Preparation and Characterization of Low Cost Ceramic and Silver-Ceramic Composite Membranes for Bacteria Filtration Applications

Thesis submitted in partial fulfillment of the requirements for the degree of

DOCTOR OF PHILOSOPHY

by

China Malakondaiah Kaniganti

Department of Chemical Engineering

Indian Institute of Technology Guwahati

Guwahati - 781039, India

Preparation and Characterization of Low Cost Ceramic and Silver-Ceramic Composite Membranes for Bacteria Filtration Applications

China Malakondaiah Kaniganti

Preparation and Characterization of Low Cost Ceramic and Silver-Ceramic Composite Membranes for Bacteria Filtration Applications

Thesis submitted in partial

fulfillment of the requirements for the degree of

DOCTOR OF PHILOSOPHY

by

China Malakondaiah Kaniganti
Roll No.: 10610711

Department of Chemical Engineering

Indian Institute of Technology Guwahati

Guwahati – 781039, India

January, 2015

Dedicated

To

My Mother

Department of Chemical Engineering
Indian Institute of Technology Guwahati
Guwahati – 781039, Assam, India

CERTIFICATE

This is to certify that **Mr. China Malakondaiah Kaniganti** worked under my supervision for the Ph.D. thesis entitled **"Preparation and Characterization of Low Cost Ceramic and Silver-Ceramic Composite Membranes for Bacteria Filtration Applications".** No portion of the work presented in this thesis has been submitted elsewhere for the award of any degree or diploma.

(Prof. Ramagopal V.S. Uppaluri)

Acknowledgements

Doing a Ph.D. requires a combination of hard work, intelligence, sincerity and supporting colleagues. In the final stages of the Ph.D., thesis writing enormously increases creative thinking. With these experiences and realizations, I would like to express my gratitude to all those who helped me in different ways in completing this research work within the time span of four years and seven months, directly or indirectly.

First and foremost, I would like to express my sincere and heartfelt gratitude to my thesis supervisor, **Prof. Ramgopal V. S. Uppaluri** who has been a continuous source of inspiration throughout the entire Ph.D. tenure. He always supported me to take up the stiffer challenges of dead end and cross flow MF studies using synthetic bacterial solutions. During the Ph.D. thesis work, there were many experimental runs that were inconclusive and further research required utmost patience and resolute determination. For all this, the role of my thesis guide as a mentor and supporter is very important. I am indebted to him for his useful suggestions and constant encouragement throughout the entire period. I am grateful to his expertise in analyzing experimental data and modelling them suitably. His uncompromising approach to complete the experimental part, data analysis, writing manuscripts as well as thesis within stipulated short period of time has been instrumental in completing my research work with minimal additional time.

My most heartfelt thanks is also due to my doctoral committee members **Dr. Vaibhav V.Goud, Dr. Sasidhar Gumma** of the Department of Chemical Engineering and **Dr. Vinayak Kulakarni** of the Department of Mechanical Engineering, for their valuable suggestions and contributions which further improved and enhanced the quality of my research work.

I am also thankful to **Dr. Animes Golder** for allowing me to use laminar flow hood equipment, **Dr. Ranjan Tamuli** and **Prof. R. Swaminathan** and their research groups including, Mr. Jagadeesh, Mr. Abrar Ali Khan, Mr. Sudhir Morla, Mr. Raghuveer Yadav Pulala, Ms. Saumya Prasad, Ms. Shrutidhara Biswas and Dr. Rekha Deka. All of them from the Department of Biotechnology, IIT Guwahati have made me learn working with procurement, preparation and analysis of microbial samples using DH5α bacterial strains.

I also thank all the faculty members of the Department of Chemical Engineering for their kind cooperation during my stay in the department. I also acknowledge the financial support provided by IIT Guwahati**.** My Ph.D. thesis is fully supported by CSIR extra mural funding and I am sincerely thankful to **CSIR** for providing the monetary support to carried out research.

I am also deeply grateful to the scientific officers **Mr. K. K. Senapati** and **Dr. D. Gogoi**, Scientific Officers, at the Central Instruments Facility of IIT Guwahati for allowing me to carry out SEM, TGA and XRD analysis on my own. I am also grateful to the **Mr. B. Choudhury** of Central Workshop, IIT Guwahati for helping me in the fabrication of my experimental setup which was very much essential in my research work. I am also thankful to DBT for providing cross flow microfiltration setup (in the other juice clarification project taken by Prof. Uppaluri) due to which my thesis has a very unique contribution. Special thanks to **Dr. C. Mallikarjuna** (Faculty member, Civil Engineering Dept., IIT Guwahati) for continuous motivation and support during the Ph.D. tenure at IIT Guwahati.

I was fortunate enough to get excellent lab mates i.e., Mr. E. Sri Harsha, Ms. Amrita Agarwal, Mr. Y. Rajesh, Mr. B. Chandrasekhar, Mr. Prashant Thorat; my friends i.e., Mr. B. Rajsekhar Reddy, Mr. S. Yadav, Mr. Ashish Kumar Thokchom, Mr. Ravi Bolleddu, Mr.

Satyannarayana Edubilli, Mr. Omar Syed, Mr. D. Anand Babu, Mr. Santhi Raju Pilli and Mr. T. Anil Kumar. All of them have provided valuable friendly support and timely assistance whenever I needed it. I am also thankful to summer internship students namely Ms. Doli Hazarika, Ms. Snigdha Baruah, Ms. Kakali Priyam Goswami, Ms. Aparna Nath, Ms. Banalata Kaibarta, Ms. Supriya Basumatary and Mr. Souradeep Sinha, Mr. Himanshu Arora, Mr. Manikantaprasad Munna, Mr. Shubham Gupta, Mr. Mohd Adil, Mr. Charan Sai and Mr. Dwipjyoti Saloi (DST project staff), for their wonderful support during the experimental investigations. Special thanks to Mr. Nagireddi Srinu for his assistance and co-operation in editing the thesis files of my research work.

Last but not the least, I would like to express my deepest gratitude to my beloved parents and family members. Their love, care, sacrifice and encouragement have made it possible for me to come so far. I am especially thankful to Srimati Seetamma Ramineni (honorable mother) for her motherly affection towards me. I appreciate the courage, understanding and dedicated support shown by all of them despite many testing times at their end.

I am also indebted to the love and affection I received from my youngest sister **Gowripriya Kaniganti** with whom I have a very good brotherly relation. I will be forever indebted to the courage, understanding and dedicated support shown by my wife **Spandana Kaniganti.** The timing of the Thesis submission made me so happy that another family member joined us in life's journey. She is none other than my daughter **Reshitha Sri Kaniganti**.

China Malakondaiah Kaniganti

Abstract

A unique study in the literature indicated promising opportunities for bacteria filtration applications of low cost ceramic membranes. Commercial silvertech composite membranes have been reported to be effective for bacteria filtration, alcoholic beverage filtration, XRD analysis media, silica and carbon black analysis media. Considering the state-of-the-art associated to fabrication engineering and application aspects of low cost ceramic and silver-ceramic composite membranes, this work addresses experimental investigations in five major areas namely:

- Preparation and characterization of low cost ceramic membranes
- Dead end microfiltration (MF) of synthetic bacterial solutions using low cost ceramic membranes
- Cross flow MF of synthetic bacterial solutions using low cost ceramic membranes
- Rate enhanced electroless fabrication of silver-ceramic composite membranes and optimality of processes and process parameters
- MF of synthetic bacterial solutions using silver-ceramic composite membranes.

From a novelty perspective, the Ph.D. thesis can be summarized as follows:

a) Dead end bacteria MF studies with low cost ceramic membranes possessing higher pore size (4 – 5 μm).

b) Dead-end MF studies with low cost ceramic membranes prepared with literature reported membrane morphologies (0.7 and 1.5 μm) using synthetic bacteria solutions in the concentration range of 0.05 – 61×10^6 CFU/mL. Dead end bacteria MF studies with wide pore size (4 – 5 μm) low cost ceramic membranes.

c) Cross-flow MF studies with low cost ceramic membranes and synthetic bacteria solutions. Specific novelty refers to the cross-flow MF data itself which has not been reported till date for low cost ceramic membranes (pore size 0.7 – 4.5 μm) and synthetic bacteria solutions (concentration range of 2.52 – 40.4×10^5 CFU/mL).

d) Identification of optimal rate enhanced silver electroless plating processes and their parameters for the fabrication of low cost silver-ceramic membranes with bulk addition mode of the hydrazine reducing agent.

e) Comparative assessment of bulk and drop wise reducing addition contacting pattern for optimal rate enhanced Ag electroless plating process to fabricate low cost silver-ceramic composite membranes.

f) Dead end MF performance of low cost silver-ceramic membranes for MF of synthetic bacteria solutions and their comparative assessment with respect to the low cost ceramic membranes.

Using literature reported inorganic precursor formulations, membranes CM1 and CM2 with low (0.7 μm) and moderate (1.5 μm) pore size respectively were fabricated using uniaxial dry compaction method. In addition, a new composition has been identified to achieve wider pore size (4.5 μm) using uniaxial dry compaction method. The membranes were subjected thermogravimetric analysis (TGA), field emission scanning electron microscopy (FESEM) and X-ray diffraction (XRD) analysis. Based on flux characterization techniques, membranes CM1 - CM3 have been analyzed to possess an average pore size of 0.7 – 4.5 μm, porosity of 39.4 - 19.3%.

During dead end MF of synthetic DH5α bacterial solutions, at a ΔP of 206.7 kPa, CM1 membrane provided an optimal flux and percent reduction value (PRV) of 1.50×10^{-3} $m^3/m^2.s$ and 100% respectively at a time of 23 min. respectively. On the other hand, CM3 membrane with its wider pore size provided an optimal flux and PRV value of 3.51×10^{-3} $m^3/m^2.s$ and 99.9999% respectively at a time of 10 min. respectively. The pertinent flux decline for the membranes has been analyzed to fit well with the cake filtration pore blocking model.

Similar results were obtained during cross flow MF but with lower separation potential of the low cost ceramic membranes. At a ΔP `of 206.7 kPa and circulation rate of 1 LPM, CM1 and CM3 membranes provided an optimal flux initial and rejection of 1.41×10^{-4} $m^3/m^2.s$ and 6 LRV ($\log_{10}$ reduction value) and 2.11×10^{-4} $m^3/m^2.s$ and 4 LRV respectively. Based on the resistances in series model analysis, CM2 and CM3 membranes at intermediate and low feed concentrations respectively have been inferred to be competent for commercial applications, as the membranes underwent low insitu fouling for these operating conditions.

The electroless fabrication of porous silver-ceramic composite membranes was first targeted with conventional (CEP), surfactant (SIEP with 2 CMC surfactant concentration), sonication (SOEP) and sonication coupled (SSOEP with 2 CMC surfactant concentration) Ag electroless plating (ELP) baths and bulk mode of hydrazine reducing agent contacting pattern. Combinatorial plating characteristics such as conversion, efficiency, percent pore densification (PPD), metal loading index (MLI) and average plating rate have evaluated for the alternate ELP processes. Among these, for a variation in plating time of 1 – 3 h, 0.01 M Ag SOEP process provided optimal plating characteristics of conversion (83%), efficiency (58 – 62%), PPD (2 – 5.7%), MLI ($2.73 - 9.09\times10^{-3}$ g/cm^3) and average plating rate ($2.31 - 2.35\times10^{-6}$ mol/L.s). For a similar plating time variation, the Ag SSOEP plating baths performed with combinatorial

characteristics of 84 – 83% conversion, 63 – 69% efficiency, 9.4 – 2% PPD, 3.07×10^{-3} – 1.01×10^{-2} g/cm^3 MLI and 2.39 – 2.34×10^{-6} mol/L.s average plating rate. Further investigations in parametric optimization of SOEP and SSOEP processes indicated that 0.01 M Ag solution concentration and 2 CMC CTAB solution concentrations are optimal choices for Ag SOEP and SSOEP baths respectively.

To further evaluate upon the competence of the contacting pattern of the hydrazine reducing agent, Ag SOEP and SSOEP plating baths were analyzed for drop wise contacting pattern of the hydrazine reducing agent for various solution concentrations (50 – 400% excess). Thereby, it has been evaluated that among all cases, the best case corresponds to SOEP process at a plating time of 1 h, where the optimal combinatorial plating characteristics of 46.24% conversion, 69.24% efficiency, 0.7% PPD, 1.82×10^{-3} g/cm^3 MLI and 1.17×10^{-6} average plating rate were obtained.

The MF studies of low cost silver-ceramic composite membranes did not indicate their competence with respect to the ceramic composite membranes. While silver membranes fabricated with CM3 porous supports provided poor performance, the silver membranes fabricated with CM1 porous support performed marginally poorer than the CM1 membrane. For a low feed concentration of 4.40×10^4 CFU/mL, the silver-ceramic composite membrane fabricated with CM1 membrane provided LRV values of 3 – 2.3 which were poorer than the LRV values obtained for the CM1 membrane. Similarly, for a higher feed concentration of 8.86×10^6 CFU/mL, LRV values of silver composite membranes were 5.1 – 3.8 which are lower than those obtained for the CM1 membrane. This indicates that low cost silver ceramic composite membranes fabricated with electroless plating are not applicable for bacteria filtration applications and further investigations are required to judge upon their competence with respect to low cost ceramic membranes. Thereby, this work highlighted the need to always refer to the

support performance for the comparative assessment of silver ceramic membranes. This was not the case in few literatures that highlighted upon the efficacy of silver membranes for bacteria filtration applications.

Conceptual retail cost analysis (inclusive of chemical, electrical, sonication etc.,) of the fabricated low cost ceramic and silver ceramic membranes indicated their costs to be 1656.96 and 5837.51 $/m^2 respectively. Thus, it has been inferred from cost analysis that the silver membranes are 3.5 times expensive than the low cost ceramic membranes. Further, a cost comparison with commercial silvertech membranes indicated that the fabricated membranes are at least 40 % inexpensive on a retail basis which can be further improved to 60% cost effectiveness by process scale up studies.

In summary, the Ph.D. thesis highlights the relevance and promising opportunities for low cost ceramic membranes towards bacteria filtration. In addition, the thesis provides useful insights into the fabrication engineering aspects of low cost silver-ceramic composite membranes using rate enhanced electroless fabrication techniques. Further research in the field of electroless fabricated low cost silver ceramic composite membranes needs to be towards consolidating the technical data related to their commercial applications such as bacteria filtration, alcoholic filtration, XRD, silica and carbon black analyses media.

Contents

List of Tables

Table No: **Table Caption** **Page No.**

Table No: **Table Caption** **Page No.**

List of Figures

Fig. No: **Fig. Caption** **Page No.**

Fig. No: **Fig. Caption** **Page No.**

Fig. No: **Fig. Caption** **Page No.**

Chapter 1:

Introduction and Literature Review

Chapter 1

Introduction and Literature Review

In this chapter, after a formal introduction to potable water in section 1.1, section 1.2 addresses an overview of membrane technologies. Subsequently, section 1.3 summarizes relevant membrane technologies for bacteria filtration and bacteriostatic applications. These especially refer to polymeric membranes, ceramic membranes and silver-ceramic membranes. The state-of-the-art associated to bacteria filtration using membrane technology is presented in section 1.4. Finally, section 1.5 presents possible scope for further research followed with objectives and organization of the thesis in sections 1.6 and 1.7 respectively.

1.1 Process Technologies for Potable Water Production

1.1.1 Introduction

In a recent World Health Organization (WHO) report, contaminated drinking water was identified as the primary cause for 80% of the human diseases. It was estimated that about 2.2 million people die every year with diarrheal diseases that are primarily caused due to waterborne infections (WR1). Thus, amongst several industries, industries that produce drinking water have high degree of significance due to their direct relevance to human consumption. With 66% of water content in their bodies, human beings require clean and potable drinking water that is free from pathogens. Potable water standards indicate that drinking water must contain fecal and total *coliform* count of 0 in 100 mL sample (Lv et al., 2009; Simonis and Basson, 2011a; van Halem et al., 2009).

Table 1.1: Common diseases caused by microbes to human beings (Source: WR2).

	Microorganism	Disease
Bacterial Infections	*Bacterium Vibrio cholera*	*Cholera*
	Escherichia coli (E.coli)	*Diarrhea*
	Clostridium Botulinum	*Botulism*
	Campylobacter jejuni	*Campylobacteriosis*
Viral Infections	*Poliovirus*	*Poliomyelitis (Polio)*
	Hepatitis A Virus (HAV)	*Hepatitis A*
	Astrovirus, Calcivirus, Enteric Adenovirus and Parvovirus	*Gastroenteritis*
Parasitic Infections	*Members of the genus Shistosoma*	*Schistosomiasis*
	Dracunculusmedinensis	*Dracunculiasis (guinea worm disease)*
	Tapeworms of the genus Taenia	*Taeniasis*
	Fasciolopsisbuski	*Fasciolopsiasis*
	Hymenolepis nana	*Hypemolepiasis*
	Echinococcusgranulosus	*Echinococcosis (Hydatid disease)*
	Ascaris lumbricoides	*Ascariasis*
	Enterobiusvermicularis	*Enterobiasis*
Protozoal Infections	*Entamoebahistolytica*	*Amoebiasis*
	Cryptosporidium parvum	*Cryptosporidiosis*
	Cyclosporacayetanensis	*Cyclosporiasis*
	Giardia lamblia	*Giardiasis*
	Microsporidia	*Microsporidiosis*

Generally, water available in fresh water ponds appears to be clean but cannot be regarded to be healthy for human consumption. This is due to the presence of bacteria and other toxic impurities. In fact, most pond pollutants are not visible and contaminants in water affect health and cause taste and odor problems due to the presence of harmful bacteria (Lv et al., 2009). Despite having such knowledge, poverty stricken rural communities consume such pathogen

contaminated water due to which endemic gastrointestinal diseases occur. A summary of various health risks for human beings due to micro-organism contamination in drinking water is presented in Table 1.1.

Further, it has also been reported in the literature that diseases can also occur due to the existence of some heavy metals at concentrations more than permissible levels in water bodies (Pindi et al., 2013). In the North-eastern region of India, iron content is very high in ground water (Paul and Mishra, 2011). In fact, almost most of the surface water bodies are having Fe in permissible limits in ground water. In nature, iron exists in +2 or +3 states. However, anaerobic conditions favor the higher concentration of Fe (II) due to the reduction of Fe (III). According to the Bureau of Indian Standards (BIS), the permissible level of iron content in drinking water is about 0.3 - 1.0 mg/L.

Therefore, the provision of safe drinking and clean potable water using low cost technologies is the need of the hour in developing countries. To implement such technologies, water quality testing is very important as testing procedures enable the measurement and monitoring of several contaminants in potable water. Thereby, these procedures provide significant insights into suitability of various competent technologies and their combinations. In summary, water treatment technologies need to address the removal of particulate matter, suspended solids, parasites, fungi, algae, bacteria and viruses from contaminated water resources.

1.1.2 Alternate process technologies

Inadequately treated water may contain disease-causing organisms, or pathogens. Pathogens include various types of protozoan parasites, other organisms, bacteria and viruses. Generally, water-borne diseases occur due to the consumption of drinking water contaminated by human or animal faeces. For human consumption, potable water must have zero content of pathogenic

micro-organisms. Water purification is the process of removing undesirable chemicals, biological contaminants, suspended solids and gases from contaminated water. The purification process of water may reduce the concentration of particulate matter including suspended particles, parasites, algae, fungi, bacteria, viruses etc. Since a single technology cannot eliminate the enlisted contaminants, often combinations of various technologies are adopted. These are further classified into physical and chemical processes.

Physical processes constitute an important sub-class of various prominent technologies (WR3) adopted for drinking water production in the lab and pilot scale. These especially refer to filtration, sedimentation, distillation and membrane technology using polymeric, ceramic and silver composite membranes. Amongst physical processes, filtration is commonly used mechanical or physical operation for the separation of solids from fluids. This is achieved by using a filter medium through which only the fluid can pass. Sedimentation explores the principle of suspended particle removal by gravity setting. Eventually, separation of solids is targeted through centrifugal acceleration or electromagnetism. Distillation is a method of separating mixtures based on differences in volatility of components in a boiling liquid mixture. Membrane technology involves the separation of contaminants using selective polymeric/ceramic/silver-ceramic membranes for the elimination of contaminants in the water resources. Amongst these membranes, polymeric membranes have been documented to be sensitive to temperature and bio-fouling and with their short life cycle, they are not advisable as long term solutions for bacteria filtration applications to generate potable water. On the other hand, ceramic and silver ceramic composite membranes/filters have the additional flexibility to withstand temperature variations and mostly importantly bio-fouling.

Table 1.2: A summary of commercially available water purifiers in India.

S. No	Company Name	Technology
1.	Eureka Forbes Aquaguard (WR4)	Reverse osmosis, Ultra filtration, ultra violet unit
2.	Hindustan Unilever Pureit (WR5)	Ultra violet Unit, Germ killer kit,
3.	Tata Swach (WR6)	Silver nanotechnology
4.	Kent RO Water purifier (WR7)	Reverse osmosis, Ultrafiltration, TDS controller, Ultra violet Unit
5.	Philips UV water purifier (WR8)	Advanced UV technology, Sediment filter unit, Activated carbon unit
6.	Hi-Tech water purifier (WR9)	Reverse osmosis
7.	Kenstar water purifier (WR10)	Ultra violet radiation, Nano silver technology
8.	Whirlpool RO Purifier (WR11)	Reverse osmosis, Silver Antimicrobial Filtration Enhancer(S.A.F.E)
9.	Livpure RO water purifier (WR12)	Reverse osmosis, Ultrafiltration, Ultra violet radiation.
10.	Ushabrita water purifier (WR13)	Reverse osmosis, Ultra violet radiation

Amongst biological processes, biologically active carbon/sand filters are prominent. These are constructed using either graded layers of sand/biological active carbon from higher to finest size. With strong filtration and adsorption capability, biological active carbons have been reported to remove colour and odour of contaminated water.

As on date, several commercial organizations have developed water purifier products to meet the drinking water requirements of Indian population. Table 1.2 presents the few best and cost effective water purifiers of India. Generally, commercial water purifier systems involve a combination of physical and chemical processes. For example, commercial water purifier systems such as Kent include a combination of several physical and chemical processes such as ultraviolet

radiation and membrane technology. Amongst various technologies, membrane technology is promising due to its ability to provide compact and low cost operation. Among various membrane technologies, polymeric membrane filters are highly popular in comparison with ceramic and silver-ceramic composite membranes. However, ceramic and silver-ceramic composite membranes can be referred to be upcoming technologies for bacteria filtration applications.

Chemical processes especially refer to ultraviolet irradiation, ozonation, chlorination, pasteurization and flocculation. Among these technologies, the widely practiced technology in rural communities is pasteurization. From a technological perspective, ultraviolet irradiation is one of the most versatile technologies adopted in household drinking water purifiers such as Aquaguard etc., to generate potable drinking water. Ozonation is a process for infusing water with ozone. Ozone is used to kill bacteria and other organisms but in turn also affects the colour, taste and odour of the potable water. Chlorination as well is an important technology adopted for the large scale production of pathogen free drinking water. Pasteurization involves the sequential boiling and natural cooling of water and is a traditional approach adopted in many Indian households and has the potential to retard microbial growth and spoilage. Flocculation is a process in which colloids are generated from a suspension which eventually settles as a floc or a flake. Generally, clarifying agents such as alum are used to remove suspended solids from liquids by inducing flocculation. After flocculation, the particles will be large enough to settle and can be removed from the potable water. For potable water production from open source water reservoirs and marshy ponds, microfiltration (MF) and ultrafiltration (UF) using membrane technology are cost effective.

1.1.3 Salient features of process technologies

Among various physical and chemical processes, each process has its own advantages and disadvantages for potable water generation from the perspective of the elimination or limitation of various contaminants in raw water resources. Technologies such as ozonation, chlorination, ultraviolet radiation etc., are significantly expensive due to utilization of chemicals. Further, these technologies enable the formation of disinfection byproducts, which might be carcinogenic in nature and unpotable for human consumption. Further, chlorination plants are well known to have the risk of chlorine leakage which is detrimental to human health. Further, distillation is energy intensive and is not economical for potable water generation. Sedimentation and flocculation do not address the desired feature of higher efficiency for bacteria removal. These technologies only refer to the elimination of suspended particles but not bacteria. For bacteria filtration applications, low cost portable technologies refer to biologically active carbon/sand filters and membrane technology. In this regard, silver membranes are expensive than membrane technology and hence, their wider application towards bacteriostatic application has not been reported to a large extent.

While biologically active filters are inexpensive, they may or may not refer to the complete elimination of bacteria. This is due to the higher pore size of these filters. Nonetheless, a careful design of biologically active filters might serve the purpose of bacteria elimination from contaminated water resources. On the other hand, membrane technology provides additional flexibility to offer wider pore sizes to suite the requirement of stage wise elimination of suspended particles and bacteria. However, it can be noted in this regard that while membrane technology is an important technology for advanced waste water treatment, it cannot be regarded to be only technology for advanced water treatment. In summary, as an important technology for

advanced water treatment, membrane technology has received significant world-wide research emphasis for the development and deployment of membranes for cost effective potable water production.The elimination of several water contaminants using filtration is highly dependent upon the amount, size and charge of the contaminant particle. Membrane filtration has the potential to remove many contaminants from water, including bacteria, salts, and various heavy metals. For operation, two classes of membrane filtration can be considered. These refer to low-pressure technologies (microfiltration and ultrafiltration) and high-pressure technologies (nanofiltration and reverse osmosis). Low-pressure operated membranes have larger nominal pore sizes, and are operated at pressures from 68.9-700 kPa. The tighter high-pressure membranes are typically operated at pressures upto 10, 000 kPa.

The basic principle of membrane separation is transport through the membrane for which a specific type of driving force (pressure drop or concentration difference or electrical potential) is responsible. Large quantities of potable water are typically produced using hybrid systems comprising of multi-flash and reverse osmosis membrane systems. Such plants have been installed in gulf countries and recently, reverse osmosis based system has been successfully installed in Chennai, India to supply potable drinking water. On a small scale basis, however, the hybrid desalination system is not cost effective. Therefore, for applications such as household and medical usage, water purifiers and other technologies are adopted.

1.1.4 Summary

Biological active carbon and ceramic membrane provide the most feasible and low cost option for the generation of microbe pathogen free potable water from contaminated water resources. While biological active filters are highly relevant for bacteria filtration, ceramic membranes are

attractive from the perspective of compact operation. Ceramic membranes with wider pore size can offer water filtration via gravity principle and can serve even as biological filter. Therefore, research in this thesis has been exclusively focused towards ceramic membranes and silver-ceramic composite membranes. In the next section, a brief overview of various membrane technologies is presented.

1.2 An overview of membrane technologies

Among novel separation processes that were invented in chemical engineering research, membrane technology remains one of the foremost and prominent technologies. In general, the research emphasis in membrane technology refers to the preparation, characterization and application of selective polymeric/ceramic membranes for the desired separation task in process industries. For a typical feed fed to a membrane process plant, in comparison with the feed concentration, streams consisting of higher and lower concentration of separated components are termed as retentate and permeate respectively.

Further, irrespective of the type of material being deployed as a selective membrane, based on the inherent structure of the membrane, these are classified into symmetric and asymmetric membranes. Among these, the symmetric membranes consist of porous single phase structures with thickness and average pore size of 10 – 200 μm and 0.2 – 10 μm respectively. On the other hand, asymmetric membranes refer to at least two layered membranes in which a thin dense layer of about 0.01 – 0.5 μm pore size is being deposited on a symmetric membrane structure. Compared to the symmetric membranes, asymmetric membranes have the additional flexibility to provide desired lower pore size for functional applications. Further, they do have higher mechanical strength due to the macroporous membrane support.

1.2.1 Classification based on pore size and species dimension

From an operational point of view, membrane processes are classified into microfiltration ultrafiltration, reverse osmosis, nanofiltration, dialysis and electrodialysis processes. Microfiltration, ultrafiltration and reverse osmosis processes are pressure driven processes where the pressure applied across the membrane serves as a driving force for the membrane flux. Typically, in a microfiltration process, the applied pressure is 0.1 – 2 bar which increases to 5 – 20 bar for nanofiltration and 10 – 100 bar for reverse osmosis processes. From the perspective of the solutes getting separated, microfiltration is capable to separate micro and macrosolutes (100 – 10,000 µm). These specifically refer to colloidal materials, bacteria and yeast cells. The operating pressure for the separation of these solutes is lower due to the higher particle size of the solutes. Since the particle sizes are high, the membrane pore size for microfiltration is in the range of 0.1 – 10 µm.

Virus, proteins and colloidal silica having a molecular weight of 100000 – 500000 (equivalent to 100 – 500 kDa) possess an average particle size of 0.01 – 0.1 µm and these separation problems are addressed with ultrafiltration processes. Aqueous salt, metal ions and sugars have even lower particle size (0.001 – 0.1 µm) and their separation is targeted by nanofiltration and reverse osmosis. Thus, membranes with larger pore size can be applied for microfiltration, membranes with moderate pore size for ultrafiltration and membranes with finer pore size for reverse osmosis processes. A summary of membrane characterization based on pore size and target species for removal is presented in Table 1.3.

Table 1.3: Pore size and Target species based characterization of membrane processes.

Pore Type (nm)	Membrane Technology	Species	Dimensions(nm)
Macro pore (>50)	Microfiltration	Yeasts & fungi	1000-10000
		Bacteria	300-10000
		Oil emulsions	100-10000
Mesopores (2-50)	Ultrafiltration	Colloidal solids	100-1000
		Viruses	30-300
		Protein/Polysaccharides	3-10
		Humics/Nucleic acids	<3
Micropores (0.2-2)	Nanofiltration &	Common antibiotics	0.6-1.2
	Reverse Osmosis	Organic antibiotics	0.3-0.8
		Inorganic ions	0.2-0.4
		Water	0.2

1.2.2 Classification based on materials

From a materials perspective, polymeric and ceramic membranes have their own pros and cons. While polymeric membranes can be prepared with promising features such as wider pore size range, hydrophilic and hydrophobic applications, low cost, easy fabrication processes and scalability, they suffer with the basic limitations of low solvent resistance, pH resistance and

Table 1.4: Efficacy of various membrane technologies towards the removal of chemical and biological species (Source: WR14)

Membrane Technology	Capabilities	Limitations
Microfiltration (0.1– 10 µm)	• Very high and moderate effectiveness in removing protozoa (*Cryptosporidium, Giardia*) and bacteria (*Campylobacter, Salmonella, Shigella, E. coli*) respectively	• Not effective in removing viruses (*Enteric, Hepatitis A, Norovirus, Rotavirus*) and chemicals.
Ultrafiltration (0.01-0.1 µm)	• Very high effectiveness in removing protozoa (*Cryptosporidium, Giardia*),bacteria (*Campylobacter, Salmonella, Shigella, E. coli*)	• Moderate effectiveness in removing viruses (*Enteric, Hepatitis A, Norovirus, Rotavirus*) and low effectiveness in removing chemicals.

temperature range applicability, lower mechanical strength and shorter life span. On the other hand, ceramic membranes have promising features such as corrosion resistance, wider pH applicability, wider temperature applicability, longer life span, less fouling tendencies and higher mechanical strength. However, they have the basic limitation of limited pore size range (typically in MF range for symmetric membranes and UF range for asymmetric membranes), higher process cost and brittle nature. Despite having these limitations, ceramic membranes are

often desired for several commercial applications due to their higher corrosive resistance and wider pH and temperature applicability, which are very relevant with respect to the physico-chemical characteristics of various streams generated in the process industries.

1.2.3 Classification based on species removal efficacy

The efficacy of various membrane technologies towards bacteria filtration and removal of other similar microbes (such as bacteria, viruses etc.,) is summarized in Table1.4. Further, the table also summarizes the limitations of various membrane technologies for the removal of specific chemicals/microbes. From the table, it can be analyzed that microfiltration technique is not effective in removing chemicals and only reverse osmosis processes are effective to remove both microbes and chemicals.

1.2.4 Commercial silver membrane filters

Silver membranes constitute an important section of chemical and sterile filtration systems. Generally, silver membranes refer to a thin silver film deposited on a symmetric or asymmetric metal/ceramic support. Silver membranes are regarded to be one of the latest technologies for bacteriostatic applications. Other applications of silver membranes include filtration of alcoholic beverages (WR15), high temperature sterilization procedures (WR16) and collection and analysis of coke oven emissions, where the silver membrane is used directly to collect coal tar pitch volatiles (WR17). However, silver composite membranes are often regarded to be of higher cost due to the thicker silver metal film. As an alternative, silver nanoparticle embedded

Table 1.5: A summary of commercially available silver membranes.

S.No	Company Name	Pore size (µm)	Applications
1.	Zefon International (WR17)	0.45, 0.8	• Collection and analysis of carbon and carbon black
2.	Germlyser, Germany (WR18)	0.2	• Removes bacteria from tap water
3.	Purificup potable natural water purifier (WR19)	1	• Elimination of bacteria • In the Medical industries
4.	SKC Filters (WR20)	0.45, 0.8	• Analysis of biological specimen • Filtration on of alcoholic beverages
5.	Sterlitech (WR21)	0.2-5	• Elimination of bacteria from water
6.	General Electric (WR22)	0.8	• Used to get potable water
7.	SPI-Pore (WR23)	0.2 – 5	• Filtration of alcoholic beverages • High temperature sterilization procedure
8.	Wacorp Hyundai Private Ltd. (WR24)	0.01	• Treatment of contaminated water
9.	Merck Millipore (WR25)	0.45, 0.8	• Use for air monitoring of carbon black, coal tar products, coke oven emissions, and silica.

composite membranes have been suggested to be effective for bacteriostatic application. Since silver nanoparticles are embedded in a ceramic matrix, the cost of the nano-material embedded ceramic filter is expected to enhance marginally in comparison with the cost of the ceramic membranes. Despite the higher cost of silver membranes, several companies manufacture silver composite membranes. A summary of different manufactures of commercial silver membranes is presented in Table 1.5. Among these manufacturers, Germlyser developed by Aqua-free Membrane Technology GmbH, Hamburg, Germany (WR18) possessed an average pore size of 0.2 µm with a silver layer on the filtration membrane, due to which the biofilm growth on the bacteriostatic silver membrane is anticipated to diminish.

An important issue for the maintenance of silver membranes is with respect to the regeneration procedures adopted for their effective cleaning after water filtration. After usage, silver membranes have been recommended by Millipore filters (WR25) to undergo cleaning procedures via four different approaches. These have been outlined as follows:

a) *Chemical Cleaning*

Immerse contaminated silver membrane in a strong alkaline solution, a solvent, or an acid. The membrane should not be immersed in nitric acid, sulphuric acid, or cyanide solutions.

b) *Ignition Cleaning*

Place the silver metal membrane filter in a laboratory muffle furnace at not more than 300^{o}C for approximately 30minutes to effectively remove organic contaminants from the membrane.

c) *Combination Cleaning*

A combination of chemical and ignition cleaning may be the best method to completely regenerate the membrane. In this procedure, the silver membrane is first immersed in 10% of hydrofluoric acid for 10 minutes followed by ignition cleaning in a muffle furnace. The combination cleaning is regarded to be effective for regenerating the membrane for at least 10 times usage without any further cleaning.

d) *Ultrasonic Cleaning*

Low intensity ultrasonics can be used to clean the silver metal membrane. The cleaning intensity and time will depend on the degree and type of contamination encountered. High intensity ultrasonics are not recommended for silver membrane cleaning as they may deteriorate the silver film bondage with the ceramic/metal matrix.

1.2.5 Summary

In comparison with ceramic membranes, polymeric membranes are highly susceptible for bio-fouling and therefore have short span of life for application towards potable water generation. Among various processes, only reverse osmosis technology is the most competent to eliminate almost all chemical and biological species. However, reverse osmosis is highly expensive due to the utilization of sophisticated membrane and pump with higher pressure delivery. For contaminated water resources, pump costs may not be very high due to lower osmotic pressure of the feed stream. However, the cost of reverse osmosis membrane is bound to be very high. Further, compared to microfiltration membranes, RO membranes will provide lower flux. On the other hand, though microfiltration is attractive, it suffers with the basic limitation that it cannot eliminate all chemical and biological species. Despite having such limitations, microfiltration is

attractive with the fact that microfiltration requires lowest operating pressure differentials and provides highest flux due to large pore size. Due to this reason MF processes are cost effective in comparison with RO. Henceforth, it can be inferred that low cost microfiltration membrane technology needs further research and development studies for its application towards potable water production and water purification from contaminated water resources.

1.3 Overview of Membrane Technologies for Bacteria filtration/Bacteriostatic applications

In this section, the relevance of various membrane technologies for bacteria filtration/bacteriostatic applications has been summarized. The low cost ceramic membranes specifically refer to those that being fabricated using materials such as kaolin and clay.

1.3.1 Polymeric membranes

From a materials perspective, polymeric membranes with their lower cost, scalability and good separation characteristics are familiar for industrial liquid phase separation schemes such as wastewater treatment (Salahi et al., 2010) and juice clarification (Girard and Fukumoto, 1999). Few literature also exists that address upon the relevance of polymeric membranes (Yang et al., 2010) towards bacteriostatic applications using synthetic microbial solutions. However, it is well known that polymeric membranes have lower shelf life due to their lower fouling resistance towards biological activity and pH variations. Porous polymeric membranes (i.e., MF/UF) have been studied and well for various water treatment processes, including water and wastewater filtration applications. Further, they are also applied for NF and RO applications. Membrane technology research for the polymer membranes is primarily aimed at varying the membrane morphological, flux and rejection characteristics with variations in casting conditions, polymer

selection and concentration, solvent/non-solvent system and additives and coagulation bath conditions. Among polymeric materials, cellulose acetate (CA) was one of the first polymers employed in aqueous membranes and continues to be employed to form membranes with properties ranging from MF to RO. CA is hydrophilic and produces smooth membranes with low fouling propensity. Cellulosic membranes are also relatively easy to manufacture with a wide range of pore sizes and are relatively inexpensive. Disadvantages of CA include limited temperature range (less than 30°C), pH range (approximately 3-5) of operation. Also, due to the cellulose backbone, CA membranes are biodegradable and can, in fact, be consumed by organisms growing in biofilms.

Other more widely applied MF/UF membrane polymers include polysulfone (PSf), polyethersulfone (PES), polyacrylonitrile (PAN), polypropylene (PP), polytetrafluoroethylene (PTFE), polyamide (PA) and polyvinylidine fluoride (PVDF). These materials exhibit excellent permeability, selectivity and stability in water treatment applications. Among these polymers, PP and PVDF are more popular materials for MF operations.

1.3.2 Low cost ceramic membranes

While ceramic membranes have promising opportunities in microfiltration applications, their higher cost is limiting their applicability. Therefore, the development of low cost ceramic membranes using low cost inorganic precursors and cheaper fabrication technologies would be useful to enhance the economic competitiveness of ceramic membranes in process industries. Typically, kaolin and clay are inexpensive inorganic materials that are deployed for laboratory scale ceramic membrane fabrication using paste and uniaxial dry compaction methods. For

commercial process scale applications, ceramic membranes are typically manufactured using extrusion processes.

Symmetric ceramic membranes have been tested for the following microfiltration applications:

a) Industrial wastewater treatment for various cases such as oily wastewater, paper and pulp effluents, tannery wastewaters etc.

b) Potable water production from various contaminated natural water resources by targeting bacteria filtration.

c) Clarification of fruit juices such as pineapple, mosambi and orange juices.

d) Bio-separation technologies such as protein recovery, milk concentration and fat separation from milk.

Among these applications, the production of potable water from various natural water resources remains one of the most important application in which research activity is targeted in this work. This is also due to the fact that several researchers have focused upon the application of low cost ceramic membranes for wastewater treatment (Emani et al., 2013; Nandi et al., 2009b; Vasanth et al., 2011) and juice clarification (Emani et al., 2013; Nandi et al., 2009a) but only few researchers (Vasanth et al., 2011) have studied bacteria filtration using low cost ceramic membranes.

1.3.3 Silver composite membranes

Research emphasis in the field of silver-ceramic composite membranes refers to fabrication engineering (preparation and characterization) and their applications. In the following sub-

section, a brief summary of various fabrication engineering methodologies is presented for the silver composite membranes.

1.3.3.1 Fabrication methods

The fabrication of silver-ceramic composite membranes is typically achieved using either one of the following methods: magnetron sputtering, chemical vapor deposition and electroless plating. A brief account of these techniques is being presented in the following sub-sections.

Magnetron sputtering

The sputtering technique involves the creation of plasma (low pressure gas with large number of ions and free electrons) using high energy electrical field. Eventually, sputtering involves the bombardment of the solid target by high energy chemically inert ions. Due to this effect, the atoms to be deposited are ejected from the target and are deposited on the surface of a substrate using a magnetic field generated with permanent magnets. Sputtering enables the generation of ultra thin nano-structured films with minimal impurity. Therefore, greater flexibility can be achieved in achieving alloys and controlled film structure with maximum degree of uniformity. Since sputtering involves heated substrate during deposition procedure itself, additional heating for the formation of an alloy is not required. A major disadvantage of the sputtering process is its high cost due to the higher capital costs and energy costs involved for the generation of plasma. Therefore, despite providing very good quality silver films, sputtering is not the preferred choice due to very expensive sputtering process. Also, sputtering process is not scalable as the technology would be highly costly for higher capacity requirements.

Chemical vapor deposition

The chemical vapor deposition (CVD) process involves the fabrication of a silver-ceramic membrane using vapor-phase chemical reaction at a controlled temperature. The gaseous compounds of the silver precursors are transported to a substrate surface where thermal reaction/deposition is facilitated. Eventually, the reaction byproducts are exhausted out of the system. CVD process provides high purity and high performance metal composite structures. CVD is usually favored for metallic or dielectric metal depositions of low and high melting points. The metal film thickness can be easily controlled to the level of submicron scales using the CVD. On the other hand, high purity alloy deposition cannot be achieved using CVD. CVD process is economically favored and compared to sputtering technique as the CVD is relatively easy to scale up. However, controls and instrumentation make up significantly towards the process cost and hence the cost of the CVD is as well high. However, CVD is economical in comparison with the magnetron sputtering process.

Electroless plating

Electroless silver deposition involves the autocatalytic reduction of silver precursors on the palladium seeded ceramic surface using a reducing agent such as hydrazine or sodium hypophosphite. Compared to other techniques, electroless plating is inexpensive given the fact that the technique only requires a very simple experimental setup. Further, electroless deposition has been opined to be promising due to several features such as uniformity of deposition, ability to deposit on non-conducting surfaces and complex shapes, scalability etc., Besides these, electroless plating is highly inexpensive and only involves the cost of the chemicals and manpower as major costs for fabrication of silver composite membranes. Controlled deposition

on the desired surface of the ceramic substrate is often targeted by not seeding other surfaces of the substrate prior to electroless deposition.

Electroless plating process is strongly influenced by support quality, surface activation procedures, electroless plating process parameters and bath chemistry. Conventional electroless plating constitutes two hierarchical steps namely sensitization-surface activation and metal deposition. The sensitization-activation process involves the sequential exposure of the porous substrate to very dilute acidic solutions of Sn^{+2} and Pd^{+2} salts with intermittent rinsing using deionized water. While sensitization favors adsorption of Sn^{+2} on the substrate surface in hydrolytic form, the activation step further involves the reduction of Pd^{+2} to Pd^{0} via the following redox reaction on the substrate:

$$Sn^{+2} + Pd^{+2} \rightarrow Sn^{+4} + Pd^{0} \qquad (1.1)$$

In the conventional ELP process, Pd activation is the most critical step that could detrimentally or favorably influence the electroless deposition of the silver film. Poor Pd activation on the surface would not enable uniform metal deposition on the surface and hence the sensitization-activation process is repeated sequentially at least 10 times to achieve the uniform Pd activation.

After uniform Pd activation is achieved, the uniformly seeded Pd support is subjected to silver electroless plating. The electroless silver deposition involves placing the seeded Pd support into a plating solution that consist of silver precursors, complexing agent, reducing agent and a pH regulator in aqueous media. Electroless plating occurs on the solid liquid interface between the ceramic support and the plating solution. The electroless silver deposition happens due to the reduction of Ag^{+2} ions in the solution on the Pd seeded ceramic support with the electrons

provided by the reducing agent. Typically, reducing agents such as dialkyl amine borane, borohydride, hypophosphite, formaldehyde and hydrazine are used for the electroless plating process. Among these, sodium hypophosphite is commonly used for chrome plating but involves the deposition of phosphorus as well to thereby reduce the quality of the silver film. On the other hand, formaldehyde is not preferred due to the fast release of H_2 gas during plating process and lower reducing ability of the formaldehyde. Hydrazine appears to be the most relevant reducing agent due to good reducing ability and heavy N_2 gas generation from the substrate surface.

To further aid quality of electroless plating and to enhance the rate of electroless deposition, surfactant and or sonication is typically coupled to the electroless plating process. While surfactant reduces the pitting effect that occurs due to the faster release of N_2 bubbles from the substrate surface, sonication enhances the rate of electroless plating due to cavitation effect. Thereby, agglomerates of silver crystals form metal clusters on the membrane surface with narrow or marginal variations in their grain boundaries. In summary, surfactant chemistry and sonication process parameters offer additional degrees of freedom for rate enhance silver electroless plating processes in comparison with the conventional electroless plating processes. These flexibilities in the process parameters enable to judiciously infer upon the efficacy of electroless plating process to achieve porous silver-ceramic composite membranes. The morphology of the silver film (thickness and pore size) is strongly influenced by the ceramic support properties (average pore size, porosity and pore size distribution), bath chemistry, rate enhancement process parameters etc.,

Summary

Among all techniques, electroless plating is the most inexpensive process to fabricate porous silver-ceramic composite membranes. This is due to the very fact that all other processes require

sophisticated instrumentation and control setup, which are very expensive in comparison with the electroless plating process which only requires simple setups such as water bath, beakers and chemicals. Henceforth, among the available technologies, electroless plating shall be regarded as the most feasible process technology to achieve low cost silver-ceramic composite membranes with lowest investment for the experimental setup.

1.3.3.2 Applications

Based on extensive literature survey, silver ceramic composite membranes have been summarized to be relevant for the following applications:

a) Bacteria removal (filtration as well as bacteriostatic application) from tap water and water produced from medical industries.

b) Analysis of biological specimens

c) Filtration of alcoholic beverages

d) Analysis of carbon black in air and dusty environment samples

e) Monitoring of silica content in air samples.

While some of these applications were elaborately described in the literature, some of them have been mentioned without further details with respect to the applications. The following sub-sections present relevant information summarized for the above mentioned applications.

a) Bacteria filtration/Bacteriostatic applications

It has been reported that the commercial silver membrane filter PurifyCup (WR19) can eliminate microbes and provide a separation efficiency of 3 - 4 LRV. With antibacterial activity, the silver

composite filter has been evaluated to specifically eliminate various microbial species such as pathogen bacteria (*E. coli, Staphylococcus aureus, Pseudomonas aeruginosa, Cryptosporidia etc.),* parasites etc. from streams, falls, creeks and rivers. The PurifyCup technology involves three filters namely ion exchange resin, activated carbon and silver membrane (1 µm). The silver film has been evaluated to be non-toxic and provide strong oxidation along with insensitivity to pH due to its ionic form of silver content and thereby eliminate more than 600 kinds of bacteria. Also, the mechanism of silver-pathogen interaction has been specified to refer to the destruction of the microbe cell wall during the oxidization of sulphur functional group on the surface protein of pathogens. On the other hand, the antibacterial effect of silver presumes the neutralization of positively charged ions and negatively charged bacteria cell walls. This eventually causes effective disruption of growth and bacteria lysis. Further, silver not only denatures the bacteria protein and also affect the metabolism of pathogens. However, the product information does not explicitly refer to the separation potential of each of the components of the technology namely ion-exchange resin, activated carbon and silver filter.

b) Analysis of biological specimen

The NIOSH 6011 method elaborates upon the potential of silver membrane filters for the analysis of biological specimen such as chlorine (WR26). Chlorine measurement has been suggested by passing the media (such as air) through the silver membrane filter which enables the formation of silver chloride on the filter. Eventually, the silver chloride on the silver filter is desorbed using sodium thiosulfate and further analysis can be conducted using ion chromatography. Thus, the suggested method is based on the positive and negative interference from both hydrogen chloride and hydrogen sulfide respectively. The suggested chlorine detection limit is about 0.007 – 0.5 ppm for a 90 L air sample at a flow rate of 0.3 – 1.0 L per min.

c) Filtration of alcoholic beverages

A patent (No. 2222586) conveys the potential of silver filtration technology for the filtration of alcoholic beverages (WR27). Developed by the Technofilter Research and Manufacturing Enterprise Ltd., the catridge filter consists of silver-impregnated cocoanut shell carbon and has been evaluated to possess high alcoholic processing rate and could enhance the organoleptic properties of water-alcohol mixtures. Other promising features of the silver impregnated filters include the achievement of stable quality of the alcohol mixtures, removal of objectionable tastes and odours of alcoholic tones in the aroma. The filters were also evaluated to provide good life cycle with lower replacement costs in comparison with their counter parts.

d) Analysis of carbon black in air and dusty environment samples

Mehler et al. (1982) reported the utilization of silver filters for the evaluation of carbon black. The method is referred to as the standard NIOSH method and involves the capture of carbon black from air and dusty environmental samples after filtration through the filter. Eventually, the collected contaminants could be removed from the filter by using suitable organic solvents and heating the filter to 500^{o}C. By doing so, only carbon black and other inorganics are selectively eliminated from the silver membrane and the difference in the weights of the silver filter before and after elimination of carbon black would enable the estimation of carbon black in the air/dusty environmental sample. The NIOSH method has been suggested to be useful to evaluate carbon black, organic and inorganic additives.

e) ***Monitoring of silica content in air samples***

The concentration of 50 µg/m^3 airborne silica particles is regarded to be a carcinogenic threat for human beings. Commercial silver filters (0.45 µm pore size and 25 mm dia.) from Millipore

Corp., Poretics Corp. etc. have been reported to analyze silica dust using standard NIOSH method (WR25). Also, silver membranes manufactured by SPI silver membranes were also reported to be useful for the evaluation of free silica using SEM and XRD techniques. The reported silica content is typically expressed in terms of mass of SiO_2 phase per volume of air sampled directly onto the silver membrane.

1.3.4 Summary

From the research and application perspective, low cost ceramic membranes are confirmed for bacteria filtration applications. However, for silver-ceramic composite membranes significant data is not available and only a preliminary database is available from available literature resources. Nonetheless, considering the wider scope of silver-ceramic composite membranes in several other applications (such as analysis of carbon black, silica, alcohol beverage filtration), their fabrication using low cost electroless plating technology would be beneficial.

1.4 State-of-the-art

In this section, we present a brief overview of the state-of-the-art in the bacteria filtration membrane technology. Our specific emphasis is towards microfiltration applications which are inexpensive and easy to operate in comparison with the reverse osmosis process which are comparatively expensive than microfiltration due to higher cost of polymeric membranes with very low average pore size.

1.4.1 Polymeric membranes

Yazgan et al. (2014) synthesized biodegradable low cost polymeric membranes with a pore size of 4 – 35 nm. The polymeric membranes refer to poly (amic) acid (PAA), glutaraldehyde-

derivatized PAA (PAA-GA) and chitosan-modified poly (amic) acid (PAA-CS) based membranes that were fabricated using phase-inversion method. Subsequently, the membranes were characterized using NMR, FT-IR, SEM and cyclic voltammetry. Both dead end filtration (circular membranes of 60 mm diameter and 0.30 mm thickness) and tangential flow filtration (rectangular membrane of dimensions120 mm ×18 mm ×0.25 mm) were carried out with the prepared membranes and mixed culture (*Escherichia coli, Citrobacterfreundii and Staphylococcus epidermidis*). All bio-functionalized PAA membranes provided 100% removal efficiency using a mixed feed concentration of 3×10^8 CFU/mL in both dead end and tangential flow filtration.

Using Gram negative *E. coli* (15597) and Gram positive *S. aureus* (ATCC 6538), Zhu et al. (2013) conducted two different experiments namely immersion of membranes in bacterial solution and filtration of bacterial suspension. The time periods for the experiments were 2 and 6 days for Gram negative and Gram positive microbes respectively. Five flat sheet PVDF matrix polymer configured membranes M0-M5 were prepared by blending the PVDF membranes with various concentrations of polymeric additives. The membranes contained both hydrophilic and oleophobic segments. Based on SEM images, no noticeable pores were observed for M0 (PVDF) membrane and an average pore size of 0.075, 0.095, 0.112 and 0.115 μm was evaluated for M1(PVDF+PEG 600), M2(PVDF+AP1), M3 (PVDF+AP1) and M4 (PVDF+AP1) membranes, respectively. A mixed bacterium suspension with a feed concentration of about ~ 10^2 CFU/mL was used to evaluate the resistances of various membranes for bio-fouling in both static and dynamic experimental conditions. The membranes (M1-M4) provided pure water flux, permeate flux, relative flux decay (RFD), relative flux recovery (RFR) and retention values of 2.55 - 176.79 L m^{-2} h^{-1}, 0.57- 98.65 L m^{-2} h^{-1}, 78 - 44%, 51 - 100% and 98 - 95% respectively.

Hilal et al. (2004) modified polyvinilidene fluoride (PVDF) microfiltration polymeric membranes (Millipore) using photo initiated grafting technique. For the grafting purpose, quaternary 2-dimethylaminoethylmethacrylate (qDMAEM) and 2-acrylamido-2-methyl-1-propanesulfonic acid (AMPS) were used. Eventually, the membranes were evaluated for biofouling using *E. coli* bacteria (size 2×0.5 μm) within the feed concentration range of 20 – 100 cells/mL. It was analyzed that the grafted qDMAEM membrane provided few colonies at degrees of modification (DM) of 224 and 714 μg/cm^2 rather than PVDF membrane, which provided 240 colonies of *E. coli*. Further, the initial PVDF membrane that provided 172 colonies performed better with the addition of AMPS to the initial membrane at a DM of 350 μg/cm^2.At this condition, 85 colonies were being counted for the permeate sample.

Furthermore, the membranes modified with qDMAEM as well as polyethileneimine (PEI) did not show *E. coli* colonies in the colony count and also had a strong bactericide effect in comparison with initial PVDF membrane (172 colonies). On the other hand, the combination of qDMAEM and PEI could be a cause for leakage of low molecular weight cytoplasmic components from the bacteria and finally changed the integrity of the cytoplasmic membrane. Also, another explanation was provided that the electrostatic attraction between cationic polymeric chains and negatively charged the lipopopysaccharide surface leads to the death of cells.

1.4.2 Ceramic membranes

Simonis and Basson (2011b) studied microporous ceramic water filters (CWF) for bacteria separation application. Two bacteriological approaches were followed by the authors for the evaluation of bacteria concentration in influent and effluent from the CWF. In the first technique,

spread plate technique was used to count the colony forming units (CFU). 100 mL of pure cultures (*E. coli*, *S. feacalis* and *B. cereus*) of different bacterial strains were inoculated in 1000 mL of sterile distilled water for influent water. 0.1 mL of water sample was pipetted out for 10 fold dilution to spread on different agar plates and then incubated at 37°C for 24 h. In the second technique, membrane filter with 0.45 μm pore size was used to analyze both influent and filtered water for the evaluation of bacteria. Adopting spread plate method and membrane filter technique, the authors evaluated that the membrane provided a $\log_{10}$ reduction value (LRV) of 5.5, 4.2 and 3.6 respectively for *E. coli*, *S. Feacalis* and *B. Cerues* microbes at their feed concentrations of 6, 0.02, 1.1×10^{4} CFU/mL respectively.

Ciston et al. (2008) studied the role of membrane skin layer on the microbe stability on zirconia ceramic UF membranes coated with anatase and mixed phase titanium dioxide photo catalysts. It was analysed that the TiO_2 coatings insignificantly influenced membrane roughness but reduced *Pseudomonas putida* attachment. However, further details with respect to reduction in fouling resistance were not elaborated by the authors.

Srivastava et al. (2004) investigated the potential for carbon nanotubes (CNT) filters in two important environmental applications namely separation of heavy hydrocarbons from petroleum during crude oil post distillation and removal of microbial contaminants from drinking water. Macro scale hollow carbon cylinders are produced with densely packed, radially aligned, micron-length multi-walled CNTs through the continuous spray pyrolysis method. To confirm the bio-adsorption of contaminants, *E. coli* (2-5 μm), *Staphylococcus aureus* (~1 μm), and the poliovirus (~25 nm), from drinking water, unfiltered biological suspension and post-treatment filtrate are incubated in both solid and liquid media and then subjected to plate count procedures.

It was found that the biological growth existed in the unfiltered samples but not in the filtrate. Hence, the CNT biofilters are regarded to be efficient for water treatment on an economical basis. Due to strong mechanical and thermal stability, CNT filters could be cleaned (by ultrasonication and autoclaving) and reused which was not the case with conventional polymeric filtration membranes that could only be disposed off after permanent damage occurred in these membranes due to bio-fouling.

Bielefeldt et al. (2009) studied the separation efficiency of clay based commercial ceramic water filters for the separation of *E. coli*. The authors inferred that the membranes did not provide satisfactory performance during long term permeation tests. For a feed bacterial concentration of 1×10^6 CFU/mL, the permeate stream concentrations were about $10 – 10^3$ CFU/mL. On the other hand, the filters improved their separation efficiency after silver coating was deposited using colloidal silver solutions. Thus, it is apparent that commercial filters did not provide efficient separation capabilities.

Vasanth et al. (2011) prepared a ceramic membrane from the raw materials of kaolin, quartz, calcium carbonate, sodium carbonate, boric acid and sodium metasilicate by using uniaxial dry compaction method at a sintering temperatures ranging between 900 – 1000^{o}C. The membrane was characterized to have an average pore size and porosity of 1.3 µm and 30% respectively. For a bacteria concentration of 6×10^4 CFU/mL at 69 kPa, the maximum observed rejection is found to be 63% at a permeate flux of 3.64×10^{-4} m^3/m^2s. However, at a higher feed concentration of 6×10^5 CFU/mL, the rejection is found to be above 99% for all applied pressures. Further, the observed rejection decreased with an increase in applied pressure and increased with an increase in feed concentration.

1.4.3 Silver membranes

1.4.3.1 Mechanism of silver-pathogen interaction

Elemental silver has not only antimicrobial property but also a release system for silver ions. Materials containing silver species hold the prospect of performing as an excellent antibacterial coating, because these coatings can be prepared on the surface with a wide variety of morphologies and variant silver content. Thereby, they allow the easy control for sustained silver release. However, if metal nano-particles are absorbed onto the surface of a porous ceramic by a weak force such as the Vander Waals attraction, they can easily be washed away by impulse force when water passes through the channels of the porous ceramic structure. Eventually the washed silver nano particles would get dispersed into the surrounding liquid medium. Therefore, the long term performance efficacy of silver composite membranes that constitute silver nano-particles is not clearly addressed at this moment and needs long term experimental investigations for the evaluation of the shelf life of the membranes.

Microorganisms can attach to the surface of porous ceramic and can grow into biofilms. A biofilm (Quang et al., 2011) is generally defined as a structured community of bacterial cells enclosed in a self-producing matrix that adheres to an inert or living surface. The biofilm can exhibit more resistance to antimicrobial treatment than the individual cells grown in suspension. Therefore it is difficult to remove a biofilm with the ordinary methods that are typically used to treat individual cells grown in suspension. To restrict the pathogen, a composite membrane of appropriate pore size is required so as to enable the formation of biofilm on the membrane surface.

Other mechanisms of silver-pathogen interaction have been presented by the manufacturer of Purificup tap/natural water purifier product (WR19). The company hypothesized that the nano-silver composite membrane enables the interaction of positively charged silver particle with the negatively charged bacterial cell wall and will adhere to the cell wall to disrupt the growth mechanism causing bacterial lysis. Further, silver can also cause bacterial protein to denature, thereby affecting the pathogen metabolism and restricting the multiplication of the pathogens by creating a difficult environment to survive. Considering these issues, biofilm would lose its activity and eventually would decay in a shorter period of time.

1.4.3.2 Preparation and characterization of silver-ceramic composite membranes

Research in the field of silver composite membranes can be dovetailed to several areas. Broadly, these include

a) Optimization of fabrication process involving the development of methodologies to relate the fabrication process parameters to the membrane performance variables.

b) Optimization of the membrane performance i.e., to fabricate an efficient silver- composite membrane that has low silver film thickness (and cost), high trans-membrane flux and very good separation efficiency for the elimination of pathogens.

Research studies in the field of silver-composite membranes need to be cautioned with respect to the sensitivity involved in generating data. This is due to the fact that contaminated surfaces can act as a reservoir of pathogenic microorganisms and potentially enhance the risk of infection. Therefore, finer relationships between silver membrane thickness and support porosity need to be more critically studied and examined for the case of silver-composite membranes.

There are very few literatures available with respect to the fabrication engineering details of porous silver-ceramic composite membranes. The available literatures are primarily in the field of silver doped on dense Pd composite membranes.

Koura (WR28) explained the silver electroless plating process and the reaction mechanism of silver in which silver cations were reduced by hydrazine anions. The role of temperature, pH, reducing agents, stabilizers, complexing agents and redox reactions of silver plating were also presented. Various reducing agents refer to glucose, rachelle salt, formaldehyde, organic borane, aldonic acid-lactone and hydrazine during Ag ELP. The obtained silver film has been characterized using X-ray Diffraction method. However, the available literature is in the public domain of silver electroless plating and does not suffice to the exact requirements of fabrication engineering of porous silver-ceramic composite membranes.

Mei and Shi (2005) conducted the modification of inner pore surfaces of reticulated alumina with thin silver film using electroless plating method. The authors also studied the film bonding strength to the substrate, effects of sintering, conduction mechanism of silver film and influence of accelerator (0.15 g/L KBr) on plating performance. Finally, the authors concluded that KBr not only accelerated the reduction of Ag^{+} but also enabled the achievement of uniform silver film with grain size of 3 - 4 μm on the substrate at a sintering temperature of 400^{o}C. The film thickness and kinetics had been studied using SEM and XRD. The simulation results concluded upon an excellent agreement between the silver deposition behavior and developed physical model.

Zhao and Cui (2007) carried out electroless plating of silver on AZ31 magnesium alloy by introducing organic coating (organosilicon heat-resisting varnish) as an inter-diffusion layer

between the substrate and silver film. The plating was carried out in five stages including pre-cleaning, inter-diffusion layer coating, surface roughing, surface sensitization and electroless deposition. The thickness of the silver film obtained was 45 μm. The potentiodynamic polarization curves for corrosion studies of the coated substrate were conducted in a corrosive environment of 3.5 wt% NaCl at a neutral pH. From this experiment, it was analyzed that the corrosion resistance was higher for organic coated membrane but not the substrate.

Huang et al. (2003) investigated the co-deposition behavior of palladium and silver on porous alumina by means of electroless plating technique. They also investigated fabrication parameters of the membranes in electroless plating process for the preparation of dense Pd-Ag composite membrane. For the Pd_{90}-Ag_{10}/α-alumina composite membrane prepared at 333 K, the thickness of the Pd-Ag layer on the α -Al_2O_3 support for plating 8 h was 20 μm. The authors used the Pd_{90}-Ag_{10}/α-alumina composite membrane (20 μm) for hydrogen and nitrogen permeation experiments under 473 - 616 K and 80 - 250 kPa and found that the ideal separation factor of H_2/N_2 through the membrane was in the range 30 - 178. Eventually, the authors deployed a resistance in series model to account for the simultaneous transport of hydrogen through the α-alumina support and skin layer of the dense Pd_{90} - Ag_{10}/ α-alumina composite membrane. Their studies inferred that the transport behavior of hydrogen through the skin layer of the membrane was a combination of solution-diffusion and Knudsen diffusion with minimal contribution from viscous flow.

Keuler et al. (1999a) prepared palladium alloy membranes by successive electroless plating steps on an alumina-zirconia support membrane. The authors deposited palladium-silver and palladium-nickel in layers and eventually carried out heat treatment of the metal films for 5 h in

a hydrogen atmosphere at 650°C. The membrane topographical characterization was conducted for the metal coatings and cross-sections of the films (before and after heating) using scanning electron microscopy (SEM). The crystal phase and alloy existence was confirmed by the XRD. In addition to the surface information, the authors also extracted in-depth information of the alloy coating using micro-PIXE (proton induced X-ray emission). Eventually, the authors constructed concentration profiles across the thickness of the films to determine the penetration of the coating into the support membrane pores during electroless plating and to investigate diffusion of coated layers during the heating step. It was observed that when palladium was deposited first (for both Pd-Ag and Pd-Ni films), the Pd penetrated at least 3 μm into the support. However, when silver was deposited first, it showed very little pore penetration (in the order of 1 μm) and hence poor metal to adhesion to ceramic surface occurred. Variable concentration profiles were obtained (after heating) when silver was deposited on palladium. The silver concentration declined from a high percentage at the outer edge of the film to a low value at the edge of the support. A constant palladium to silver ratio, across the thickness of the film, was obtained when palladium was deposited on silver and subsequent heat treatment of the prepared membrane.

Keuler et al. (1999b) prepared palladium and silver coated membranes using electroless plating and palladium-silver alloy membranes by successive palladium and silver depositions on the same membrane support and heat treated the metal coated membranes for 5 h in a hydrogen atmosphere at 650^{o}C. The authors noticed that the palladium deposit was about 99.75% pure with the main impurities being tin (deposited during the pre-treatment step), 700 ppm silver, 100 ppm mercury and 100 ppm lead and the silver film was about 99.5% pure with tin (0.49%) and 250 ppm iron. They also found that the palladium deposit was column-like, but formed a

continuous dense layer covering the entire substrate surface. The silver deposit on the support was non-homogeneous and clusters were deposited randomly over the palladium film or the activated substrate. No layer of even thickness was visible.

Kikuchi and Uemiya (1991) studied the characterization of composite membranes, consisting of a dense palladium-silver alloy film on the outer surface of an inorganic porous support (alumina), for hydrogen separation. The authors prepared the membranes with consecutive electroless-plating of palladium and silver, and then with heat treatment in a stream of inert gas (argon) at 1173 K for 12 h. The prepared membranes had a complete selectivity for hydrogen separation and exhibited an extremely high rate of hydrogen permeation in comparison with commercial palladium-based membranes. The authors found that the hydrogen permeation was about 30 times faster when 23 wt% silver existed in a dense metal film thickness of 5.7 μm. The higher hydrogen permeability was due to enhanced hydrogen solubility into the metal film as well as its reduced thickness.

Cheng and Yeung (1999) carried out electroless plating kinetic studies with hydrazine based plating baths and palladium/silver precursors. Electroless plating (Pd-Ag) was conducted on 5 cm^2 cleaned and activated vycortube at constant temperature. The sample was removed after 60 min and rinsed in deionized water. The cross section of the membranes was analyzed for film structure and composition. The microstructure of the deposited film was examined using a scanning electron microscope. The thickness of the film was evaluated from the SEM micrographs and was used to evaluate the average plating rate. The gas permeation rates were measured using a bubble flow meter at room temperature and pressure. Their study proved that

Pd-Ag alloy membrane had superior performance in comparison with pure palladium membrane of similar thickness.

Ma et al. (2009) obtained a nano-composite coating of Ni-P/Ag by adding silver nano-particles (1×10^{-7}M) to the Ni-P electroless plating solution operated at 85ºC and pH (4 - 5). Silver nano-particles were obtained by adding $AgNO_3$ (1×10^{-3} M) solution to $NaBH_4$ (4×10^{-3} M) solution containing sodium oleate (2.5×10^{-4} M) with vigorous stirring at ice-cold temperature. The authors noticed that the silver nano-particles changed the properties of the composite coating. In summary, the authors inferred that the Ni-P/Ag composite coating had better hardness and less P content than that of Ni-P alloy coating.

1.4.3.3 Bacteria filtration/Bacteriostatic applications

Padilla et al. (1997) conducted studies on the synthesis, characterization and ultrafiltration of a cylindrical porous silver ceramic membrane. The tubular supports (3 mm) were obtained using slip casting method. The silver membranes possessed an average silver film thickness of 27.5 μm. In their work, cross flow ultra-filtration was conducted to treat the public water. Experimental observations indicated that the specific surface area from the BET method, average pore radius determined from mercury intrusion porosimetry, effective area and intrinsic resistance of the composite membrane were 5 $m^2.g^{-1}$, 4.4 μm, 104 cm^2 and 5.97×10^7 $s^2.cm^{-2}$ respectively. Parameters evaluated for the estimation of water quality include removal turbidity, heterotroph plate count and humics (determined by removing substances that absorbed UV light at 254 nm). These values were observed to be 20 – 0.2 NTU, 100% and around 35% for turbidity removal, heterotroph plate count removal and humics removal respectively.

1.4.4 Frontier technologies

1.4.4.1 Silver impregnated filters

Oyanedel-Craver and Smith (2007) studied on colloidal- silver-impregnated ceramic filters for household water filtration (point-of-use) and tested their bacterial separation efficacy for various flow rates. The filters were also tested without any colloidal-silver application. Hydraulic conductivity and pore-size distribution varied with filter composition and hydraulic conductivities were on the order of 10^{-5} cm/s and more than 50% of the pores for each filter had diameters ranging from 0.02 to 15 μm. The filters removed the *Escherichia coli* (*E. coli*) between 97.8% and 100% for raw water fed to these units. Silver concentrations in effluent filter water were initially greater than 0.1 mg/L, but dropped to insignificant quantity after 200 min of continuous operation.

Mwabi et al. (2012) evaluated various filters such as silver-impregnated porous pot, ceramic candle filter, bio-sand filter-standard, bio-sand filter-zeolite and bucket filter as alternate household drinking water systems. Amongst all filters, the authors concluded that silver-impregnated porous pot is the best in terms of flux (0.05 – 2.49 L/h) and 100% separation efficiency (LRV > 5) for feed concentrations varying from 3×10^{2} – 3.68×10^{6} CFU/mL. For similar feed concentrations, the ceramic candle filter provided a flux and separation efficiency of 1 – 4 L/h and 2 – 4 LRV respectively.

Brown (WR29) loaded 600 L of water with 10^{4}–10^{7} (CFU/mL) of *E. coli* CN13 on three ceramic water purifiers (CWP). These purifiers refer to ceramic water purifier with $AgNO_3$ fabricated by Resource Development International (CWP1), CWP1 modified by adding FeOOH (CWP2) and CWP1 without $AgNO_3$ or other amendments (CWP3). The membranes were tested in Cambodia

and provided 99 – 99.9999% (2 – 6 LRV) disinfection. The primary aim of the study was to evaluate the microbiological effectiveness of locally produced ceramic filters. The ceramic water filters were evaluated for up to 44 months in household usage in three provinces of Cambodia. Over time as batches of water are treated, the silver leached out into the water. This decreases the amount of silver left on the filter which eventually influenced pathogen inactivation.

1.4.4.2 Silver nanoparticle embedded filters

Among chemical agents, silver emerged as an antibacterial property for water treatment applications. However, it is difficult to apply for domestic water treatments due to low ion release and high cost of fabrication. Silver nano-particles are best compared with the silver for water treatment applications. Therefore, nano-particles are expected to play a vital role in the water disinfection and other applications related to disinfection. Silver nano-particles have recently attracted much research interest due to their distinctive properties, large surface area, unique physical, chemical and biological properties. All these are regarded to be highly relevant for hygiene, medical applications, and antibacterial water filters. Among nano-materials such as copper, zinc, titanium, magnesium, gold, alginate and silver, silver nano-particles have proved to be most effective as it has good antibacterial efficacy against bacteria, viruses and other eukaryotic micro-organisms. Silver nano-particles not only possess a strong antibacterial activity but can also inhibit a broad spectrum of bacteria and fungi.

Silver nano-particles can be synthesized by various methods. These include the reduction of silver ions in aqueous solution using stabilizers, reducing silver ions in porous materials, and reducing silver ions on the surface of functionalized materials. Two sequential approaches have

been recommended to integrate silver nano-particles into water filtering materials. In the first approach, silver nano-particles are synthesized in an aqueous solution in the presence of stabilizers. Eventually, silver is absorbed onto the surface of polymer materials, substrates or filter materials that are modified with functional groups. Silver nano-particles are subsequently created by chemical reduction to bond on to the surface.

Lv et al. (2009) used silver nano-particle-decorated porous ceramic composites prepared by overnight exposure to a sliver nano-particle colloid solution of an aminosilane coupling agent, 3-aminopropyltriethoxysilane (APTES). The connection between the nano-particle and the ceramic relies on the coordination bonds between the $–NH_2$ group at the top of the APTES molecule and the silver atoms on the surface of the nano-particles. The other end of the aminosilane coupling agent attaches to silicon atoms in the ceramic through a Si–O–Si bond. On-line tests were conducted with a mimetic water filter. At a flow rate of 0.01 L/min, for an initial bacterial concentration of $\sim 10^5$ CFU/mL, the output count of *E. coli* was zero. Combined with low cost and effectiveness in prohibiting the growth of *E. coli*, such materials might have wide application to drinking water treatment.

Quang et al. (2011) studied on silver nano-particle containing silica micro beads (Ag-NPBs) which were successfully prepared by using inexpensive sodium silicate precursor and chemical reduction method. The presence of silver nano-particles as well as structure of materials was characterized with FTIR, XRD, BET, FE-SEM, TEM, UV–vis spectrophotometer, and optical microscope. Silver nano-particles with an average size of about 5 nm were found in the pore and on the surface of amino functionalized silica beads. Ag-NPBs samples were tested for their antibacterial activity against Escherichia coli (*E. coli*). The antibacterial activity was examined

by both zone inhibition and test tube methods. Biological studies indicated that the synthesized materials have an excellent antibacterial performance against *E. coli* which was completely inhibited after 5 min contact with Ag-NPBs.

1.4.5 Summary

Based on the contents presented in this section, a summary of the discussion is outlined as follows:

a) Alpha-alumina based ceramic membranes are expensive and therefore low cost ceramic membranes need to be fabricated with inexpensive precursors such as kaolin and clay.

b) Low cost silver-ceramic composite membranes can be fabricated only using electroless plating technique due to insignificant investments in fabricating these membranes. While silver could be expensive, the electroless process is inexpensive among available alternate technologies. Therefore, the electroless plating process has the maximum potential to fabricate low cost silver-ceramic composite membranes with research dividends in the process itself.

c) The applicability of silver-ceramic composite membranes for bacteria filtration/bacteriostatic applications might be not competitive on an economic basis. However, other applications do exist for these membranes for which they might be the only case. For instance, the filtration of alcoholic beverages is an important area of research in which the relevance of silver filters is being conveyed. Therefore, irrespective of their applications towards bacteriostatic application, silver-ceramic composite membranes shall be investigated for their fabrication engineering using optimized

electroless plating process. However, at the same time, their applicability towards bacteriostatic applications also needs to be considered on a comparative basis with low cost ceramic membranes. In other words, if a silver composite membrane offers similar performance as that provided by low cost ceramic membrane, then the silver ceramic composite membrane cannot be recommended for bacteria filtration applications. However, silver-ceramic composite membrane fabrication engineering needs to be addressed due to available limitations in the literature.

In other words, research is highly active in the field of silver filters and silver composite filters for drinking water treatment and bacteriostatic applications. However, electroless plating technique has been extensively used to deposit silver on palladium composite membranes but not for silver composite membranes. There is a need to understand and optimize the fabrication of silver ceramic composite membranes that infer upon the minimization of silver metal used on the ceramic matrix. Needless to convey, the ceramic membranes also have separation efficiencies towards bacterial and microbial suspensions. Therefore, a systematic investigation appears to be the need of the hour.

1.5 Possible scope for further research

Based on the extensive literature survey that has been conducted in various fields associated to the preparation, characterization and applications of low cost ceramic and low cost silver-ceramic composite membranes, the following areas of research have been highlighted:

a) Preparation and characterization of low cost ceramic membranes for bacteria filtration applications.

b) Dead end microfiltration of prepared low cost ceramic membranes

c) Cross flow microfiltration of bacterial solutions using low cost ceramic membranes

d) Preparation and Characterization of low cost silver-ceramic composite membranes

e) Comparative assessment of dead end MF of low cost silver-ceramic and ceramic membranes.

Further insights into various gaps in existing research trends in the above areas of research are presented in the following sub-sections.

1.5.1 Preparation and characterization of low cost ceramic membranes for bacteria filtration applications

With their enhanced mechanical, thermal and chemical stability, ceramic materials are promising for challenging water purification processes such as industrial wastewater, oil/water separations and hazardous waste treatment. The flux through ceramic membranes is more easily recovered after fouling as ceramics can withstand harsh chemical and thermal treatment and cleaning procedures. Hence, ceramic membranes possess extended shelf life even when subjected to extreme fouling and cleaning process operations. On the other hand, ceramic membranes are highly expensive for large-scale membrane applications, such as municipal drinking water production and wastewater treatment. Therefore, their application has been historically limited to relatively small-scale industrial separations, where polymeric membrane technology could also be applied. On the other hand, being compact technologies, the insitu utilization of membrane technology for the generation of household potable water is potentially advantageous and it is

this application of membrane technology for small scale generation of potable water that makes them attractive in comparison with large scale industrial processing schemes.

Also, the cost of ceramic membranes is often very high, as they are prepared typically using α-alumina. On the other hand, low cost porous ceramic supports are typically prepared using kaolin, quartz, calcium carbonate, sodium carbonate, boric acid and sodium metasilicate. Compared to standard alpha-alumina ceramic membranes, low cost ceramic membranes provide similar flux and separation characteristics at a lower cost and are therefore attractive for faster research commercialization. Therefore, research towards low cost ceramic membranes is on the rise. Hence, along with the utilization of ceramic supports such as α-alumina, there is a need to also develop membranes using low cost ceramic precursors that can withstand desired pressure differentials and that possess the desired corrosion resistance so to eventually offer similar shelf life provided by the α -alumina membranes. Polymeric and ceramic membranes have variant characteristics for bacteria separation. This is primarily due to their pore size distributions. While ceramic membranes have wider pore size distributions, polymeric membranes have narrow pore size distributions. Hence, their separation and fouling characteristics are also distinct.

Till date, only few researchers have investigated upon the performance of ceramic membrane technology for the separation of microbes. A critical analysis of the available literature provides several insights. Firstly, the literature is highly focused towards drinking water treatment applications but not bacteria filtration applications, which are also important from the perspective of industrial biotechnology. Commercial bacteriostatic applications include pasteurization followed with centrifugation, which involve a heat treatment step. Heat treatment steps could damage heat sensitive compounds that are of immense value in bioprocess streams.

Therefore, low cost ceramic membrane technology might be promising in such scenarios. Secondly, only Vasanth et al. (2011) studied upon the efficacy of low cost ceramic membranes for bacteria filtration applications, who did not present a detailed investigation with respect to bacteria removal from water. The research work of Vasanth et al. (2011) has proven that low cost ceramic membranes with a pore sizes in the range of 1.42 – 2.72 μm are also efficient for drinking water treatment and bacteriostatic applications. Therefore, it will be interesting to observe how membranes with different morphologies would be effective to separate microbes from synthetic solutions.

An important issue for the developed low cost ceramic membranes is to achieve 100% separation efficiency, which is very much dependent on both pore size distributions, morphologies and feed concentrations of the separated microbes. Thus, it is apparent that significant amount of research activity needs to be dovetailed towards the development and application of low cost ceramic membranes for bacteria filtration applications. In this regard, a systematic investigation that accounts for the optimality of membrane morphological characteristics to suite the desired application is very important. While literature does provide few data sets for low cost ceramic membranes, systematic insights with respect to the performance characteristics are not available. For instance, the literature does not elaborate upon the dependence of membrane fouling on membrane morphology. This is an important issue in the context of the shelf life of the low cost ceramic membranes. Thus, research emphasis shall be towards minimizing the insitu fouling performance and maximizing the shelf life of low cost ceramic membranes. Such efforts will further enhance the adaptability of low cost ceramic membranes for drinking water treatment and bacteria filtration applications.

1.5.2 Dead end Microfiltration of synthetic microbial solutions using low cost ceramic membranes

In the field of the low cost ceramic membrane based dead end MF of synthetic microbial suspensions, there is only one literature Vasanth et al. (2011) that elaborated upon the fouling and separation characteristics of low cost ceramic membranes. However, ongoing research in the application of low cost ceramic membranes needs to emphasize upon the following issues. Firstly, the appropriate optimal combinations of pore size and feed concentration are required. Diverse membrane morphologies need to be investigated in the context of low to high pore size. Secondly, fouling indices need to be evaluated for various combinations of membranes and feed concentrations. Thirdly, the fitness of various standard fouling models to represent obtained flux decline data is required to assess upon the extent of reversible and irreversible fouling mechanisms.

1.5.3 Cross flow Microfiltration of synthetic microbial solutions using low cost ceramic membranes

In the field of low cost ceramic membranes and their applications, there is no data in the literature with respect to the cross flow microfiltration of synthetic microbial solutions. Such data is of paramount relevance to judge upon the insitu performance of the low cost ceramic membranes for drinking water treatment and bacteria filtration applications. While dead end MF data is useful to judge upon the performance of the membrane under severe conditions of operation, the cross flow MF provides data with respect to the proximity of the membrane for real time applications. Hence, cross flow MF of microbial suspensions using low cost ceramic membranes is an important area of research and needs to be addressed once dead MF data is

available for the developed low cost ceramic membranes. Areas of specific interest in this field include (a) optimality of feed and membrane morphological combinations (b) extent of irreversible and reversible fouling and (c) contributions of biofilm and internal fouling resistance towards the total fouling resistance of the membrane.

1.5.4 Identification of optimal process and membrane parameters for the electroless fabrication of silver-ceramic composite membranes

A critical analysis of the available literature can be summarized as follows in the field of porous silver-ceramic composite membranes.

a) There is no literature data with respect to the combinatorial plating characteristics of electroless silver composite membrane fabrication. Few literatures refer to the silver deposition using electroless plating for dense Pd-Ag composite membranes whose application has been suggested for hydrogen energy. Few other literatures refer to the electroless plating of silver in the general domain of silver plating and do not refer to the silver composite membrane fabrication. As far as literatures available for silver filters, they confine to the product related information but not engineering aspects associated to the product development of silver filters. Thus, there is a need to evaluate upon the competence of the engineering aspects of silver composite membranes/filters.

b) In the field of electroless plating for porous metal-ceramic composite membrane fabrication, research has been confined to (i) fabrication of porous nickel-ceramic composite membranes using electroless plating and (ii) competence of rate enhance electroless plating for metal-ceramic composite membrane fabrication.

c) A further study into the field of rate enhanced electroless plating is indicative towards the fact that while stirring, sonication, surfactant, surfactant-sonication, vacuum and hydrothermal rate enhancement supplements are available, only sonication (SOEP), surfactant (SIEP) and sonication-surfactant (SSOEP) combined modes of electroless plating are the most competent rate enhancements in the context of scalability perspective.

d) Available literatures for SOEP, SIEP and SSOEP processes are confined to the fabrication of nickel-ceramic composite membranes, palladium-ceramic composite membranes and palladium-stainless steel composite membranes. No literature data is available for the efficacy of the SOEP, SIEP and SSOEP processes to fabricate silver-ceramic composite membranes.

e) The contacting pattern of the reducing agent has been evaluated to be an important aspect to significantly influence the combinatorial electroless plating characteristics of nickel-ceramic composite and palladium-stainless steel composite membranes. However, the same needs to be assessed for the fabrication of porous silver-ceramic composite membranes.

f) Irrespective of the ability of silver composite filters for bacteriostatic applications, silver-ceramic composite membranes need to be evaluation for fabrication engineering aspects due to several other applications such as filtration of alcoholic beverages, analysis of carbon black and silica in air quality evaluation. Considering these aspects, advances in engineering of silver filters need to be considered from a research perspective.

Considering these aspects, research in the field of silver-ceramic composite membranes is required in the following areas:

i) Efficacy of conventional (CEP), sonication (SOEP), surfactant (SIEP) and surfactant-sonication (SSOEP) assisted silver electroless plating for the fabrication of silver-ceramic composite membranes.

ii) Efficacy of reducing agent contacting mode (bulk addition vs. drop wise addition) based on the evaluation of combinatorial plating characteristics of silver ceramic composite membranes.

It will be further interesting to examine the optimality of electroless plating process parameters in conjunction with those reported in the literature. Given the fact that the literature data corresponds to the optimality of rate enhanced electroless process parameters for dense nickel ceramic and palladium ceramic composite membrane fabrication, it will be very interesting to evaluate, compare and contrast these parameters with the optimal rate enhanced electroless process parameters for porous silver-ceramic composite membranes. Thereby, useful insights could be gained in the field of electroless silver-ceramic composite membrane fabrication.

1.5.5 Microfiltration performance of silver ceramic composite membranes

With respect to the efficacy of silver-ceramic composite membrane filters for bacteriostatic applications, it is not clear whether silver film on its own has the potential to totally eliminate or mitigate the microbial contamination of the membranes. Thus, data is available with respect to the efficacy of silver composite filters which does not explicitly convey the competence of the support or substrate. In this regard, it is very important to note that if the support itself is highly

competitive towards bacteria filtration, there will be no need to suggest silver-ceramic composite membranes as the silver filters are highly expensive in comparison with ceramic filters.

Thus, research needs to examine at least dead end MF of bacterial suspensions using silver-ceramic composite membranes and their competence with respect to the low cost silver-ceramic membranes. Thereby, it will be affirmed whether silver-ceramic filters are required for drinking water treatment/bacteriostatic applications or not.

1.6 Objectives of the Thesis

1.6.1 Preparation and Characterization of low cost ceramic membranes

The first objective of this work is to prepare low cost ceramic membranes with uniaxial dry compaction method. Membranes with diverse morphological characteristics with low to high average pore size (0.7 – 4.5 μm) are being targeted. The high pore size membrane is targeted to be relevant for application in gravity based water permeation. Thereby, characterization is targeted using SEM, XRD, corrosion resistance, hydraulic permeability and porosity.

1.6.2 Dead end Microfiltration Performance of low cost ceramic membranes and flux decline modeling analysis

The second objective of this work is to evaluate the dead end microfiltration performance of fabricated low cost ceramic membranes. The MF experimental investigations refer to feed preparation and their microbial count followed with permeate flux measurement and permeate microbial count. Experimental procedures need to eliminate the permeate sample contamination by targeting a leak proof dead end MF operation. Plate count method will be adopted to estimate the concentration of microbes in the feed and permeate samples.

The obtained flux decline data for various membranes needs to be targeted from both conceptual and standard flux decline modeling perspectives. Average fouling indices needs to be evaluated for the obtained data so as to evaluate upon the optimality of feed concentration for various membranes. Flux decline modeling needs to be conducted for the evaluation of insitu membrane fouling during the MF operation and extent of irreversible fouling. Thereby, dead end MF tests aim to identify the most competent combinations of feed concentrations and membrane morphologies.

1.6.3 Cross flow microfiltration of microbial solutions using low cost ceramic membranes

The third primary objective of the thesis is to conduct cross flow MF of microbial suspensions. This will enable to identify maximum steady state water flux values for various cases of membrane morphology and feed concentrations. Subsequent flux decline modeling analysis will identify potential fouling mechanisms and avoid conditions that tend to maximize irreversible membrane fouling during the MF operation. In the end, optimal operating condition of feed concentration and membrane morphology can be obtained for the cross flow MF operation of synthetic microbial solutions.

1.6.4 Optimal rate enhanced electroless plating processes and reducing agent contacting pattern for porous silver-ceramic composite membrane fabrication

The previous steps of membrane preparation and characterization, dead end and cross flow MF are indicative towards the optimal membrane morphology. With the identified optimal membrane, silver composite membrane will be fabricated to achieve the following objectives:

- Evaluation of plating and membrane characteristics for wide variety of plating process parameters and selected rate enhanced electroless processes (CEP, SIEP, SOEP and SSOEP). The plating process parameters refer to silver ion concentration in the solution, loading ratio, plating temperature and total time of plating. The plating characteristics refer to metal conversion and metal plating efficiency. The membrane characteristics refer to metal loading index or thickness and pore densification.
- Identification of optimal rate enhanced electroless plating process and its process parameters at which optimal combinations of plating and membrane characteristics could be achieved.
- Conduct a comparative cost analysis of the membrane fabrication for both low cost ceramic and low cost silver-ceramic composite membranes.

1.6.5 Dead end Microfiltration studies of low cost silver-ceramic composite membranes

The final objective of the thesis is to evaluate the microfiltration performance of low cost silver composite membranes and evaluate them in comparison with the low cost ceramic membranes. For this purpose, firstly, the obtained silver membranes are subjected to compaction studies using Millipore/water purifier and then to hot air sterilization. Eventually, microfiltration studies using synthetic microbial solutions are targeted to evaluate the microfiltration performance of silver composite membranes. Thereby, the separation efficiency of the low cost silver composite membranes is compared with the corresponding low cost ceramic membranes so as to deduce valuable conclusions and insights related to the potential of the silver film and ceramic membranes.

1.7 Organization of the Thesis

From the detailed discussion presented in section 1.5, it is apparent that there is significant scope for further research in the field of membrane technology towards bacteria filtration/bacteriostatic applications. From the objectives of the thesis presented in the earlier section, the following paragraphs briefly summarize the contents of the thesis in the context of the preparation, characterization and application of ceramic and silver ceramic composite membranes.

The thesis has been classified in six additional chapters. **Chapter 2** addresses the experimental work and modeling involved throughout the thesis. It includes a) preparation and characterization procedures of ceramic and silver-ceramic membranes from their precursors b) preparation of bacterial solution using *DH5*α strain c) dead end microfiltration test procedures with batch loading of feed solution d) cross flow microfiltration test procedures with continuous loading of feed and e) time dependent silver electroless plating on ceramic membranes with variant metal, reducing agent and surfactant concentrations. In summary, low cost ceramic membranes CM1-CM3 have been fabricated in the thesis using which further experiments were conducted for silver-ceramic membrane preparation and characterization.

The ceramic and silver-ceramic membrane characterizations have been conducted using TGA, XRD, BET and FESEM. A huge number of trial and error methods have been carried out for the dead end and cross flow MF studies. Subsequently, dead end flux decline data was modeled using pore blocking methods and Trapezoidal rule for the fouling indices. Thereafter, these two models have been used for best fit model and fouling index respectively. Also, cross flow flux decline data was modeled using the resistances in series model to evaluate the contribution of biofilm fouling resistance towards the overall hydraulic resistance of the membrane. Lastly,

electroless silver plating has been studied on ceramic membrane for the desired efficiency and minimum metal film thickness. Eventually, combinatorial plating characteristics for various combinations of metal, reducing agent and surfactant concentrations have also been evaluated prior to dead end MF experiments with low cost silver-ceramic composite membranes. Further details on all these are presented in the relevant sections of Chapter 2 in the Ph.D. thesis.

Chapter 3 summarizes the time dependent dead end MF flux data obtained for various ceramic membranes. The discussion is dovetailed with respect to various relevant membrane performance characteristics such as flux ($m^3/m^2.s$), and removal efficiency (LRV), for various combinations of feed concentrations and membranes (CM1-CM3). Eventually, average fouling index and competence of standard fouling models to represent obtained flux decline data has been addressed. Thereby, the optimality of membranes CM1-CM3 at various feed concentrations is being evaluated. The optimality refers to combinations of lower average fouling index value and higher separation efficiency. Also, the chapter presents a retail cost based analysis of the prepared low cost ceramic membranes. The retail cost data is anticipated to serve as a benchmark for the fabrication of low cost ceramic membranes.

For membranes CM1- CM3, **Chapter 4** summarizes the results and analysis of the data obtained during cross flow MF of synthetic microbial solutions. The membrane performance has been quantified in terms of flux and removal efficiency at various feed concentrations. Flux decline modeling was carried out using resistances in series model. Thereby, optimal combinations of membrane and feed concentrations have been identified for the cross flow MF performance of the low cost ceramic membranes.

Chapter 5 addresses the preparation and characterization of silver-ceramic composites using electroless plating processes. Various alternate processes such as CEP, SIEP, SOEP and SSOEP have been investigated using bulk addition mode of the reducing agent and surfactant (if any). Subsequently, details with respect to evaluated process and membrane characteristics have been presented. The primary aspect of the experimental investigations is to identify the rate enhanced process that provides high plating efficiency and minimum metal film thickness at lower plating time. Based on this criteria, the optimal rate enhanced electroless plating process has been identified along with its process parameters.

Chapter 6 elaborates upon the results obtained for 3 h of SOEP based electroless plating baths with drop wise reducing agent addition. The effects of various process parameters such as metal and reducing agent concentration have been evaluated in the context of combinatorial plating characteristics. Primarily, plating efficiency and metal film thickness have been targeted for their optimality. Thereby, the optimal combination of process parameters has been identified for SOEP process and drop wise reducing agent addition. Also, the retail cost analysis of the fabricated low cost silver-ceramic membrane is being presented in the chapter. The retail cost analysis is anticipated to be useful for the comparative assessment of the costs of low cost silver-ceramic membranes.

Chapter 7 presents the data obtained for dead end MF of low cost silver-ceramic composite membranes using synthetic microbial suspension. Only separation efficiency has been targeted in the chapter for two different feed concentrations and two types of silver-ceramic composite membranes. Thereby, the separation efficiency of silver composite filters has been compared with that of the ceramic membranes.

Chapter 8 summarizes the conclusions obtained from the research output in this work. Eventually, based on the insights of the obtained data and research methodologies, the chapter also presents a brief overview of the future research work that can targeted in the field of preparation, characterization and applications of low cost silver-ceramic membranes.

Chapter 2:

Experimental and Modeling Procedures

Experimental and Modeling Procedures

Section 2.1 addresses the preparation and characterization of low cost ceramic membranes CM1 – CM3, that were fabricated with variant pore sizes by altering the compositions of the low cost ceramic precursors. Along with modeling approaches, section 2.2 addresses dead end microfiltration of low cost ceramic membranes CM1 – CM3 for the separation of bacteria from synthetic microbial solutions. Section 2.3 summarizes cross flow microfiltration of synthetic microbial solutions with the low cost ceramic membranes. Section 2.4 addresses the preparation and characterization of low cost silver-ceramic membranes.

2.1 Low cost ceramic membranes

2.1.1 Fabrication of ceramic membranes

Three ceramic membranes CM1, CM2 and CM3 with distinct membrane morphologies were fabricated using low cost inorganic precursors such as kaolin (CDH, India), quartz (Research Lab Fine Chem Industry, India), calcium carbonate (Merck, India), sodium carbonate (Merck, India), boric acid (Merck, India) and sodium metasilicate (CDH, India). The variations in the membrane morphologies were achieved by targeting the variation in the inorganic precursor composition and their particle size distributions in the dry powder mixture. Table 2.1 summarizes the compositions of the inorganic precursors to fabricate CM1 - CM3 membranes. For CM1 and CM2 membranes, polyvinyl alcohol (PVA, Loba Chemicals Ltd., India) was also used with a solution composition of 2 and 4 wt% respectively.

Table 2.1: Inorganic precursor compositions for the fabrication of low cost ceramic membranes.

Material	CM1 (wt %)	CM2 (wt %)	CM3 (wt %)
Kaolin	40	40	40
Quartz	15	15	15
Calcium carbonate	25	25	20
Sodium carbonate	10	10	10
Boric acid	5	5	5
Sodium metasilicate	5	5	10

From a novelty perspective, compositions for CM1 and CM2 were taken from Vasanth et al. (2011), which did not refer to the utilization of PVA. More precisely composition of CM1 and CM2 is similar to that reported by Emani et al. (2014), who did not investigate the membrane performance for bacteria separation applications. Membrane CM3 was developed with wide pore size and its composition is obtained based on trial and error approaches. In other words, composition of CM3 membrane is contributed in this work and compositions for CM1 – CM2 membranes were taken from Emani et al. (2014). Similar is the case of characterization studies and hence characterization of CM1 – CM2 membranes was not addressed in the Ph.D. thesis due to the availability of results elsewhere (Emani et. al. (2014)). The inorganic precursors with distinct functional attributes and compositions enabled the achievement of membranes within the pore size range of 0.5 – 5 μm. For CM1 and CM2 membranes, the powder mixture recipe (Table 2.1) was dry sieved with 36 (425 μm) and 72 (212 μm) mesh screen respectively. The sieving step was not deployed to prepare the CM3 membrane. Thus, it is apparent that the sieving procedure is crucial to affect the particle size distributions of the precursors, which in turn contributed to desired membrane morphologies for CM1 and CM2 membranes

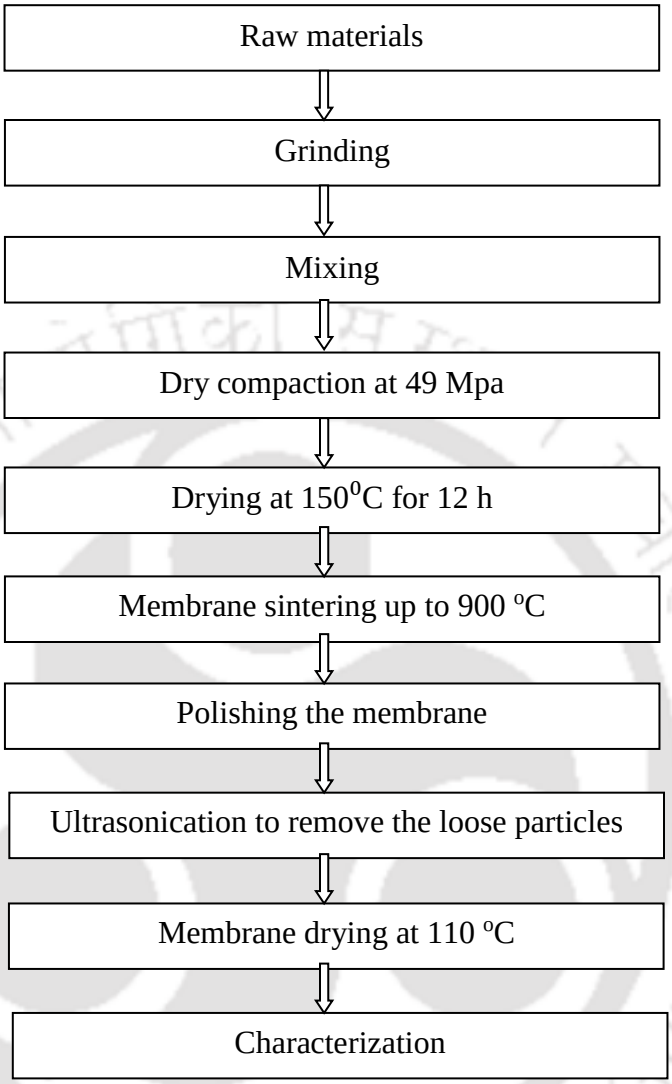

Figure 2.1: Low cost ceramic membrane fabrication procedure.

The experimental procedure was similar to that presented by Vasanth et al. (2011). The membrane fabrication procedure adopted uniaxial dry compaction method after thorough mixing of the raw materials using a ball mill. After this step, 20 g of the resulting powder was compacted using a stain less steel mould and a hydraulic press (Make: Velan Engineering, Tamil Nadu, India) at a fabrication of 49 MPa to fabricate circular disc shaped supports of 55 mm diameter and 5 mm thickness. Following this, several heat treatment steps were followed. These include

drying at 150^{o}C for 12 h followed with heating at a rate of 2^{o}C/min up to 900^{o}C and sintering at 900^{o}C for 4h. Also, it is important to note that the membranes were dried at 150^{o}C but not at 100^{o}C. This is due to the reason that even though the green membrane has low moisture content (due to dry compaction method), additional thermal stresses are not desired.

Finally, the membranes were cooled to ambient temperature by natural cooling process. This was achieved by switching off the power supply to the muffle furnace. For all membranes, subsequent steps such as polishing and sonication assisted surface cleaning were similar to those reported by Vasanth et al. (2011). The overall membrane fabrication procedure is illustrated in Figure 2.1.

The raw materials used for the fabrication of low inorganic membranes contribute towards diverse functional attributes. Kaolin provides low plasticity and high refractory properties. Quartz contributes towards the mechanical and thermal stability of the membrane. The regulation of porous texture is due to calcium carbonate ($CaCO_3$) and sodium carbonate (Na_2CO_3). These two materials under sintering condition would dissociate into calcium oxide (CaO) and sodium oxide (Na_2O), respectively and release CO_2 gas. The path taken by the released carbon dioxide (CO_2) gas thereby contributes to the porous texture and porosity of the membrane during sintering process. On the other hand, sodium carbonate and boric acid act as a colloidal agent and improved dispersion properties of the inorganic precursors. Due to these features, the homogeneity in the membrane structure is being taken care. Boric acid also enhances the membrane mechanical strength with the formation of metallic metaborates at the sintering temperature. In a similar way, sodium metasilicate acts as a binder by creating silicate bonds with other precursors to induce higher mechanical strength in the ceramic membrane. Also, the

suggested precursor formulations provided crack free membranes with good structural consistency to achieve integrity and desired average pore size of the membrane.

2.1.2 Surface characterization

The structural characterization of membrane involved thermogravimetric analysis (TGA), X-ray diffraction analysis (XRD), morphological study using field emission scanning electron microscope (FESEM), total porosity determination and evaluation of pore size distributions from FESEM images.

2.1.2.1 Thermogravimetric analysis (TGA)

Membrane characterization was carried out using thermogravimetric analyzer (TGA, Make: NETZ5CH, Model No. STA 449 F3, Jupiter, Switzerland). The TGA working principle involved increasing temperature of the sample at a constant heating rate for inducing physical and chemical transformation of the sample. TGA was conducted for the raw material also. From the TGA, weight loss and thermal transformation curves were obtained. Using these curves, the minimum sintering temperature required for membrane fabrication can be evaluated. Thereby, appropriate justification can be sought for selected sintering temperature to fabricate the membranes.

2.1.2.2 XRD analysis

X-ray diffraction (XRD, Make: BRUKER, Model No. D8 Advance, Germany) was carried out to evaluate the extent of various phase transformations and membrane crystallinity during sintering.

2.1.2.3 Brunauer–Emmett–Teller (BET) analysis

The BET analysis refers to the physical adsorption of gas molecules on a solid surface. Thereby, the analysis enables the evaluation of the specific surface area of a material. Based on the gas adsorption BET method, using the BET instrument (Make: COULTER, SA3100), liquid N_2 was used to determine the specific surface of the inorganic membranes.

2.1.2.4 Surface morphology

Membrane morphological studies were carried out using field emission scanning electron microscopy (FESEM, Make: ZEISS, Model No. ∑IGMA, USA). FESEM enabled to analyze the presence of possible defects by careful observation of the micrographs.

2.1.2.5 Porosity and Chemical Stability

The total porosity of the membrane was estimated using Archimedes principle with water as the wetting agent. For this purpose, the membranes were first dried in a hot air oven at 110^{o}C for 6 h to remove the moisture. After this step, the dry weight of the membrane (w_1) was measured. Eventually, the membrane was kept in water for 24 h at room temperature. After this step, the wet weight (w_2) of the membrane was measured after wiping the surfaces of the membrane with tissue paper. The overall porosity of the membrane (including dead and permeable pores) was determined using the following relation.

$$\varepsilon = \frac{(w_2 - w_1)/\rho_w}{\pi \times \left(d/2\right)^2 \times \delta} \qquad (2.1)$$

w_1 Dry weight of the membrane, g

w_2 Wet weight of the membrane, g

ρ_w	Density of water, g/cm^3
d	Diameter of the membrane, cm
δ	Membrane Thickness, cm

The chemical stability of the membrane was evaluated by soaking the membrane into acid and alkali solution individually using HCl (pH 1) and NaOH (pH 14) for one week at atmospheric condition. The stability was determined in terms of weight loss after exposure to the chemical environment.

2.1.2.6 Characterization of physico-chemical parameters

For few samples, the physicochemical parameters were also tested for feed and permeate using the water analysis kit (Make: VSI Electronics, Model: VSI - 06D1, India). The purpose of this analysis is to ensure the quality of the permeate samples, in relation with the feed samples. The physical parameters such as pH and conductivity were determined using water analysis kit.

2.2 Dead end Microfiltration

2.2.1 Experimental setup

A schematic of experimental set up used for water or synthetic solution dead end MF experiment is presented in Figure 2.2. The set up constitutes a stainless steel (SS316) cylindrical unit (320 mL capacity) with rubber sheets placed at the top and bottom portion of the membrane (55 mm diameter). In addition, the top surface the membrane was covered with another rubber disc (43mm diameter) to avoid leakages at the circumference of the membrane. Eventually, the total set up under gas-tight condition with seals was subjected to hydraulic test and dead end MF tests. For either case, the membranes were compacted at 40 psi to ensure the structural compaction of the membrane structure with applied pressure.

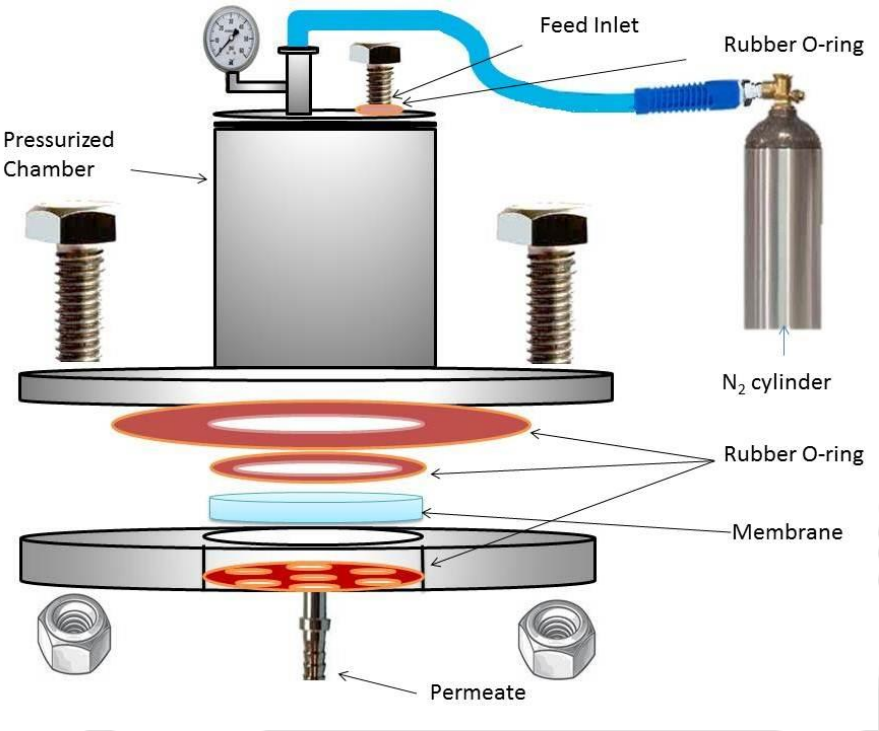

Figure 2.2: Schematic of hydraulic permeability and dead end microfiltration setup.

2.2.2 Hydraulic permeability experiments

During liquid permeation experiments, the feed (de-ionized water) was filled in the tubular section of the setup using the feed in let (as shown in Figure 2.2) and the chamber was pressurized by high purity nitrogen gas (99.99%). The permeate from the membrane was collected in a beaker (500 mL), which was placed over the digital scale weight balance. The experiment was carried out at various trans-membrane pressure differentials. At these conditions, the weight of the water collected was noted using a digital scale weighing balance.

2.2.3 Dead end MF of bacterial suspensions

DH5α strain is a typical organism and *coliform* to indicate upon the potential contamination of a water source. The *E. coli* organism is a very common rod-shaped (2×1 μm) bacterium of well-

defined dimensions. In this work, *DH5α strain* has been used to evaluate the bacteria filtration performance of the MF membranes. This is also due to the reason that the testing of *coliform* bacteria is faster and cheaper than the testing for specific organisms and pathogens.

E. coli (DH5α strain*)* was obtained from the Department of Biotechnology, IIT Guwahati, India, and was maintained on nutrient agar plates and incubated at 37°C for 24 h. One full loop of the bacterial culture was inoculated into 50 mL sterile nutrient broth and was incubated again overnight at 37°C in an orbital shaking incubator (Make: DaihanLabTech India Pvt. Ltd., Model: LSI-3016R) at a speed of 200 rpm. The volume specification of the culture was based on the desired feed concentration in MF run. In this regard, it is further important to note that it is extremely difficult to precisely control the feed concentration due to variations in the culture activity. Nonetheless, the procedures adopted for dilution are based on the expertise obtained with trial and error based approaches.

To conduct the dead end MF of the synthetic microbial suspensions, a specified volume of the overnight culture was diluted wit 10 L of sterile physiological water (0.9% w/v NaCl). For this purpose, the spread plate method was deployed to evaluate the resulting colonies in both feed and permeate samples. The end point of the analysis is the number of colony forming units per mL (CFU/mL) rather than the total no. of bacteria (WR30).The main assumption in the analysis is that each viable cell in the suspension will form an individual colony. In some early trials, such colonies could not be obtained for even feed samples. This was due to poor sampling and analysis procedures. The dead end MF experiments were terminated when either 10 L solution was exhausted or when the membranes underwent substantial fouling and the permeate flux reduced considerably.

2.2.4 Modeling Approaches

2.2.4.1 Pure water permeation

Based on permeation data obtained at various pressure differentials, the hydraulic permeability (L_h) has been evaluated using the expression (Almandoz et al., 2004; Marchese and Pagliero, 1991)

$$J = \frac{n\pi r^4 \Delta P}{8\mu l} = L_h \Delta P \qquad (2.2)$$

where J (m/s) is the flow density (flux) of permeated water, n is the pore density (number of pores per m^2), μ is the water viscosity, l is the pore length (m), ΔP (Pa) is the trans-membrane pressure. Using the above expression, L_h can be obtained as the slope of 'J' versus 'ΔP' plot. Using the porosity values obtained from Archimedes principle and assuming $\varepsilon = n\pi r^2$ the average pore radius has been evaluated using the expression:

$$r = \left[\frac{8\mu l}{\varepsilon} L_h \right]^{1/2} \qquad (2.3)$$

2.2.4.2 Flux and Rejection

The room temperature (25°C) dead end MF of bacterial suspensions was conducted with the synthetic microbial solutions that were prepared using the principle of dilution. The experimental procedure for dead end MF was similar to that presented in the previous sub-section 2.2.3. However, few variations existed. Firstly, the dead end MF setup could hold only 320 mL and due to high permeability's of the fabricated membranes, sample loading had to be taken up after the filled up solution in the setup was exhausted during the batch run. Permeate samples were collected periodically for permeate analysis of bacterial concentration.

The permeate flux (J, $m^3/m^2.s$) and the percent reduction value (PRV) were evaluated using the following expressions

$$J = \frac{V}{A \times \Delta t} \tag{2.4}$$

$$PRV = \left(1 - \frac{C_p}{C_f}\right) \times 100 \tag{2.5}$$

where A (m^2) is the effective membrane area, V (m^3) is the volume of permeate, Δt (s) is the sampling time, C_f (CFU/mL) and C_p (CFU/mL) are the concentration of bacterial colonies (expressed in terms of colony count) in the feed and permeate respectively.

Another alternative index for the evaluation of the separation efficiency has been proposed by Simonis and Basson (2011). The index is termed as the Log_{10} Reduction Value (LRV) and is not applicable for cases with 100% separation/rejection efficiency. The LRV could be evaluated using the following equation:

$$LRV = \log_{10}(C_f) - \log_{10}(C_p) \tag{2.6}$$

The co-relation between LRV and PRV values has also been presented by Simonis and Basson (2011). This is presented in the following Table 2.2:

Table 2.2: Relationship between LRV and PRV

LRV	PRV (%)
1	90
2	99
3	99.9
4	99.99
5	99.999
6	99.9999

Thus it is apparent from the above Table 2.2 that the numerical value of LRV refers to the number of nines in the PRV value.

2.2.4.3 Fouling Index

Fouling indices are often ignored in MF studies. The extent of membrane fouling is an important parameter for the competence/inefficiency of a chosen process condition (feed concentration and pressure differential) and membrane morphology (pore size distribution and average pore size). To delineate upon the conceptual relations between fouling and membrane/process parameters, various fouling indices have been evaluated based on the time dependency flux data.

For an MF run, the time dependent fouling index (*F (t)*), total fouling index (*FI*) and average fouling index (*AFI*) of a combination of membrane and process condition have been estimated using Trapezoidal rule. The following expressions summarize the mathematical transformations (Agarwal et al., 2013):

$$F(t) = \left(1 - \frac{J}{J_0}\right) \times 100 \tag{2.7}$$

$$FI = \int_0^{t_{max}} F(t)dt \tag{2.8}$$

where t_{max} is the maximum time duration at which the MF run is terminated

$$AFI = \frac{FI}{t_{max}} \tag{2.9}$$

Thus operating conditions with lowest combinations of F (t), FI and AFI refer to optimal process and membrane parameters.

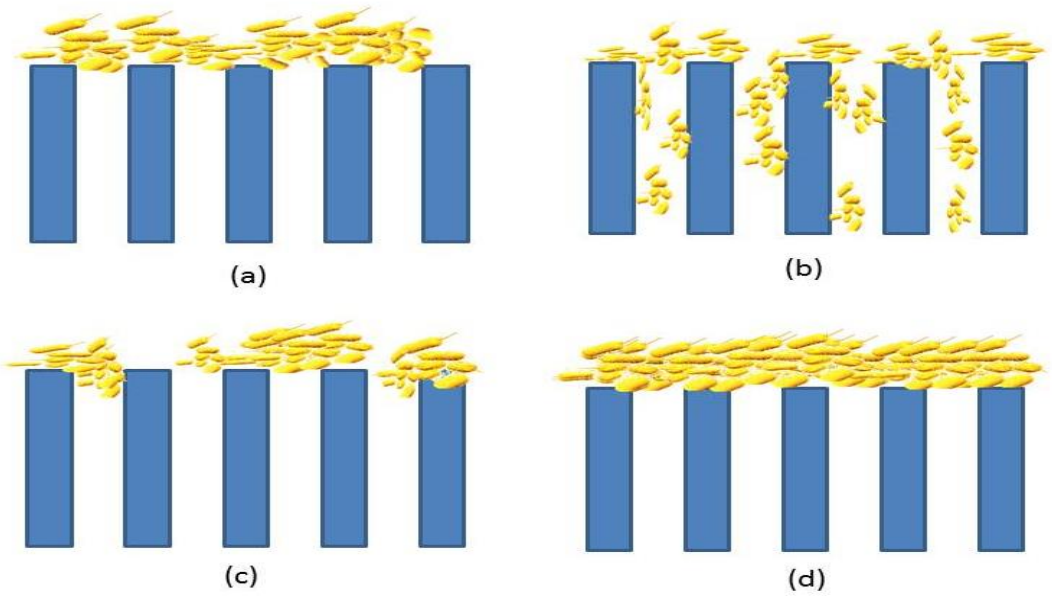

Figure 2.3: Schematic representation of various pore blocking mechanisms (a) complete pore blocking, (b) standard pore blocking, (c) intermediate pore blocking and (d) cake filtration.

2.2.4.4 Fitness of standard pore blocking models during dead end MF

The dead end MF of microbial suspensions using low cost ceramic membranes was addressed using pore blocking models namely complete pore blocking, standard pore blocking, intermediate pore blocking and cake filtration. Obtained parameters for the models do have physical relevance. Hermia (1982) presented a generalized fouling model for constant pressure batch microfiltration. This is presented as:

$$\frac{d^2t}{dV^2} = K_p\left(\frac{dt}{dV}\right)^n \tag{2.10}$$

where the discrete selection of 2, 1.5, 1 and 0 for parameters *n* corresponds to complete pore blocking, standard pore blocking, intermediate pore blocking and cake filtration, respectively. The physical interpretation of these pore blocking mechanisms is presented in Figure 2.3. As

shown, in Figure 2.3 (a), complete pore blocking occurs when the sizes of the solute particles are greater than the size of the membrane pores. As a result, pore blocking occurs over the membrane surface and not inside the membrane pores. Standard pore blocking hypothesizes that the molecules enter the membrane pores and deposit over the pore walls due to the irregularity of pore passages. Thereby, they reduce the membrane pore volume. Thus, standard pore blocking occurs due to particles having sizes smaller than the membrane pore size and pore blocking occurs inside the membrane pores. Thereby, the volumes of membrane pores decrease proportionally to the filtered permeate volume (Figure 2.3 (b)). Intermediate blocking occurs when the solute particle size is similar to the membrane pore size. For such a scenario, it is assumed that a membrane pore is not necessarily blocked by the solute molecules and some particles may settle over others. Therefore, the non-blocked membrane surface area diminished with time and some molecules are expected to obstruct the membrane pore entrance without blocking the pore completely (Figure 2.3 (c)). Cake filtration corresponds to a scenario where particles larger than the average pore size accumulate on the membrane surface and thereby enable the formation of a "cake" (Figure 2.3 (d)). The cake grows with time and provides an additional porous barrier (and hence hydraulic resistance) to the permeating liquid.

The linearized expressions for various pore blocking models are presented as follows (Emani et al., 2013):

a) Complete pore blocking (n = 2)

$$\ln\left(J^{-1}\right) = \ln\left(J_0^{-1}\right) + k_b t \tag{2.11}$$

b) Standard pore blocking (n = 1.5)

$$J^{-0.5} = J_0^{-0.5} + k_s t \tag{2.12}$$

c) Intermediate pore blocking (n = 1)

$$J^{-1} = J_0^{-1} + k_i t \tag{2.13}$$

d) Cake filtration (n = 0)

$$J^{-2} = J_0^{-2} + k_c t \tag{2.14}$$

Therefore, a plot of $\ln\left(J^{-1}\right)$ vs. t, $J^{-0.5}$ vs. t, J^{-1} vs. t and J^{-2} vs. t shall be a straight line with slope of k_b, k_s, k_i and k_c and with y-intercept of $\ln\left(J_0^{-1}\right)$, $J_0^{-0.5}$, J_0^{-1} and J_0^{-2} for complete pore blocking, standard pore blocking, intermediate pore blocking and cake filtration model, respectively. Using expressions (2.11 - 2.14), the appropriate fitness and competence of various fouling models can be confirmed by comparing the values of coefficient of correlation (R^2) obtained from appropriate plots of time dependent flux data.

2.3 Cross flow microfiltration

2.3.1 Experimental setup

Unlike dead end MF, cross flow MF involves tangential feed flow across the membrane. This is not the case during dead end MF where the feed is contacted perpendicular to the membrane surface. Since cross flow enables tangential shear forces, the membrane fouling during the cross flow is relatively low. Thereby, membrane performance is effective in comparison with the dead end MF.

A schematic of experimental set up used for water or synthetic solution cross flow MF permeation experiment is presented in Figure 2.4. As shown, the feed tank is supplemented with

a compressor to increase the temperature and a chiller jacket to decrease the temperature of the feed stream. A gear pump connected to the feed tank provides the necessary pressure and flow rate, which is further regulated using bypass, reflux valves and variable frequency drive device. The dampener located after the gear pump enables the reduction of flow fluctuations in the feed channel. The membrane permeation module referred to the housing of a circular membrane disc which was sandwiched between rubber gaskets to facilitate fluid permeation only through the membrane. A typical cross flow run refers to the measurement of time dependent flux using a weighing balance and a 500 mL beaker. Similar to the dead end MF, both feed and permeate colony count were evaluated using plate count method.

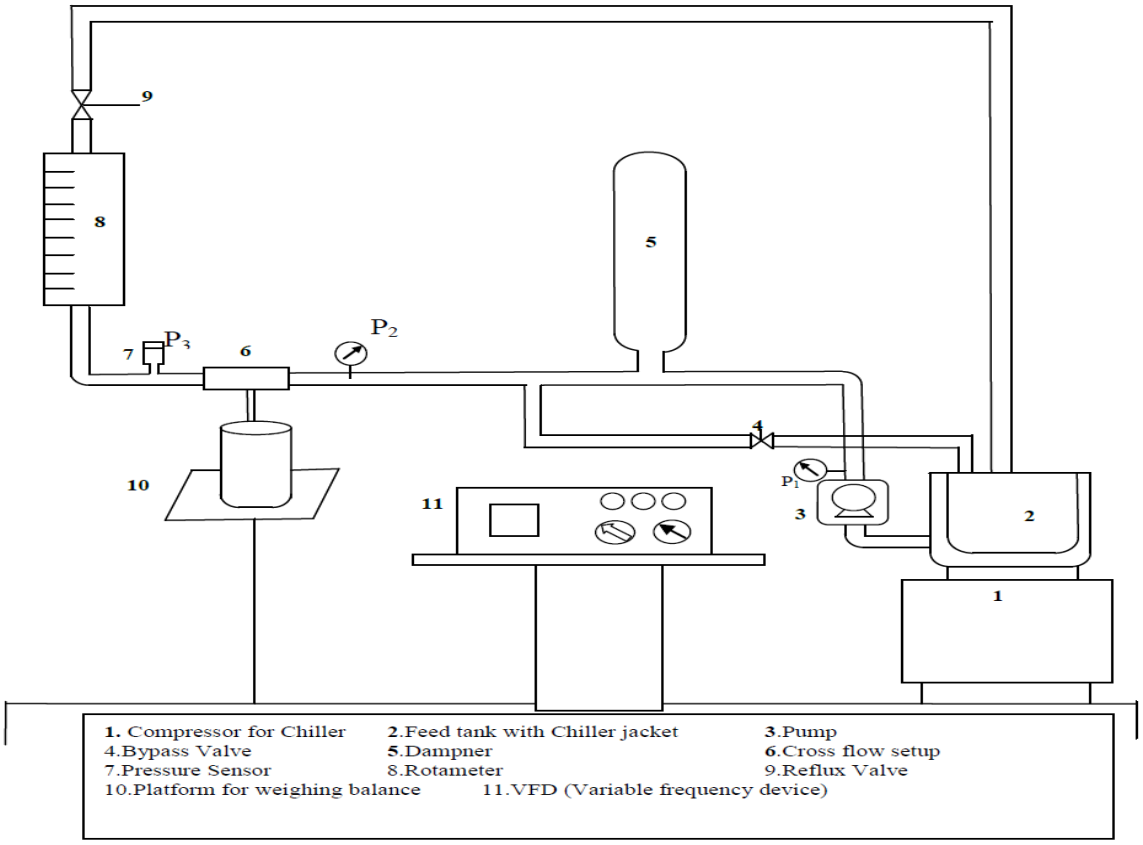

Figure 2.4: Schematic of crossflow microfiltration setup

2.3.2 Cross flow MF tests

A typical cross flow MF run involved the leak proof housing the disc shaped membrane first in the membrane permeator module. Eventually, after ensuring that the setup has been assembled carefully with all connections, the cross flow MF setup was first run at 1 LPM circulation rate and Millipore water at 40 psi so as to subject the membrane to compaction. Eventually, cross flow MF run was conducted by changing the feed as synthetic microbial suspension which was prepared a priori using dilution method that was outlined in section 2.2.3. For all cross flow MF runs, the circulation rate and ΔP have been taken as 1 LPM and 30 psi respectively. This is based on some preliminary trial and error approaches that .indicated that circulation rates greater than 1 LPM do not enhance the flux significantly and ΔP should be maximum for higher flux.

2.3.3 Flux decline analysis using resistances in series model

The total time dependent permeation resistance during a typical cross flow run can be evaluated from the measured flux Vs. time data using the expression:

$$R_t = \frac{\Delta P}{\mu J} \tag{2.15}$$

where μ is the viscosity of the permeate sample (and is same as that of water).

R_t can be further expressed as a combination of two resistances namely the resistance of support (R_s) and fouling resistance due to pore blocking and bio-film growth (R_f)

$$R_t = R_s + R_f \tag{2.16}$$

The fouling resistance R_f is due to (a) pore blocking of the ceramic structure and (b) formation of a thin bio-film on the ceramic surface. Therefore, the fouling resistance is the net effect of

both reversible (bio-film) and irreversible (pore blocking) fouling mechanisms. The fouling resistance thereby can be evaluated using the expression:

$$R_f = R_t - R_s \tag{2.17}$$

Where R_s can be evaluated using water permeation flux data using the expression:

$$R_s = \frac{\Delta P}{\mu_w J_w} \tag{2.18}$$

Where μ_w is the viscosity of water and J_w is the steady state water flux at ΔP.

The ratio of time dependent fouling resistance (R_f) and total hydraulic resistance (R_t) will indicate upon the severity of fouling. For instance, if the ratio is very close to a value of 1, it indicates that the support hydraulic resistance is negligible and total permeation resistance is contributed by the fouling due to pore blocking and bio-film. If severe pore blocking occurs due to the blockage of the ceramic structure with the microbes, then irreversible fouling could occur. On the other hand, if the film deposition occurs on the membrane surface, then it could cause reversible fouling. Hence, the magnitude of fouling resistance and total permeation resistances and the variation in fouling resistance with time are very important to indicate upon the extent of fouling.

The time dependent fouling index (*F (t)*), total fouling index (*FI*) and average fouling index (*AFI*) of the ceramic membrane for the cross flow MF data can be evaluated using the expressions presented in sub-section 2.2.4.3.

2.4 Preparation and Characterization of silver-ceramic composite membranes

2.4.1 Overall methodology

The overall methodology adopted in hierarchy for the preparation and characterization of silver-ceramic composite membranes is summarized as follows:

a) **Preparation of support for electroless plating:** The fabricated low cost ceramic membrane obtained from sintering process was first subjected to polishing and sonication assisted cleaning using Millipore water. Eventually, the membrane was dried in an oven at 110^{o}C for 12 h.

b) **Measurement of ceramic membrane flux:** The flux measurement of the low cost ceramic membrane was carried out using dead end MF setup presented previously in section 2.2.1. Using the setup, N_2 gas permeation tests were carried out to thereby obtain N_2 flux Vs. ΔP data. The N_2 flux measurements were carried out using gas rotameter which was calibrated before measurement. Using the N_2 flux Vs. ΔP data, the average membrane flux of the support was evaluated using modelling approaches.

c) **Sensitization and activation:** The ceramic membrane was once again dried at 110^{o}C for 12 h and following this step, it was fastened with Teflon tape on the rear side so as to disallow sensitization and activation on the Teflon covered side and allow the activation on the surface exposed to sensitization and activation solutions. Eventually, sensitization and activation steps were carried out to obtain a Pd nucleated ceramic membrane.

d) Electroless plating: The Pd nucleated ceramic membrane support was subjected to Ag electroless plating using CEP, SIEP, SOEP and SSOEP baths. Bulk and drop wise reducing agent contacting pattern was adopted. For both cases, the maximum time of deposition was 3 h with 1h as maximum time for one plating step.

e) Membrane and ELP process characterization: The fabricated silver-ceramic composite membrane was subjected to overnight drying at 110^{o}C. Following this step, the silver-ceramic composite membrane was evaluated for its N_2 permeation flux Vs. ΔP using the procedure presented above (header b) in the sub-section 2.4.1. Further, membrane characterization was conducted by evaluating the weight gained by the membrane after Ag composite membrane fabrication. The ELP process characterization was carried out by analysing the Ag solution concentration before and after plating using titration method.

f) Surface characterization: The membrane after process and membrane characterization was subjected to XRD and SEM based surface characterization.

2.4.2 Evaluation of average ceramic membrane support flux

The nitrogen flux through the membrane (J) for a chosen ΔP was evaluated from the volumetric flow rate data

$$J = \frac{Q}{A_m} \tag{2.19}$$

Where Q represents the volumetric flow rate in LPM, A_m is the permeable area of the membrane, m^2 and J is the flux through the membrane, $\left(\frac{mol}{m^2 s}\right)$

Eventually, J vs ΔP can be obtained for various values of ΔP. There by, the average trans-membrane flux $\overline{J}$ is evaluated using the expression:

$$\overline{J} = \frac{\int_{p_1}^{p_2} JdP}{P_2 - P_1} \tag{2.20}$$

where $\overline{J}$ represents the average flux through the membrane, $\int_{P_1}^{P_2} JdP$ corresponds to the area under the curve of a plot between the membrane flux $\left(\frac{mol}{m^2 s}\right)$ and pressure (psi). The term $P_2 - P_1$ corresponds to the lowest and highest values of the trans-membrane pressure differential.

In the above expression, the area under the curve was determined using trapezoidal rule.

2.4.3 Sensitization and Activation

Electroless plating is a chemical method for the deposition of silver metallic layer onto the surface of a substrate. For electroless silver plating, it is necessary that the ceramic membrane is activated using Pd. Therefore, prior to electroless plating sensitization and activation steps are repeated at least 10 – 12 times using respective baths. The procedure adopted is similar to that presented by Agarwal et al. (2013). In between these two steps, intermittent water rinsing was also carried out which improved the activation process. Thereby, the activation process is regarded to be complete by observing a dark brown Pd layer on the porous ceramic membrane support.

2.4.4 Ag Electroless Plating

Ag electroless plating was carried out using various ELP bath configurations namely conventional electroless plating (CEP), surfactant induced electroless plating (SIEP), sonication induced electroless plating (SOEP) and coupled sonication and surfactant induced electroless plating (SSOEP). For all cases, the Ag ELP bath composition refers to that presented in Table 2.3. As presented, the bath composition refers to silver nitrate as source of Ag ions and hydrazine hydrate as a reducing agent for providing electrons for the autocatalytic reaction. Besides these, sodium EDTA and ammonia are used as stabilizing agent and pH controlling agent. The plating process referred to a loading ratio (defined as average membrane surface area per volume of plating solution used for one plating step), temperature and pH of 441 cm^2/L, 35^oC and 11 – 12 respectively. While the silver ion solution concentration was varied from 0.005 – 0.015 mol/L, the reducing agent concentration was varied from 50 – 800% excess with 800% excess being used for bulk addition mode of reducing agent. The higher concentration of reducing agent during bulk addition mode of the reducing agent is due to the instantaneous decomposition of hydrazine in the plating conditions. Due to this reason, it is desired that the electrons shall be available for the Ag ions during the prolonged plating time of about 1h for each plating step. Further, where surfactant was utilized, CTAB surfactant with a solution concentration of 1 – 4 CMC was being used. The basis for the chosen composition is based on (a) available literature data (Alvar et al., 2008) and (b) prior expertise in the research group (Agarwal et al., 2014; Bulasara et al., 2012). For a total plating time of 3 h, 3 sequential Ag ELP was carried out using fresh solutions prepared for each plating step. For each plating step, except reducing agent, all other components were mixed thoroughly using a sonication/water bath and were brought to the required plating temperature. Once the solution reached the desired plating temperature, the

Table 2.3: Composition and parameters for silver electroless plating bath

S. No.	Constituent	Formula	Amount (mol/L)
1.	Silver Nitrate	$AgNO_3$	0.005-0.015
2.	$Na_2EDTA.2H_2O$	$C_{10}H_{14}N_2Na_2O_8.2H_2O$	0.07
3.	Aqueous NH_3	$NH_3.H2O$	0.007
4.	Surfactant (CTAB),CMC		1- 4
5.	Plating Temperature, ^oC		25
6.	pH		11-12

ceramic substrate was contacted with the ELP solution and reducing agent of specified Ag, hydrazine and CTAB (if any) solution concentrations. Subsequently, plating was carried out in either of the following processes: CEP, SIEP, SOEP and SSOEP and accordingly compositions were chosen. For example, for the SIEP and SSOEP, surfactant induced compositions were used and for CEP and SOEP no surfactant was used in the composition. The overall ELP reaction can be presented as per the following reaction:

$$4AgNO_3 + 4NH_4OH + N_2H_4H_2O \xrightarrow{Pd} 4Ag + N_2 + 4NH_4NO_3 + 5H_2O \quad (2.21)$$

All Ag electroless plating experiments were conducted in a fume hood. Since hydrazine is a carcinogenic toxic chemical it was handled very carefully and was diluted and added only in fume hood conditions along with the usage of a mask. Further, hydrazine was always prepared in diluted condition only prior to the experiments and was always stored in refrigerator. This was also due to the fact that hydrazine undergoes instantaneous decomposition even at room temperature.

Further details of the CEP, SIEP, SOEP and SSOEP processes are presented in the following sub-sections:

2.4.4.1 Conventional Electroless Plating (CEP)

The CEP process involved electroless plating carried out in a water bath and was named as CEP due to not utilizing rate enhancement techniques such as sonication and/or surfactant. To initiate the plating process, the solutions without reducing agent were preheated in the water bath to reach the plating temperature (35°C) after which, the reducing agent is added to the solution in bulk mode. Once the reducing agent is added, the solution was stirred and the seeded ceramic support was placed in the plating bath. The membrane was taken out only after 1h of the plating time which was the time duration taken for one plating step.

2.4.4.2 Surfactant Induced Electroless Plating (SIEP)

During SIEP process, procedures similar to those presented in section 2.4.4.1 were followed. However, the plating solution referred to an additional CTAB component within the concentration range of 1 – 4 CMC. The selection of CTAB surfactant is with prior knowledge of the cationic surfactant to be more effective than other types of surfactants such as SDS. Compared to the CEP, SIEP process has been reported in the literature to maximize the quality of plating by reducing the pitting effect. This is mainly due to the reason that the surfactant inclusion in the composition reduces the interfacial tension and thereby enables the generation of smaller N_2 bubbles on the substrate surface, which could leave the surface without inducing significantly higher shear stresses on the loosely deposited Ag metal. Only bulk mode of reducing agent contacting pattern was studied for Ag SIEP processes.

2.4.4.3 Sonication induced Electroless plating (SOEP)

Similar to the CEP process, the SOEP process was conducted. However, the major difference is that while water bath was being used in the CEP for the ELP, an ultrasonic cleaning bath (Make: Elmasonic, S30 H) was used in the SOEP. Other specifications of the bath refer to 280 W power consumption at a frequency of 37 kHZ in degas mode and inner dimensions of the rectangular bath (240 mm ×137 mm× 100 mm). The ultrasound assisted ELP has been proven in previous studies to be very effective to achieve low cost porous metal ceramic composite membranes and this work intends to focus towards the plating characteristics of SOEP baths for porous silver-ceramic composite membranes. Sonication has been proven to be effective to cause controlled shear forces on the substrate surface due to cavitation effect. With faster elimination of N_2 gas bubbles and enhanced Pd ion concentration on the substrate surface, the cavitation effect is anticipated to enhance the autocatalytic silver deposition rate. Both bulk and drop wise contacting pattern of the reducing agent was studied for Ag SOEP processes.

2.4.4.4 Sonication and surfactant induced electroless plating (SSOEP)

Using a similar procedure summarized in section 2.4.4.1 of the thesis, the Ag SSOEP process was carried out using a combination of surfactant and sonication. In other words, the SSOEP was achieved by carrying out the Ag ELP in an ultrasonic cleaning bath using Ag ELP bath compositions consisting of CTAB surfactant. The combined effect of sonication and surfactant is an interesting feature to investigate upon to evaluate the tradeoffs associated with enhanced shear rate based on cavitation and minimized pitting effect due to the surfactant. In particular, the case studies aimed to evaluate whether SSOEP provides better combinatorial plating characteristics in comparison with SIEP and SOEP processes. Both bulk and drop wise contacting pattern of the reducing agent was studied for Ag SSOEP processes.

2.4.5 Ag composite membrane and ELP process characterization

After 3 h of sequential Ag ELP, the membrane was first thoroughly rinsed with Millipore water to clean the surface from loose particles and was eventually dried at 110^{o}C. Eventually, membrane and process characterization parameters were evaluated based on three important measurements namely

a) Dry weight of the porous Ag-ceramic composite membrane (w_2)

b) Nitrogen flux Vs. ΔP data for the Ag-ceramic composite membrane

c) Initial (C_i) and final (C_f) solution concentration of the Ag ELP solution using titration method. Along with this, the final solution volume after plating was also measured to precisely consider solution losses in evaluation procedures.

2.4.6 Evaluation of ELP process and membrane characteristics

The efficacy of various ELP processes to fabricate low cost Ag-ceramic composite membranes has been evaluated based on five major parameters namely bath conversion (x), plating efficiency (η), metal loading index (MLI) and percent pore densification (PPD). In the following paragraphs, the procedure adopted to evaluate these plating characteristic parameters is being presented.

The plating bath conversion (x) is defined as the ratio of the amount of metal ion reacted during the plating process to the amount of metal present initially in the plating solution and is expressed as

$$x = \frac{V_i C_i - V_f C_f}{V_i C_i} \tag{2.22}$$

where V_i, V_f are the initial and final loading volume and C_i, C_f are initial and final concentrations of silver metal loading solution. Titration procedure along with sample calculation for the evaluation of Ag ion solution concentrations is presented in Appendix D and E of the thesis.

The plating efficiency η (%) is defined as the ratio of amount of metal deposited on the ceramic support to the amount of metal converted during the reaction and is evaluated using the equation:

$$\eta = \frac{w_2 - w_1}{w_0 x} \tag{2.23}$$

where x corresponds to the conversion in the plating bath.

Pore densification was presented as the fractional volume of the pores covered by the deposited silver metal and it is expressed as:

$$PPD_i = \frac{\overline{J_0} - \overline{J_i}}{\overline{J_0}} \times 100 \tag{2.24}$$

where $\overline{J}_0$ represents the average flux through the support and $\overline{J}_i$ represents the average flux through the silver membrane after ith hour. The average flux is evaluated using the procedure presented in section 2.4.2 of the thesis.

The metal loading index MLI can be evaluated using the expression:

$$MLI = \frac{w_2 - w_1}{A_m \delta} \tag{2.25}$$

where w_2 is weight of the silver- ceramic membrane (g), w_1 is weight of ceramic support (g), δ represents the thickness of ceramic membrane (cm) and $A_m (cm^2)$ the membrane surface area for nitrogen permeation experiments.

2.4.7 Surface Characterization

For the porous Ag-ceramic composite membrane, X-ray diffraction studies were conducted to evaluate the presence of various crystalline materials other than Ag. Also, FESEM analysis was as well carried out to identify the presence of surface defects in the metal composite membrane porous structure.

Chapter 3:

Dead End Microfiltration Performance of Low Cost Ceramic Membranes

Dead End Microfiltration Performance of Low Cost Ceramic Membranes

After a brief overview of surface, physical and flux characterization is addressed in section 3.2 for the fabricated membranes, section 3.3 elaborates upon the dead end MF performance and its modelling aspects for low cost ceramic membranes. Following this, section 3.4 summarizes the retail cost analysis followed with the summary of the research findings in section 3.5.

3.1 Overview

In this chapter, results obtained from surface, physical, flux characterization of CM1- CM3 membranes is presented first. Eventually, dead end MF performance of the membranes is summarized. Following this, flux decline analysis using standard pore blocking models is addressed. Finally, the evaluated conceptual retail cost of the membrane is being presented.

3.2 Surface and physical characterization

3.2.1 BET and TGA analysis

From BET analysis, the specific surface area of CM1, CM2 and CM3 membranes have been obtained as 13.593, 7.688 and 6.940 m^2/g respectively. Based on the data, it can be analyzed that the BET surface area decreased with an increase in membrane pore size.

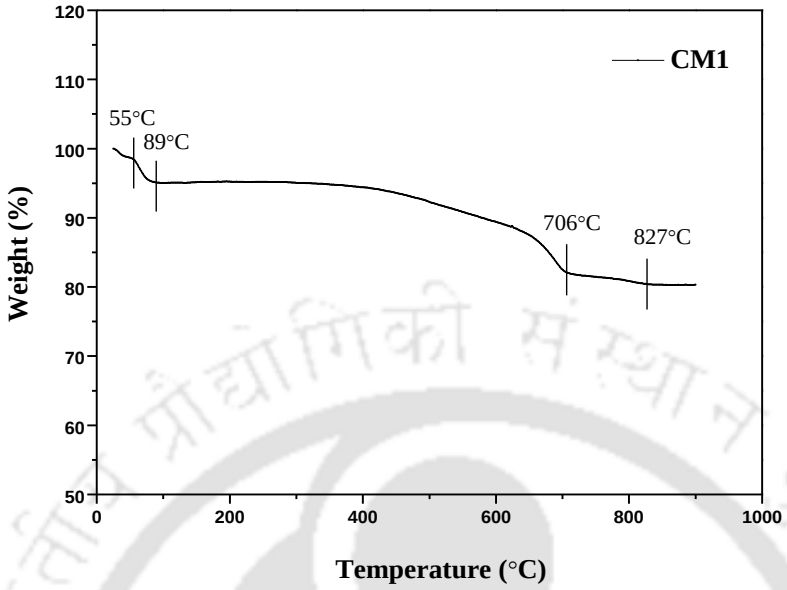

(a)

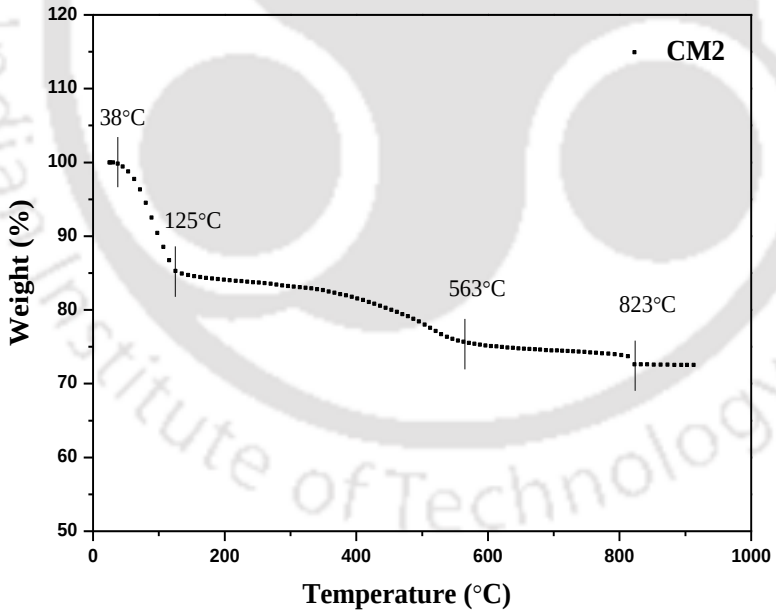

(b)

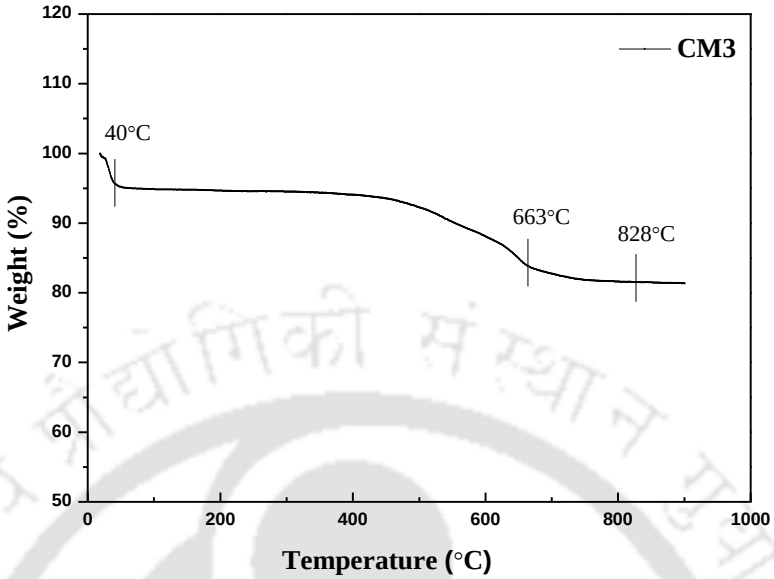

(c)

Figure 3.1: TGA of the raw material mixture for (a) CM1 (b) CM2 and (c) CM3 membranes.

Figure 3.1 (a - c) presents the variation of weight (%) as a function of temperature. This was obtained from the TGA analysis of the raw material mixture. It can be observed that significant weight losses existed up to 827, 823 and 818^{o}C for CM1, CM2 and CM3 membranes respectively and beyond these temperatures, there was no weight loss. Hence, the maximum sintering temperature of 900^{o}C is acceptable to achieve defect free fabrication of low cost ceramic membranes. Also, it can be observed that for all membranes, weight loss that occurred up to 125^{o}C is due to moisture removal and weight loss that occurred between 563 - 706^{o}C is due to decomposition of carbonate salt to oxide and CO_2. For the membranes, the maximum weight loss was evaluated to be about 73 - 81%.

3.2.2 XRD analysis

For membranes CM1- CM3, the XRD pattern for unsintered raw material mixture and sintered inorganic material membrane is presented in Figure 3.2 (a - c) respectively. As shown, for all cases, peaks corresponding to kaolin disappeared after sintering the inorganic precursors at 900ºC. This is due to the conversion of kaolinite and metakaolinite at the sintering temperature (Emani et al., 2014). The XRD pattern also confirms upon significant phase transformations during sintering which refer to the appearance of a nephiline phase after sintering.

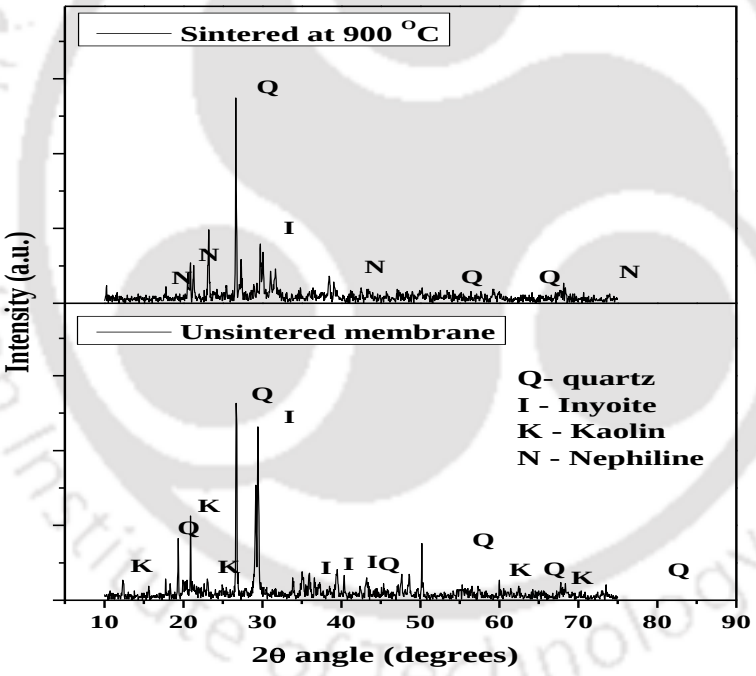

(a)

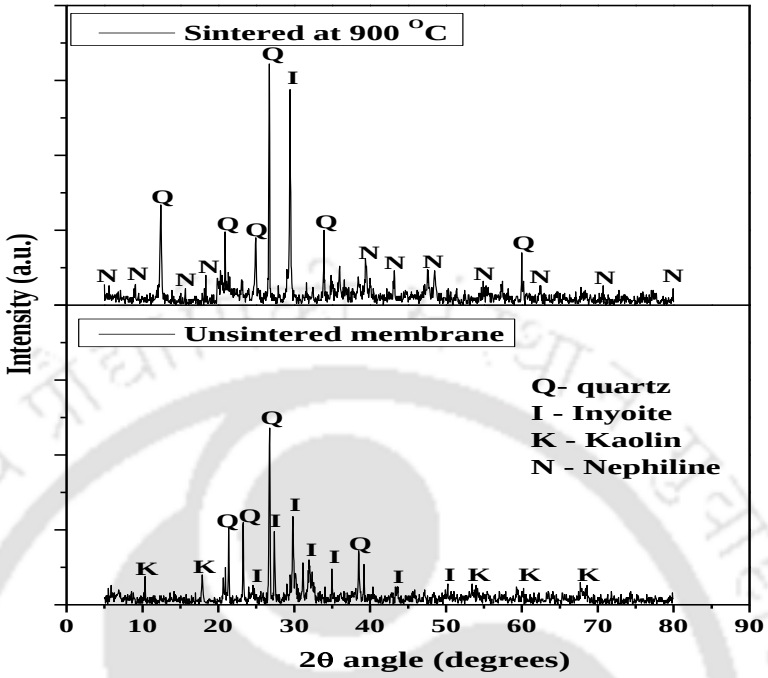

(b)

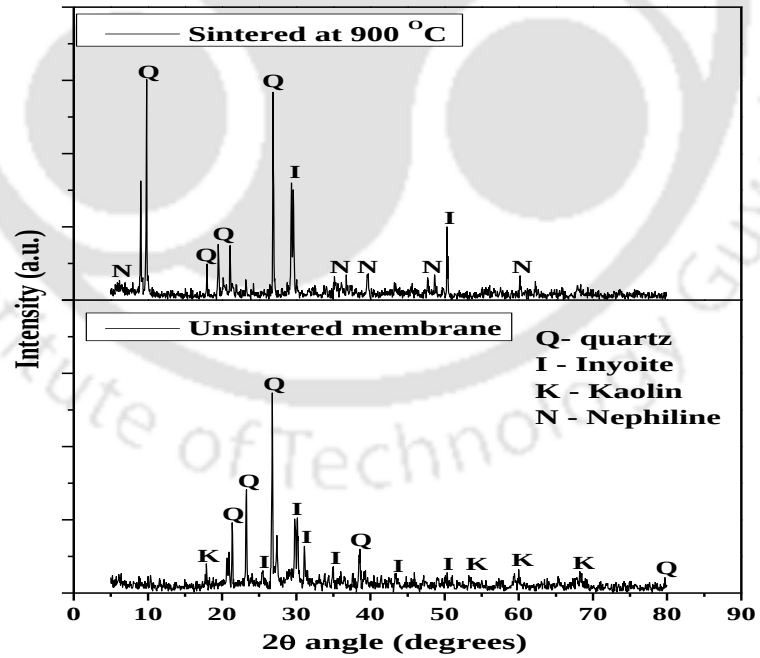

(c)

Figure 3.2: XRD spectra of unsintered powder mixture and sintered membranes (a) CM1 (b) CM2 and (c) CM3.

3.2.3 FESEM

Figure 3.3 (a - c) presents the FESEM images for CM1, CM2 and CM3 membranes respectively. The images indicate highly porous texture of the membranes without surface defects such as cracks and pinholes. The maximum observable pores for all membranes are in the range of 2 - 6.5 µm. Based on analysis of the image, the pore size distributions in various membranes have been determined using ImageJ software (Version 1.40) and has been illustrated in Appendix A. Based on the FESEM image analysis, the average pore size is 1.1, 1.9 and 4.9 µm for membranes CM1, CM2 and CM3 respectively.These values are in good agreement with the corresponding pore size values determined using pure water permeation experiments, which will be elaborated later in this Chapter. A critical comparison of obtained morphologies with those presented in the literature for low cost ceramic membranes indicates that the average pore size

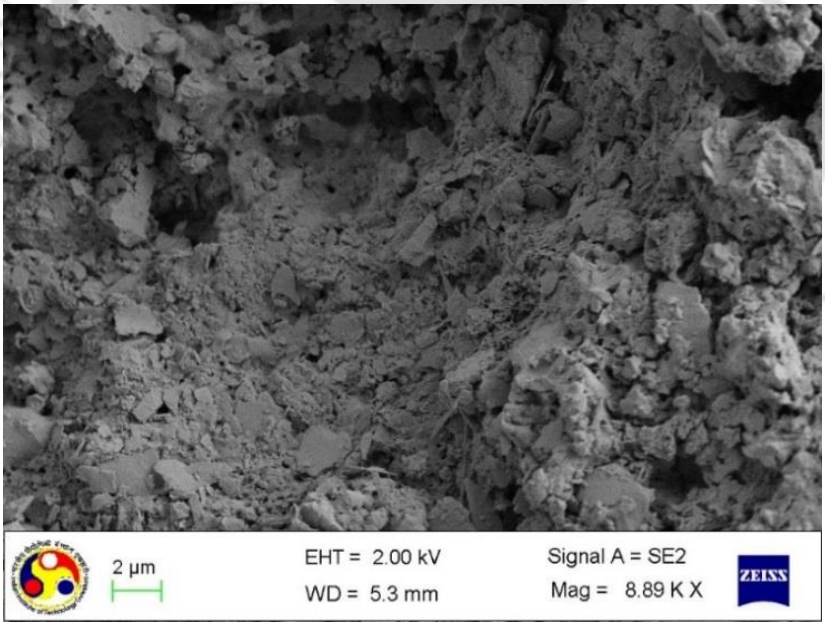

(a)

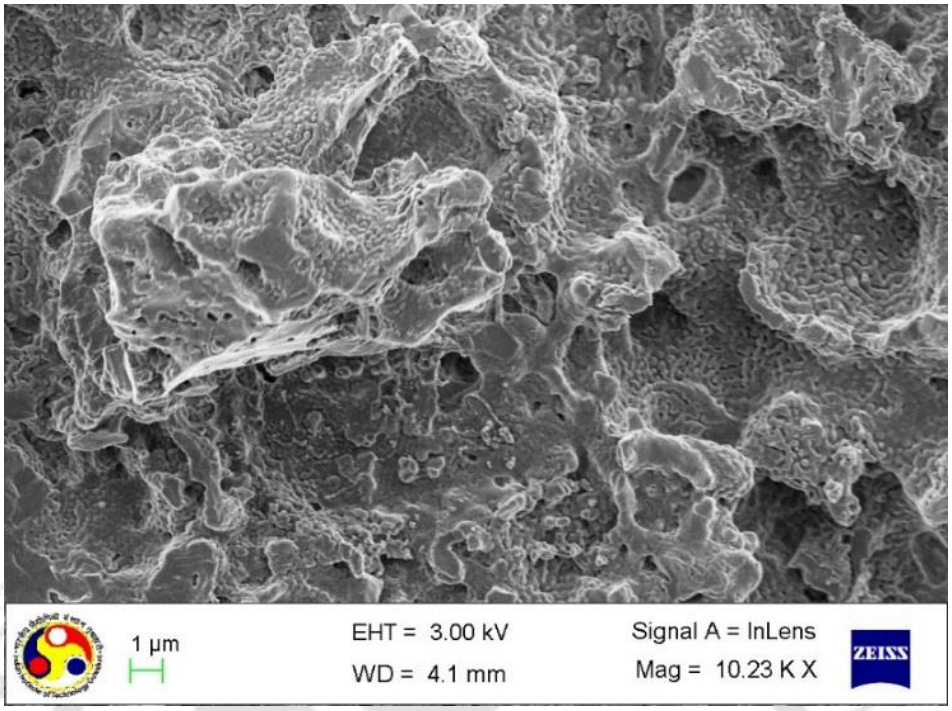

(b)

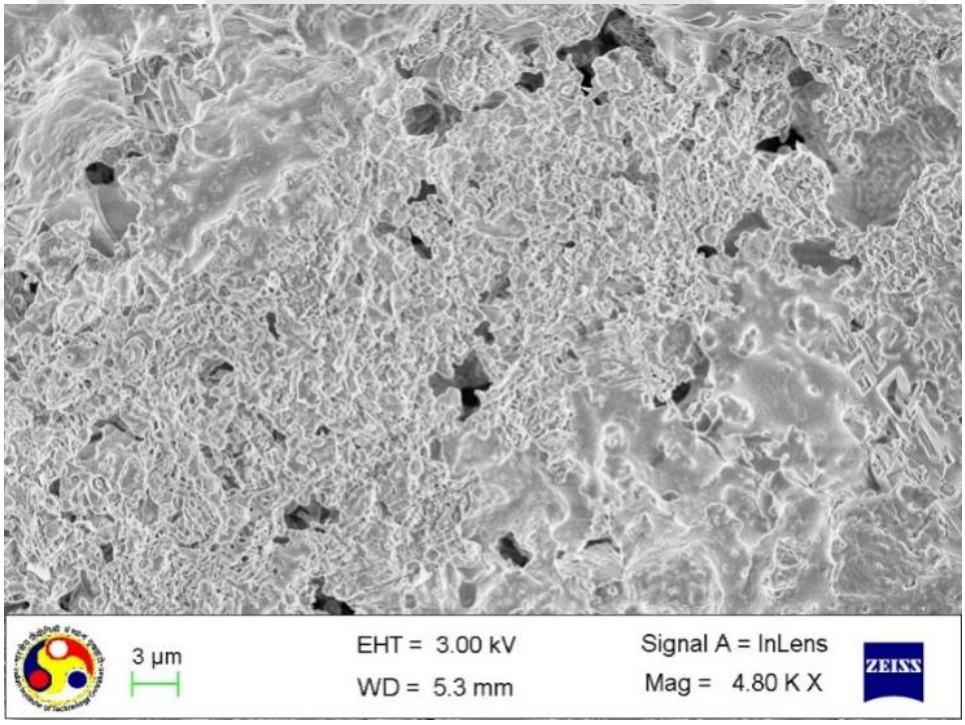

(c)

Figure 3.3: FESEM images of (a) CM1 (b) CM2 and (c) CM3 membranes.

and porosity of membrane CM2 is comparable with those presented by Vasanth et al. (2011). Using a similar inorganic precursor formulation, Vasanth et al. (2011) obtained an average pore size and porosity of 1.3 µm and 30% at a fabrication pressure of 50 MPa, a value slightly higher than the fabrication pressure adopted in this work (49 MPa). Compared to their experimental procedure for the fabrication of the membrane, it is apparent that both precursor composition and particle size distributions significantly influenced morphologies of CM2 and CM3 membranes.

3.2.4 Pure water flux and porosity

The variation of pure water flux with applied pressure for the membranes is presented in Figure 3.4 (a). As shown, for a variation in ΔP from 68.9 - 206.7 kPa, the pure water flux varied from 1.312 - 3.893×10^{-4}, 4.728 - 14.145 × 10^{-4} and 33.245 - 88.552 × 10^{-4} m^3/m^2.s for CM1, CM2 and CM3 membranes respectively. The variation in average membrane porosity (determined with Archimedes principle) and average pore size (determined using Hagen-poiseuille equation) for the membranes are presented in Figure 3.4 (b). As shown, the membrane porosity reduced from 39.4 - 19.3% with an enhancement in pore size from 0.7 - 4.5 µm for membranes CM1 - CM3 respectively. Membranes with different compositions are considered and therefore variation in porosity and pore size cannot be correlated.

The significant variation in both pore size and porosity of the membranes is due to the variation in both inorganic precursor compositions and particle size distributions of the inorganic precursor mixture. A critical analysis of the fabrication procedure and inorganic precursor composition indicates that both CM1 and CM2 have almost similar compositions but with variant PVA concentrations. On a trial and error basis, these variations in PVA concentrations have been identified to be important to achieve the desired membrane morphology. However, experimental fabrication procedures were also slightly different. For CM1 membrane, 36 (425

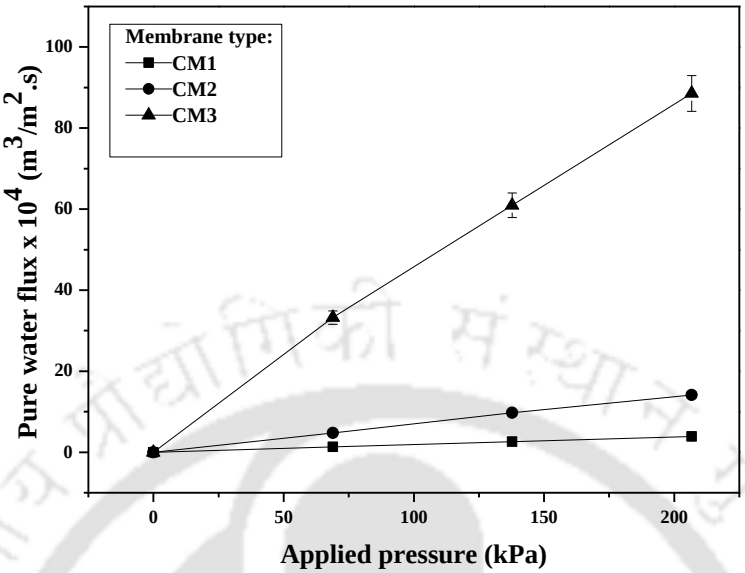

(a)

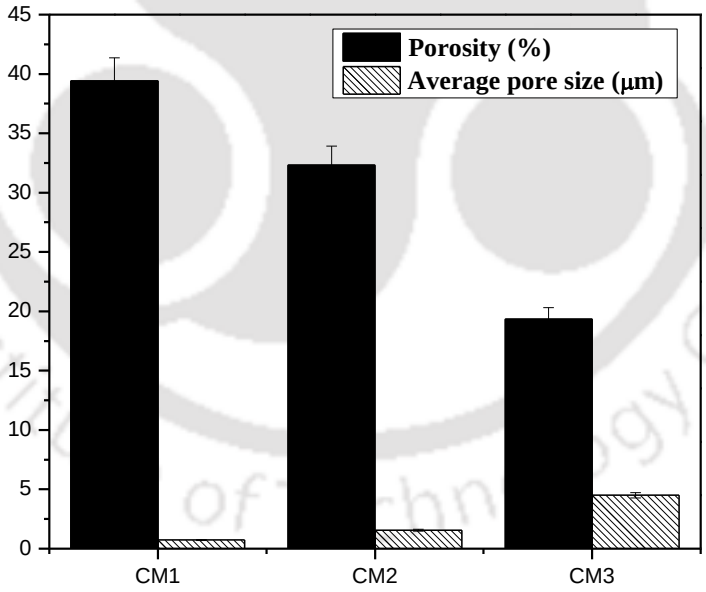

(b)

Figure 3.4: Variation of (a) Pure water flux with applied pressure and (b) Average pore size and porosity for CM1, CM2 and CM3 membranes.

μm) mesh screen was used to screen the precursor mixture where as for CM2 membrane, 72 (212 μm) mesh screen was used. Thus, for a similar PVA concentration, it is expected that CM2 membrane should have had lower average pore size due to the finer particle size distributions. However, since higher average pore size was obtained for the CM2 membrane, it is apparent that PVA concentration significantly influences membrane morphology and higher PVA concentration in the inorganic precursor mixture enhances the average membrane pore size.

On the other hand, the CM3 membrane inorganic precursor formulation does not involve the utilization of PVA and with wide particle sizes of inorganic precursors, the membrane properties are anticipated to be distinct from CM1 - CM2 membranes. In summary, the achievement of low cost ceramic membranes with larger pore size (4.5 μm) is anticipated to be useful for the MF of synthetic microbial solutions, as it is expected that the wider pore size of the membrane could also serve for gravity filtration applications.

3.3 Microfiltration studies

3.3.1 Flux decline Profiles

Figure 3.5 (a - c) presents the microbial (DH5α) flux decline profiles for CM1, CM2 and CM3 membranes respectively. The feed concentration (CFU/mL) and initial flux ($m^3/m^2.s$) values corresponding to these membranes have been presented in Table 3.1. For the CM1 membrane, for a variation in time from 1 - 24 min., the membrane flux varied from 2.34 -1.79×10^{-3}, 7.08 - 4.95×10^{-4} and 1.83 - 1.50×10^{-3} $m^3/m^2.s$ for feed concentrations of 1.6×10^6, 1.7×10^6 and 8.4×10^6 CFU/mL respectively. For the case of CM2 membrane, for a variation in time from 1 - 22 min., the flux decline from 9.68 - 4.64×10^{-4}, 8.41 - 7.11×10^{-4} and 6.39 - 2.44×10^{-4} $m^3/m^2.s$ for

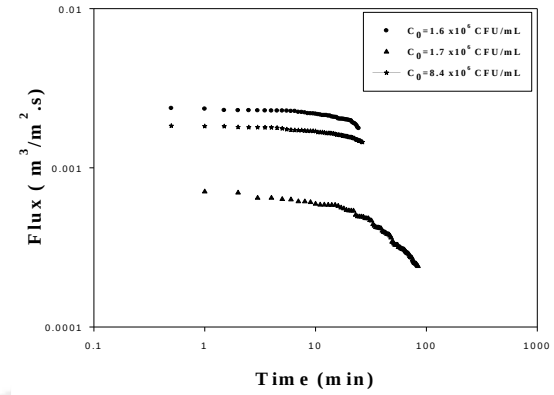

(a)

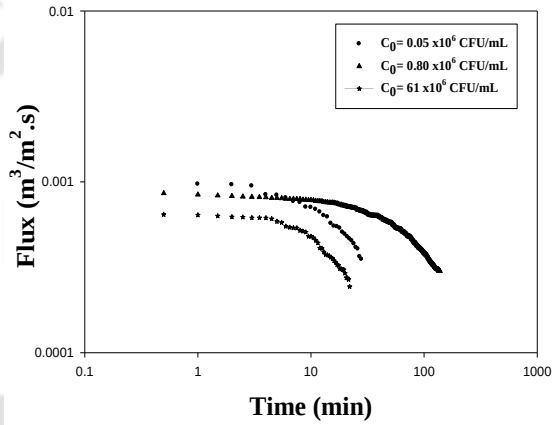

(b)

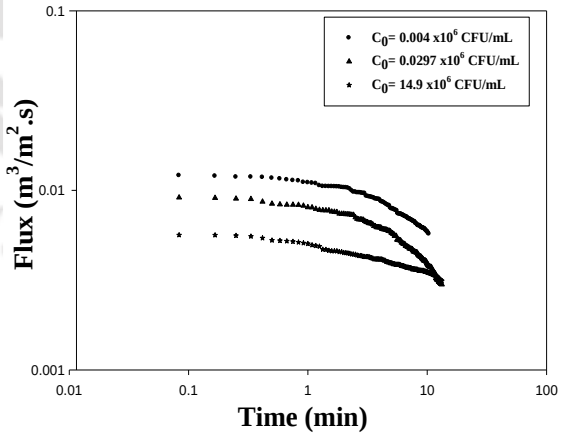

(c)

Figure 3.5: Variation of trans-membrane flux with time at ΔP = 206.7 kPa at various feed microbial concentrations: (a) CM1 (b) CM2 and (c) CM3 membrane.

feed concentration of 0.05×10^6, 0.80×10^6 and 61×10^6 CFU/mL respectively. Further for the CM3 membrane, for a variation in time from 1-10 min., the flux varied from 1.10×10^{-2} - 5.90×10^{-3}, 8.05 - 3.89×10^{-3} and 5.05 - 3.51×10^{-3} $m^3/m^2.s$ for 0.004×10^6, 0.0297×10^6 and 14.9×10^6 CFU/mL feed concentration respectively.

It can be observed that in Figure 3.5 (a-c), the total experimental run period varied from 12 – 120 min. Also, a common time period does not exist for all membranes. This is due to the fact that J_0 is different for various membranes due to their variant pore size distributions and average pore size values. Among all membranes, for the CM3 membrane, it can be observed that the total MF run period did not exceed more than 10 - 12 min. This is due to the large pore size of the membrane, which in turn enabled lower insitu membrane fouling and higher trans-membrane flux.

For CM1 and CM2 membranes, the flux decline profiles did not follow a systematic trend with increasing feed concentrations. For these two membranes, the flux profile for an intermediate feed concentration was located below the flux profile obtained at low and higher feed concentration. These observations are possibly due to the variation in the morphologies of the cultivated microbes in the feed samples which can either significantly contribute towards pore blocking or enable the formation of a dynamic cake filtration layer on the membrane surface. On the other hand, for the CM3 membrane, flux profiles reduced with enhancement in feed concentration. This is due to significant pore blocking at higher feed concentrations. Thus, from an operational perspective, it can be inferred that the membrane CM3 provided pore size distributions that enabled a systematic reduction in flux with increasing feed concentrations.

Therefore, among all cases, CM3 membrane provided highest flux and underwent minimal fouling due to wider pore size.

It is further to noted that the variation in flux decline trends in CM1 and CM2 membranes and relevant hypothesis in conjunction with variant feed bacteria morphology needs to be further investigated to infer whether cell morphology has a potential role in influencing the flux trends. However, since similar flux trends were obtained for the CM3 membrane and alternate trends were obtained for CM1-CM2 membranes, the presented data can be at best regarded to be conceptual in nature and further experimental investigations are necessary to ensure upon the role of membrane pore size and cell morphology in influencing the pertinent flux decline trends for CM1 and CM2 membranes. No such experiments are required for the CM3 membrane where an enhancement in feed concentration significantly reduced the flux decline.

3.3.2 Separation efficiency

Figure 3.6 (a - c) illustrate the separate efficiency of CM1 - CM3 membranes respectively in terms of the cumulative permeate count for various permeate volume samples. For the CM1 membrane (average pore size of 0.7 µm), the cumulative permeate count varied from 0 - 380, 0 - 10 and 0 CFU/mL for feed concentrations of 1.6×10^6, 1.7×10^6 and 8.4×10^6 CFU/mL respectively. These correspond to an LRV value of 5 and 6 for feed concentrations of 1.6×10^6 and 1.7×10^6 CFU/mL respectively, given the fact that LRV cannot be defined for zero permeate

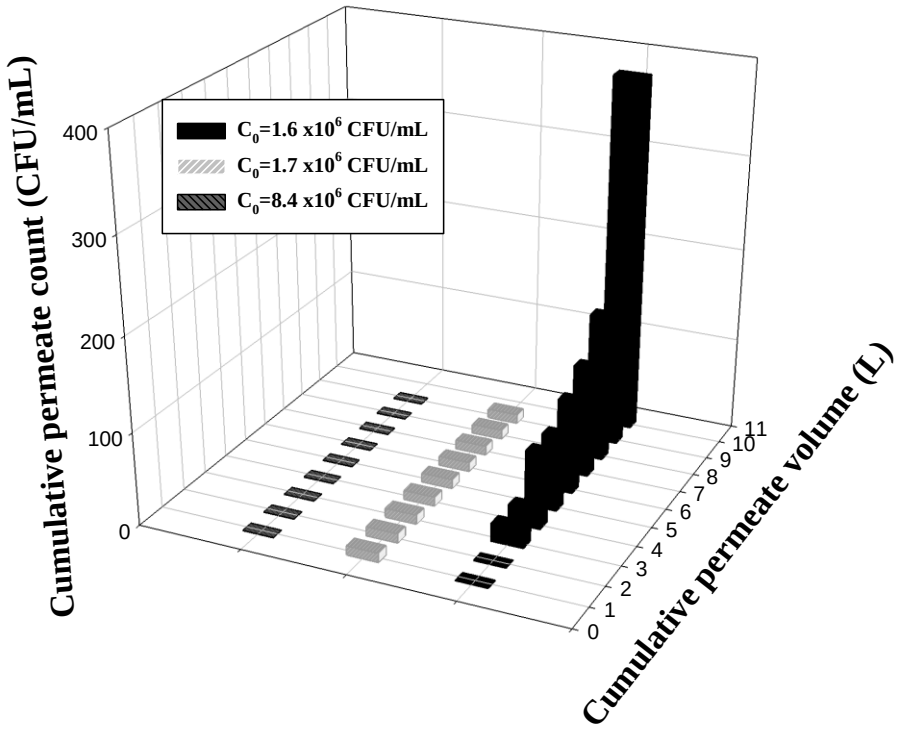

(a)

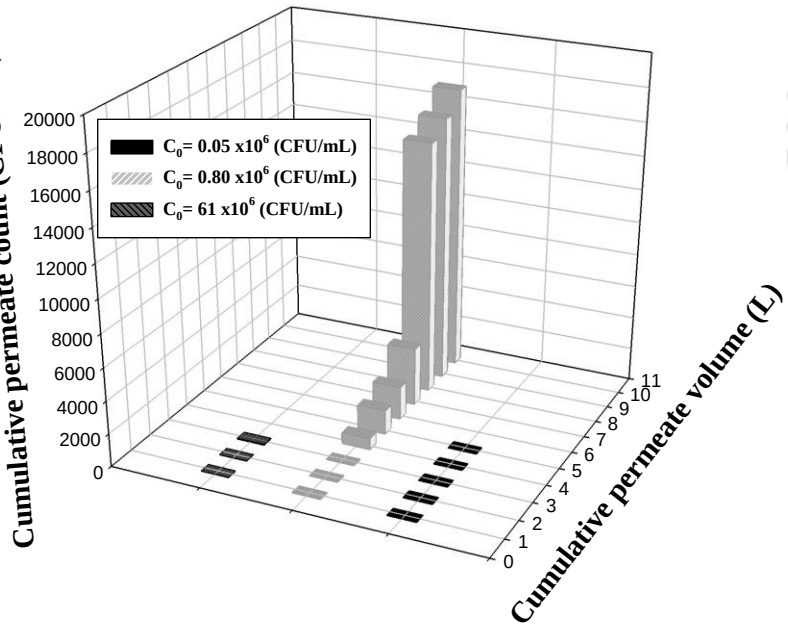

(b)

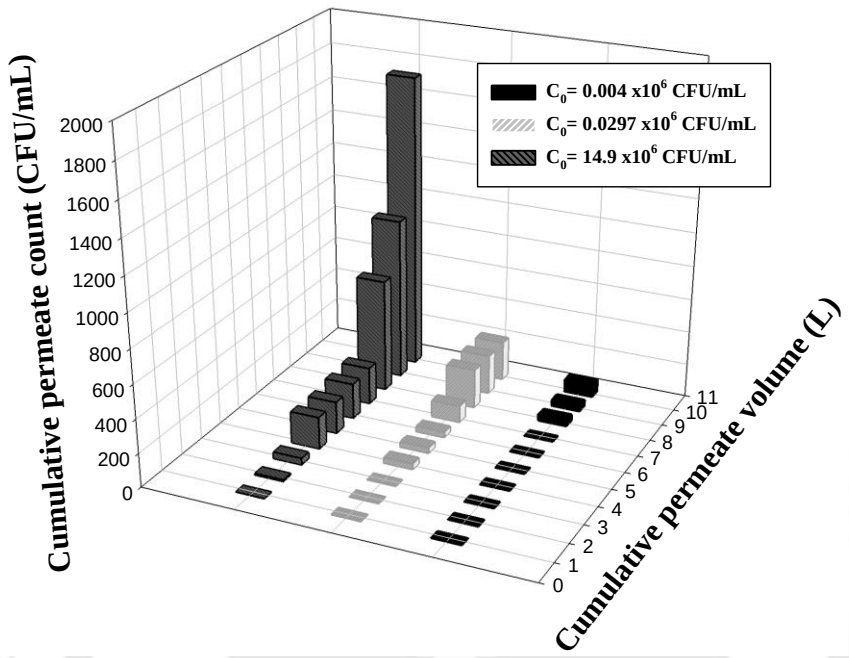

(c)

Figure 3.6: Variation of cumulative permeate count (CFU/mL) with cumulative permeate volume (L) at various feed concentrations: (a) CM1 (b) CM2 and (c) CM3 membrane.

count cases. Similar trends were obtained for CM2 and CM3 membranes. For CM2 membrane (average pore size of 1.5 µm), 100% removal efficiency was obtained at a feed concentration of 0.05×10^6 CFU/mL and the LRV increased from 3 - 6 with an increase in feed concentration from 0.80 - 61×10^6 CFU/mL. For the case of CM3 membrane (average pore size of 4.5 µm), the LRV was found to be 2, 3 and 6 respectively for a feed concentrations of 0.004×10^6, 0.0297×10^6 and 14.9×10^6 CFU/mL respectively. Thus, for the CM3 membrane, the separation efficiency increased with increasing feed concentration, and since CM3 membrane provided the highest flux amongst all the membranes, it can be inferred to possess the most desirable pore size

distributions and average pore size for the MF of microbial solutions with chosen feed concentrations. However, it is important to note that 100% separation efficiency was not achieved and this indicates further engineering of the ceramic membrane is required. This could refer to an additional bacteriostatic skin layer (such as silver film) to deactivate the growth of the bacterial film on the membrane and omit the passage of microbes into the permeate stream.

3.3.3 Fouling indices

Figure 3.7 presents the variation of time dependent fouling index (FI) and average fouling index (AFI) of CM1, CM2 and CM3 at various feed concentrations. Table 3.1 summarizes the relevant values corresponding to the obtained data for all membranes. For CM1 membrane, for a variation in time from 3 - 24 min, the FI values varied from 5.88 - 239.99, 5.84 - 384.05 and 3.06 - 218.36 at feed concentrations of 1.6×10^6, 1.7×10^6 and 8.4×10^6 CFU/mL respectively. Corresponding AFI values varied from 1.96 - 10, 1.95 - 16 and 1.02 - 9.10 respectively. Similarly, for the CM2 membrane, for a variation in time from 3 - 21 min, the FI and AFI values varied from 1.92 - 568.28, 7.68 - 193.67, 5.61 - 589.78 and 0.64 - 27.06, 2.56 - 9.22, 1.87 - 28.08 at feed concentrations of 0.05×10^6, 0.80×10^6 and 61×10^6 CFU/mL respectively. For the CM3 membrane, for a variation in time from 2 - 10 min, the FI and AFI values varied from 16.30 - 308, 21.31 - 348.31, 21.75 - 271.54 and 8.15 - 30.80, 10.65 - 34.83, 10.88 - 27.15 for feed concentrations of 0.004×10^6, 0.0297×10^6 and 14.9×10^6 CFU/mL respectively.

Thus, it can be observed that while AFI values for CM1 membrane were the lowest (1.02 - 16), they were highest (8.15 - 34.83) for the CM3 membrane. This is due to significant pore blocking for wider membrane morphologies. However, CM1 membrane provided an almost negligible flux after 100 min. of operation due to which reason flux experiments could not be carried out

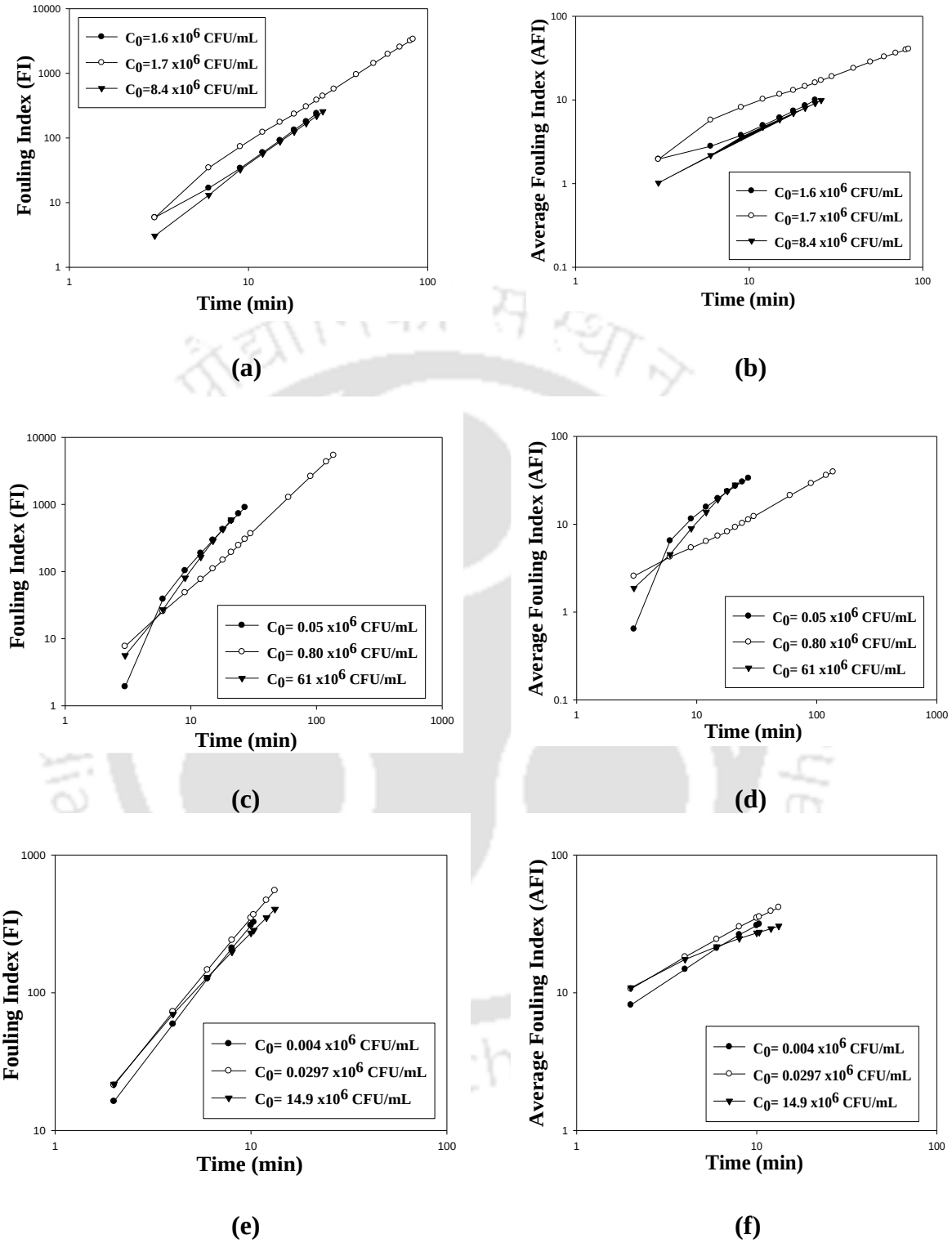

Figure 3.7: Variation of FI (a, c and e) and AFI (b, d, f) for various membranes: CM1 – (a) and (b); CM2 - (c) and (d) and CM3 (e) and (f).

Table 3.1: A summary of dead end MF fouling index and average fouling index data for CM1 – CM3 membranes.

Membrane Type	Feed (CFU/mL) × 10^6	Flux ($m^3/m^2.s$)	Fouling Index (FI)	Avg. Fouling Index (AFI)	Fouling Mechanism
CM1	1.6	2.36×10^{-3}	240	10	Complete pore blocking
	1.7	7.07×10^{-3}	3366	40.6	Standard pore blocking
	8.4	1.83×10^{-3}	2573	9.9	Complete pore blocking
CM2	0.05	9.68×10^{-4}	901.2	33.4	Complete pore blocking
	0.80	8.57×10^{-4}	5397.5	39.4	Complete pore blocking
	61	6.44×10^{-4}	589.8	23.1	Complete pore blocking
CM3	0.004	1.21×10^{-2}	325.3	31.5	Intermediate pore blocking
	0.0297	9.11×10^{-3}	555.8	4.7	Complete pore blocking
	14.9	5.65×10^{-3}	404.2	30.5	Cake filtration

after 100 min of MF operation. On the other hand, for the CM3 membrane, despite obtaining a very high value of AFI (34.83), flux experiments were conducted up to a time frame of 10 minutes and further experiments were not conducted due to minimal variation in the flux after additional 3 minutes time frame. Therefore, despite undergoing significant fouling, the CM3 membrane is regarded to be the best membrane among CM1 - CM3 due to its ability to provide measurable flux values even after prolonged time of operation. The FI and AFI profiles could not be regressed using mathematical expressions. This is due to their strong dependence on membrane morphology, feed concentrations and microbe morphologies in the feed samples.

Along with the most relevant data presented in the literature, Table 3.2 presents a summary of the performance of various ceramic membranes towards bacteria filtration. It can be observed that CM3 membrane performance is comparable with those reported in the literature.

Table 3.2: A summary of ceramic membrane performance for bacteria filtration applications.

S.No	Authors	Average pore size (µm)	Porosity (%)	Feed concentration (CFU/mL)	Flow rate (LPH)/Flux ($m^3/m^2.s$)	Pressure (kPa)	Removal Efficiency (LRV)
1	Simonis and Basson (2011)	-	64	6×10^4	-	-	4
2	Vasanth et al. (2011)	1.3	30	6×10^5	1×10^{-4} $m^3/m^2.s$	69	2
3	Mwabi et al. (2012)	-	-	-	1 - 4LPH*	-	2 - 4
4	Bielefeldt et al. (2009)	-	-	10^6	1.9 LPH*	-	3 - 4
5	This Work	4.5±0.2	19.3 ±1.07	14.9 ±0.5×10^6	3.15±0.05×10^{-3}	206.7	6

*Membrane area is not given

Table 3.3: Physico – chemical properties of feed and permeate samples of synthetic bacteria solutions during MF at ΔP = 206.7 kPa.

Membrane type	Feed concentration (CFU/mL) × 10^6	Feed		Permeate	
		pH	Conductivity (µs/cm)	pH	Conductivity (µs/cm)
CM1	0.36±0.03	6.60±0.05	6.69±0.12	8.13±0.04	7.86 ±0.13
CM2	0.16±0.02	6.50±0.06	12.52±0.14	8.73±0.07	12.79±0.16
CM3	14.9±0.04	7.34±0.05	11.30±0.11	8.98±0.06	11.89±0.14

3.3.4 Physico-chemical parameters

Table 3.3 presents a summary of physico-chemical properties of feed and permeate samples for membranes CM1 - CM3 for selected experimental data. Similar results were obtained for other sets of MF runs and have not been reported. It can be observed that for feed samples the pH and conductivity values varied from 6.60 - 7.34 and 6.69 - 11.30 µs/cm respectively. Corresponding pH and conductivity samples for permeate streams varied from 8.13 - 8.98 and 7.86 - 11.89 µs/cm respectively. These observations indicate that the pH and conductivity of the permeate samples increased significantly. The enhancement in the pH of the permeate samples is due to the presence of alkaline oxides and carbonates in the membrane matrix (Nandi et al., 2009). The conductivity of both feed and permeate samples remained fairly constant. Thus, calcium leaching is a prominent limitation of the prepared low cost ceramic membrane and therefore further research needs to be taken up to achieve low cost ceramic membranes without calcium leaching effect. This can be targeted by choosing alternative low cost pore modification agents during membrane fabrication.

3.3.5 Fitness of standard pore blocking models

Figure 3.8 presents the best fit models for all membranes at distinct feed concentrations. Corresponding parameters associated to correlation coefficient, slope and intercept of the best fit fouling models for all membranes is presented in Table 3.4. Thus, it is apparent that except for a single case for the CM3 membrane, all other cases correspond to the existence of pore blocking mechanisms, which can significantly contribute towards irreversible membrane fouling. However, very high trans-membrane flux values were obtained for the CM3 membrane for a short total MF run time period of 10 - 12 min, which indicates that the CM3 membrane provided lowest insitu fouling. Also, the fitness of cake filtration model for the CM3 membrane at highest feed concentration is indicative towards lower irreversible membrane fouling. In summary, the variation in best fit models for variant feed concentrations and membrane morphology (or average pore size) is indicative towards the complexity associated with morphology and activity of microbes.

Based on general rule of thumb, CM3 membrane should undergo maximum membrane fouling during the MF operation, which is not the case. This is indicative to the fact that the dynamic cake filtration layer formed on the membrane surface behaved distinctly for different membrane pore sizes. While the cake filtration layer for the CM1 - CM2 membrane restricted the membrane flux, it favoured higher membrane flux for the CM3 membrane. Thus, it can be analyzed that the dynamic microbial cake filtration layer morphology is a strong function of the membrane morphology. Thus, it is apparent that larger average pore size of the membrane is favourable to achieve good properties of the dynamic microbe based cake filtration layer that develops during the MF operation.

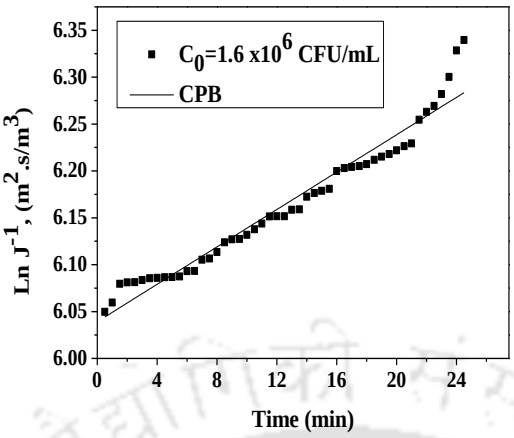

(a)

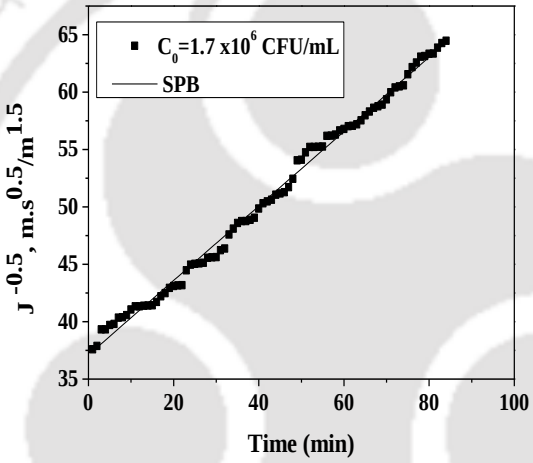

(b)

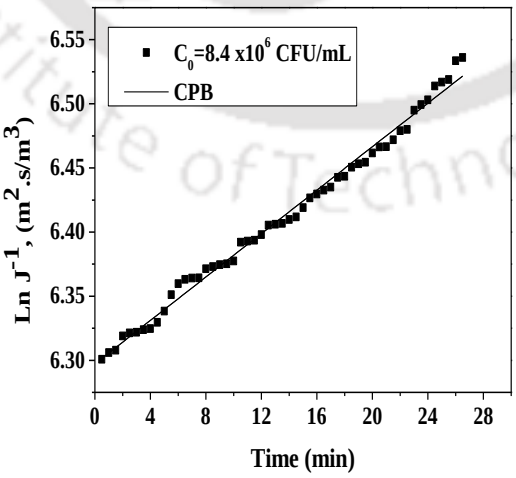

(c)

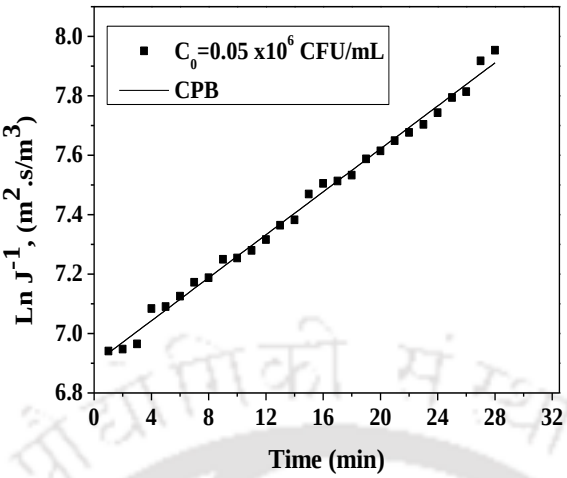

(d)

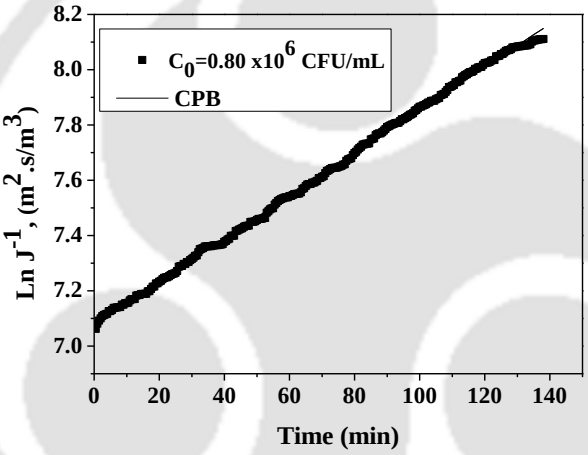

(e)

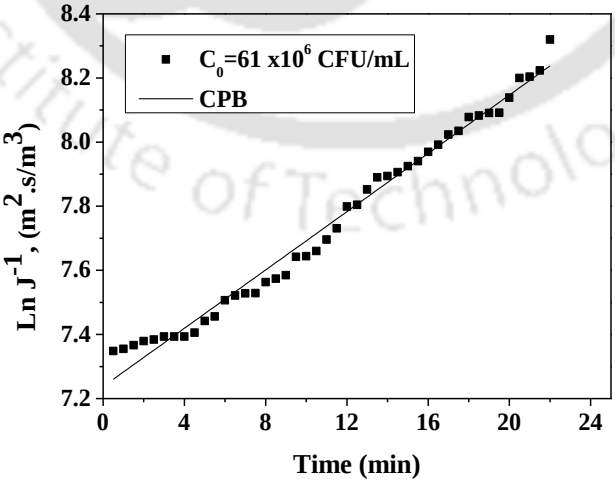

(f)

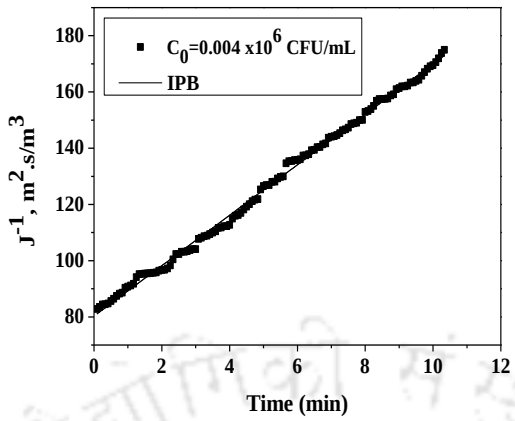

(g)

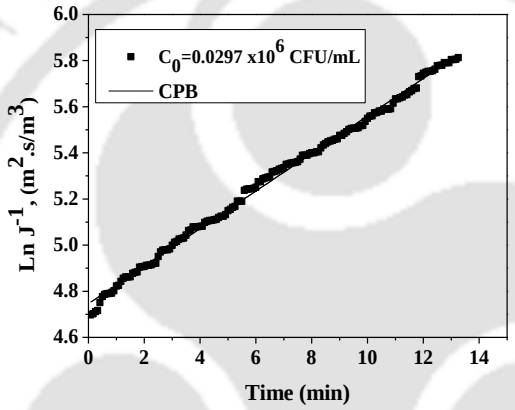

(h)

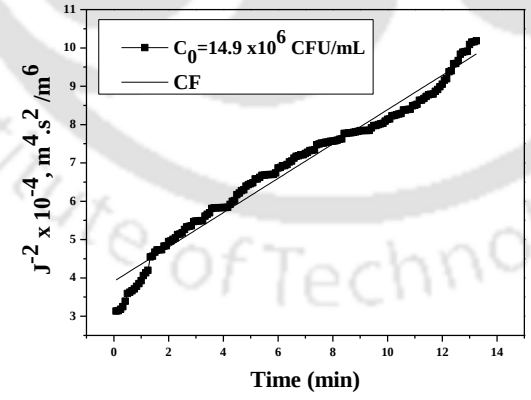

(i)

Figure 3.8: Cake filtration fitness plots for dead end MF flux data of various membranes: CM1 - (a-c); CM2 – (d –f) and CM3 (g – i).

Table 3.4: Summary of fouling model parameters for all membranes during dead end MF at ΔP = 206.7 kPa.

Membrane type	Feed Concentration (CFU/mL) × 10^6	Complete pore blocking			Standard pore blocking			Intermediate pore blocking			Cake filtration		
		$k_b \times 10^{-4}$	$\ln(J_0^{-1})$	R^2	$k_s \times 10^{-4}$	$J_0^{-0.5}$	R^2	$k_i \times 10^{-4}$	J_0^{-1}	R^2	k_c	J_0^{-2}	R^2
CM1	1.6	2	6.04	0.954	18	20.45	0.947	800	416.48	0.938	77	170247	0.919
	1.7	2	7.29	0.994	54	37.10	0.995	5522	1243.5	0.987	2999	37024	0.952
	8.4	1	6.30	0.991	17	23.28	0.990	863	540.26	0.988	106	288205	0.981
CM2	0.05	6	6.90	0.994	124	30.54	0.987	10386	842.79	0.970	3777	25105	0.910
	0.80	1	7.08	0.999	29	33.39	0.995	2702	1005.7	0.982	1190	8101.4	0.937
	61	8	7.24	0.985	185	36.16	0.974	18363	1180.8	0.955	9341	64964	0.899
CM3	0.004	12	4.44	0.991	67	9.11	0.996	1494	80.29	0.997	38	4956.4	0.987
	0.0297	14	4.75	0.997	96	10.41	0.995	2747	97.89	0.983	118	8.82	0.930
	14.9	6	5.32	0.917	46	14.25	0.937	1464	201.75	0.953	75	39092	0.974

The data presented in this work corresponds to flux measurements carried out using batch microfiltration cell using membranes with very high water permeability. About 50 - 60 batches of microfiltration run were conducted in a span of 100 minutes for some membranes. However, the reduction in membrane flux after 10 batches is significantly low. This indicates that the membranes are promising for commercial applications. Further flux data was not measured, as it did not contribute significantly towards additional flux decline.

Figure 3.9(a - c) depict parity plots for the fitness fouling models to represent measured experimental MF flux data for membranes CM1 - CM3 respectively. It can be observed that all best fit fouling models had very good fitness with the measured flux data. The maximum and minimum errors have been evaluated to vary from 6 - 7% and 0.002 - 0.007% respectively for membranes CM1 - CM3. Corresponding RMS error values were evaluated to vary in the range of 1.43 - 1.81%.

3.4 Membrane Cost

Based on retail cost of the materials, the average cost of the fabricated membranes is about 62 $/m^2. Procedures adopted for the retail conceptual cost analysis are presented in Appendix B. Inclusive of other fabrication costs such as electrical and labor costs, the average cost of fabricated membranes is estimated to be about 80 $/m^2. Typical ceramic filter candles for gravity fed applications have a dimension of 7×10^{-2} m length and 2×10^{-2} m dia. This corresponds to a membrane surface area of 4.71×10^{-3} m^2. Each ceramic pot filter costs about 1.19 $. Thereby, the retail cost of the ceramic pot filter has been evaluated as 251 $/m^2. Thus, the fabricated

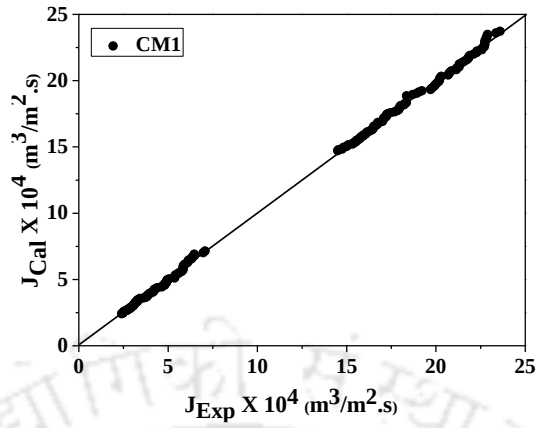

(a)

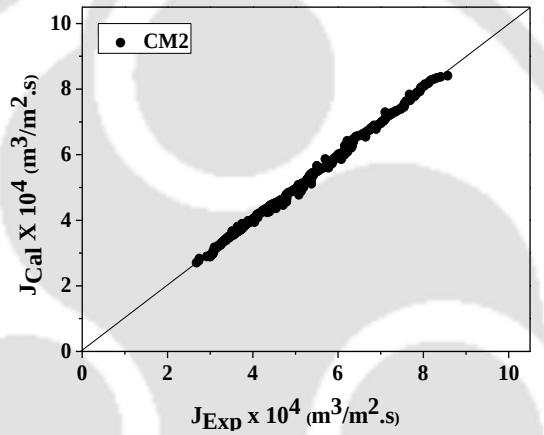

(b)

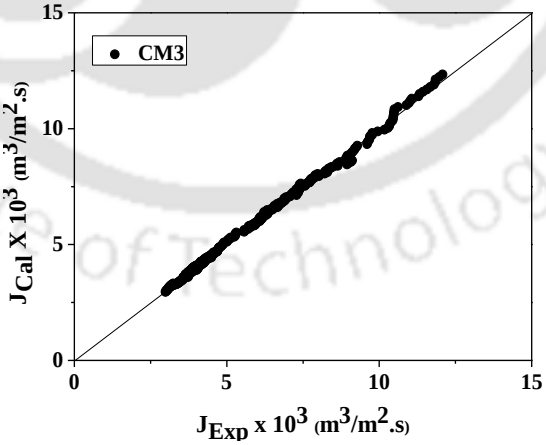

(c)

Figure 3.9: Parity plots for measured and best fit fouling model flux for (a) CM1 (b) CM2 and (c) CM3 membranes.

membranes are about 70% less expensive in comparison with the commercially available membranes. With respect to other incurred costs during operation, both for CM1 and CM2 membranes, additional costs are incurred to provide sufficient pressure. But the CM3 membrane with wider pore size is envisaged to be applicable for gravity fed application. Thus, CM3 membrane is inferred to be the low cost membrane for gravity fed application as a ceramic pot filter.

3.5 Summary

Among all membranes, for the chosen feed concentrations, CM3 membrane provided promising performance during dead end MF of synthetic microbial suspensions. For a feed concentration of 14.9×10^{6} CFU/mL, and for a time of 10 min, the membrane flux and separation efficiency (LRV) was 3.51×10^{-3} $m^3/m^2.s$ and 6 respectively. For chosen high feed concentrations, all membranes underwent significant fouling, but CM3 membrane provided considerable flux even after significant amount of fouling. The separation efficiency of the membranes has been evaluated to be a strong function of the dynamic cake filtration layer morphology which is in turn a function of the chosen membrane morphology. While CM1 and CM2 membranes provided higher LRV for chosen higher feed concentrations, they fouled significantly. Therefore, it is expected that CM1 and CM2 membranes are applicable for lower feed concentration with lower fouling. However, in such a case, PRV values of the membranes may not be close to 100%, given the fact that the bio-film under those operating conditions may not be able to serve as a dynamic filter aid to promote the retention of the microbes. All in all, it is apparent that the membrane morphology strongly influences insitu membrane fouling (and flux) and the separation efficiency (LRV) during the MF of synthetic microbial solutions.

Chapter 4:

Cross Flow Microfiltration Performance of Low Cost Ceramic Membranes

Cross Flow Microfiltration Performance of Low Cost Ceramic Membranes

After a brief overview of cross flow microfiltration studies in section 4.1, section 4.2 presents the flux and removal efficiency characteristics of the low cost ceramic membranes possessing diverse membrane morphologies (average pore size of 0.7 - 4.5 μm). Section 4.3 summarizes the time dependent permeation resistance profiles and its subsequent analysis using the resistance in series in model. Section 4.4 presents the average fouling index values of the membranes during microfiltration studies. Finally, section 4.5 presents a summary of the cross flow microfiltration data.

4.1 Overview

Apart from dead end Microfiltration (MF) studies, cross flow MF studies have been conducted for low cost membranes CM1 - CM3. The objective of the cross flow MF studies is to evaluate the real time performance of the prepared membranes for bacteria filtration applications as cross flow MF operation is widely followed in commercial membrane installations. The major emphasis of the experimental investigations is to evaluate the flux, removal efficiency and fouling characteristics and thereby identify optimal combinations of feed concentrations and morphologies for which membranes undergo lower insitu fouling. Another objective of the cross flow MF studies it to examine the separation potential of the low cost ceramic membranes in terms of the LRV.

Due to infeasibility of standard pore blocking models to represent the pertinent flux decline trends, resistances in series model has been adopted for the flux decline analysis. The resistances in series model has been targeted to evaluate the contributions of fouling resistances to the overall hydraulic resistance during cross flow MF.

4.2 Flux and Rejection characteristics

4.2.1 Flux

The bacterial flux decline profiles for CM1, CM2 and CM3 membranes have been presented in Figure 4.1 a, b and c respectively. For all cases, cross flow MF studies were conducted after compaction with Millipore water. For a variation in time from 5 – 150 min, it can be observed in Figure 4.1 (a) that the CM1 membrane flux reduced from 2.54×10^{-4} - 2.92×10^{-5}, 2.21×10^{-4} - 2.93×10^{-5} and 1.41×10^{-4} - 2.77×10^{-5} $m^3/m^2.s$ for 2.80×10^5, 4.40×10^5 and 15.2×10^5 CFU/mL feed concentrations respectively. For all cases, the flux decline can be observed to be significant during the first 65 min., which reached to the steady state value at about 120 min. Despite having significant variations in the initial flux, the final flux has been evaluated to be almost independent of the initial concentrations and is indicative towards similar morphology of the fouled CM1 membrane after prolonged MF experimental run.

Figure 4.1 (b) illustrates the flux decline profiles for CM2 membrane at various feed concentrations. For a variation in time from 5 - 150 min, it has been evaluated that the CM2 membrane flux varied from 2.24×10^{-4} - 1.59×10^{-5}, 1.91×10^{-4} - 1.45×10^{-5} and 1.65×10^{-4} - 1.34×10^{-5} $m^3/m^2.s$ with a variation in bacterial concentrations from 2.52×10^5, 6.80×10^5 and 40.4×10^5 CFU/mL respectively. It can be further observed that the flux decline profiles are distinct initially up to 100 min. after which the steady state values are very close for all feed

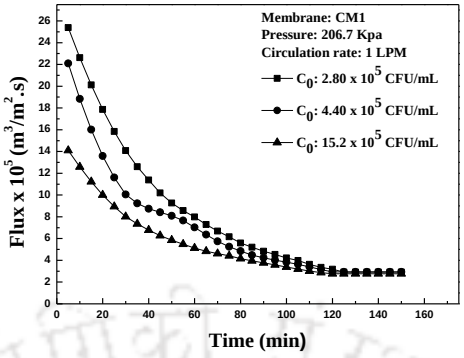

(a)

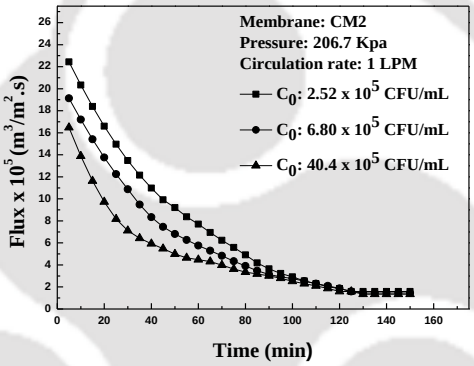

(b)

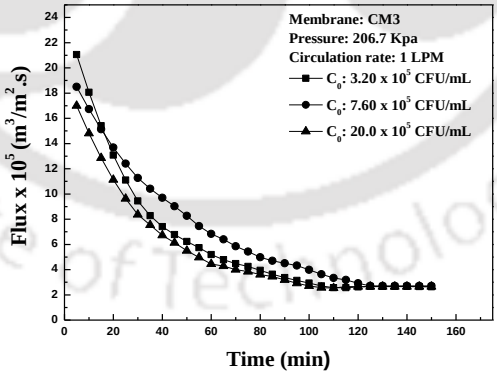

(c)

Figure 4.1: Variation of cross flow MF flux with time at ΔP = 206.7kPa: (a) CM1, (b) CM2 and (c) CM3 membrane.

concentrations. Compared to CM1 membrane, CM2 membrane took higher time to reach steady state. This is possibly due to its wider pore size which enabled significant fouling to occur in comparison with the CM1 membrane.

For CM3 membrane, the time dependent flux is presented in Figure 4.1 (c). As shown, for a variation in time from 5 - 150 min, the flux varied from 2.11×10^{-4} - 2.64×10^{-5}, 1.85×10^{-4} - 2.71×10^{-5} and 1.70×10^{-4} - 2.65×10^{-5} $m^3/m^2.s$ for feed concentrations of 3.20×10^5, 7.60×10^5 and 20.0×10^5 CFU/mL respectively. During the initial stages of cross flow MF, the intermediate concentration of 7.60×10^5 CFU/mL gave lower flux but eventually better flux profiles than those obtained for feed concentrations of 3.20×10^5 and 20.0×10^5 CFU/mL. This indicates that the initial fouling of the membrane assisted towards better morphology of the fouled membrane during the later stages of the cross flow MF. Highest membrane flux was obtained for CM3 membrane due to its highest pore size. Flux comparison plots for various fixed choices of feed concentrations cannot be presented due to difficulty in precisely controlling the feed concentration. From flux decline analysis, the membrane choice is in the order of CM3>CM2>CM1 which is in accordance with the hypothesis that the wider pore size membrane even after undergoing substantial fouling can provide better fluxes.

4.2.2 Removal efficiency

Figure 4.2 a, b and c present the removal efficiency plots of various permeate capacities (250, 500 and 750 mL) for CM1, CM2 and CM3 membranes and different feed concentrations. The removal efficiency is being expressed in terms of $\log_{10}$ reduction value (LRV) which was introduced by Simonis and Basson (2011) to quantify the separation potential of filtration media. For the CM1 membrane, the LRV varied from 6 - 3.5, 4 - 6 and 6 for 2.80×10^5, 4.40×10^5 and

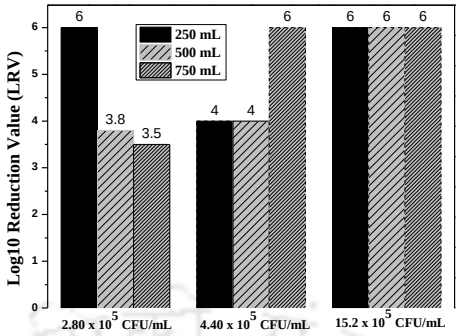

(a)

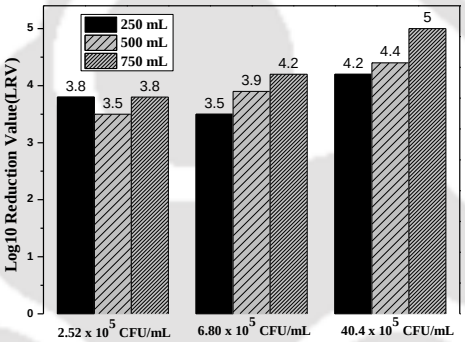

(b)

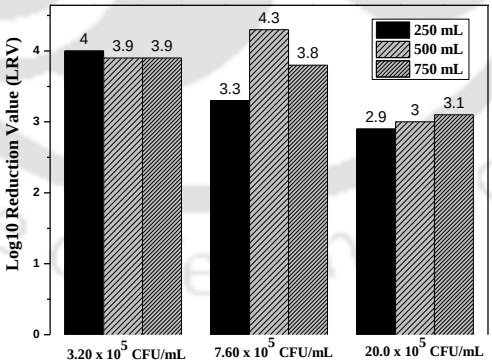

(c)

Figure 4.2: Variation of permeate quality (LRV) with permeate capacity (mL) during cross flow MF: (a) CM1, (b) CM2 and (c) CM3 membrane.

15.2×10^5 CFU/mL feed concentrations respectively. Thus, an increase in feed concentration enabled an increase in LRV or removal efficiency. For the CM2 membrane, the LRV varied from 3.5 - 3.8, 3.5 - 4.2 and 4.2 - 5 for 2.52×10^5, 6.80×10^5 and 40.4×10^5 CFU/mL feed concentrations respectively (Figure 4.2 b). These LRV values were significantly lower than those obtained for CM1 membrane and similar feed concentrations. Similarly, for the CM3 membrane (Figure 4.2 c), the LRV varied from 3.9 - 4, 3.3 - 4.3 and 2.9 - 3.1 for feed concentrations of 3.20×10^5, 7.60×10^5 and 20.0×10^5 CFU/mL respectively. These LRV values are similar or inferior to those obtained with CM2 membrane and significantly lower than those obtained for the CM1 membrane. Hence, the separation efficiency of various membranes is in the order of CM1>CM2>CM3. This is in agreement with the hypothesis that larger pore size membranes provided lower LRV and vice-versa.

For commercial applications, both flux and LRV needs to be judged and membranes that do not undergo significant fouling and that provide acceptable LRV have to be identified for further experimental investigations and pilot plant studies. Considering these issues, the optimal choice for CM1 membrane is lower feed concentration of 2.80×10^5 CFU/mL where LRV values of 3.5 - 6 have been achieved. For high concentration of 20×10^5 CFU/mL, despite obtaining low LRV, CM3 membrane is recommended due to its lower fouling ability.

4.3 Analysis of fouling resistances using resistances in series model

The variation of total fouling resistance (R_f) with time at various feed concentrations for CM1, CM2 and CM3 membranes is presented in Figure 4.3 a, b and c respectively. As shown, for the CM1 membrane, the time dependent R_f varied from 6.97×10^5 - 6.97×10^6, 6.40×10^5 - 6.77×10^6

and 1.34 - 7.34×10^6 m^2.s.kPa/m^3 for 2.80×10^5, 4.40×10^5 and 15.2×10^5 CFU/mL feed concentrations respectively. Thereby, the graph indicated that the fouling resistance profiles were lowest for low feed concentration and highest for high feed concentration. For CM2 membrane (Figure 4.3 c), the R_f varied from 1.86×10^4 - 1.21×10^7, 7.52 $\times10^5$ - 1.40×10^7 and 9.15×10^5 - 1.51 $\times10^7$ m^2.s.kPa/m^3 for 2.52×10^5, 6.80×10^5 and 40.4×10^5 CFU/mL feed concentrations respectively. These fouling resistance profiles are similar to those obtained for the CM1 membrane. For CM3 membrane (Figure 4.3 e), the R_f varied from 6.98×10^5 - 7.28 $\times10^6$, 1.29×10^5 - 6.66 $\times10^6$ and 6.18×10^5 - 7.48×10^6 m^2.s.kPa/m^3 for 3.20×10^5, 7.60×10^5 and 20.0×10^5 CFU/mL feed concentrations respectively. Based on the time dependent R_f values, it can be observed that the intermediate feed concentrations gave highest membrane flux. The reason for the same would be presented later in this section.

While R_f profiles can be analyzed to evaluate upon the optimality of feed concentration and membrane selection, they may be misleading as well. Therefore, to get an accurate account of the fouling resistances, plots of time dependent variation of R_f / R_t have been prepared and have been presented in Figure 4.3 b, d and f for CM1, CM2 and CM3 membranes respectively. These plots provided significantly different insights with respect to the optimality of membrane and feed concentration choices. For CM1 membrane, Figure 4.3 (b) depicts the R_f / R_t increased from 85.43 - 98.17%, 68.28 - 95.79% and 91.09 - 98.25% for 2.80×10^5, 4.40×10^5 and 15.2 $\times10^5$ CFU/mL feed concentrations respectively. The graph indicates that the resistances ratio profile is highest for low feed concentration and lowest for intermediate solution concentration. This is possibly due

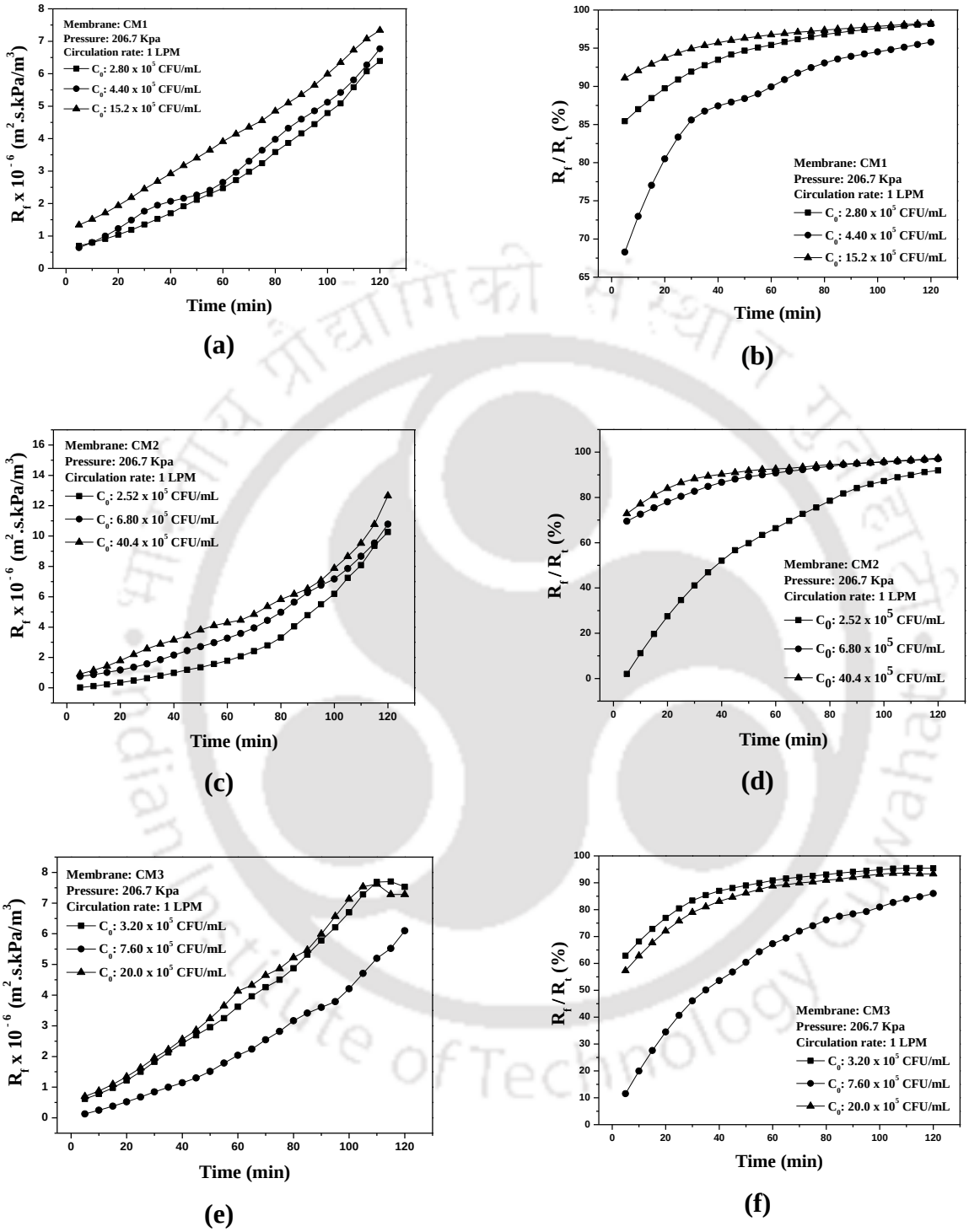

Figure 4.3: Variation of cross flow MF fouling membrane resistance (R_f) and % (R_f/R_t) with time for various feed concentrations: CM1 - (a-b); CM2 - (c-d); and CM3 - (e-f).

to the variations in the membrane fouling and dynamic variations of the bio film morphology with time. It is further interesting to note that the internal membrane fouling strongly affects the dynamic morphology of the bio-film with time and the optimality of internal membrane fouling could indicate the optimality of the bio-film for membrane flux. Nonetheless, based on obtained analysis from the resistances in series model, the CM1 membrane cannot be recommended for microfiltration of bacterial solutions with chosen feed concentrations as the (R_f / R_t) varied very high from 68 - 98%. Therefore, despite providing high LRV values and good separation potential, the CM1 membrane cannot be recommended for bacteria filtration applications due to its substantial fouling.

For the CM2 membrane (Figure 4.3 d), the R_f / R_t varied from 2.02 - 91.91%, 69.49 - 97.03% and 72.86 - 97.38% for feed concentrations of 2.52×10^5, 6.80×10^5 and 40.4×10^5 CFU/mL respectively. The obtained fouling resistances ratio profiles indicated that the profiles are highest for highest feed concentration and lowest for lowest feed concentration. Also, it can be observed that the fouling resistances ratio profiles for intermediate and highest feed concentration are located close to one another. In contrast to the CM1 membrane, the CM2 membrane provided lower fouling values for the intermediate feed concentration during the initial stages of the cross flow MF run. Therefore, for the CM2 membrane, since low fouling was achieved, lowest feed concentration of 2.52×10^5 CFU/mL is applicable for commercial applications of bacteria filtration.

Further for the CM3 membrane (Figure 4.3 f), R_f / R_t varied from 62.88 - 95.38%, 11.51 - 86.03% and 57.30 - 93.33% for feed concentrations of 3.20×10^5, 7.60×10^5 and 20.0×10^5

CFU/mL. The fouling resistance profiles for CM3 membrane are distinct in comparison with those obtained for CM1 and CM2 membranes. For the CM3 membrane, the intermediate feed concentration of 7.60×10^5 CFU/mL provided lowest fouling resistance. This is explained with the following hypothesis. For the chosen low feed concentration, the membranes underwent substantial pore blocking within their morphology and the dynamic cake filtration layer as well as internally fouled membrane significantly restricted the passage of the permeate with time. For the highest feed concentration, cake filtration layer might have had very poor morphology and could have completely blocked the wider pores of the membranes. Due to this reason, the membrane flux would have been poor. On the other hand, for the intermediate feed concentration, the membrane internal fouling and dynamic morphology of the cake filtration layer is optimal to enable higher membrane flux. Therefore, among all membranes, CM3 membrane is the optimal choice along with a feed concentration of 7.60×10^5 CFU/mL, where lowest fouling resistance profiles have been obtained.

In summary, the fouling resistances ratio profiles gave significant insights into the competence of membrane average pore size and feed concentration parameters. These insights are relevant for the ongoing research in the field of low cost ceramic membranes based cross flow microfiltration of bacteria solutions.

4.4 Average fouling index

The time dependent variation of average fouling index profiles for CM1, CM2 and CM3 membranes is presented in Figure 4.4 a, b and c respectively. As shown, for the CM1 membrane, the time dependent average fouling index values varied from 86.97 - 94.50, 72.81 - 88.72 and

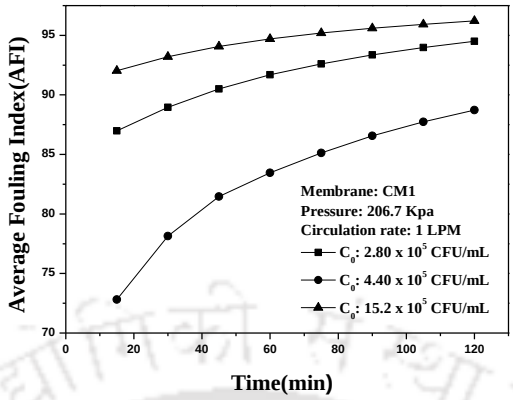

(a)

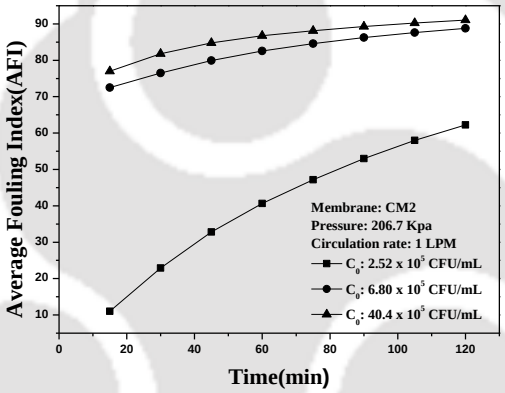

(b)

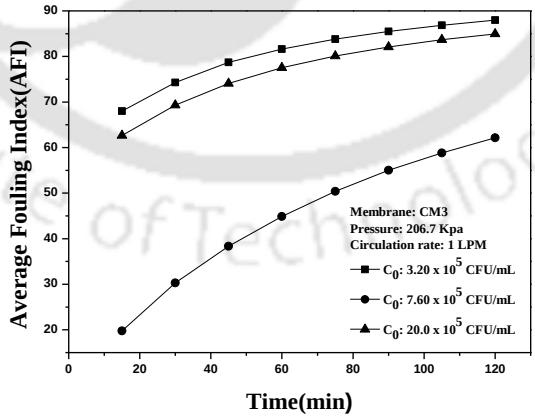

(c)

Figure 4.4: Variation of cross flow MF average fouling index (AFI) for (a) CM1 (b) CM2 and (c) CM3 membranes.

Table 4.1: A summary of various parameters obtained during cross flow MF at ΔP = 206.7kPa.

Membrane type	Feed Concentration (CFU/mL) $\times 10^5$	Pure water flux ($m^3/m^2.s$)	Initial flux of bacterial solution ($m^3/m^2.s$)	AFI	Removal Efficiency (LRV)
CM1	2.80	2.32×10^{-3}	2.54×10^{-4}	86.97- 94.50	3.5 - 6
	4.40	9.29×10^{-4}	2.21×10^{-4}	72.81- 88.72	4 - 6
	15.2	2.11×10^{-3}	1.41×10^{-4}	92.02- 96.21	6
CM2	2.52	3.05×10^{-4}	2.24×10^{-4}	11- 62.25	3.5 - 3.8
	6.80	8.36×10^{-4}	1.91×10^{-4}	72.51- 88.79	3.5 - 4.2
	40.4	8.09×10^{-4}	1.65×10^{-4}	77- 91.08	4.2 – 5
CM3	3.20	7.56×10^{-4}	2.11×10^{-4}	68- 87.97	3.9 - 4
	7.60	2.79×10^{-4}	1.85×10^{-4}	19.74- 62.14	3.3 - 4.3
	20.0	5.31×10^{-4}	1.70×10^{-4}	62.65- 84.96	2.9 - 3.1

92.02 - 96.21 for feed concentrations of 2.80×10^5, 4.40×10^5 and 15.2×10^5 CFU/mL respectively. For the CM2 membrane, these values varied for 11 - 62.25, 72.51 - 88.79 and 77 - 91.08 for feed concentrations of 2.52×10^5, 6.80×10^5 and 40.4×10^5 CFU/mL respectively. For the CM3 membrane, the average fouling index values varied from 68 – 87.97, 19.74 – 62.14 and 62.65 – 84.96 for feed concentrations of 3.20×10^5, 7.60×10^5 and 20.0×10^5 CFU/mL respectively. The obtained average fouling index trends are similar to those presented for the resistances ratio profiles in Figure 4.3 b, d and f. Possible reasons for the observed variations in the trends are similar to those presented in the previous sub-section. Based on the AFI profiles, the optimal membrane and feed concentration corresponds to CM2 membrane and low feed concentration and CM3 membrane with intermediate feed concentration. A summary of obtained membrane

data including AFI values, removal efficiency, initial flux for bacterial solutions, feed concentrations etc., for various membranes is presented in Table 4.1. Among all cases, AFI values are minimal for CM2 membrane and CM3 membrane at low and intermediate feed concentrations respectively.

4.5 Summary

The cross flow MF studies for CM1- CM3 membranes provided valuable insights. The CM1 and CM2 ceramic membranes provided 99.99 - 99.9999% removal efficiency which is quite high in comparison to the CM3 ceramic membrane (99.9 - 99.99%). However, despite obtaining high LRV values for the CM1 membrane, it is not the optimal choice due to significant fouling. The resistances in series model is a valuable tool to identify the extent of insitu fouling during cross flow MF and has indicated that misleading inferences can be deduced by carrying out total fouling resistance analysis but not analysis of the various resistances. Based on extensive experimental investigations, the cross flow MF studies indicated that CM3 membrane with intermediate feed concentration is the optimal choice and despite obtaining low LRV values it needs to be considered due to very low fouling tendencies. The next choice for the optimal membranes is the CM2 membrane which also gave low values of the AFI in comparison with both CM1 and CM3 membranes. Compared to CM1 and CM2, CM3 gave lower fouling for all feed concentrations. Considering these insights, the cross flow MF studies have indicated that promising opportunities exist for low cost ceramic membranes for the microfiltration of bacterial solutions.

Chapter 5:

Identification of Optimal Rate Enhanced Silver ELP Processes for Silver-Ceramic Composite Fabrication

Chapter 5

Identification of Optimal Rate Enhanced Silver ELP Processes for Silver-Ceramic Composite Fabrication

Section 5.1 summarizes various targeted objectives of rate enhanced Ag ELP processes for the fabrication of low cost silver-ceramic composite membranes. Section 5.2 elaborates with respect to the results obtained during preliminary set of investigations carried out for CEP, SIEP, SOEP and SSOEP processes for the membrane fabrication. Eventually, for the identified optimal processes (SOEP and SSOEP), few other parametric investigations were carried out and their results are presented in sections 5.2 and 5.3 respectively for SOEP and SSOEP processes. Section 5.4 summarizes results obtained from few surface characterization studies such as FESEM and XRD. Finally, section 5.5 presents a summary of the chapter.

5.1 Targeted Objectives

Conventional and rate enhanced ELP processes such as CEP, SIEP, SOEP and SSOEP were investigated to identify optimal processes for low cost silver-ceramic composite membranes. Conversion, efficiency, percent pore densification (PPD) and metal loading index (MLI) have been regarded to be the plating process variables with which optimal processes are being identified. Among these variables, PPD is not highly relevant given the fact that porous composite membranes were fabricated and PPD values would not be significantly high. Similarly, conversion does not also account for the efficacy of the ELP process due to its inability to provide insights with respect to the quality of the plating. Hence, efficiency and MLI have been regarded to be important variables and ideally for similar process parametric

conditions (silver solution and reducing agent concentration) for alternate ELP processes, both efficiency and MLI should be significantly high.

During Ag ELP, a reduction in efficiency could be due to significant metal attrition from the ceramic membrane surface which eventually contributes to significant metal nucleation in the solution and hence poor efficiency values. The MLI value should be as high as possible and is a potential indicator for the metal attrition effects. An ELP process with high MLI profile indicates lower metal attrition from the ceramic surface during Ag ELP. Thus, the efficacy of rate enhanced Ag ELP process is an interesting field of research. Also, it is important to note that both efficiency and MLI may indicate similar trends i.e., processes with higher time dependent efficiency profiles could have higher time dependent MLI profiles. Nonetheless, these are two diverse characterization parameters as efficiency is related to the process performance and MLI is related to the product development (low cost porous silver-ceramic composite membrane). The experimental investigations for the identification of optimal rate enhanced Ag ELP processes were carried out with a systematic hierarchy. The first set of experiments were carried out as preliminary set of investigations to identify the most competent processes among CEP, SOEP, SIEP and SSOEP. For these investigations, 0.01 Ag ELP baths were adopted. Eventually, for identified rate enhanced ELP processes, few parametric investigations were carried out to identify the role of some important parameters in influencing the combinatorial plating characteristics. For all cases, bulk mode of hydrazine reducing agent addition has been adopted and CM3 membranes were used as membrane supports for porous metal ceramic membrane fabrication.

In the next section, the results obtained for the preliminary set of experimental investigations for CEP, SIEP, SOEP and SSOEP Ag ELP processes are presented based on the insights obtained from such investigations. A comparative assessment with literature data is not possible due to the non-availability of such data. This is also due to the fact that there has been no literature available till date with respect to the fabrication engineering aspects of porous Ag-ceramic composite membranes using electroless plating technique or any other technique such as magnetron sputtering.

The working principle of various rate enhanced ELP processes is presented as follows:

a) **SOEP**: During sonication induced Ag ELP, cavitation effect occurs due to which plating rate enhancement contributes to the faster deposition of Ag metal on the seeded porous substrate surface. However, previous works Bulasara et al. (2012a) and Agarwal et al. (2014b) have highlighted that SOEP is effective to enhance metal deposition but not pore densification. Such an option would be highly relevant for porous metal-ceramic composite membrane since higher PPD significantly reduced porosity.

b) **SIEP**: During surfactant induced Ag ELP using CTAB surfactant, the surfactant enables the reduction of interfacial tension at the ceramic support and solution interface. Thereby, gas bubbles generated during the plating reaction would be smaller in size and would slowly leave the membrane surface without causing significant mechanical stress. Hence, SIEP process has been documented in the literature to reduce pitting effect which refers to the formation of pits or uncovered portions of the ceramic support surface due to mechanical stresses caused during conventional metal deposition. On the other hand, competitive adsorption of surfactant to the ceramic support is a significant problem

during SIEP and complex tradeoffs could exist due to which the process may not be optimal. Thus, it would be interesting to examine these for Ag SIEP baths.

c) **SSOEP**: The SSOEP process facilitates additional cavitation effect to an SIEP Ag ELP bath. Due to this, the SSOEP process could enable significant rate enhancement by reducing competitive CTAB adsorption to the ceramic support surface. Thereby, SSOEP has been evaluated to provide optimal performance in previous works (Agarwal et al., 2014a) for dense Ni-ceramic composite membrane fabrication. Therefore, in the context of Ag ELP for porous Ag-ceramic composite membrane fabrication, SSOEP process assumes paramount relevance and the obtained results for the process could infer upon the optimality of the process in conjunction with other processes such as CEP, SIEP and SOEP processes.

5.2 Combinatorial plating characteristics of Ag ELP processes

5.2.1 Conversion and efficiency profiles

The time dependent conversion profiles for CEP, SOEP, SIEP and SSOEP processes are illustrated in Figure 5.1 (a). As shown, for the CEP process, the conversion varied from 80 – 61% for a variation in plating time from 1 – 3 h. On the other hand, for rate enhanced ELP processes such as SOEP, SIEP and SSOEP processes provided better conversion profiles. For SOEP, SIEP and SSOEP processes, the conversions varied from 83 – 83%, 73 – 76% and 84 – 83% respectively for a variation in plating time from 1 – 3 h. Among all processes, SOEP and SSOEP provided better conversion profiles. It is further interesting to note that the SIEP process

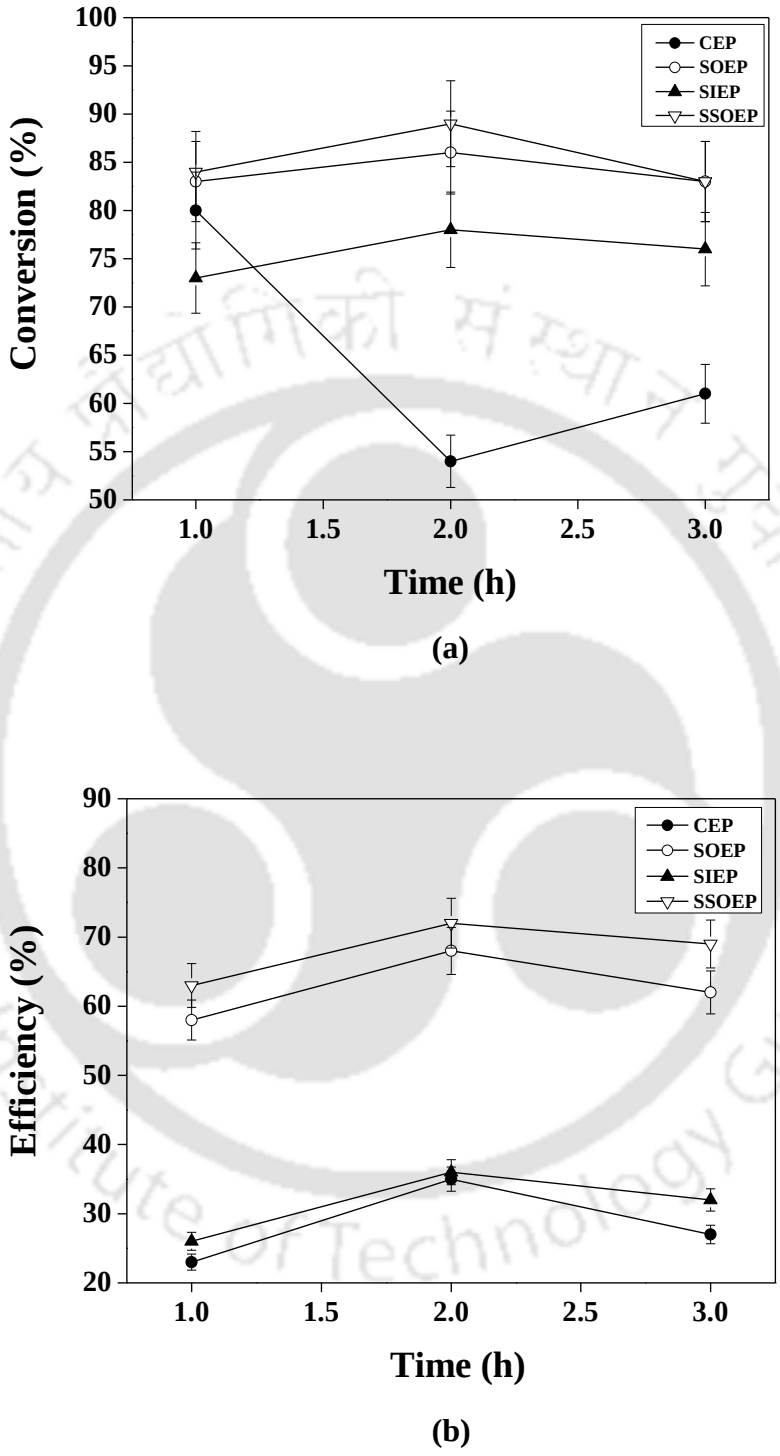

Figure 5.1: Variation of (a) Conversion and (b) Efficiency with time for Ag CEP, SOEP, SIEP and SOEP processes.

despite being rate enhanced only provided moderate conversion profiles. This could be due to significant metal nucleation in the solution due to significant metal attrition from the ceramic support. The significant metal attrition from the ceramic support could be due to competitive adsorption of CTAB and metal ion on the support surface due to which adhesion strength of the metal film could be poor.

In summary, based on conversion profiles, SOEP and SSOEP processes performed better than CEP and SIEP processes. It is further interesting to note that the conversion profiles of SSOEP baths are far better than the SIEP process. In other words, it is apparent that the metal attrition from the ceramic support could be significantly reduced by the induced cavitation affect during Ag ELP with SSOEP process. In summary, sonication can be seen as a potential rate enhancement technique with which even competitive surfactant adsorption to the ceramic support surface can be altered and maximum conversions can be obtained. The obtained conversion profile trends are in agreement with the results reported by Agarwal et al. (2013) who also inferred that SSOEP baths provide optimal conditions for dense nickel ceramic composite membrane fabrication.

Figure 5.1 (b) presents the time dependent variation of efficiency profiles for CEP, SIEP, SOEP and SSOEP Ag ELP baths during bulk addition of the reducing agent. It is interesting to note that despite using significantly excess quantity of the reducing agent, the rate enhanced ELP processes provided good efficiency values. This is indicative to the fact that hydrazine undergoes instantaneous decomposition during plating and its concentration in the solution could be significantly lower than that evaluated based on the concept of the limiting reactant. Conceptually, inferences similar to those obtained for conversion profiles can be drawn from the

time dependent efficiency profiles. For a variation in plating time from 1 – 3 h, the efficiency varied from 23 – 27%, 58 – 62%, 26 – 32% and 63 – 69% for CEP, SOEP, SIEP and SSOEP Ag ELP baths. Thus, the efficiency based performance of the Ag ELP baths is in the order of SSOEP>SOEP>SIEP>CEP. Also, it can be observed that for SIEP process, the conversion profiles are significantly lower than those obtained for SOEP and SSOEP processes. This observation is in agreement with the conversion profiles for the said processes in Figure 5.1 (a). Thus, efficiency profiles confirmed the hypothesis that metal attrition from the ceramic support surface during plating is significant during SIEP process due to which it cannot be recommended for porous Ag-ceramic composite membrane fabrication. Thereby, poor adhesion of Ag with the ceramic support is evident which might be due to competitive adsorption of CTAB surfactant to the ceramic support surface.

5.2.2 PPD and Metal Loading Index (MLI) profiles

The time dependent variation of PPD for CEP, SOEP, SIEP and SSOEP is presented in Figure 5.2 (a). As shown, the profiles do not indicate a definitive trend among processes and convey the complexity of the PPD variation with time and rate enhancement technique. For the CEP, the PPD steadily increased from 2.8 – 9.7% with an increasing in plating time from 1 – 3 h. However, for the SOEP process, the PPD initially increased from 2 – 7.6% from 1 – 2 h of plating which eventually decreased to 5.7% for a plating time of 3 h. The reduction in PPD at longer plating times is indicative towards significant variation in film morphology. For SIEP, the PPD reduced initially with time (from 6.2 – 3.7% for a variation in plating time from 1 – 2 h) which later increased to 8% for a plating time of 3 h. For the SSOEP, the PPD reduced with

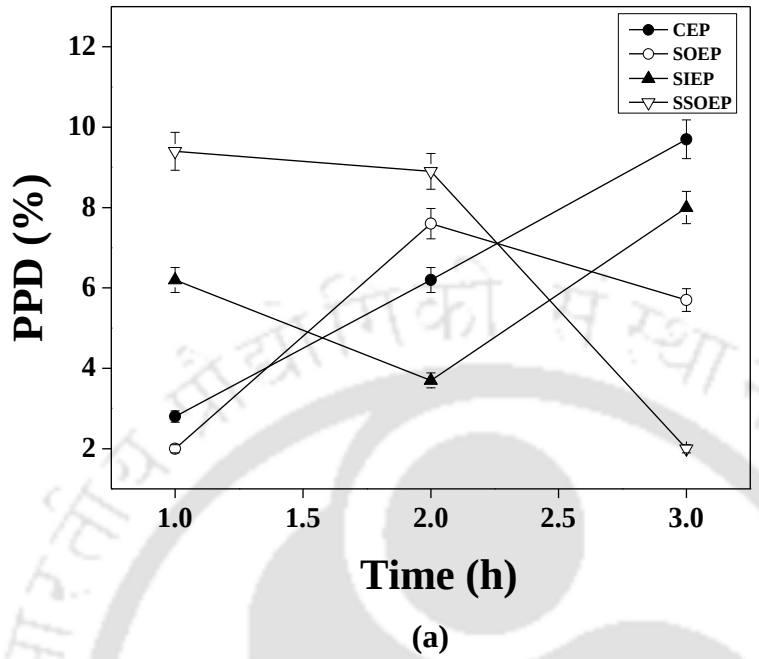

(a)

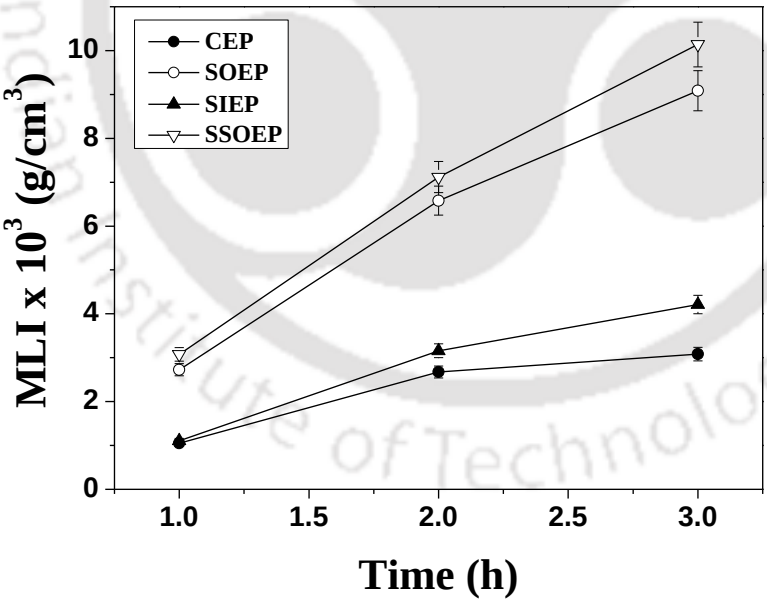

(b)

Figure 5.2: Time dependent variation of (a) PPD and (b) MLI for Ag CEP, SIEP, SOEP and SSOEP processes.

plating time. This indicates that the film porosity increased with plating time which could be due to substantial variation in the structural distribution of Ag metal on the ceramic support. The same can be only confirmed after evaluating the metal loading index. Overall, the PPD values varied from 2 – 9.7% for all processes and have clearly indicated the fabrication of porous silver-ceramic membranes. This is not the case in the literature where dense metal ceramic composite membranes have been reported (Agarwal et al., 2014a; Bulasara et al., 2012b). Hence, a comparative assessment of literature data and the data obtained in this work is not relevant, given the fact that literature data refers to dense nickel-ceramic composite membranes and the presented data in this work refers to porous Ag-ceramic composite membranes. In summary, the complexity of time dependent profiles is critically attributed to the complexity of the rate enhancement process in terms of variations brought forward towards structure and porosity of the as deposited Ag film. The following reasons have been presented for the apparent complexity of the time dependent PPD profiles:

a) An enhancement in PPD with time for CEP is indicative towards the negation of other rate enhancements in influencing PPD trends.
b) The steady decline in PPD with time for SSOEP baths is indicative towards the poor rate enhancement brought forward by combination of sonication and surfactant.
c) For SIEP, the PPD reduced first and then increased. This confirms that surfactant and porosity of the as deposited Ag films might have conversing effect at times and contributory effect at other times.
d) For SOEP, the PPD increased first and then reduced. This confirms that the Ag film characteristics (porosity and thickness) could strongly influence further deposition characteristics.

Figure 5.2 (b) presents the time dependent MLI profiles for CEP, SOEP, SIEP and SSOEP processes. As shown, the MLI increased with increasing plating time. The time dependent MLI values varied from 1.05 - 3.09×10^{-3}, 2.73 - 9.09×10^{-3}, 1.11 – 4.21×10^{-3} and 3.07 - 10.14×10^{-3} g/cm^3 for a variation in plating time from 1 – 3 h for CEP, SOEP, SIEP and SSOEP processes respectively. Also, the MLI profiles of SSOEP and SOEP are close and significantly higher than those obtained for SIEP and CEP processes. The MLI profiles are in good agreement with the efficiency profiles. Among all processes, SSOEP provided optimal and highest MLI profiles and based on the efficiency and MLI profiles, both SOEP and SSOEP can be regarded to be the optimal processes for porous silver-ceramic composite membrane fabrication. Thereby, it can be inferred that surfactant on its own would not suffice as a potential rate enhancement technique for the Ag-ceramic composite fabrication.

5.2.3 η/ (MLI.PPD) index

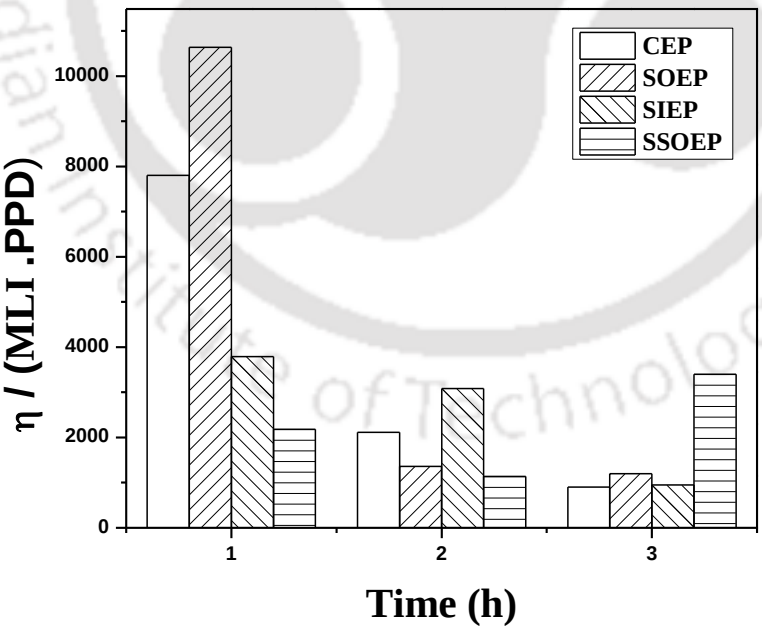

Figure 5.3: Variation of η/(MLI.PPD) index with time for various ELP processes.

Table 5.1: Average plating time data for Ag CEP, SIEP, SOEP and SSOEP processes.

Rate enhancemen technique	Average plating rate (mol/L.s)×10^6 for various total plating time (h)		
	1	**2**	**3**
CEP	2.26	1.51	1.73
SOEP	2.31	2.40	2.35
SIEP	2.09	2.22	2.11
SSOEP	2.39	2.45	2.34

Conceptually, an optimal Ag ELP should provide maximum combinations of η and minimal combinations of MLI and PPD. In this regard, it may be hypothesized that higher η refers to higher MLI and vice-versa. While this may be true, an efficient Ag ELP should provide minimal Ag film thickness with maximum efficiency and minimal variation in PPD for porous silver-ceramic composite membrane fabrication. Thus, a convenient index for the screening of alternate ELP process is to refer to a factor termed η/(MLI.PPD) which should be maximum for the optimal process. Figure 5.3 illustrates the η/(MLI.PPD) index for CEP, SOEP, SIEP and SSOEP processes. It can be observed that while SOEP provided maximum value of the index during the 1st h of plating (10635.38), it reduced to 1359.79 and 1197.18 after 2 and 3 h of sequential Ag ELP. After 3 h of Ag ELP, only SSOEP provided maximum value of the η/(MLI.PPD) index. This indicates that complex tradeoffs exist for the Ag ELP process to fabricate porous Ag ceramic composite membranes.

5.2.4 Average plating rate

A summary of the average plating rate for various plating processes at different plating time values is presented in Table 5.1. As presented, both SOEP and SSOEP provided higher plating rate values. The CEP and SIEP also provided moderate plating rate values along with poor

combinations of efficiency and MLI. Thus, the evaluation of combinatorial plating characteristics is very much relevant to identify the most competent plating processes for Ag-ceramic composite membrane fabrication.

5.2.5 Summary

Among various alternate Ag ELP processes, the optimal process and conditions with bulk mode of reducing agent addition refer to

a) SSOEP process for t = 3 h, where conversion, efficiency, PPD, MLI and η/MLI.PPD) have been evaluated as 83%, 69 %, 2%, 10.14×10^{-3} g/cm^3 and 3402.89 respectively.

b) SOEP process for t = 3 h, where conversion, efficiency, PPD, MLI and η/(MLI.PPD) have been evaluated as 83%, 62%, 5.7%, 9.09×10^{-3} g/cm^3 and 1197.18 respectively.

Since SOEP and SSOEP performed significantly better than CEP and SIEP, further parametric investigations have been targeted only for these processes. For the SOEP, with bulk mode addition of the reducing agent, parametric optimality of Ag solution concentration was investigated for Ag solution concentrations of 0.005 and 0.015 mol/L. For such cases, the reducing agent concentration was maintained 800% excess to the revised Ag solution concentration. Since surfactant solution concentration could be a very sensitive parameter to influence combinatorial plating characteristics of SSOEP Ag ELP baths, surfactant solution concentration was varied from 1, 3 and 4 CMC for SSOEP baths. For such cases, the reducing agent concentration is similar to that presented for Ag SOEP baths. Thereby, the optimality of Ag solution concentration and surfactant solution concentration were investigated for SOEP and SSOEP processes respectively.

5.3 Effect of Ag solution concentration on combinatorial plating characteristics of SOEP process

5.3.1 Conversion and Efficiency profiles

Figure 5.4 (a) presents the time dependent conversion profiles at various Ag solution concentrations for the SOEP. It can be observed that the conversions varied significantly with Ag solution concentration from 79% at 0.005 mol/L to 85% at 0.015 mol/L after plating time of 3 h. Also, it can be analyzed that while conversions steadily increased at lower solution concentration (0.005 mol/L), they varied non-linearly at higher solution concentration. This indicates that complex plating characteristics exist at higher solution concentrations that involve enhancement in conversion after plating time of 2 h but not 3 h. The reduction in conversion at higher solution concentrations is possibly due to inhibitory effect of concentration at prolonged plating time.

As shown in Figure 5.4 (b), similar efficiency profiles exist for the SOEP. For a variation in plating time from 1 – 3 h, the efficiency profiles varied from 40 – 46%, 58 – 62%, 24 – 30% for Ag solution concentrations of 0.005, 0.01 and 0.015 mol/L respectively. It is interesting to note that the optimal Ag solution concentration corresponds to 0.01 mol/L at which maximum efficiency values were obtained. This is due to the optimality of the solution concentration in terms of the metal adhesion to the ceramic support, as Ag film mechanical strength is a strong function of Ag solution concentration. Based on obtained efficiency profiles, the maximum efficiency of the SOEP process corresponds to a value of 68% at 0.01mol/L solution concentration and 2 h. The optimality of efficiency value at intermediate plating time is indicative towards significant variations in metal nucleation in the solution for prolonged plating time. This can be avoided by enhancing the solution concentration due to which Ag

film characteristics could be significantly altered and better adhesion of the film can be achieved.

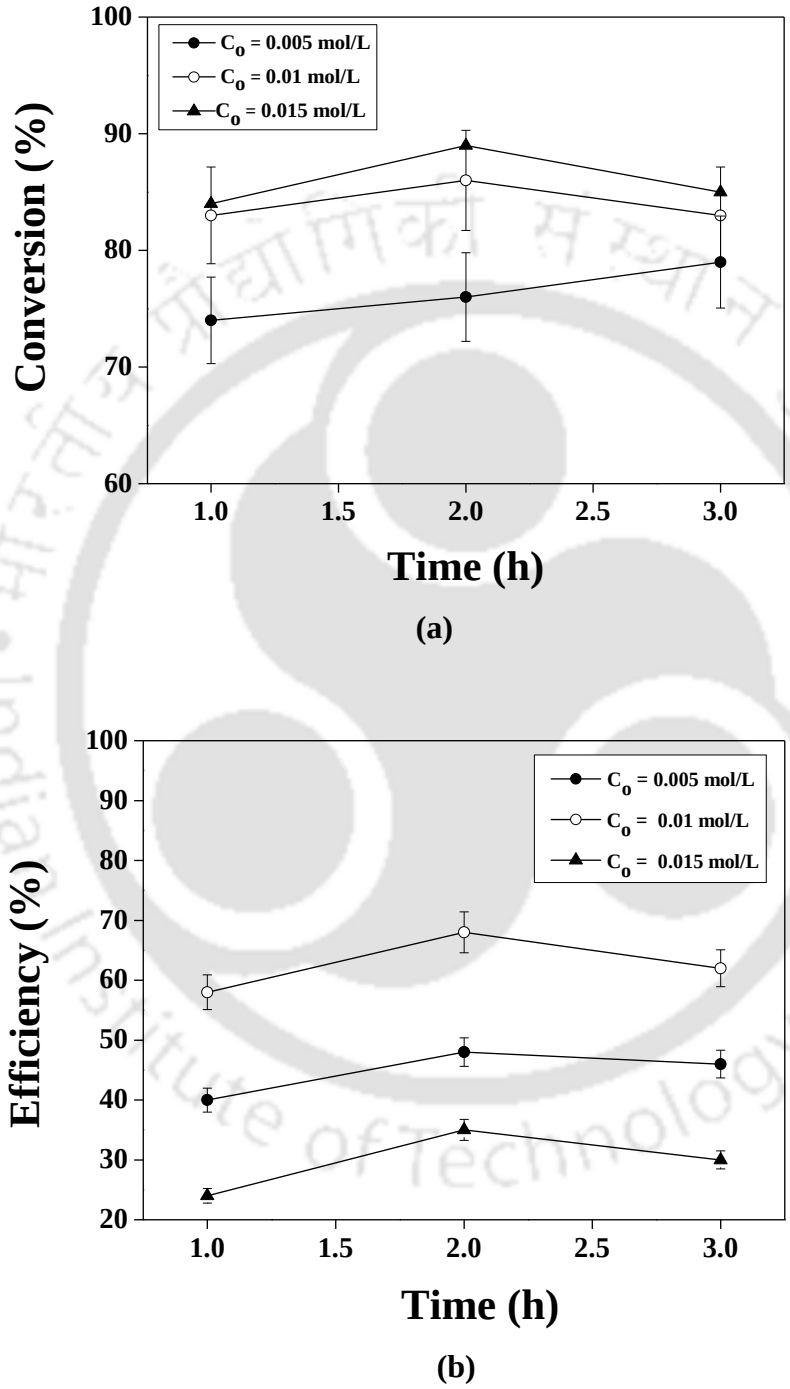

Figure 5.4: Effect of Ag solution concentration on time dependent (a) Conversion and (b) Efficiency profiles for SOEP process.

5.3.2 PPD and MLI profiles

Figure 5.5 (a) presents the time dependent PPD profiles for various solution concentrations. It can be observed that for SOEP process, significant variation in PPD profiles exist for variation in Ag solution concentration. At the lower solution concentration of 0.005 mol/L, the PPD reduced

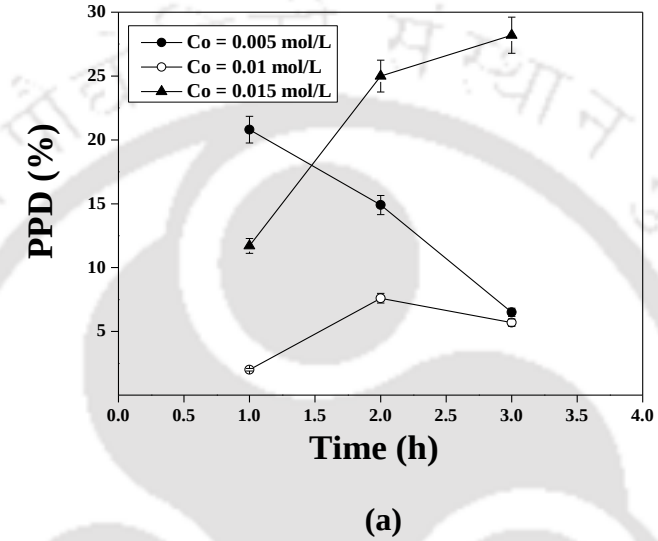

(a)

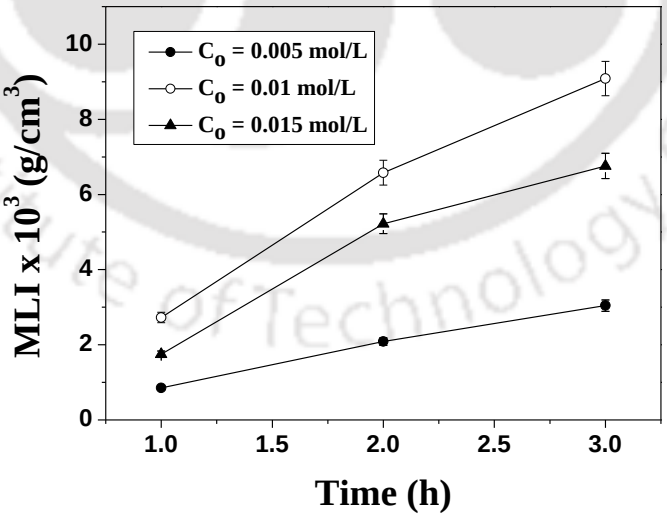

(b)

Figure 5.5: Effect of Ag solution concentration on time dependent (a) PPD and (b) MLI profiles for SOEP process.

with increasing time from 20.8 – 6.5%. However, for higher solution concentrations, the PPD profile reduced to 5.7% at 0.01 mol/L which later increased to 28.2% at 0.015 mol/L after 3 h of plating time. Thus, it is apparent that the PPD values were lowest for 0.01 mol/L Ag concentration. This is possibly due to deposition of metal in the pores but not on the surface of the membrane. Such a hypothesis appears to be valid due to the fact that the weight gain (or MLI) always increased with increasing plating time. Thus, it is apparent that the solution concentration (0.01 mol/L) is optimal with the fact that PPD's reduced with time and metal composite membranes with more porosity were achieved than those obtained at other solution concentrations. In this regard, it is important to note that the objective of Ag ELP is to achieve porous but not dense metal ceramic composite membranes.

Figure 5.5 (b) presents the MLI profiles for various solution concentrations and SOEP baths. It can be observed that distinct MLI profiles were obtained for various solution concentrations. The time dependent MLI varied from 0.85 – 3.04×10^{-3}, 2.73 – 9.09×10^{-3}, 1.75 – 6.76×10^{-3} g/cm^3 at solution concentrations of 0.005, 0.01 and 0.015 mol/L respectively. The enhancement in MLI with time has confirmed that despite obtaining complex PPD tradeoffs, the Ag film thickness increased with time.

5.3.3 η/(MLI.PPD) index

Figure 5.6 illustrates the η/(MLI.PPD) index for variation solution concentrations and SOEP process. Among various cases, the index value obtained at t = 1 h is significantly high and indicates highly complex tradeoffs and combinatorial characteristics. The index does not indicate the optimality of solution concentrations.

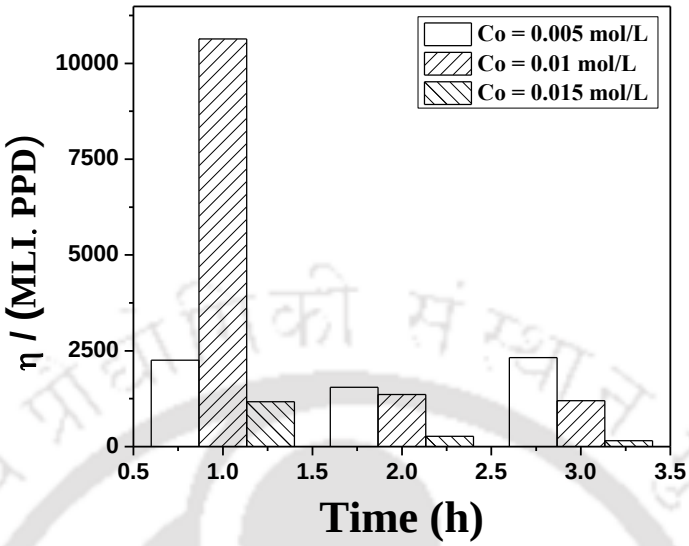

Figure 5.6: Effect of Ag solution concentration on time dependent variation of η/ (MLI.PPD) index for SOEP baths.

5.3.4 Average plating rate

A summary of average plating rate for various solution concentrations is presented in Table 5.2. As presented, the average plating rate is lowest (1.04 – 1.11×10^{-6} mol/L.s) and highest (3.58 – 3.81×10^{-6} mol/L.s) for 0.005 and 0.015 mol/L Ag solution concentration respectively. It is

Table 5.2: A summary of average plating rate data for SOEP processes with variant Ag solution concentrations.

Silver concentration (mol/L)	Average plating rate (mol/L.s)×10^6 for various total plating time(h)		
	1	2	3
0.005	1.04	1.09	1.11
0.01	2.31	2.40	2.35
0.015	3.58	3.81	3.65

further interesting to note that significant variation in the average plating rate does not exist, which further confirmed that SOEP process is ideal for prolonged plating and achievement of thicker Ag films in case they are required.

5.3.5 Summary

Based on obtained results for the SOEP baths, the optimal solution concentration refers to 0.01 mol/L, where conversion, efficiency, PPD, MLI and η/(MLI.PPD) were obtained as 83%, 62%, 5.7%, 9.09×10^{-3} g/cm^3 and 1197.18 respectively for a plating time of 3 h. It is further interesting to note that for this solution concentration, lowest PPD is obtained along with good combinations of efficiency and MLI, which confirmed the optimality of the deployed solution concentration.

5.4 Effect of surfactant solution concentration on Ag SSOEP process performance

5.4.1 Conversion and efficiency profiles

Figure 5.7 (a) presents the time dependent conversion profiles for various surfactant solution concentrations during Ag SSOEP process. It can be observed that the conversions increased with increasing surfactant solution concentrations. However, all profiles indicate a non-linear trend that confirmed upon the optimality of 2 h plating time but not 3 h plating time. For a variation in plating time from 1 - 2 h, the conversions varied from 83 – 86, 84 – 89, 85 – 89.5 and 86 – 90% for CTAB surfactant solution concentrations of 1, 2, 3 and 4 CMC respectively. However, a further increase in plating time from 2 – 3 h enabled the conversions to reduce from 86 – 80, 89 – 83, 89.5 – 84, 90 – 85% for 1, 2, 3 and 4 CMC surfactant concentrations respectively. The optimality of intermediate plating time is possibly due to the optimality of the surfactant

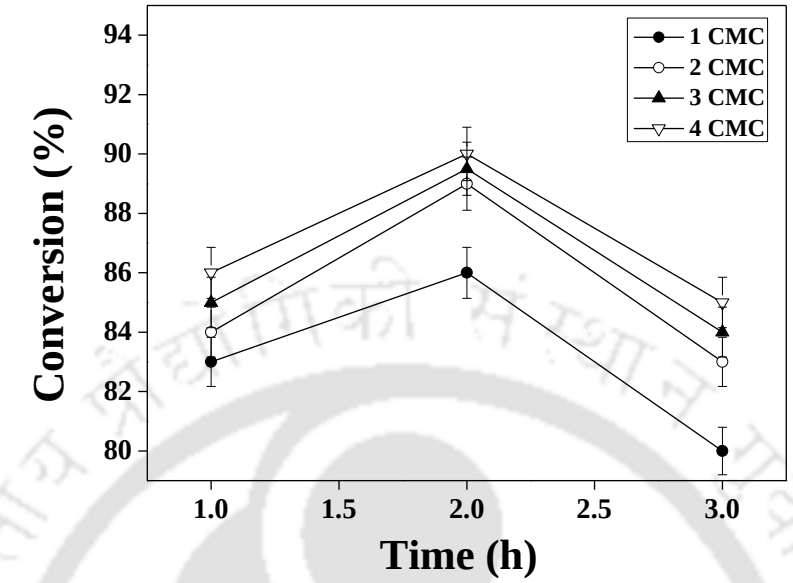

(a)

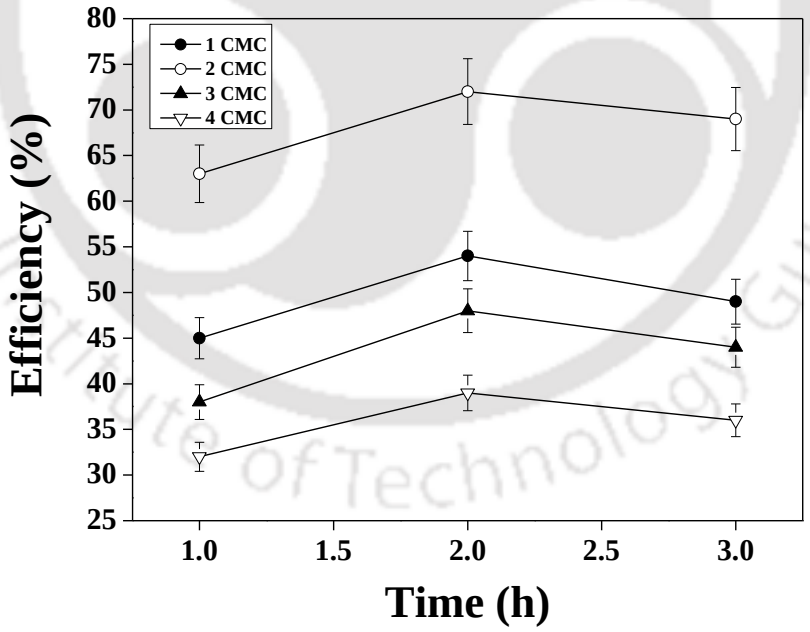

(b)

Figure 5.7: Effect of surfactant solution concentration on time dependent (a) Conversion and (b) Efficiency profiles for Ag SSOEP processes.

adsorption at the plating time. During SSOEP, surfactant adsorption to the ceramic support can be insignificant. The surfactant adsorption is a complex function of metal film porosity, metal film adhesion strength etc., which are complex functions of the solution chemistry. Thus, it is possible that the surfactant adsorption is significant at low and high plating times, but not the moderate plating time. At low plating time (1 h), surfactant adsorption appears to be significant with the ceramic support which may not be the case for intermediate plating time (2 h) with the as deposited Ag metal. However, at higher plating time (3 h), the surfactant adsorption appears to be significant with the metal film deposited on the porous support, due to which conversion values are lower. In summary, the surfactant solution concentration appears to be very strongly influencing optimality of plating time.

Figure 5.7 (b) presents the variation of time dependent efficiency with surfactant solution concentration. For a variation in plating time from 1 – 3 h, the efficiency varied from 45 – 49, 63 – 69, 38 - 44 and 32 – 36% for surfactant solution concentrations of 1, 2, 3 and 4 CMC respectively. It is apparent that the efficiency values reduced after 2 h for all cases. This is due the reduction of metal adhesion to the ceramic support for prolonged plating time, which thereby promoted greater metal nucleation in the solution and thus inefficiency. Thus, based on conversion and efficiency profiles, the optimal operating condition for the Ag-ceramic composite membrane refers to a plating time of 2 h.

5.4.2 PPD and MLI profiles

The PPD profiles (Figure 5.8 (a)**)** for various surfactant solution concentration cases refer to complex time dependent characteristics. For a low surfactant solution concentration of 1 CMC, the PPD reduced almost linearly from 17.3 – 11.3% for an increase in plating time from 1 – 3 h.

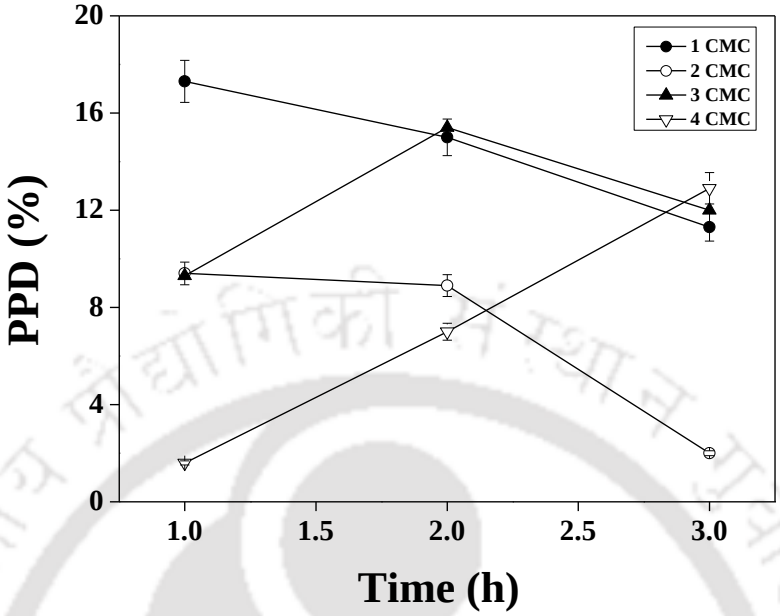

(a)

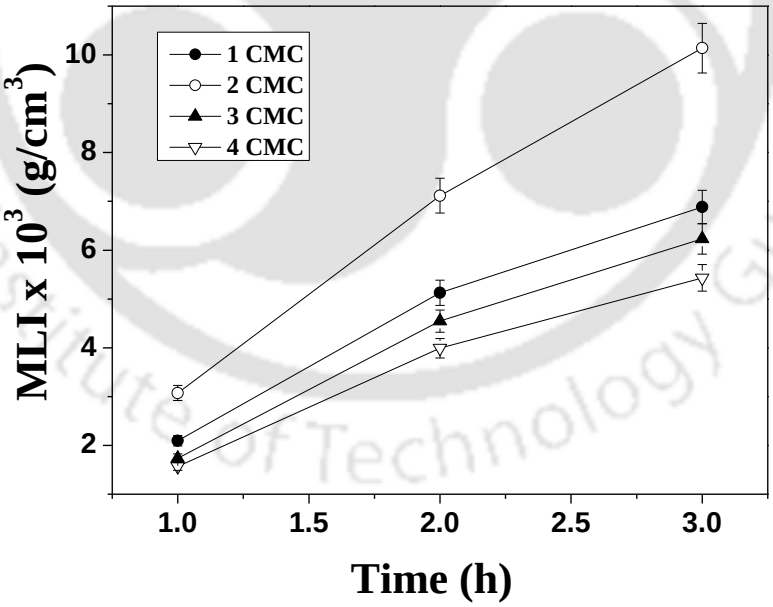

(b)

Figure 5.8: Effect of surfactant solution concentration on time dependent (a) PPD (b) MLI profiles for Ag SSOEP processes.

However, for the surfactant solution concentration of 2 CMC, the PPD reduced non-linearly from 9.4 – 2% for similar plating time variation. The PPD profile for 3 CMC surfactant solution concentration indicated a nonlinear increasing trend from 9.3 – 12% with an optimal value of 15.4% at 2 h plating time. The 4 CMC solution concentration enabled a linear enhancement in the PPD from 1.6 – 12.9 % for a variation in plating time of 3 h. With these observations, it can be analyzed that the surfactant solution concentration strongly influenced surfactant adsorption and metal film morphology to provide complex tradeoffs. While MLI increased, it indicated that CTAB surfactant does play a significant role in altering the membrane morphology and metal adhesion strength. Since low PPD values were obtained for 2CMC surfactant solution concentration, it is regarded as the optimal case among the cases investigated.

The MLI profiles for various surfactant solution concentration cases are illustrated in Figure 5.8 (b). For all cases, the MLI increased and thereby inferred that metal thickness increased with increasing plating time. Among all cases, the MLI at 2 CMC surfactant solution concentration is maximum and varied from 3.07 – 10.14×10^{-3} g/cm^3 for a plating time variation from 1 – 3 h. This is possibly due to one main reason namely optimal surfactant adsorption with the ceramic support due to which metal adhesion and morphology to the ceramic support is appropriate and does not enhance metal nucleation in the solution for further deteriorating plating quality or efficiency. Substantial reduction in MLI with increasing surfactant solution concentration from 3 to 4 CMC is indicative to the fact that strong surfactant adsorption inhibited metal deposition on the surface and 2 CMC is the optimal surfactant solution concentration.

5.4.3 η/(MLI.PPD) index

For the SSOEP process, Figure 5.9 illustrates the η/(MLI.PPD) index for various surfactant solution concentrations. As shown, highest index was obtained for 4 CMC value and plating time of 1 h at which condition, efficiency is poor. Further, it is notable that maximum index of 3402.89 is obtained for 2 CMC surfactant solution concentration for a total plating time of 3 h. At the optimal plating time of 2 h, the index values remained fairly similar for 2 CMC and 4 CMC but since 2 CMC provided higher efficiency and MLI values, 2 CMC is inferred to be the optimal choice for SSOEP plating baths.

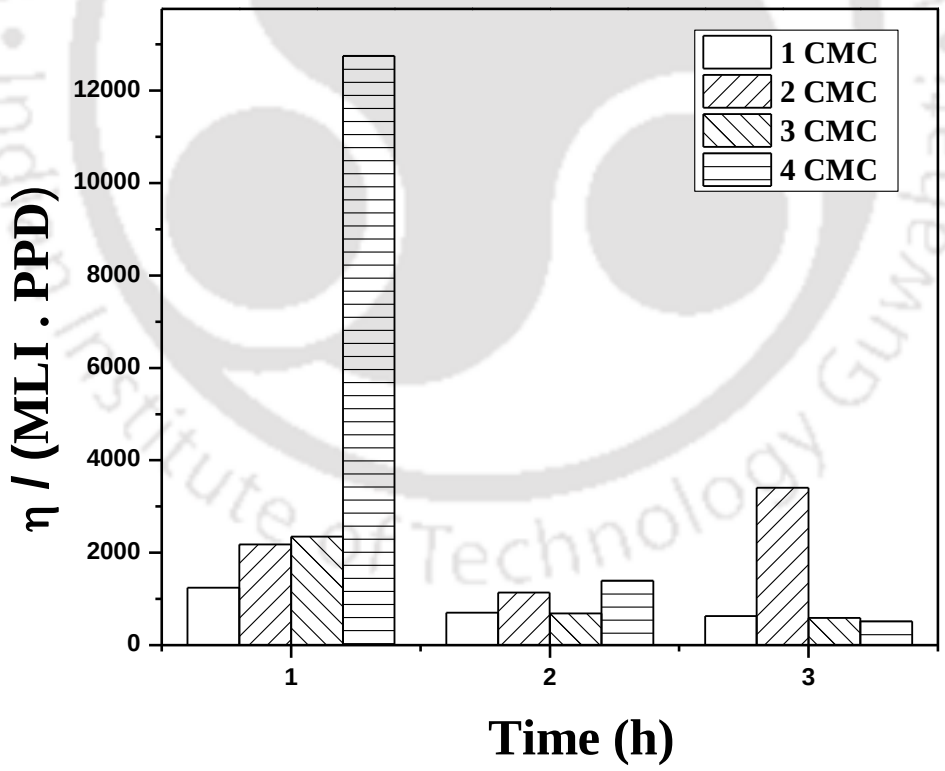

Figure 5.9: Variation of η/(MLI.PPD) index with time and CTAB surfactant solution concentrations for Ag SSOEP processes.

Table 5.3: A summary of average plating rate data for Ag SSOEP baths with variant CTAB surfactant solution concentrations.

Surfactant concentration	Average plating rate (mol/L.s)×10^6 for various total plating time (h)		
	1	2	3
1 CMC	2.30	2.37	2.23
2 CMC	2.39	2.45	2.34
3 CMC	2.24	2.40	2.30
4 CMC	2.40	2.61	2.37

5.4.4 Average plating rate

A summary of the average plating rates for SSOEP Ag ELP baths with variant surfactant solution concentrations is presented in Table 5.3. As presented, the average plating rates varied from 2.23 – 2.61×10^{-6} mol/L.s for all the cases and no significant variation in the plating rate occurred despite varying the surfactant solution concentrations. Thereby, these trends indicate that surfactant solution concentration critically influences metal adhesion strength and metal nucleation in the solution despite providing similar average plating rate values.

5.4.5 Summary

Based on the experimental investigations carried out for the SSOEP process, the optimal operating condition corresponds to 2 CMC surfactant solution concentration and plating time of 2 h, where conversion, efficiency, PPD, MLI and η/(MLI.PPD) index were obtained as 89%, 72%, 8.9%, 7.12×10^{-3} g/cm^3 and 1136.71 respectively.

5.5 Surface characterization

The surface morphology of porous silver-ceramic membrane fabricated using bulk wise addition of reducing agent for SSOEP baths at optimal process parameters (0.01 M silver concentration, 2 CMC surfactant concentration, plating time of 1 h and loading ratio of 441 cm^2/L) was characterized by FESEM Figure 5.10 (a) presents the surface morphology of silver-ceramic membrane obtained from FESEM. It can observed that pore modification occurred on

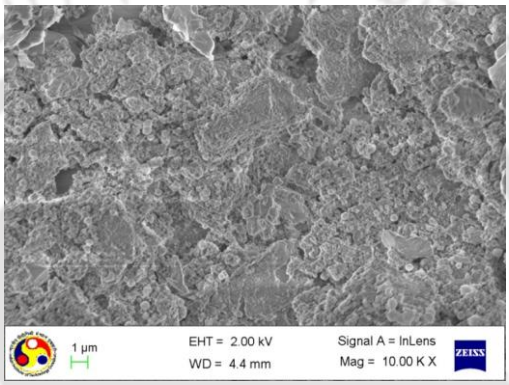

(a)

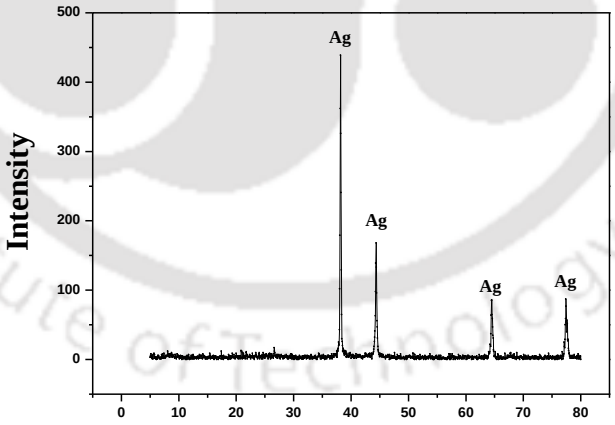

(b)

Figure 5.10: (a) Surface FESEM image and (b) XRD pattern of silver-ceramic composite membrane fabricated with SSOEP process at 0.01 M Ag and 2 CMC CTAB solution concentration.

the ceramic support due to the formation of Ag grain agglomerates and porous structure existed on the membrane surface despite undergoing surface modification. Figure 5.10 (b) presents the XRD pattern of silver-ceramic membrane fabricated with optimal process parameters presented for Figure 5.10 (a). The XRD pattern confirmed that silver (Ag) reflection peaks exist in the face centered cubic phase at (111), (200), (220) and (220) planes. Further, no other peaks were observed for the silver-ceramic membrane. Thereby, the XRD pattern confirmed that the surface coverage with silver film is effective.

5.6 Summary

During bulk addition of the reducing agent, both SOEP and SSOEP Ag ELP processes have been identified as optimal cases. Based on further process optimization studies, the optimal parameters refer to 0.01 mol/L Ag solution concentration for SOEP and 2 CMC solution concentration for SSOEP process. The MLI profiles confirmed that both rate enhanced ELP processes provide promising opportunities for the cost effective fabrication of silver-ceramic composite membranes. For both SOEP and SSOEP Ag ELP process, till date, to the best of our knowledge, no literature is available and therefore the obtained results are anticipated to serve as guidelines and benchmarks for further optimizing the fabrication engineering aspects of low cost porous Ag ceramic composite membranes, which have potential applications such as XRD media, silica and carbon analysis media and bacteria filtration.

The obtained experimental trends for porous silver-ceramic composite membrane fabrication using electroless plating using relevant characterization parameters can be extended to similar systems of fabrication and thereby enable the deduction of useful inferences with minimal experimentation. Further, the experimental approach presented in this work also negates the trial and error based approaches that might be followed by other researchers in the field of rate enhanced electroless metal ceramic composite membrane fabrication.

Chapter 6:

Efficacy of Reducing Agent Contacting Pattern on the Plating Characteristics of Ag SOEP and SSOEP processes

Chapter 6

Efficacy of Reducing Agent Contacting Pattern on the Plating Characteristics of Ag SOEP and SSOEP processes

After a brief introduction to the necessity of addressing reducing agent contacting pattern in section 6.1, section 6.2 summarizes the performance characteristics of SSOEP Ag ELP baths supplemented with drop wise addition of the reducing agent. Eventually, sections 6.3 – 6.5 summarize the results obtained for drop wise reducing agent facilitated SOEP baths at different Ag solution concentrations in terms of the combinatorial plating characteristics and surface characterization. Eventually surface characterization results of few samples is presented in section 6.6 followed with summary of the chapter in section 6.7.

6.1 Introduction

In Chapter 5 of the thesis, both SOEP and SSOEP processes have been identified to be optimal rate enhanced Ag ELP processes for porous Ag ceramic composite membrane fabrication. These baths were facilitated with bulk mode of reducing agent addition. The recent research of Agarwal et al. (2013) in the field of dense nickel-ceramic and palladium-ceramic composite membrane fabrication has highlighted that the variation in the reducing agent contacting pattern by adopting drop wise addition strategy can significantly alter and improve the combinatorial plating characteristics of ELP baths. Therefore, it is important to visualize whether drop wise reducing agent addition would be beneficial or not for porous Ag ceramic composite membrane

fabrication. Hypothetically, the drop wise addition of the reducing agent may improve or deteriorate the combinatorial plating characteristics of Ag ELP baths. For the case where the Ag ELP bath characteristics are improved, the drop wise addition can be regarded to be very effective in improving metal adhesion to the ceramic support which eventually reduces metal nucleation in the solution and thereby plating inefficiency. Conversely, the drop wise addition of the reducing agent may also deteriorate the plating characteristics. This may be due to enhanced metal nucleation of the solution due to poor metal adhesion of the metal to the ceramic support, and hence lower plating efficiency. In addition, it is also important to observe that Ag solution concentration also strongly influences metal film adhesion strength and morphology. Therefore, with drop wise addition of the reducing agent being a sensitive parameter, it would be as well important to visualize the role of Ag solution concentration to influence combinatorial plating characteristics.

6.2 Performance of Ag SSOEP baths

Several experiments were conducted for Ag SSOEP baths supplemented with drop wise reducing agent and variant solution concentrations of the hydrazine (50 – 200% excess) and Ag solution concentrations (0.005 – 0.015 mol/L). In all such investigations, it has been evaluated that significant nucleation occurred in the solution and metal efficiencies as low as 10 – 20% were obtained. Thus, it is apparent that drop wise addition of the reducing agent strongly influenced metal adhesion to the support and SSOEP rate enhancement was detrimental towards metal bonding. Hence, Ag SSOEP baths with drop wise reducing agent addition can be concluded be ineffective in improving the combinatorial plating characteristics reported in Chapter 5 of the thesis.

Considering these observations, the next section addresses the combinatorial plating characteristics of Ag SOEP plating baths.

6.3 Plating Characteristics of 0.005 M Ag SOEP baths

This section addresses the combinatorial plating characteristics of Ag SOEP baths with 0.005 M Ag solution concentration and 50 – 400% excess hydrazine reducing agent concentration.

6.3.1 Conversion and Plating Efficiency

Figure 6.1 (a) presents the variation of time dependent conversion profiles for various reducing agent concentrations. For 50% excess concentration case, the conversion insignificantly reduced from 33.22 –26.54% with plating time variation from 1 – 3 h. This was not the case for 200% excess and 400 % reducing agent excess cases, where the conversion increased from 36.53 – 44.29% and 56.25-72.8% respectively. Further, it can be noted that the conversion profiles indicated greater non-linearity for higher reducing agent concentration. This indicates that reducing agent concentration strongly influenced time dependent metal adhesion characteristics. Also, for 400 % hydrazine excess case, the conversion values significantly reduced after 2 h of plating and this indicates that greater nucleation occurred for these operating conditions. Overall, the conversions obtained are moderate to high for higher reducing agent concentration. Therefore, it is important to note that excess reducing agent concentration is useful to promote conversions.

Figure 6.1 (b) presents the time dependent efficiency profiles for 0.005 Ag SOEP baths. For 50 % hydrazine excess case, the time dependent efficiency values varied non-linearly from 41.08 – 36.86% for plating time variation from 1 – 3 h. This is also the case for 400% excess hydrazine

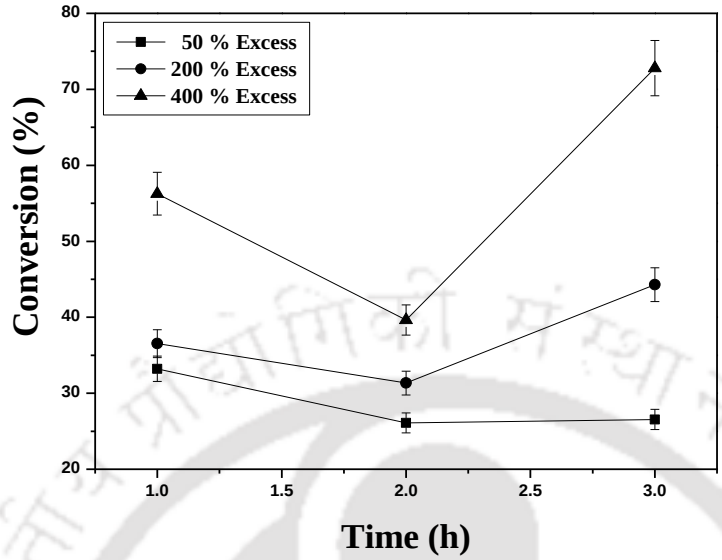

(a)

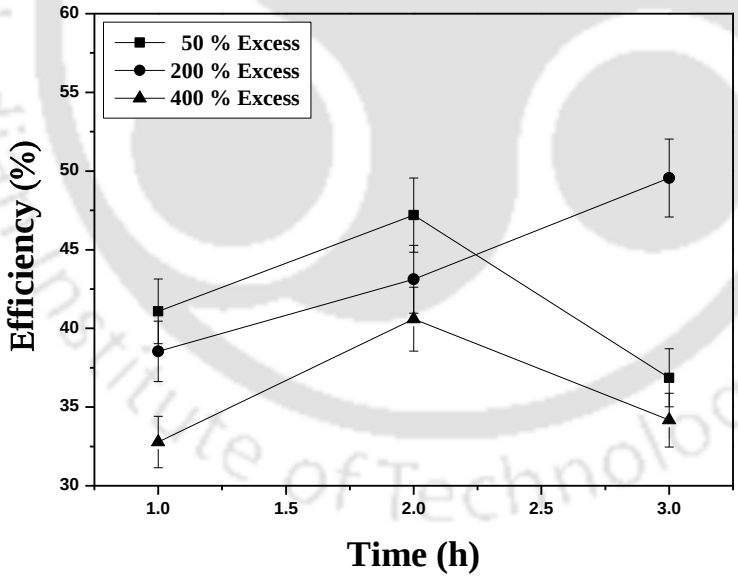

(b)

Figure 6.1: Effect of drop wise contacted hydrazine concentration on time dependent (a Conversion and (b) Efficiency profiles for 0.005M Ag SOEP baths.

case, where the efficiency values varied from 32.78 – 34.17% for similar variation in plating time. However, at the intermediate reducing agent concentration of 200% excess, the efficiency values increased from 38.54 – 49.55% for a variation in total plating time from 1 – 3 h. Thus, it is apparent that the metal adhesion characteristics with the ceramic support are significantly influenced by the reducing agent concentration during its drop wise addition.

The optimality of reducing agent concentration specifically refers to its ability to enable Ag metal deposition with good adhesion strength. This is specifically valid with respect to the counter influence of cavitation effect, which may induce additional agitation on the membrane surface and thereby adverse effect to the strong metal bonding with the ceramic support. In summary, even though plating efficiency can be evaluated to be optimal for 200% excess case, the obtained values for drop wise reducing agent addition are not better(38.54 – 49.55%) than those obtained for SOEP baths supplemented with bulk mode of reducing agent addition (58 – 62%).

6.3.2 PPD and MLI profiles

Figure 6.2 (a) presents the time dependent PPD profiles for 50%, 200% and 400% excess hydrazine cases. It can be observed that the time dependent PPD varied from 3.48 – 13.19%, 17.9 – 33.39%, 5.71 – 13.81% for a variation in time from 1 – 3 h for 50%, 200% and 400% excess cases respectively. Among all cases, maximum PPD has been obtained for 200 % excess case. This is possibly due to significant variation in membrane morphology and metal adhesion with a variation in excess hydrazine concentration during drop wise addition of the reducing agent. The excess hydrazine reducing agent in turn enables significantly higher plating rates.

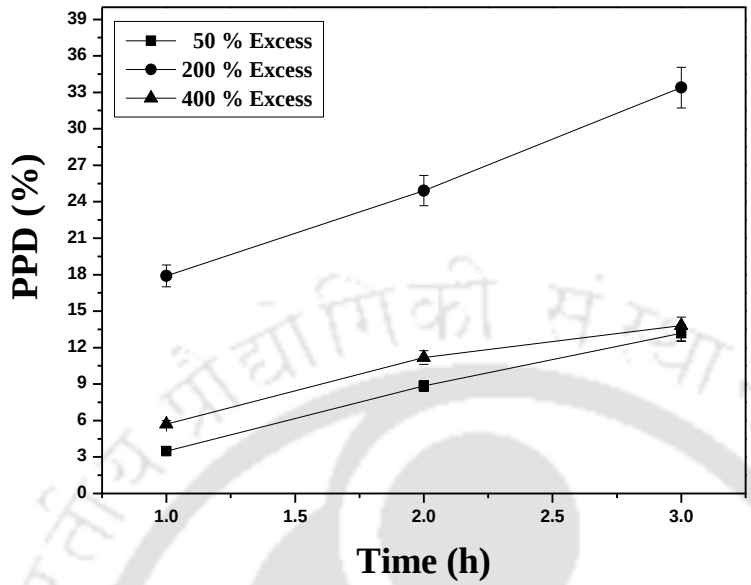

(a)

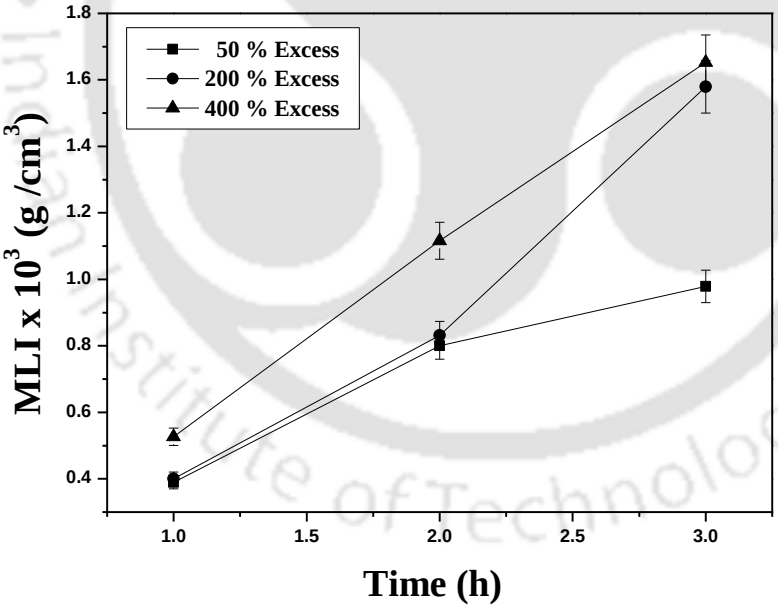

(b)

Figure 6.2: Effect of drop wise contacted hydrazine concentration on time dependent (a) PPD and (b) MLI profiles for 0.005 M Ag SOEP baths.

However, along with cavitation effect, it also enabled a variation in the membrane morphology and metal adhesion to the ceramic support and thereby PPD. While PPD values are significantly higher for 200% excess case which is not desired, since higher efficiency values have been obtained only for this case, it is regarded to be optimal. Figure 6.2 (b) presents the time dependent variation of MLI for various excess hydrazine cases. The MLI profiles varied from 0.39 – 0.98×10^{-3}, 0.40 – 1.58×10^{-3} and 0.53 – 1.65×10^{-3} g/cm^3 for a variation in plating time from 1 – 3 h for 50%, 200% and 400% excess hydrazine cases respectively. In general, the MLI profiles increased with increasing hydrazine excess concentrations. However, the optimal MLI corresponds to that obtained for best efficiency profiles and hence 200% excess hydrazine case is regarded as optimal concentration of the reducing agent.

6.3.3 η/(MLI.PPD) index

Figure 6.3 depicts the η/(MLI.PPD) index with time at various reducing agent concentrations for silver concentration of 0.005 M. It can be observed that the η/(MLI.PPD) index values are varied from 30304.31 – 3086.49, 5381.83 – 939.70 and 10905.80 – 1496.95 for 50, 200 and 400% excess reducing agent concentrations respectively. Highest index value is obtained for 50% excess hydrazine case and plating time of 1 h. This is due to poor plating during the initial 1 h of plating, due to which reason lower MLI values have been obtained. However, at this condition the efficiency value is significantly low for the case. Considering this issue, the optimal η/(MLI.PPD) index value at 200 % excess hydrazine solution concentration is 939.70 at plating time of 3 h.

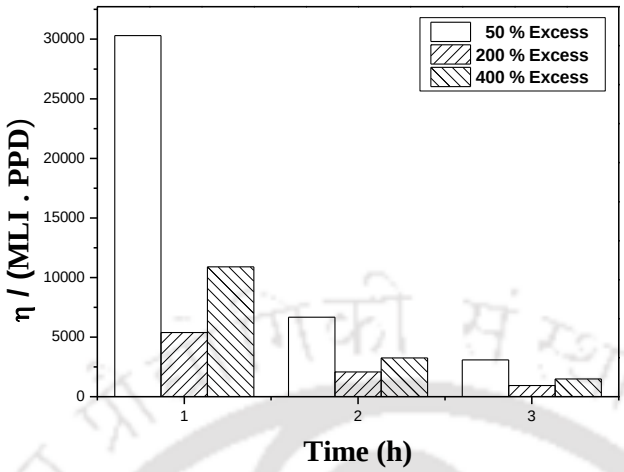

Figure 6.3: Time dependent variation of η/(MLI.PPD) index for 0.005 M SOEP (DW) baths at various hydrazine solution concentrations.

6.3.4 Average plating rates

Table 6.1 presents a summary of the average plating rates for various hydrazine excess concentration cases. It can be observed that the average plating rate varied from 4.22-3.39×10^{-7}, 4.62-5.60×10^{-7} and 7.14-9.29×10^{-7} mol/L.s for 50%, 200% and 400% excess hydrazine cases. Despite obtaining higher plating rates for 400% excess hydrazine concentration, it cannot be regarded to be optimal due to poor efficiency profiles.

Table 6.1: Average plating rate data for 0.005M SOEP (DW) baths and variant reducing agent concentrations.

Reducing agent concentration (% Excess)	Average plating rate (mol/L.s)×10^{7} for various total plating time (h)		
	1	2	3
50	4.22	3.32	3.39
200	4.62	3.96	5.60
400	7.14	5.09	9.29

6.3.5 Summary

For 0.005 M Ag baths, at a plating time of 3 h, the optimal hydrazine concentration of 200% excess provided a conversion, efficiency, PPD, MLI, η/(MLI.PPD) and average plating rate values of 44.29%, 49.55%, 33.39%, 1.58×10^{-3} g/cm^3, 939.70 and 5.6×10^{-7} mol/L.s respectively.

6.4 Plating Characteristics of 0.01 M Ag SOEP baths

6.4.1 Conversion and Plating Efficiency

Figure 6.4 (a) presents the variation of time dependent conversion profiles for various reducing agent concentrations. It can be observed that for 50% and 200% excess hydrazine concentration cases, the conversions increased with increasing plating time. For these cases, the time dependent conversions varied from 50.93 – 71.32% and 46.24 – 66.84% for increasing plating time respectively. However, for 400 % excess hydrazine concentration case, the conversion reached a saturation value at a plating time of 2 h and then reduced for a plating time of 3 h (from 72.82 – 69.02% for a plating time of 1 – 3 h). The reduction in conversion for highest excess hydrazine solution concentration case is due to significant metal nucleation in the solution and is indicative of poor adhesion of the silver film to the ceramic support.

Figure 6.4 (b) presents the time dependent efficiency profiles for 0.01 M Ag SOEP baths. For 50% hydrazine excess case, the time dependent efficiency values varied linearly from 43.24 – 36.82% for plating time variation from 1 – 3 h. However, for 200 % excess hydrazine case, the efficiency values reduced from 69.24 – 52.68 % for similar variation in plating time. For 400% excess hydrazine case, the efficiency varied non-linearly with an increase from 30.24 – 47.65% from 1 – 2 h plating time and then to a lower value of 34.03% for 3 h plating time. Thus, it is

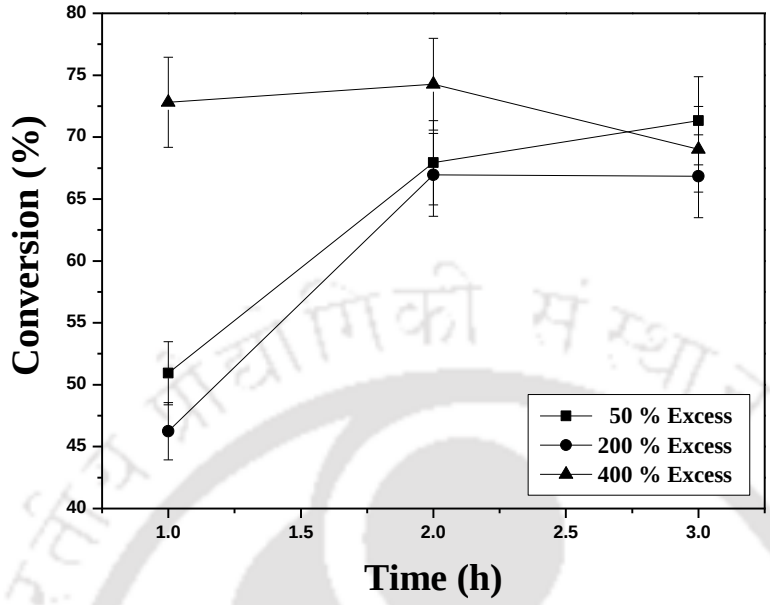

(a)

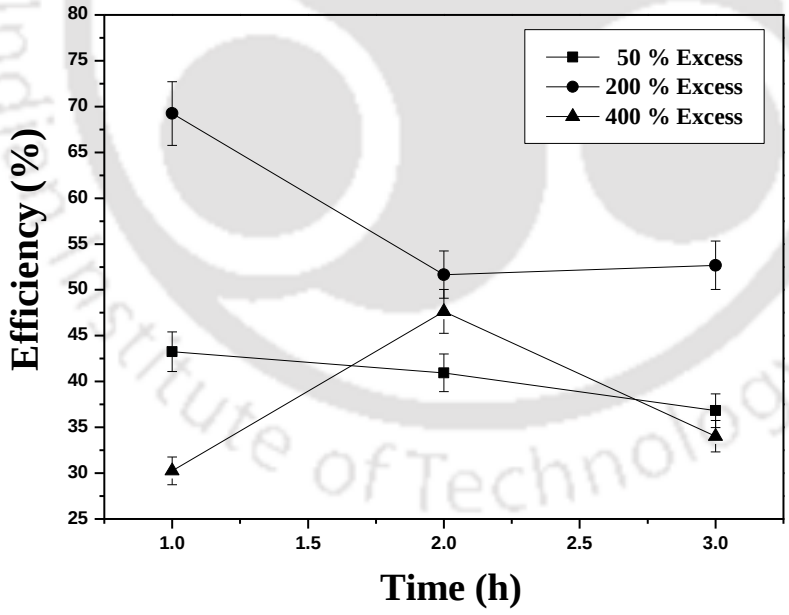

(b)

Figure 6.4: Effect of hydrazine concentration on time dependent (a) Conversion and (b) Efficiency profiles for 0.01 M Ag SOEP (DW) process.

apparent that metal nucleation is strongly promoted by higher excess hydrazine solution concentration and prolonged plating times. Among all cases, the best efficiency profile corresponds to that obtained at 200% excess hydrazine solution concentration. The possible reasons for the variations in efficiency with excess hydrazine solution concentration are similar to those presented for efficiency profiles of 0.005 M Ag SOEP baths.

6.4.2 PPD and MLI profiles

For the 0.01 M Ag SOEP baths, Figure 6.5 (a) presents the time dependent PPD profiles for 50%, 200% and 400% excess hydrazine cases. It can be observed that the time dependent PPD varied from 18.65 – 22.47%, 0.7 – 5.15%, 5.95 – 15.54% for a variant in time from 1 – 3 h for 50%, 200% and 400% excess cases respectively. Among all cases, maximum PPD has been obtained for 50% excess case and lowest values have been obtained for 200% excess case. Thus, the PPD profiles indicate that excess hydrazine concentration profoundly influences metal film morphology as the reducing agent concentration along with cavitation effect could potentially alter the morphology of achieved silver films. This is an important observation in the thesis as desired and undesired membrane morphologies can be addressed by varying the solution concentration of hydrazine during drop wise addition of the reducing agent. In case thinner porous Ag films are desired, 200% excess hydrazine is recommended and thicker porous Ag films are desired, 50% excess hydrazine is recommended. Typically thinner Ag films are desired and hence 200 % excess hydrazine concentration is the optimal case from PPD perspective.

Figure 6.5 (b) presents the time dependent variation of MLI for various excess hydrazine cases. For 50% and 200% excess hydrazine cases, the MLI profiles increased from 1.25 – 4.01×10^{-3} and 1.82 – 5.43×10^{-3} g/cm^3 for plating time variation from 1 – 3 h. However, for the 400%

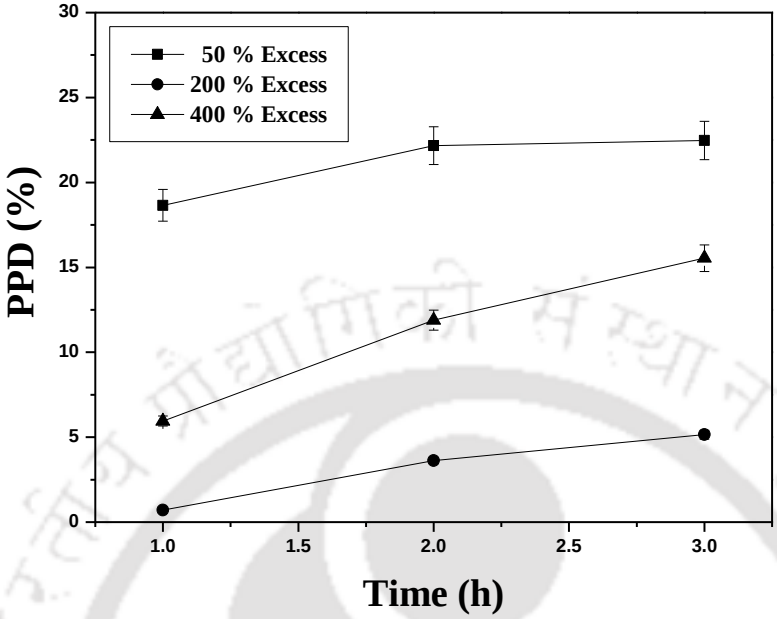

(a)

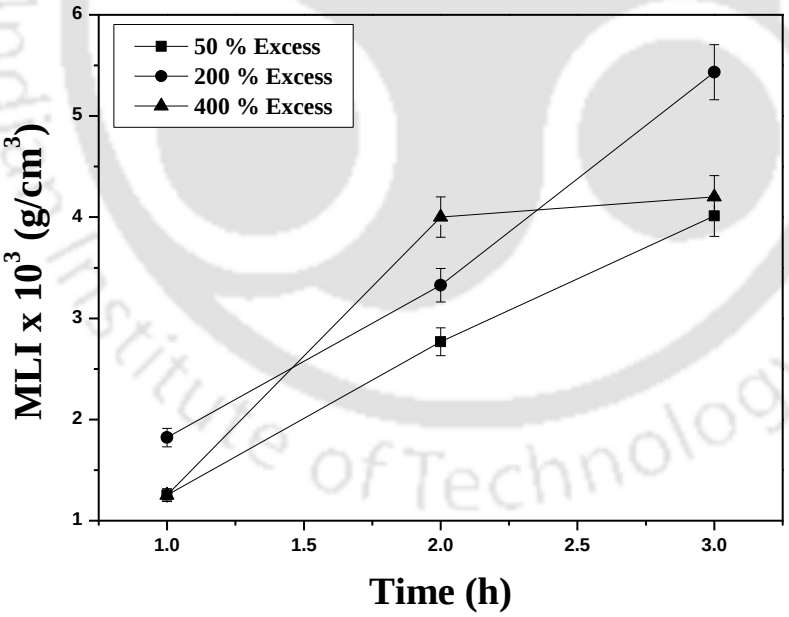

(b)

Figure 6.5: Effect of hydrazine concentration on time dependent (a) PPD and (b) MLI profiles for 0.01 M Ag SOEP (DW) process.

excess hydrazine case, the MLI profiles increased to a value of 4.20×10^{-3} g/cm^3 for a plating time of 3 h. These variations in MLI profiles with a variation in excess hydrazine concentrations is due to enhancement in solution metal nucleation with plating time and hydrazine concentration.

6.4.3 η/(MLI.PPD) index

Figure 6.6depicts the η/(MLI.PPD) index with time at various reducing agent concentrations for Ag solution concentration of 0.01M.It can be observed that the η/(MLI.PPD) index values are varied from 1850.61 – 408.52, 54308.51 – 1882.97 and 4056.70 – 521.31 for 50, 200 and 400% excess reducing agent concentrations respectively. Highest index value is obtained for 200% excess hydrazine case and plating time of 1 h. However, since higher efficiency values have been obtained for a plating time of 3 h, the optimal η/(MLI.PPD) index value corresponds to 1882.97 for 200% excess hydrazine solution concentration and a total plating time of 3 h.

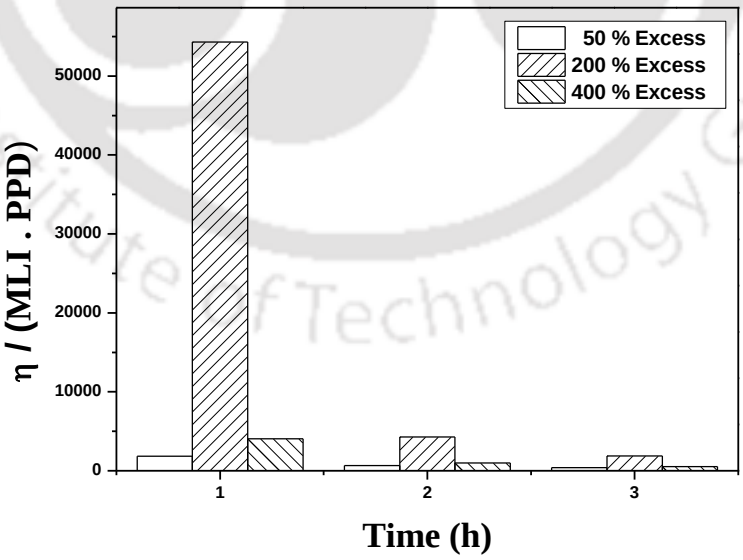

Figure 6.6: η/(MLI.PPD) index graph for 0.01M Ag SOEP (DW) process.

Table 6.2: A summary of average plating rate data for 0.01 M SOEP (DW) processes with variant hydrazine concentrations and plating time.

Reducing agent concentration (% Excess)	Average plating rate (mol/L.s)×10^6 for various total plating time (h)		
	1	2	3
50	1.29	1.72	1.84
200	1.17	1.69	1.72
400	1.84	1.89	1.76

6.4.4 Average plating rates

Table 6.2 presents a summary of the average plating rates for various hydrazine excess concentration cases. It can be observed that the average plating rate varied from 1.29 – 1.84×10^{-6}, 1.17 – 1.72×10^{-6} and 1.84 – 1.76×10^{-6} mol/L.s for 50%, 200% and 400% excess hydrazine cases. This indicates that significant variation in average plating rates could not be achieved by varying the excess hydrazine solution concentration. Thereby, the optimal plating rate corresponds to a value of 1.17×10^{-6} mol/L.s that was obtained for the 200% excess hydrazine solution case.

6.4.5 Summary

For 0.01 M Ag baths, at a plating time of 1 h, the optimal hydrazine concentration of 200% excess provided a conversion, efficiency, PPD, MLI, η/(MLI.PPD) and average plating rate values of 46.24%, 69.24%, 0.7%, 1.82×10^{-3} g/cm^3, 54308.52 and 1.17×10^{-6} mol/L.s respectively. This choice is based on the maximum plating efficiency obtained for a plating time of 1 h. The optimal plating time of 1 h for 0.01 M Ag is not the same value that was obtained for 0.005 M Ag baths. Hence, it is apparent that the Ag solution concentration is an important parameter to

influence the combinatorial plating characteristics of Ag SOEP baths for porous metal-ceramic composite membrane fabrication.

6.5 Plating characteristics of 0.015M Ag SOEP baths

6.5.1 Conversion and Plating Efficiency

For 0.015 M Ag SOEP baths, Figure 6.7 (a) presents the variation of time dependent conversion profiles for various reducing agent concentrations. For all cases, the conversions increased from 1 – 2 h plating time which later reduced for a plating time of 3 h. For a plating time variation from1 – 2 h, the conversions varied from 76.15 – 84.45%, 77.71 – 81.77% and 79.39 – 84.60% for 50%, 200% and 400% excess hydrazine concentrations respectively. For a total plating time of 3 h, these values reduced to 80.78%, 76.89% and 80.97% for corresponding cases. The optimality of intermediate plating time of 2 h is possibly due to variations in the metal nucleation in the solutions, which occurred due to variations in the Ag adhesion to the ceramic support. The obtained conversion values are significantly higher in comparison to those obtained for 0.005 M and 0.01 M Ag SOEP baths. However, the optimality of 0.015 M could be only judged with the efficiency profiles.

Figure 6.7 (b) presents the time dependent efficiency profiles for 0.015 M Ag SOEP baths. For 50% hydrazine excess case, the time dependent efficiency values reduced linearly from 40.68 – 34.72% for plating time variation from 1 – 3 h. This confirms that significant metal nucleation occurred with prolonged plating time and the porous Ag film underwent substantial variations in its morphology due to poor adhesion to the support. On the other hand, for both 200% and 400% excess hydrazine cases, the time dependent efficiencies increased from 38.48 – 43.19% and

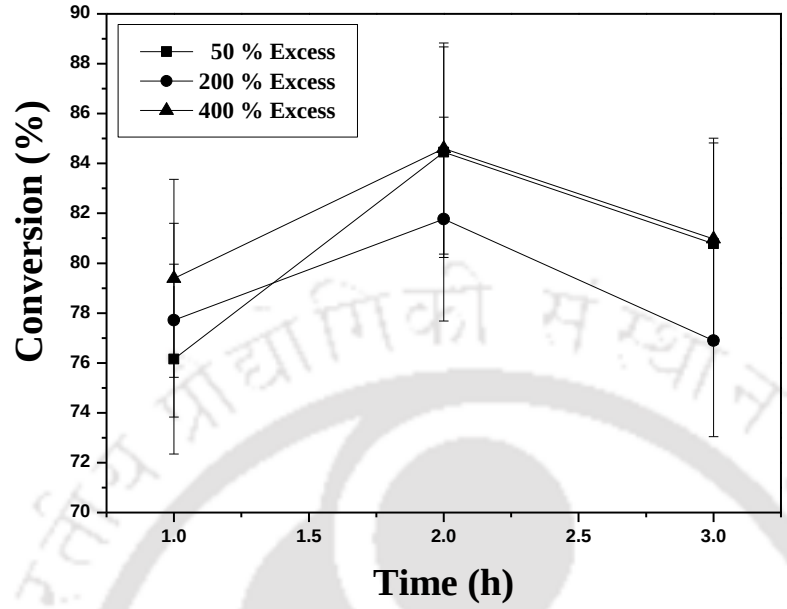

(a)

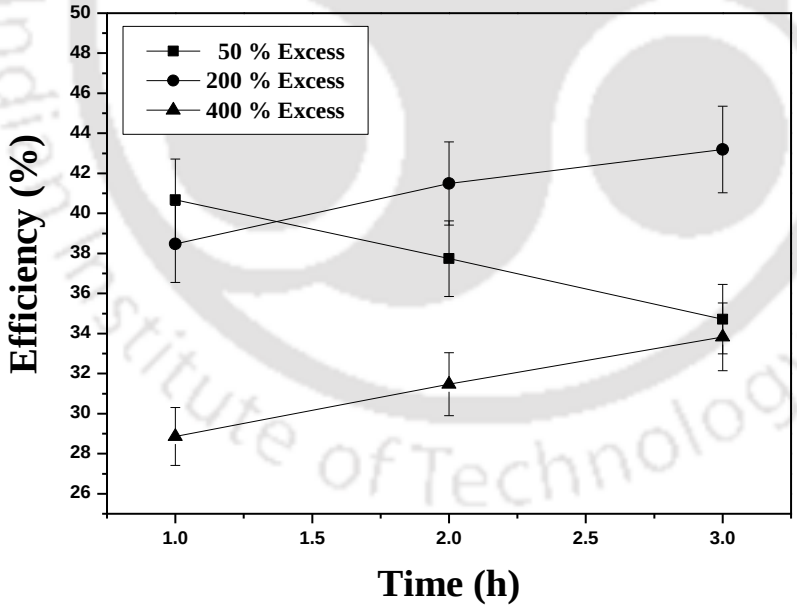

(b)

Figure 6.7: Effect of hydrazine solution concentration on the time dependent (a) Conversion and (b) Efficiency profiles for 0.015M Ag SOEP (DW) process.

28.86 – 33.83% respectively for a variation in plating time from 1 – 3 h. Among all cases, 200% excess hydrazine concentration provided optimal efficiency profiles and indicated that the chosen hydrazine concentration enabled the fabrication of metal composite membrane morphology that improved with plating time. These observations are in good agreement with inefficiency profile reported in the literature (Agarwal et al., 2014) for Ni solution concentration effect during dense metal ceramic composite membrane fabrication.

6.5.2 PPD and MLI profiles

Figure 6.8 (a) presents the time dependent PPD profiles for 0.015 M silver solution concentration. It can be observed that for plating time from 1-3 h, the PPD varied from 2.04-11.14%, 2.58-14.38% and 2.95-10.68% for 50, 200 and 400% excess hydrazine concentrations, respectively. Further, it can also be observed that for 200% excess hydrazine concentration, the maximum PPD of 14.38 % was obtained and it is about 23-26% higher than the PPDs obtained for lower and higher hydrazine solution concentrations. The PPD reduction with plating time for 50% and400% excess hydrazine concentration cases is due to the unwanted metal nucleation in the solution.

The MLI profiles for 0.015 M Ag SOEP baths are presented in Figure 6.8 (b). As shown, the MLI profiles varied from 2.65 – 7.18×10^{-3}, 2.57 – 8.76×10^{-3} and 1.96 – 7.09×10^{-3} g/cm^3 for 50%, 200% and 400% excess hydrazine concentration cases. Among all cases, highest MLI have been obtained for 200% excess hydrazine case and confirms its optimality with respect to obtained efficiency and PPD profiles. Further, both 50% and 400% excess hydrazine concentration cases enabled a reduction in PPD after 3 h of plating time in comparison with that obtained for 200% excess hydrazine concentration case.

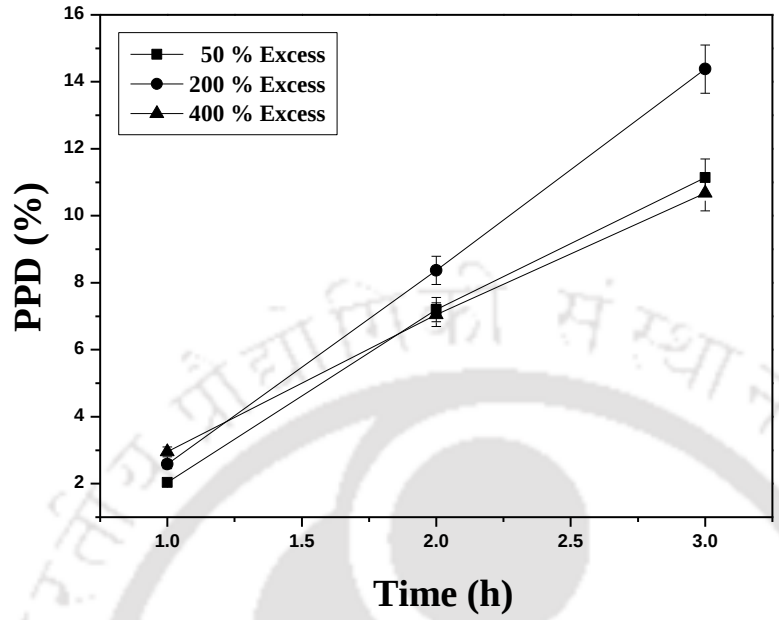

(a)

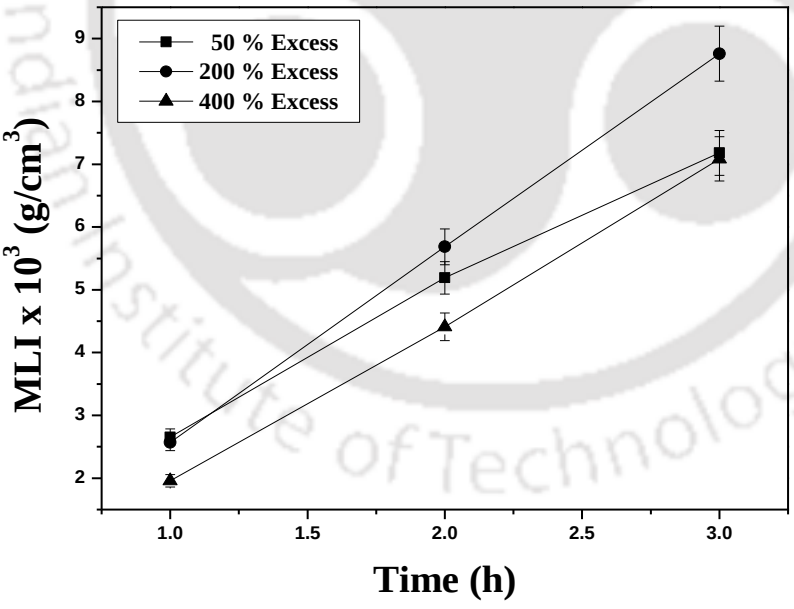

(b)

Figure 6.8: Variation of time dependent (a) PPD and (b) MLI profiles with hydrazine solution concentration for 0.015 M Ag SOEP (DW) process.

This is attributed to the dynamic degradation of membrane morphology to support metal adhesion in the former two cases.

6.5.3 η/(MLI.PPD) index

The η/(MLI.PPD) index values for various plating times and hydrazine solution concentrations are presented in Figure 6.9 as a bar chart. As shown, maximum index is obtained for 50 % excess hydrazine concentration case where efficiencies are not the optimal. Based on best efficiency value, the optimal η/(MLI.PPD) index is about 342.89 for 200 % excess hydrazine concentration and plating time of 3 h.

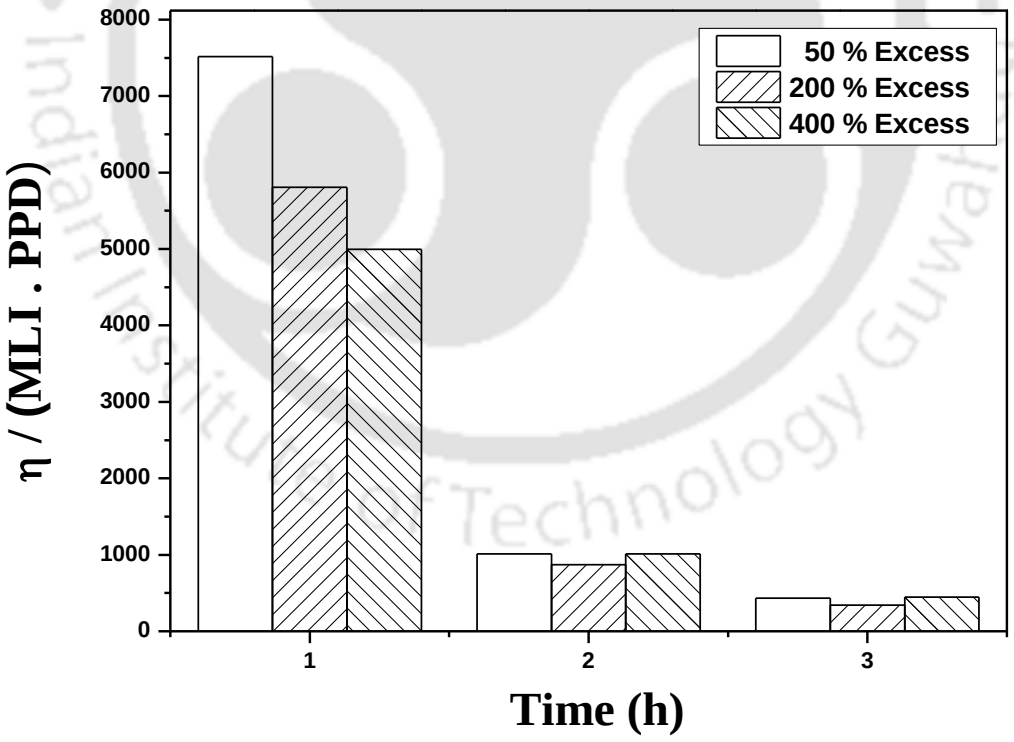

Figure 6.9: η/(MLI.PPD) index graph for 0.015M Ag SOEP (DW) process.

Table 6.3: Average plating rate data for 0.015 M Ag SOEP (DW) process.

Reducing agent concentration (% Excess)	Average plating rate (mol/L.s)×10^6 for various total plating time (h)		
	1	2	3
50	2.90	3.22	3.08
200	2.97	3.12	2.93
400	3.02	3.22	3.08

6.5.4 Average plating rates

For 0.015 M Ag SOEP baths, Table 6.3 presents a summary of the average plating rates for various hydrazine excess concentration cases. It can be observed that the average plating rate varied from 2.90 – 3.08×10^{-6}, 2.97 – 2.93×10^{-6} and 3.02 – 3.08×10^{-6} mol/L.s for 50%, 200% and 400% excess hydrazine cases. This indicates that the average plating rates did not vary significantly with variation in excess hydrazine concentration. These results are in agreement with those obtained at 0.01 M Ag solution concentration.

6.5.5 Summary

For 0.015 M Ag baths, at a plating time of 3 h, the optimal hydrazine concentration of 200 % excess provided conversion, efficiency, PPD, MLI, η/(MLI.PPD)and average plating rate values of 76.89%, 43.19%, 14.38%, 8.76×10^{-3} g/cm^3, 342.89 and 2.93×10^{-6} mol/L.s respectively. This choice is based on the maximum plating efficiency obtained for a plating time of 3 h. The optimal plating time of 3 h for 0.01 M Ag is significantly different from that obtained for 0.015 M Ag baths. Hence, generalization of process parameters such as plating time appears to be invalid for porous Ag ceramic composite membrane fabrication using SOEP baths.

6.6 Surface characterization

Porous silver-ceramic membrane fabricated using drop wise addition of reducing agent for SOEP baths at optimal process parameters (0.01 M Ag concentration and 200 % excess hydrazine concentration, plating time of 1 h) was characterized by FESEM and the obtained micrograph is presented in Figure 6.9 (a). It can be observed that pore modification occurred on the ceramic support with the formation of Ag metal grain agglomerates on the porous structure. Figure 6.10 (b) presents the XRD pattern of silver-ceramic membrane fabricated using drop wise addition of reducing agent with optimal process parameters. The figure indicates that silver (Ag) reflection peaks have been detected in the face centered cubic phase at (111), (200), (220) and (220) planes. Further, no peaks including those of kaolin and support materials could be observed in the XRD pattern and this indicates that the Ag film coverage is effective on the porous ceramic surface.

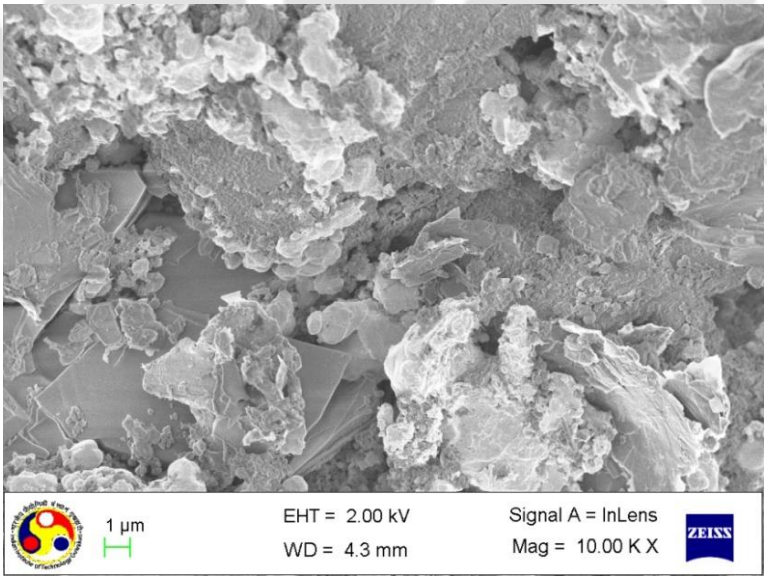

(a)

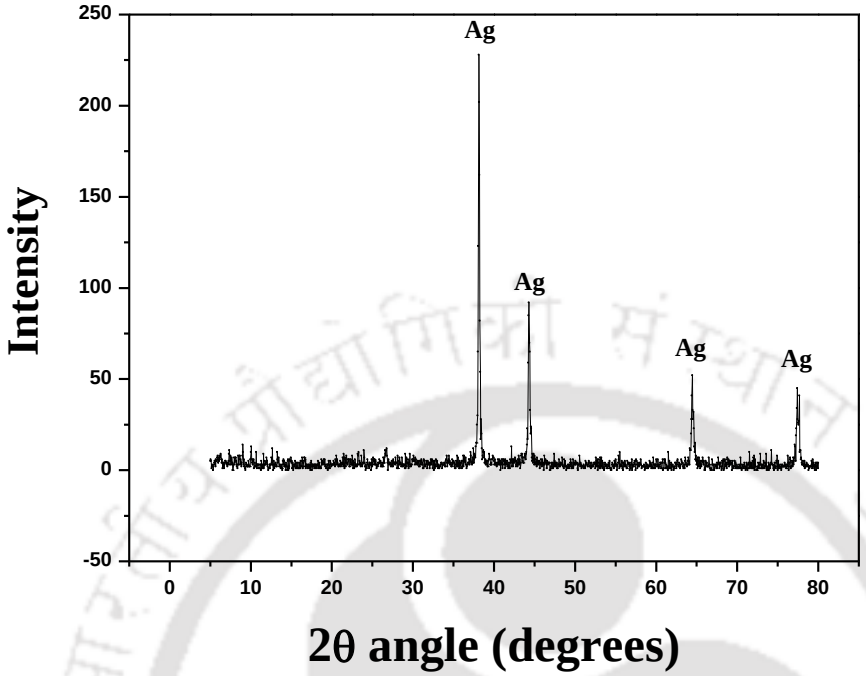

(b)

Figure 6.10: (a) Surface FESEM image and (b) XRD pattern of silver-ceramic composite membrane fabricated with 0.01 M Ag SOEP (DW) process.

6.7 Cost Analysis

The laboratory fabricated low cost silver-ceramic composite membranes from SOEP (DW) baths need to be analyzed towards cost effectiveness. Therefore, retail cost estimation has been done for the optimal silver-ceramic composite membranes. For the cost analysis, various parameters considered refers to manpower, electricity, sonication and chemicals for the retail cost estimation. The parameters considered for the cost estimation of silver-ceramic composite membrane are presented in Table 6.4. Appendix B summarizes details with respect to the cost estimation for both ceramic support and silver-ceramic composite membranes. For the cost

estimation, 150 mL total plating solution is used for a membrane area of 2.37×10^{-3} m^2 and 3 h of plating time.

The costs of the ceramic support and silver film inclusive of other costs are 1656.96 and 4180.51 $/m^2, respectively. Eventually, the total cost of silver-ceramic composite membrane inclusive of all costs is 5837.51 $/m^2. The silver-ceramic composite membrane cost is 3.5 times higher than the cost obtained for ceramic support using parameters reported in this section. Considering these parameters, the retail cost of silver-ceramic composite membrane fabricated using SSOEP silver ELP baths is also similar (5839.88 $/m^2). Therefore, in comparison with the

Ag SOEP baths, the cost of membrane fabrication with SSOEP baths has been increased by only 2.37 $/m^2. Compared to commercial silvertech membranes, the fabricated silver ceramic composite membranes are inexpensive by 40%. A further accurate estimate of the retail costs could further increase the cost effectiveness of the fabricated membranes by 50 – 60%. Thus, low cost silver-ceramic composite membranes have been fabricated which can be applied for applications such as bacteria filtration, alcoholic beverage filtration, XRD analysis media, silica and carbon black analysis media etc.,

Table 6.4: Conceptual retail cost parameters for low cost ceramic and silver ceramic composite membranes (fabricated with SOEP process).

S.No	Parameter	Chemicals cost per membrane ($/m^2)	Total cost inclusive of other costs ($/m^2)
1	Ceramic support	60.71	1656.96
2	Silver film	761.90	4180.54
3	Silver-ceramic composite membrane	822.60	5837.51

6.8 Summary

A summary of various combinatorial plating characteristics for all cases is presented in Table **6.5**. As shown, the best case corresponds to SOEP bulk plating baths at a solution concentration of 0.01 M Ag and 800 % excess hydrazine solution concentration where the optimal combinatorial plating characteristics are 83.18%, 62.98%, 5.73%, 9.09×10^{-3} g/cm^3 and 1197.18 for parameters conversion, efficiency, PPD. MLI and η/(MLI.PPD) respectively. The obtained characteristics values for drop wise reducing agent addition case are marginally poorer in comparison to those obtained for Ag baths with bulk reducing agent addition.

Table 6.5: A summary of optimal combinatorial plating characteristics for Ag SOEP and SSOEP processes for low cost Ag ceramic composite membrane fabrication.

S. NO.	Process	Mode of reducing agent contacting pattern	Process Parameters	Time of plating (h)	Average Conversion (%)	Average Efficiency (%)	Average PPD (%)	Average MLI ($g/cm^{3)}$	Average plating rate (mol/L.s)	η/(MLI.PPD)
1	SOEP	Bulk	0.01M Ag, 800% Excess Hydrazine,	3	83.18	62.98	5.73	9.09×10^{-3}	2.35×10^{-6}	1197.18
2	SSOEP	Bulk	0.01M Ag, 800% Excess Hydrazine, 2 CMC CTAB	3	83.23	69.13	1.99	1.01×10^{-2}	2.34×10^{-6}	3402.89
3	SOEP	Drop	0.01M Ag, 200% Excess Hydrazine,	3	66.84	52.68	5.15	5.43×10^{-3}	1.72×10^{-6}	1882.97
4	SSOEP	Drop	0.01M Ag, 200% Excess Hydrazine, 2 CMC CTAB	3	41.34	19.33	22.43	1.27×10^{-3}	1.06×10^{-6}	676.51

Chapter 7:

Microfiltration Performance of Silver-Ceramic Composite Membranes

Chapter 7

Microfiltration Performance of Silver-Ceramic Composite Membranes

Along with the comparative assessment with ceramic membrane supports, this chapter summarizes the separation efficiency results obtained during dead end microfiltration performance of silver composite membranes using synthetic bacteria (E. coli) solutions. Two distinct compositions have been investigated for silver composite membranes fabricated with CM1 supports. Section 7.1 presents an overview of the chapter. Eventually, in section 7.2, the comparative microfiltration performance (in terms of LRV) of silver ceramic composite membranes and membrane supports is presented for low and high feed concentration. Based on the research findings, section 7.3 presents possibilities for further research.

7.1 Overview

It has been emphasized in several literatures that silver membranes including silver composite membranes are effective towards bacteriostatic applications. However, the literature does not elaborate upon fabrication engineering aspects and the comparative performance assessment of silver membranes and their porous supports. Therefore, there is a need to assess upon the competence of the silver ceramic composite membranes for bacteria filtration applications, given the fact that silver membranes are highly expensive in comparison with the ceramic membranes.

To carry out the separation potential tests for fabricated silver ceramic membranes, silver ceramic membranes were fabricated with CM1 and CM3 membranes using SOEP process. The

operating conditions of the SOEP process are 0.01 M Ag solution concentration and plating time of 3 h. This is due to the fact that after 3 h of Ag plating, maximum silver film thickness can be achieved and hence bacteriostatic applications can be better explored with ease and confidence. Thereby, the obtained SOEP membranes were thoroughly rinsed in hot water and then dried to test their separation performance. For this purpose, dead end MF studies were carried out using low and high feed solution concentrations. During these studies, flux data was not taken and only permeate and feed analysis using colony count method was carried out to evaluate their separation potential.

It has been observed that the Ag composite membrane prepared with CM3 support provided poor microfiltration performance with LRV values of about 1. Dense colonies were observed in the permeate samples. This is possibly due to widening of pores during Ag SOEP. In this regard, it is important to note from the results presented in Chapter 5 that PPD did not reduce with plating time for the Ag SSOEP baths. Therefore, it might be the case that wider pores became wider and narrow pores became narrower to enhance PPD. This might have in turn degraded the morphology of the biofilm and easy passage of the bacteria through the fouled silver membrane during dead end MF. Thereafter, silver membranes were fabricated with CM1 support and comparable results were achieved. The obtained results are presented in the following section.

7.2 MF of silver ceramic composite membranes

7.2.1 Effect of lower feed concentration (~10^4 CFU/mL) on the separation performance of silver ceramic composite membranes

Figure 7.1 presents the separation potential (LRV) of silver-ceramic composite (fabricated with CM1 support) and CM1 ceramic membranes for low feed concentration (in the order of 10^4 CFU/mL). For the CM1 membrane, at a feed concentration of 3.72×10^4 CFU/mL, 100% PRV

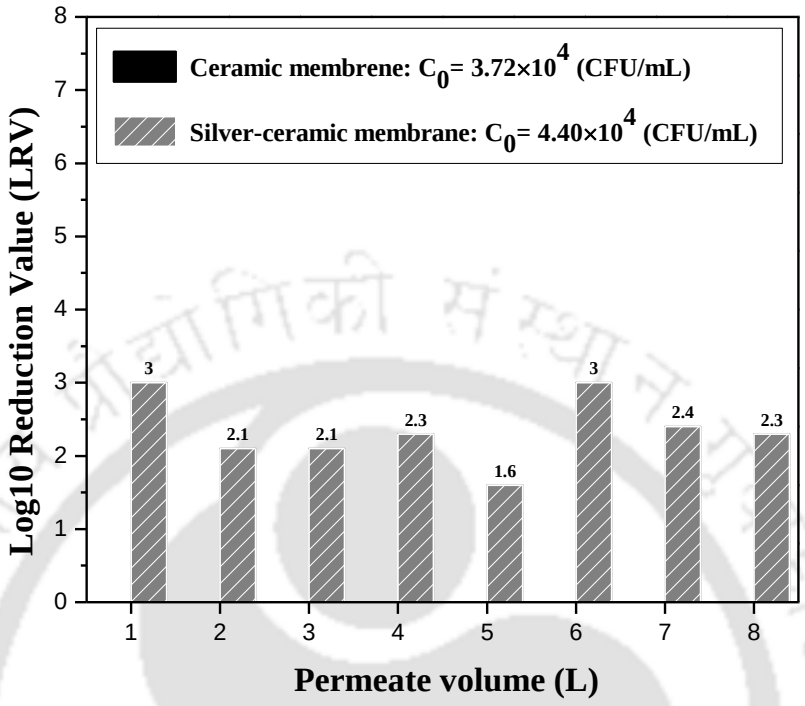

Figure 7.1: Variation of permeate quality (LRV) with permeate volume (L) for silver-ceramic composite membranes at lower feed concentration (about 10^4 CFU/mL). The removal for the ceramic membrane was greater (about 100%) than those obtained for the silver composite membranes.

was obtained. Hence, bars could not be presented in LRV bar chart presented in Figure 7.1. This is due to the fact that the governing equation of LRV (Eq.2.7) could not be applied for cases where permeate count is about 0 CFU/mL. On the other hand, for the silver-ceramic membrane, for a similar feed concentration (4.40×10^4 CFU/mL), the LRV can be observed to vary from 3.0 - 2.3 LRV for a variation in permeate volume from 1 – 8 L. Hence, it can be inferred that electroless fabrication enables deposition of elemental silver on the silver ceramic composite membrane could not provide good separation performance. Compared to the support, the reduction in LRV is possibly due to pore size enhancement during electroless plating of silver on ceramic membrane. In this regard, it is important to note from the

results presented in Chapter 5 that PPD did not reduce with plating time for the Ag SOEP baths. Therefore, it might be the case that wider pores became wider and narrow pores became narrower to enhance PPD. This might have in turn degraded the morphology of the biofilm and easy passage of the bacteria through the fouled silver membrane during dead end MF.

7.2.2 Effect of higher feed concentration (~10^6 CFU/mL) on silver-ceramic composite membrane performance

Figure 7.2 summarizes the separation efficiency of silver-ceramic and ceramic membranes prepared with CM1 support and at higher feed concentrations (~10^6 CFU/mL). The dead end LRV data for the support is based on the results presented in Chapter 3 of the thesis. For the ceramic membrane support CM1 and

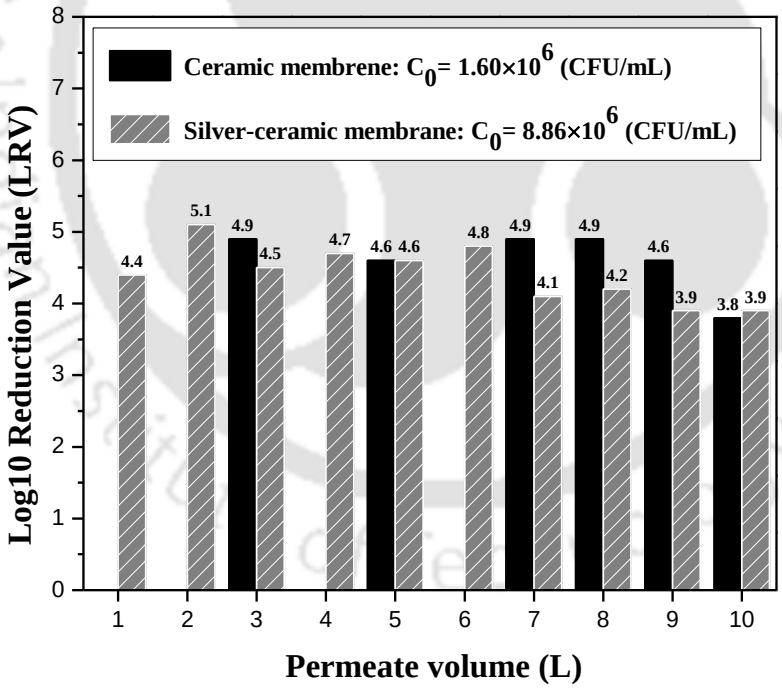

Figure 7.2: Variation of permeate quality (LRV) with permeate volume (L) for ceramic and silver-ceramic composite membranes at higher feed concentration (~10^6 CFU/mL). Bars are not shown for few cases of the ceramic membrane (100% PRV).

feed concentration of 1.60×10^6 CFU/mL, for permeate volumes of 1, 2, 4 and 6 L, LRV values are not presented in the graph as 100% PRV was obtained for these cases. On the other hand, for the silver-ceramic composite membrane and feed concentration of 8.86×10^6 CFU/mL, the silver-ceramic membrane provided lower LRVs (5.1 – 3.8) which are 8 – 16% lower than those obtained for the ceramic support. The reduction in the LRV for the silver ceramic membrane is possibly due to widening of the porous structure during prolonged plating in alkaline silver plating baths. In this regard, it is important to note from the results presented in Chapter 5 that PPD did not reduce with plating time for the Ag SOEP baths. Therefore, it might be the case that wider pores became wider and narrow pores became narrower to enhance PPD. This might have in turn degraded the morphology of the biofilm and easy passage of the bacteria through the fouled silver membrane during dead end MF. Thus, even for higher feed concentration also, silver ceramic composite membranes did not provide better performance in comparison with the ceramic membranes.

7.3 Analysis of results and further scope for future research

The bacteria filtration research using silver-ceramic composite membranes needs to be further refined. It is evident from conducted studies that the fabricated ceramic supports are incompatible to serve as materials for low cost silver ceramic composite membranes applicable towards bacteria filtration application. Therefore, the hypothesis of the electroless fabricated silver film for effective bacteriostatic application needs to be affirmed and this can be facilitated by choosing an expensive compatible support first and eventually targeting low cost ceramic membranes. Ideally, the silver ceramic composite membranes must provide 100% PRV for cases

where 1 – 3 LRV was obtained for the supports. Only in those circumstances, the silver membranes competence can be affirmed from experimental investigations.

Despite obtaining poor performance of silver membranes for MF of bacteria solutions, the research conducted in this work contributed to the directions of further research. Apart from this, there can be optimism to target electroless fabricated silver-ceramic composite membranes as alcoholic filtration media and as XRD, silica and carbon black analysis media.

Chapter 8:

Conclusions and Future Work

Conclusions and Future Work

Section 8.1 summarizes conclusions obtained from the research findings of the thesis. Section 8.2 presents possible scope for future research work.

8.1 Conclusions

Based on experimental investigations conducted in this work, the conclusions obtained for various cases are presented in the following sub-sections.

8.1.1 Dead end microfiltration performance of low cost ceramic membranes

- Extensive experimental investigations were carried out to evaluate upon the competence of low cost ceramic membranes for bacteria filtration applications. While such studies may exist in the literature, this work enabled greater insights into the application of uniaxial dry compaction based low cost ceramic membranes for bacteria filtration applications.
- A unique inorganic precursor formulation (kaolin 40 wt%, quartz 15 wt%, calcium carbonate 20 wt%, sodium carbonate 10 wt%, boric acid 5 wt% and sodium metasilicate 10 wt% on a dry basis) has been identified that provided membranes with wider morphology (average pore size and porosity of 4.5µm and 19.3% respectively) using uniaxial dry compaction method. The membranes are anticipated to serve as gravity filter applications during batch potable water treatment application.
- For the literature reported inorganic precursor formulation of CM1 membrane (other than PVA 2 wt%, kaolin 40 wt%, quartz 15 wt%, calcium carbonate 25 wt%, sodium carbonate 10

wt%, boric acid 5 wt% and sodium metasilicate 5 wt%) which yielded an average pore size and porosity of 0.7μm and 39.4% respectively, at a ΔP of 206.7 kPa and feed concentration of 8.4×10^{6} CFU/mL, the optimal dead end MF flux and rejection (PRV) corresponds to 1.83×10^{-3} $m^3/m^2.s$ and100% respectively.

- For the literature reported inorganic precursor formulation of CM2 membrane (Other than PVA 4 wt%, kaolin 40 wt%, quartz 15 wt%, calcium carbonate 25 wt%, sodium carbonate 10 wt%, boric acid 5 wt% and sodium metasilicate 5 wt%) which yielded an average pore size and porosity of 1.5 μm and 32.3% respectively, at a ΔP of 206.7 kPa and feed concentration of 0.05×10^{6} CFU/mL, the optimal dead end MF flux and rejection (PRV) corresponds to 9.68×10^{-4} $m^3/m^2.s$ and 100% respectively.
- For CM3 membrane, at a ΔP of 206.7 kPa and feed concentration of 14.9×10^{6} CFU/mL, the optimal dead end MF flux and rejection (PRV) correspond to 5.05×10^{-3} $m^3/m^2.s$ and 99.9999% respectively. Thus, CM1 and CM2 membranes provided the minimum flux with good values of permeate quality whereas CM3 membrane gave the maximum flux but low permeate quality.
- For all membranes, cake filtration fouling model fit well to represent the pertinent dead end MF flux decline.

8.1.2 Cross flow microfiltration performance of low cost ceramic membrane

- At a circulation rate and ΔP of 1 LPM and 206.7 kPa respectively, the optimal steady state flux and rejection (LRV) are $2.11\times10^{-3}m^3/m^2.s$ and 6 respectively for CM1 at feed concentration of 15.2×10^{5} CFU/mL, 8.09×10^{-4} $m^3/m^2.s$ and 5 respectively for CM2 membrane at a feed concentration of 40.4×10^{5} CFU/mL and 2.79×10^{-4} $m^3/m^2.s$ and 4.3 respectively for CM3 membrane at a feed concentration of 7.60×10^{5} CFU/mL.

Comparatively, cross flow MF provided lower LRVs with respect to those obtained with dead end MF. The optimal flux has been analyzed based on resistances in series model based analyses of the fouling resistance and average fouling index profiles. Also, CM3 membrane provided lower separation potential (2.9 – 3.1 LRV) in comparison with the CM2 and CM1 membrane (3.5 – 6 LRV).

- Resistances in series model has been very useful to judge upon the optimality of various combinations of feed concentration and membrane morphologies during cross flow MF. Without the model analysis, it has been observed that misleading inferences could be deduced with respect to process condition and membrane selection optimality.
- The resistances in series model analysis has explicitly inferred that high feed concentration (around 10×10^5 CFU/mL) will cause higher fouling (more than 90%) during cross flow MF for all membranes.
- Inclusive of chemicals, manpower and electricity costs, the retail conceptual cost of the ceramic membrane supports are 1656.96 $\$/m^2$, which is expected to reduce by 40% with process scale up and rigorous cost analysis.

8.1.3 Process optimality for electroless fabrication of porous silver ceramic composite membranes

- Among Ag CEP, SOEP, SIEP and SSOEP baths supplemented with bulk addition of the reducing agent, SOEP and SSOEP processes have been identified to be the optimal processes for porous silver ceramic composite membranes.
- For the Ag SOEP process, 0.01 M Ag solution concentration has been identified to be the optimal concentration for metal ceramic composite membrane fabrication.

- For the Ag SSOEP process, 2 CMC CTAB surfactant concentration has been identified as the optimal surfactant concentration for metal ceramic composite membrane fabrication.
- For a Ag solution concentration of 0.01 M, surfactant concentration of 2 CMC and plating time of 3 h, the optimal combinatorial plating characteristics for Ag SSOEP baths correspond to a conversion, plating efficiency, PPD, MLI and average plating rate of 83%, 69%, 2%, 10.14×10^{-3} g/cm^3 and 2.34×10^{-6} mol/L respectively.
- For a Ag solution concentration of 0.01 M and plating time of 3 h, the optimal combinatorial plating characteristics for Ag SOEP baths correspond to a conversion, plating efficiency, PPD, MLI and average plating rate of 83%, 62%, 5.7%, 9.09×10^{-3} g/cm^3 and 2.35×10^{-6} mol/L.s respectively.
- The obtained optimal combinatorial characteristics and process parameters are envisaged to be applicable for low cost silver ceramic composite membranes which have several applications such as alcoholic filtration media, XRD sample analysis media and silica/carbon black analysis media.

8.1.4 Efficacy of Reducing Agent Contacting Pattern on the plating characteristics of Ag SOEP baths

- During drop wise mode of hydrazine addition, the optimal combinatorial plating characteristics of Ag SOEP baths correspond to a conversion, plating efficiency, PPD, MLI and average plating rate of 46.24%, 69.24%, 0.7%, 1.82×10^{-3} g/cm^{3}and 1.72×10^{-6} mol/L.s respectively for 0.01 M Ag and hydrazine solution concentration of 200% excess respectively and plating time of 1 h.

- Among Ag SOEP baths facilitated with bulk and drop wise mode of the reducing agent contacting pattern, baths with drop wise mode of the reducing agent contacting pattern provided poorer combinatorial plating characteristics. This is attributed to the significant metal nucleation in the solution due to the reduction in metal adhesion that was brought forward by the combined effect of cavitation and drop wise addition of the reducing agent.
- Inclusive of manpower, electricity, sonication and chemicals, the conceptual retail cost of the silver-ceramic composite membranes is 5837.51 $/m^2$ which is 3.5 times higher than the conceptual retail cost of the low cost ceramic membranes. However, the silver composite membrane cost is estimated to be 40% lower than the cost of the commercial silvertech membranes. Thereby, it is envisaged that the porous silver-ceramic composite membranes cost could be further reduced with process scale up studies. For such a scenario, the low cost silver ceramic composite membranes have been evaluated to be at least 60% inexpensive than commercial silvertech membranes.

8.1.5 Dead end MF performance of silver-ceramic composite membranes

- In terms of the LRV, the dead-end MF performance of silver ceramic composite membranes fabricated with CM3 membranes are significantly poorer than those obtained with CM3 membranes. This is possibly due to the widening of pores during prolonged plating time of silver membrane fabrication. Since PPDs have increased with plating time, it might be the case that wider pores became wider and narrow pores became narrow during prolonged plating and this in turn affected biofilm morphology within and on the top of the silver membrane during dead end MF.

- In terms of the LRV, the dead end MF performance of silver ceramic composite membranes fabricated with CM1 membrane were marginally poorer than those obtained for CM1 membranes. This is possibly due to widening of pores during electroless fabrication of Ag composite membranes. Since PPDs have increased with plating time, it might be the case that wider pores became wider and narrow pores became narrow during prolonged plating and this in turn affected biofilm morphology within and on the top of the silver membrane during dead end MF.
- The carried out investigations provided significant insights into silver ceramic composite membrane research for effective future investigations towards bacteriostatic applications.

8.2 Future work

Based on the investigations and obtained results reported in the thesis, the following sub-sections summarize various important research themes for consideration as future work

8.2.1 Fabrication of compatible low cost ceramic membranes for bacteria filtration applications

During dead end MF studies, CM1- CM3 membranes could not provide calcium free permeate samples. This was confirmed in the physico-chemical tests conducted using water analysis kit for both feed and permeate samples. This confirms that calcium leaching occurred during MF. Hence, without varying much the identified inorganic precursor compositions (outlined in the literature for CM1 and CM2 membranes and presented in this work for CM3), future research emphasis should be dovetailed to swap carbonate precursors with alternative inexpensive pore forming agents to achieve low cost ceramic membranes with similar morphologies (average pore

size of 0.7 – 4.5 μm) and similar/better dead end and cross flow MF performance (in terms of flux and LRV data) of synthetic DH5α bacterial solutions.

8.2.2 Dead end and cross flow MF of synthetic mixed bacterial culture solutions

In this work a single bacterium (DH5α) was used for the evaluation of membrane dead end and cross flow MF performance. The real world scenario would involve more complex combinations of micro-organisms. Hence, synthetic solutions with mixed bacterial culture needs to be prepared and analyzed in the near future to evaluate upon the effect of mixed bacterial culture concentration on both flux and separation efficiency of low cost ceramic membranes using dead end and cross flow MF configurations. Deeper insights shall be gained into the relative size of bacteria with respect to pore size, charge interactions etc., for single as well as mixed species cultures.

8.2.3 Dead end and cross flow MF of real contaminated water samples

In addition to micro-organisms, real contaminated water samples collected from lakes, ponds and other open habitat resources consist of other impurities such as mud, suspended solids etc., Therefore, the ultimate applicability of the prepared ceramic composite membranes is dependent on their performance with real contaminated water samples. It can be expected that membranes could undergo significant fouling with mud, suspended solids and bacteria in comparison to the synthetic bacterial solutions. Therefore, dead end and cross flow flux and separation characteristics of low cost ceramic membranes needs to be obtained for real water samples and compared with those obtained for various synthetic solutions.

8.2.4 Alcoholic beverage filtration studies using low cost silver ceramic composite membranes

Commercial alcoholic beverage filtration technology has been proposed using porous silver catalyst/adsorbent beds (WR27). Instead, low cost silver ceramic composite membranes can be utilized which can significantly contribute to compactness of the process and overall productivity. In addition, the inexpensive fabrication of low cost Ag-ceramic composite membranes using identified electroless plating process further accounts towards the cost effectiveness of membrane fabrication as well as application towards alcoholic beverage filtration.

8.2.5 Applicability of low cost silver ceramic composite membranes for other commercial applications

There is very limited literature pertaining to the application of silver membranes for XRD, silica, carbon black analysis. Considering the fact that low cost silver composite membranes could be produced with an economic competitiveness of 40% when compared to the commercial silvertech membranes, more data needs to be generated for the commercial application of silver ceramic membranes for XRD, silica and carbon black analysis.

8.2.6 Fabrication of low cost ceramic tubular membranes using identified compositions for bacteria filtration applications

Process scale up investigations for low cost ceramic membranes targeted for bacteria filtration applications essentially involve retrofit studies. Such studies need to first consider identified compositions with uniaxial dry compaction based membrane fabrication. Using such data, the

research investigations need to identify compositions with paste method to fabricate tubular ceramic supports with similar membrane morphologies. Considering the fact that bacteria filtration has not been extensively studied with low cost ceramic membranes, systematic investigations are required to correlate the fabrication parameters of uniaxial dry compaction and paste methods to achieve membranes with similar membrane morphologies. Along with such studies, membrane composition compatibility also needs to be addressed to achieve acceptable permeate samples during dead and cross flow microfiltration.

8.2.7 Compatible silver-ceramic composite membranes for bacteriostatic applications

This work could not enable the successful application of silver-ceramic composite membranes for bacteriostatic applications. The proposed hypothesis for the same is that the elemental silver film might be ineffective. In this regard, further research investigations are required with a multi-disciplinary research emphasis. These specifically refer to (a) rigorous characterization using temperature programmed reduction (TPR), X-ray photon spectroscopy (XPS) for the identification of elemental and ionic silver species in the membrane matrix and (b) process modifications to achieve better bacteriostatic applications of the silver film. It has been widely inferred in the literature that ionic silver is more effective to achieve bacteriostatic effect. In such case, electroless silver deposition needs to be actively promote existence of ionic Ag species on the membrane surface during microfiltration and further research directions from chemistry and materials synthesis perspectives would be useful to envisage upon bacteriostatic applications. Nonetheless this work enabled that electroless fabricated low cost silver ceramic composite membranes are not compatible for bacteria filtration and significant research is required in this direction in the near future.

In summary, the research theme of low cost ceramic and silver ceramic composite membranes for bacteria filtration applications provides an exciting area of research and needs to be further addressed to enhance commercial ceramic membrane applications. The Ph.D. thesis involved the specification of bacteria feed and permeate concentration in terms of total colony count but not in terms of total number of bacteria filtered per unit membrane area. Hence, future work needs to address additional characterization during bacteria microfiltration such as total number of bacteria filtered per unit membrane area and correlate such characterization data with total colony count data.

References

References

Agarwal, A., Pujari, M., Uppaluri, R., Verma, A., 2013. Preparation, optimization and characterization of low cost ceramics for the fabrication of dense nickel composite membranes. Ceramics International 39, 7709 -7716.

Agarwal, A., Pujari, M., Uppaluri, R., Verma, A., 2014a. A novel method of reducing agent contacting pattern for metal ceramic composite membrane fabrication. Applied Surface Science 320, 52-59.

Agarwal, A., Pujari, M., Uppaluri, R., Verma, A., 2014b. Efficacy of reducing agent and surfactant contacting pattern on the performance characteristics of nickel electroless plating baths coupled with and without ultrasound. Ultrasonics Sonochemistry 21, 1382-1391.

Agarwal, A., Pujari, M., Uppaluri, R., Verma, A., 2014c. Optimal electroless plating rate enhancement techniques for the fabrication of low cost dense nickel/ceramic composite membranes. Ceramics International 40, 691-697.

Almandoz, M.C., Marchese, J., Prádanos, P., Palacio, L., Hernández, A., 2004. Preparation and characterization of non-supported microfiltration membranes from aluminosilicates. Journal of Membrane Science 241, 95-103.

Alvar, E.N., Golmohammadi, M.R., Rezaei, M., Alvar, H.N., Mardanloo, A., Nouhian, S.H., Didari, M., 2008. Preparation and thermal treatment of3 Pd/Ag composite membrane on a porous α-alumina tube by sequential electroless plating technique for H2 separation. Journal of Natural Gas Chemistry 17, 321-326.

Bielefeldt, A.R., Kowalski, K., Summers, R.S., 2009. Bacterial treatment effectiveness of point-of-use ceramic water filters. Water Research 43, 3559-3565.

Bulasara, V.K., Abhimanyu, M.S., Pranav, T., Uppaluri, R., Purkait, M.K., 2012. Performance characteristics of hydrothermal and sonication assisted electroless plating baths for nickel–ceramic composite membrane fabrication. Desalination 284, 77-85.

Bulasara, V.K., Uppaluri, R., Purkait, M.K., 2012. Effect of ultrasound on the performance of nickel hydrazine electroless plating baths. Materials and Manufacturing Processes 27, 201-206.

Cheng, Y.S., Yeung, K.L., 1999. Palladium–silver composite membranes by electroless plating technique. Journal of Membrane Science 158, 127-141.

Ciston, S., Lueptow, R.M., Gray, K.A., 2008. Bacterial attachment on reactive ceramic ultrafiltration membranes. Journal of Membrane Science 320, 101-107.

Emani, S., Uppaluri, R., Purkait, M.K., 2013. Preparation and characterization of low cost ceramic membranes for mosambi juice clarification. Desalination 317, 32-40.

Emani, S., Uppaluri, R., Purkait, M.K., 2014a. Cross flow microfiltration of oil–water emulsions using kaolin based low cost ceramic membranes. Desalination 341, 61-71.

Emani, S., Uppaluri, R., Purkait, M.K., 2014b. Microfiltration of oil–water emulsions using low cost ceramic membranes prepared with the uniaxial dry compaction method. Ceramics International 40, 1155-1164.

Girard, B., Fukumoto, L.R., 1999. Apple Juice Clarification Using Microfiltration and Ultrafiltration Polymeric Membranes. LWT - Food Science and Technology 32, 290-298.

Hermia, J., 1982. Constant pressure blocking filtration laws-application to power –law non newtonian fluids. Transactions of the Institution of Chemical Engineers 60, 183-118.

Hilal, N., Kochkodan, V., Al-Khatib, L., Levadna, T., 2004. Surface modified polymeric membranes to reduce (bio)fouling: a microbiological study using E. coli. Desalination 167, 293-300.

Huang, T.-C., Wei, M.-C., Chen, H.-I., 2003. Preparation of hydrogen-permselective palladium–silver alloy composite membranes by electroless co-deposition. Separation and Purification Technology 32, 239-245.

Keuler, J.N., Lorenzen, L., Sanderson, R.D., Prozesky, V., Przybylowicz, W.J., 1999a. Characterising palladium–silver and palladium–nickel alloy membranes using SEM, XRD and PIXE. Nuclear Instruments and Methods in Physics Research Section B: Beam Interactions with Materials and Atoms 158, 678-682.

Keuler, J.N., Lorenzen, L., Sanderson, R.D., Prozesky, V., Przybylowicz, W.J., 1999b. Characterization of electroless plated palladium–silver alloy membranes. Thin Solid Films 347, 91-98.

Kikuchi, E., Uemiya, S., 1991. Preparation of supported thin palladium-silver alloy membranes and their characteristics for hydrogen separation. Gas Separation & Purification 5, 261-266.

Lv, Y., Liu, H., Wang, Z., Liu, S., Hao, L., Sang, Y., Liu, D., Wang, J., Boughton, R.I., 2009. Silver nanoparticle-decorated porous ceramic composite for water treatment. Journal of Membrane Science 331, 50-56.

Ma, H., Tian, F., Li, D., Guo, Q., 2009. Study on the nano-composite electroless coating of Ni–P/Ag. Journal of Alloys and Compounds 474, 264-267.

Marchese, J., Pagliero, C.L., 1991. Characterization of asymmetric polysulphone membranes for gas separation. Gas Separation & Purification 5, 215-221.

Mehler, J.E., Lankenau, R.O., Mees, F.S., 1982. Determination of carbon black on silver membrane filters from rubber factory dust. American Industrial Hygiene Association journal 43, 908-911.

Mei, F., Shi, D., 2005. Electroless Plating of Thin Silver Films on Porous Al2O3 Substrate and the Study of Deposition Kinetics. Tsinghua Science & Technology 10, 680-689.

Mwabi, J.K., Mamba, B.B., Momba, M.N.B., 2012. Removal of Escherichia coli and Faecal Coliforms from Surface Water and Groundwater by Household Water Treatment

Devices/Systems: A Sustainable Solution for Improving Water Quality in Rural Communities of the Southern African Development Community Region. International Journal of Environmental Research and Public Health 9, 139-170.

Nandi, B.K., Uppaluri, R., Purkait, M.K., 2008. Preparation and characterization of low cost ceramic membranes for micro-filtration applications. Applied Clay Science 42, 102-110.

Nandi, B.K., Das, B., Uppaluri, R., Purkait, M.K., 2009a. Microfiltration of mosambi juice using low cost ceramic membrane. Journal of Food Engineering 95, 597-605.

Nandi, B.K., Uppaluri, R., Purkait, M.K., 2009b. Treatment of Oily Waste Water Using Low-Cost Ceramic Membrane: Flux Decline Mechanism and Economic Feasibility. Separation Science and Technology 44, 2840-2869.

Oyanedel-Craver, V.A., Smith, J.A., 2007. Sustainable Colloidal-Silver-Impregnated Ceramic Filter for Point-of-Use Water Treatment. Environmental Science & Technology 42, 927-933.

Paul, S., Mishra, U., 2011. Assessment of underground water quality in North Eastern region of India: A case study of Agartala City. International Journal of Environmental Sciences 2, 850-862.

Pérez Padilla, A., Rodríguez, J.A., Saitúa, H.A., 1997. Synthesis and water ultrafiltration properties of silver membrane supported on porous ceramics. Desalination 114, 203-208.

Pindi, P.K., Yadav, P.R., Kodaparthi, A., 2013. Bacteriological and Physico-Chemical Quality of Main Drinking Water Sources. Polish Journal of Environmental Studies 22.

Quang, D.V., Sarawade, P.B., Hilonga, A., Kim, J.-K., Chai, Y.G., Kim, S.H., Ryu, J.-Y., Kim, H.T., 2011. Preparation of silver nanoparticle containing silica micro beads and investigation of their antibacterial activity. Applied Surface Science 257, 6963-6970.

Salahi, A., Gheshlaghi, A., Mohammadi, T., Madaeni, S.S., 2010. Experimental performance evaluation of polymeric membranes for treatment of an industrial oily wastewater. Desalination 262, 235-242.

Simonis, J.J., Basson, A.K., 2011a. Evaluation of a low-cost ceramic micro-porous filter for elimination of common disease microorganisms. Physics and Chemistry of the Earth, Parts A/B/C 36, 1129-1134.

Srivastava, A., Srivastava, O.N., Talapatra, S., Vajtai, R., Ajayan, P.M., 2004. Carbon nanotube filters. Nat Mater 3, 610-614.

van Halem, D., van der Laan, H., Heijman, S.G.J., van Dijk, J.C., Amy, G.L., 2009. Assessing the sustainability of the silver-impregnated ceramic pot filter for low-cost household drinking water treatment. Phys Chem Earth 34, 36-42.

Vasanth, D., Pugazhenthi, G., Uppaluri, R., 2011a. Fabrication and properties of low cost ceramic microfiltration membranes for separation of oil and bacteria from its solution. Journal of Membrane Science 379, 154-163.

Vasanth, D., Uppaluri, R., Pugazhenthi, G., 2011b. Influence of Sintering Temperature on the Properties of Porous Ceramic Support Prepared by Uniaxial Dry Compaction Method Using Low- Cost Raw Materials for Membrane Applications. Separation Science and Technology 46, 1241-1249.

Yang, Y.-F., Li, Y., Li, Q.-L., Wan, L.-S., Xu, Z.-K., 2010. Surface hydrophilization of microporous polypropylene membrane by grafting zwitterionic polymer for anti-biofouling. Journal of Membrane Science 362, 255-264.

Yazgan, I., Du, N., Congdon, R., Okello, V., Sadik, O.A., 2014. Biofunctionalized poly (amic) acid membranes for absolute disinfection of drinking water. Journal of Membrane Science 472, 261-271.

Zhao, H., Cui, J., 2007. Electroless plating of silver on AZ31 magnesium alloy substrate. Surface and Coatings Technology 201, 4512-4517.

Zhu, X., Loo, H.-E., Bai, R., 2013. A novel membrane showing both hydrophilic and oleophobic surface properties and its non-fouling performances for potential water treatment applications. Journal of Membrane Science 436, 47-56.

Web References:

WR1: Safe Drinking Water Foundation, Canada: http://www.safewater.org/PDFS/PurposeofDrinkingWaterQualityGuidelinesRegulations.pdf, (accessed May 2014).

WR2: Gaia Ltd.,- in service to Africa: http://www.gaia-africa.com/cms/index.php/information/16-diseases-causen-by-contaminated-drinking-water, (accessed April 2013).

WR3: Water purification–Wikipedia, the free encyclopedia: http://en.wikipedia.org/wiki/Water_purification#cite_note-2, (accessed April 2013).

WR4: Eureka Forbes water purifiers: http://www.eurekaforbes.com/water-purifiers.aspx, (accessed April 2013).

WR5: Hindustan Unilever Pureit: http://www.pureitwater.com/IN/technology, (accessed April 2013).

WR6: Tata Swach nanotech water purifiers: http://www.tataswach.com/, (accessed April 2013).

WR7: Kent RO Water purifiers: http://kent.co.in/kent_technology/mineralro_technology.aspx, (accessed April 2013).

WR8: Philips UV water purifier: http://www.philips.co.in/c/water-purifier/pure-water-uv-wp3889_01/prd/;jsessionid=140F511860EEDCF954D64C43F541919E.app101-drp4, (accessed April 2013).

WR9: Hi-Tech water purifier: http://www.hitechro.net/, (accessed April 2013).

WR10: Kenstar water purifiers: http://www.kenstar-appliances.com/products_ha_wp.php#, (accessed April 2013).

WR11: Whirlpool RO Purifiers: http://www.whirlpoolindia.com/water-purifiers, (accessed April 2013).

WR12: Livpure RO water purifiers: http://www.livpurewater.com/, (accessed April 2013).

WR13: Ushabrita water purifiers: http://www.ushabrita.com/, (accessed April 2013).

WR14: Centers for disease control and prevention: http://www.cdc.gov/healthywater/drinking/travel/household_water_treatment.html, (accessed April 2013).

WR15: Technofilter Research and Manufacturing Enterprise Ltd Silver filtration technology for water-alcoholic mixtures, Patent No 2222586: http://www.filter-ru.com/use/food/filtration_of_wateralcohol/, (accessed October 2014).

WR16:Sterilization(Microbiology):www.frankshospitalworkshop.com/equipment/.../sterilization.pdf, (accessed March 2012).

WR17: Zefon Intenational sampling equipment specialist: http://www.zefon.com/store/silver-membrane-filters-0.8-37mm.html, (accessed March 2012).

WR18: Germlyser, Aqua-free Membrane Technology GmbH, Germany: http://www.aqua-free.com/en/general-water-hygiene., (accessed March 2012).

WR19: Purificup potable natural water purifier: http://purificup.com/index.php/natural-water-purifier-green.html, (accessed April 2012).

WR20: SKC Silver membrane filter: www.skcinc.com/prod/225-1801.asp, (accessed March 2012).

WR21: Sterlitech Corporation, USA: http://www.sterlitech.com/membrane-disc-filters/silver-membranes.html, (accessed March 2012).

WR22: General Electric Silver membranes: http://www.gewater.com/water-quality-monitoring.html?cid=ApplicationsNavBar, (accessed March 2012).

WR23: SPI-Pore^{TM} silver membranes: http://www.2spi.com/catalog/spec_prep/silver-membrane-filtration-media.html, (accessed March 2012).

WR24: Nano Silver membranes available at Wacorp Hyundai India Limited, Noida, UP, India: http://www.indiamart.com/wacorphyundai/#profile, (accessed March 2012).

WR25: Merck Millipore silver membrane filters: http://www.millipore.com/catalogue/module/C7906, (accessed March 2012).

WR26: Detection of chlorine using NIOSH method 6011: http://www.atsdr.cdc.gov/toxprofiles/tp172-c7.pdf, (accessed November 2014).

WR27: Technofilter Research and Manufacturing Enterprise Ltd Silver filtration technology for water-alcoholic mixtures, Patent No 2222586: http://www.filter-ru.com/use/food/filtration_of_wateralcohol/, (accessed November 2014).

WR28 : Electroless Plating of silver (chapter 17), N. Koura: www.sciencemadness.org/talk/files.php?pid=97774&aid=3243, (accessed March 2012).

WR29: J.M. Brown, Effectiveness of ceramic filtration for drinking water treatment in Cambodia. Ph.D Dissertation. University of North Carolina at Chapel Hill, 2007: *potterswithoutborders.com/.../Studies/joe-brown-dissertation.pdf,* (accessed March 2012).

WR30: Microbiology techniques: http://www2.hendrix.edu/biology/CellWeb/Techniques/microspread.html, (accessed May 2012).

Appendix

Appendix A: Pore Size Distributions using FESEM Image Analysis

The FESEM based analysis was used to evaluate the approximate average membrane pore size. The estimation of average membrane pore size (d_s) and pore size distribution from FESEM micrographs was carried out using ImageJ software (Version 1.40). Individual pore diameters were measured for about 500 pores using ImageJ software for different pores visible in the FESEM image. Thus, a primary assumption of the procedure is that the variation in the intensities of various sections refers to the pores, which may or may not be true for all cases. Also, pore size distribution and average pore distribution values critically dependent on the sampling procedure. Thus, micrographs were taken randomly from the selected section of the membranes in order to obtain pore size distributions that represent the overall porous texture of the membrane. While such methodology may or may not be correct, the image analysis could not be conducted without such basic limitations that cannot be eliminated. Eventually based on the obtained Image analysis data, the pore size distributions were obtained for CM1 - CM3 membranes. The average pore diameter (d_s) from FESEM analysis of the membrane was evaluated by assuming cylindrical porous texture of the membrane as

$$d_s = \left[\frac{\sum_{i=1}^{n} n_i d_i^2}{\sum_{i=1}^{n} n_i} \right]^{0.5}$$

where, n is the number of pore, d_i is the pore diameter (μm) of i^{th} pore.

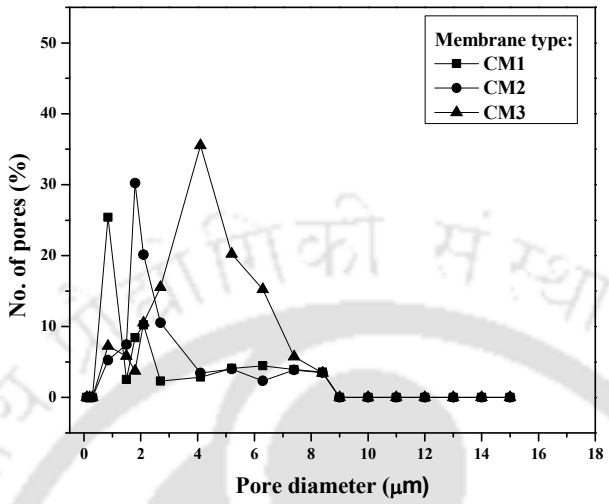

Figure A1: Pore size distribution profiles for various membranes.

It is also important to note that the FESEM based pore size refer to the total porous structure of the membranes, which includes dead and permeable pores. Thus, there could be significant variation in the pore sizes estimated by FESEM and by liquid permeation experiments.

Figure A1 illustrates the variation of pore diameters of the membrane morphology with the number of pores. For all membranes (CM1 – CM3), it can be observed that less than 10 % of the pores are within the pore diameter range of 1 – 15 μm. Also, 25% of the pores exist below 0.85 μm for CM1 membrane, 30% and 36% pores exist for CM2 and CM3 membranes below 1.8 and 4.1 μm respectively. Based on the obtained pore size distribution profiles, the average pore size of CM1, CM2 and CM3 membranes have been evaluated as 1.1, 1.9 and 4.9 μm respectively.

Appendix B: Conceptual Retail Cost Analysis of Ceramic and Silver-Ceramic Composite Membranes

In this section, the calculations related to conceptual retail cost analysis of ceramic support, film and silver-ceramic composite membrane. The following calculations represent the cost of the support, silver film and composite membrane. In these cost calculations, manpower, chemical, electricity and sonication have also been considered.

I) Support cost

Unit prices of various raw materials are as follows: Kaolin – Rs. 520/kg; Quartz – Rs. 200/kg; $CaCO_3$ – Rs. 408/kg; Na_2CO_3 – Rs. 432; Boric acid – Rs.768/kg and Sodium metasilicate – Rs. 578/kg.

Inorganic precursor formulation for CM3 membrane on a weight basis: Kaolin – 40 %, Quartz – 15 %; $CaCO_3$ – 25 %; Na_2CO_3 – 10 %; Boric acid – 5 % and Sodium metasilicate – 5 %.

Cost of one support (20 g for support)

$$\frac{(40\times 20\times 520+15\times 20\times 200+...)}{100\times 10000} = \text{Rs. } 9.01$$

The currency conversion factor used in all calculations is 1 Rs = 0.016 $

Area of the support = 23.746 cm^2

$$\text{One membrane support disc cost} = \frac{9.01Rs}{23.746cm^2} = 0.379\text{Rs}/cm^2 = 60.709\$/m^2 \qquad \text{(B1)}$$

The laboratory grade muffle furnace enables the fabrication of 12 supports in one sintering run. For fabrication, other parameters are assumed as follows:

Manpower requirement = 500 Rs/day

Total manpower requirement is for 4 days to fabricate membranes.

$$\text{Manpower cost} = \frac{500\left(Rs/days\right)\times 4days}{12\times 23.746cm^2} = 7.019Rs/cm^2 \quad \text{(B2)}$$

Electricity consumed to fabricate 12 low cost ceramic supports = 2 kW

Sintering time required to fabricate 12 supports = 2 days

Electricity tariff charge = 8.78 Rs/ kW.h

$$\text{Total electricity cost} = \frac{24h\times 2\times 2kW\times 8.78(\text{Rs/ kW.h})}{12\times 23.746cm^2} = 2.958Rs/cm^2 \quad \text{(B3)}$$

Total cost of support inclusive of manpower and electricity (B1+B2+B3) =

$$= 10.356\text{Rs}/cm^2 = 1656.963\$/m^2 \quad \text{(B4)}$$

II) Cost Ag film deposition

Cost of plating bath chemicals: $AgNO_3$ – Rs. 327.8/gm; Na_2EDTA – Rs. 260/100 gm; NH_4OH – Rs. 492/2.5 L; Hydrazine – Rs. 1182/500 mL.

Using the above unit costs of chemicals, for reported ELP bath composition, the cost of chemicals consumed to plate silver on a ceramic support with 3 h of sequential ELP = Rs. 113.429

The currency conversion factor used in all calculations is 1 Rs = 0.016 $

Area of the support = 23.746 cm^2

$$\text{Cost of Ag ELP per unit area} = \frac{113.429Rs}{23.746cm^2} = 4.777\text{Rs}/cm^2 = 764.271\$/m^2 \quad \text{(B5)}$$

Manpower requirement for one silver plating step (inclusive of drying etc.,) = Rs. 500/-

$$\text{Manpower cost per unit area of plating} = \frac{500Rs}{23.746cm^2} = 21.056Rs/cm^2 \quad \text{(B6)}$$

Electricity consumed per one silver plating step using sonication = 280 W = 0.28 kW

Time required for one silver plating = 3 h

Electricity Tariff charge = 8.78 Rs/ kW.h

Total electricity cost during Ag ELP with SOEP process =

$$\frac{3h \times 0.28kW \times 8.78(\text{Rs/ kW.h})}{23.746cm^2} = 0.311Rs/cm^2 \quad \text{(B7)}$$

Total cost for fabrication of silver film = Cost of Chemicals + Cost of Manpower + Cost of electricity = (B4+B5+B6) = $= 26.143\text{Rs}/cm^2 = 4182.918\$/m^2$ (B8)

III) Cost of silver-ceramic composite membrane fabrication

Silver-ceramic composite cost (inclusive of manpower, electricity and support costs) (B4+B8) = $36.499\text{Rs}/cm^2 = 5839.881\$/m^2$

The website of Sterlitech silver membranes (WR21) conveys that the cost of 25 nos. of 47 mm dia. and 5 μm average pore size commercial silver membranes = $ 423.76.

Area of commercial silver membranes = 25 nos. x 3.14/4 x $(47 \times 10^{-3})^2$ = 0.0433 m^2

Cost of commercial silver composite membranes = 423.76/0.0433 = 9786 $/m^2

Compared to the commercial Sterlitech membranes, the laboratory fabricated silver-ceramic composite membranes are 40 % inexpensive. Further research in scale up is anticipated to reduce the cost of silver ceramic composite membranes to about 3000 $/m^2. For such a case, the low cost silver-ceramic composite membranes will have 75 % cost lower than the commercial membranes.

Appendix C: Theoretical Porous Ag film Thickness Data

Chapters 5, 6 and 8 of the Ph.D. thesis presented weight gained during electroless fabrication of porous silver ceramic composite membranes in terms of metal loading index. However, there might be a need to evaluate the theoretical metal film thickness using appropriate correlation.

For this purpose, the average porous Ag metal film thickness is evaluated using the expression:

$$\delta_{Agp} = \frac{(w_2 - w_1)}{A_m \rho_m}$$

Process	Average porous film thickness (μm) for various total plating time cases		
	1h	2h	3h
CEP (0.01 M Ag)	2.8	7.2	8.3
SIEP(0.01 M Ag, 2 CMC)	3.2	9.1	12.2
SOEP (0.005 M Ag)	2.3	5.5	8
SOEP (0.01 M Ag)	7.8	18.8	26
SOEP (0.015 M Ag)	4.7	14	18
SSOEP (0.01 M Ag, 1 CMC)	5.7	13.9	18.6
SSOEP (0.01 M Ag, 2 CMC)	8.3	19	27.2
SSOEP (0.01 M Ag, 3 CMC)	4.6	12.2	16.7
SSOEP (0.01 M Ag, 4 CMC)	3.9	9.9	13.5

(a)

Ag solution concentration	% Excess hydrazine concentration	Average Porous film thickness (μm) for various total plating time cases		
		1h	2h	3h
0.005 M	50	1.04	2.14	2.62
	200	1.09	2.27	4.31
	400	1.4	2.97	4.39
0.01 M	50	3.4	7.51	10.88
	200	4.82	8.8	14.36
	400	3.38	10.79	11.33
0.015M	50	7.09	13.85	19.15
	200	6.95	15.37	23.65
	400	5.25	11.81	18.95

(b)

Table C1: Porous metal film thickness values for various cases (a) Bulk addition of reducing agent for CEP, SIEP, SOEP and SSOEP processes (b) Drop wise addition of reducing agent for SOEP processes.

where δ_{Agp} refers to the average porous Ag metal film thickness, $(w_2 - w_1)$ refers to the weight gained during electroless Ag membrane fabrication, A_m is the area of the membrane subjected to Ag ELP and ρ_m is the structural density of the membrane (expressed in terms of weight of the dry membrane disc per unit volume of the membrane disc).

For various experimental investigations, Table C1 (a) and (b) summarize theoretical porous Ag film thickness values for bulk and drop wise reducing agent contacting pattern respectively. The presented data in Table C1 is anticipated to serve as a standard benchmark for furthering research in the electroless fabrication of low cost silver ceramic composite membranes.

Appendix D: Sample Calculations for Combinatorial Plating Characteristics of Ag SOEP Baths

The sample calculations for evaluation of various parameters involved in the electroless fabrication of silver- ceramic membrane are presented as follows:

1. Metal Conversion (x (%))

After three sequential deposition $V_i = 3\times55\times.001$ L, $C_i = 0.01$ mol/L , $V_iC_i = 0.165 \times0.01$ mol

$= 0.00165$ mol

Titration : $N_1 = \frac{N_2 \times V_2}{V_1} = \frac{0.01\times 6.8}{10} = 0.0068N$

Volume of solution obtainedafter 3sequential deposition $V_f =$ 134 mL

$C_f = 0.0068$ mol/L, $V_fC_f = 0.00091$ mol

Conversion : $x = \frac{V_iC_i - V_fC_f}{V_iC_i}\times100$

x= 44.85 %

2. Plating efficiency ($\eta(\%)$)

$$\eta = \frac{w_2 - w_1}{w_0\, x}\times100$$

$$w_0x = (V_iC_i - V_fC_f)M_{Ag} = 0.13g$$

$w_2 - w_1 = 0.0516$ g

$\eta = 39.69$ %

3. Average Plating rate $\left(\bar{r}_i \left(\frac{mol}{\mathrm{L}.s}\right)\right)$

$$\overline{r_i} = \frac{0.0516}{169.87 \times (165 \times 0.001) \times 3 \times 3600} = 1.70 \times 10^{-7} \frac{mol}{L.s}$$

4. Percent Pore Densification (PPD(%))

$$PPD = \frac{\overline{J_0} - \overline{J_i}}{\overline{J_0}} \times 100 = \frac{179.5 - 170.25}{179.5} \times 100 = 5.16\%$$

$\overline{J_0}$ and $\overline{J_i}$ were determined from the area under the curve of plot J vs. ΔP which was plotted for both ceramic support and silver-ceramic composite membrane respectively using N_2 permeation experiments. Procedure for the same has been presented elsewhere (Agarwal et al., 2013).

5. Metal loading Index (MLI (g/cm^3)

$$MLI = \frac{w_2 - w_1}{A_m \delta}$$

$$MLI = \frac{0.0516}{23.75 \times 4} = 5.43 \times 10^{-4} g / cm^3$$

Appendix E: Determination of Ag Solution Concentration

The procedure for the determination of silver solution concentration before and after plating process is summarized as follows. Volhard's method was used to analyze the concentration of silver ions in samples collected before and after plating. The method involves titration with potassium thiocyanate (KCNS) solution. Titrations were conducted between silver samples and solution mixture of KCNS and ferric ammonium sulfate solution ($NH_4Fe(SO_4)_2.12H_2O$) indicator with few drops of concentrated nitric acid. During the titration process, silver thiocyanate (AgCNS) gets precipitated due to the reaction between silver ions and KCNS.

The $NH_4Fe(SO_4)_2.12H_2O$ solution was prepared with 8 mL of salt and 20 mL of water. This was used as an indicator. The main reactions involved in the titration process are presented as follows:

$$KCNS + AgNO_3 \xrightarrow{NH_4Fe(SO_4)_2.12H_2O} AgCNS + KNO_3$$

Thus, the solution remains pale yellow until excess (unreacted) silver ions react with the thiocyanateions. Eventually, titration end point is realized when no silver ions are available in the solution and Ferric ions available in the solution start forming a Ferrous complex as shown below:

$$CNS^- + Fe^{3+} \rightarrow Fe(CNS)^{2+}$$

The overall titration procedure is summarized in the following steps:

(i) 10 mL of silver ion containing bath sample was taken into a 250 mL beaker.

(ii) The sample is mixed with ferric ammonium sulfate indicator. The solution is pale yellow in color due to the presence of excess Ag ions in the solution.

(iii) Titration was conducted using standardized 0.01 M KCNS solution that was placed in a burette.

(iv) Titration was terminated by observing the variation in the solution color from pale yellow to deep red color.

The above steps (i – iv) were repeated at least 3 – 4 times to obtain average titration based end point. From the burette run down volume (V_2) of standard (N_2=*0.01 M*) KCNS solution, the Ag ion concentration N_1 (in terms of Normality or Molarity) in the plating bath was evaluated using the expression:

$$N_1 \times V_1 = N_2 \times V_2$$

where, (V_1) is the volume of Ag ion containing bath sample taken in the beaker (10 mL).

Appendix F: Spread Plate Colony Count Method

The feed and permeate samples collected from dead end and cross flow MF studies were analyzed using spread plate colony count method which can summarized in the following steps:

a) **Preparation of Sterile LB Agar solution:** 32 g of LB-Growth Top Agar (Himedia, India), was taken and suspended in 1000 mL Millipore water. Subsequently, the prepared solution was subjected to sterilization using an Autoclave (Make: Equitron, Medica Instrument Mfg. Co., India) at 121^{o}C (15 psi pressure) for 20 minutes. Similarly, sterile dilution water was also prepared.

b) **Preparation of sterile petriplates and micro-tips for dilution:** The petriplates and micro-tips were first subjected to sterilization in an Autoclave at 121^{o}C for 20 minutes. Subsequently, sterile LB Agar solution, Petri plates, micro-tips were transferred to Laminar flow hood.

c) **10 fold dilution procedures of feed/permeate samples:** 100 µL from feed sample was taken and diluted in 900 µL of sterilized Millipore water. The sample thus prepared is termed as 10^{-1} dilution sample. The 10^{-1} dilution sample was further diluted with similar quantities subsequently to achieve 10^{-2}, 10^{-3}, 10^{-4} and 10^{-5} dilution samples. For permeate samples, only 10^{-1} and 10^{-2} dilution was considered.

d) **Spreading:** Using L-Spreader and a micro-tip, 15 - 20 mL of sterile LB-agar was first transferred into the Petri plate in the laminar flow hood chamber, which would solidify upon cooling in the petri plate itself. Eventually, 50 µL of prepared dilution sample was spread using micro-tip and L-Spreader in a gentle manner so that the dilution sample is

spread uniformly on the solidified agar plate. Subsequently, the petri plate samples were sealed with parafilm (Bemis Flexible packaging, USA) and were transferred from the Laminar flow hood chamber to the Incubator (Make: Dass & Co, Kolkata) and were kept at 37^{o}C for 24 – 48 h.

e) **Colony count:** Visible colonies that appeared on the petri plate plates were counted using digital colony counter (Make: VSI-CC1, VSI Electronics Pvt. Ltd., India).

The basic assumption of colony count method is that one colony represents several live cells and hence, obtaining permeate samples with no colonies infers 100 % separation efficiency of the low cost ceramic membranes. Therefore, sample concentration corresponds to the number of colonies counted after incubation.

(a) **(b)**

Figure G1: Low cost (a) Ceramic and (b) Silver-ceramic membranes

Figure G2: Dead end Microfiltration Setup

Figure G3: Cross flow Microfiltration Setup (Courtesy: Department of Biotechnology Juice Clarification Project)

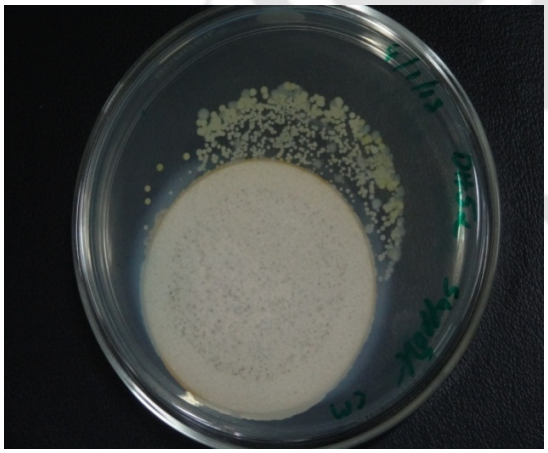

(a) Bio film formation on CM1 membrane after MF run

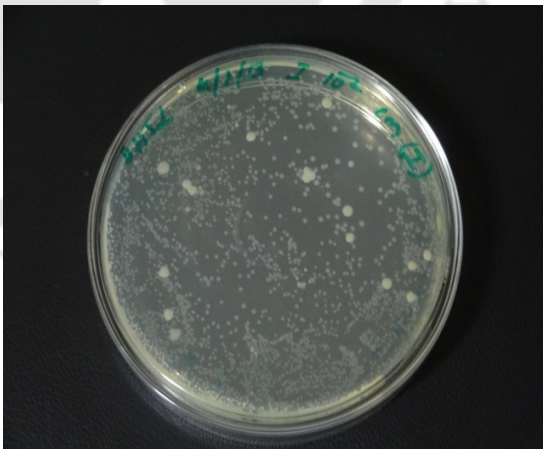

(b) Dense colonies in feed sample

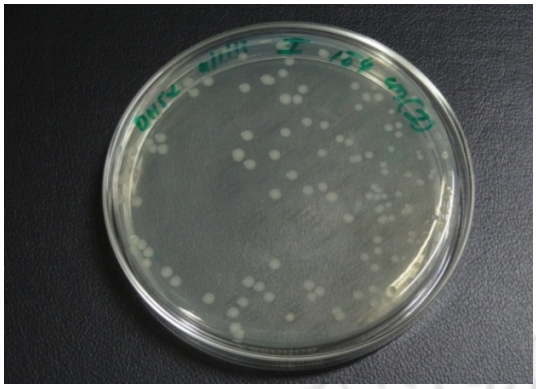

(c) Colonies for 10^{-3} Dilution of feed sample

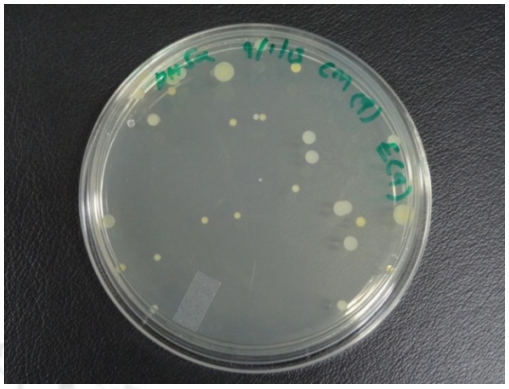

(d) Colonies for 10^{-5} Dilution of feed sample

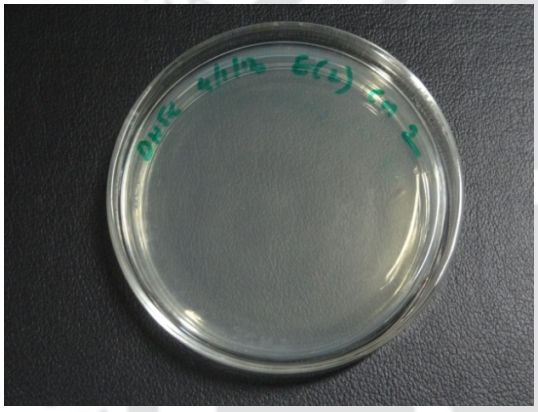

(e) CM1 dead end MF permeate sample colony count plate

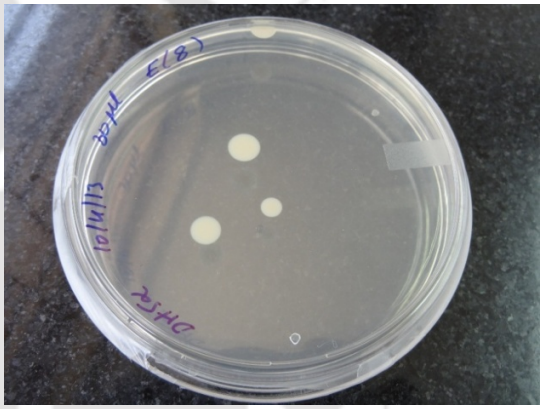

(f) CM2dead end MF permeate sample colony count plate

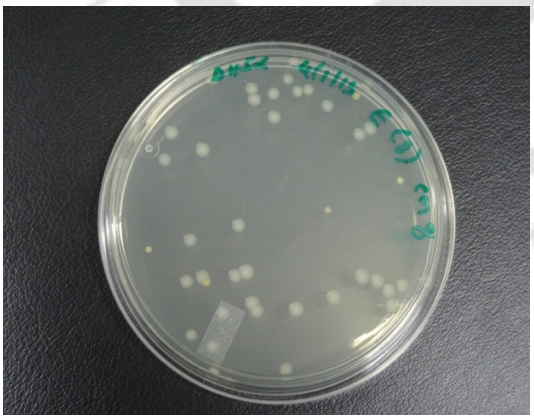

(g) CM3membrane dead-end MF permeate sample colony count plate

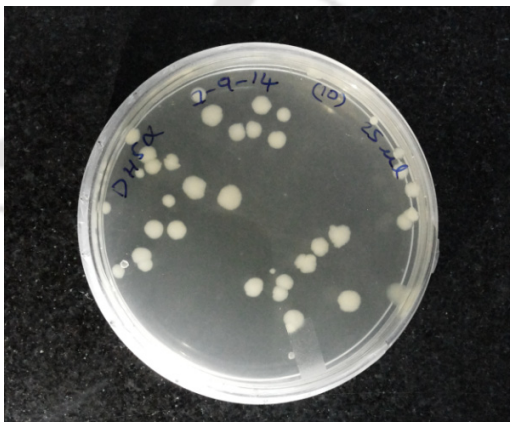

(h) Silver-ceramic membrane dead end MF permeate sample colony count plate

Figure G4: Biofilm formation and feed/permeate colony count plate samples.

List of Publications

International Journal:

1. Kaniganti, C.M., Emani, S., Thorat, P., Uppaluri, R., 2014. Microfiltration of Synthetic Bacteria Solution Using Low Cost Ceramic Membranes. Separation Science and Technology, 50, 121-135.

Manuscripts under preparation:

1. Kaniganti, C.M. and Uppaluri, R. "Cross Flow microfiltration performance of low cost Ceramic Membranes during bacteria filtration" (under preparation).

2. Kaniganti, C.M. and Uppaluri, R. "Optimality of rate enhancement techniques for electroless fabrication of low cost porous silver-ceramic composite membranes" (under preparation).

3. Kaniganti, C.M. and Uppaluri, R. "Efficacy of drop wise reducing agent contacting pattern on the sonication assisted electroless fabrication of low cost silver-ceramic composite membranes" (under preparation).

4. Kaniganti, C.M. and Uppaluri, R. "Microfiltration of bacteria solutions using low cost ceramic and silver-ceramic composite membranes" (under preparation).

International Conferences:

1. **China M. Kaniganti** and R. Uppaluri, "Development of Low Cost Ceramic Membranes for Drinking Water Treatment and Bacteriostatic Applications" International Conference on Chemical and Bio process Engineering (ICCBPE, IN), 16-17 November 2013, NIT Warangal, India.

2. **China M. Kaniganti** and R. Uppaluri, "Preparation and Characterization of Low Cost Ceramic Membranes for Bacteriostatic Applications", International Conference on Membranes and Applications (ICMA 2013), 22-23 November 2013, CSIR-CGCRI, Kolkata, India.

National Conferences:

1. **China M. Kaniganti,** Shubham Gupta, Mohd. Adil, Manikanta Prasad VVS "Preparation and Characterization of Silver Ceramic Composite Membranes Using Electroless Plating" Indian Chemical Engineering Congress (CHEMCON- 2014), 27-30 December 2014, Chandigarh, India.

2. **China M. Kaniganti,** Charan S. Bugudala and R. Uppaluri "Efficacy of Reducing Agent on the Performance Characteristics of Silver Electroless Plating Baths Coupled with Ultrasound" Indian Chemical Engineering Congress (CHEMCON-2014), 27-30 December 2014, Chandigarh, India.

International Journal Publication

Separation Science and Technology
Publication details, including instructions for authors and subscription information:
http://www.tandfonline.com/loi/lsst20

Microfiltration of Synthetic Bacteria Solution Using Low Cost Ceramic Membranes

China M. Kaniganti[a], Sriharsha Emani[a], Prashant Thorat[a] & R. Uppaluri[a]
[a] Department of Chemical Engineering, Indian Institute of Technology - Guwahati, Guwahati, Assam, India

Accepted author version posted online: 25 Sep 2014.Published online: 31 Dec 2014.

To cite this article: China M. Kaniganti, Sriharsha Emani, Prashant Thorat & R. Uppaluri (2015) Microfiltration of Synthetic Bacteria Solution Using Low Cost Ceramic Membranes, Separation Science and Technology, 50:1, 121-135, DOI: 10.1080/01496395.2014.949772

To link to this article: http://dx.doi.org/10.1080/01496395.2014.949772

Separation Science and Technology, 50: 121–135, 2015

ISSN: 0149-6395 print / 1520-5754 online
DOI: 10.1080/01496395.2014.949772

Taylor & Francis
Taylor & Francis Group

Microfiltration of Synthetic Bacteria Solution Using Low Cost Ceramic Membranes

China M. Kaniganti, Sriharsha Emani, Prashant Thorat, and R. Uppaluri
Department of Chemical Engineering, Indian Institute of Technology - Guwahati, Guwahati, Assam, India

This work addresses the development and identification of optimal low cost membrane morphologies for bacteria separation applications. Using uniaxial dry compaction method, ceramic membranes (CM1–CM3) were prepared using kaolin, quartz, calcium carbonate, sodium carbonate, boric acid, sodium metasilicate, and poly-vinyl alcohol (PVA) precursors. The fabricated membranes possessed diverse pore morphologies (0.7-4.5 μm average pore size and 39.4–19.3% porosity). Amongst all membranes, the CM3 membrane with wide pore morphology (average pore size of 4.5 μm and porosity of 19.3%) provided the best performance during the direct-flow MF of synthetic *Escherichia coli* (DH5α strain) solutions. The CM3 membrane provided a trans-membrane flux varying from 1.21×10^{-2} –3.51×10^{-3} $m^3/m^2.s$ after 10 minutes of direct-flow MF for a variation in feed concentrations of 0.004 –14.9×10^6 CFU/mL. Corresponding bacterial removal efficiency and $\log_{10}$ reduction value (LRV) values varied from 99-99.9999% and 2-6 respectively. Further, various fouling models have been evaluated for their use in measuring flux decline data. The results indicated that both membrane pore morphologies and concentration of *E. coli* strains significantly influenced the measured transmembrane flux, fouling index, and separation efficiency.

Keywords ceramic membrane; *E. coli*; LRV; fouling

INTRODUCTION

Contaminated drinking water was identified as the primary cause for 80% of the diseases in a recent World Health Organization (WHO) report (1). About 2.2 million people die every year with diarrheal diseases caused by waterborne infections (2). According to World Health Organization (WHO), the household water treatment and safe storage (HTWS) standards indicate that drinking water must contain fecal and total coliform count of 0 in a 100 mL sample. To achieve this, uses of water treatment technologies have adopted targets for the reduction of particulate matter, suspended solids, parasites, fungi, algae, bacteria, and viruses. A critical feature of such water treatment technologies is that while it is easier to eliminate suspended solids, it is very difficult to reduce or eliminate disease causing organisms.

Various competent technologies for the purification of potable water resources include physical processes (such as slow sand filters or activated carbon) and chemical processes (such as ultraviolet irradiation, ozonation, chlorination, pasteurization, flocculation, and membrane technology using polymeric, ceramic, and composite membranes). Today, commercial water purifier systems such as Kent (3) include a combination of several physical and chemical processes such as ultraviolet radiation and membrane technology. Amongst various technologies, membrane technology is promising due to its ability to simultaneously reduce or eliminate several contaminants such as salts, heavy metals, and bacteria. For potable water production from open source water reservoirs and marshy ponds, microfiltration (MF) and ultrafiltration (UF) using membrane technology are cost effective (4).

From a materials perspective, polymeric membranes with their lower cost, scalability, and good separation characteristics are familiar for industrial liquid phase separation schemes such as wastewater treatment (5) and fruit juice clarification (6). Few references from literature also exist that address the relevance of polymeric membranes (7) toward bacteria separation applications using synthetic microbial solutions. However, it is well known that polymeric membranes have lower shelf life (8) due to their lower fouling resistance towards biological activity and pH variations. On the other hand, ceramic membrane technology offers good combinations of fouling resistance and mechanical strength (9). Therefore, low cost ceramic membranes provide promising opportunities for the processing of wastewater treatment (10), juice clarification (11), and bacteria separation applications (12).

To date, only few researchers have investigated the performance of ceramic membrane technology for the separation of microbes. Simonis and Basson (2) fabricated lithium alumina-silicate ceramic membranes using slip casting method.

Received 17 January 2014; accepted 26 July 2014.
Address correspondence to R. Uppaluri, Department of Chemical Engineering, Indian Institute of Technology - Guwahati, Guwahati, 781039, Assam, India. E-mail: ramgopalu@iitg.ernet.in
Color versions of one or more of the figures in the article can be found online at www.tandfonline.com/lsst.

Adopting spread plate method and membrane filter technique, the authors evaluated that the membrane provided a $\log_{10}$ reduction value (LRV) of 5.5, 4.2, and 3.6 respectively, for *E. coli, S. feacalis* and *B. cerues* microbes at their feed concentrations of 6, 0.02, 1.1×10^4 CFU/mL respectively. Srivastava et al. (13) addressed carbon nanotube (CNT) filters for the separation of *E. coli* (2–5 μm), *Staphylococcus aureus* (~1 μm) and *poliovirus* (~0.025 μm) from drinking water. The authors used ultrasonic and autoclaving methods to clean membranes. Mwabi et al. (14) evaluated various filters such as silver-impregnated porous pot, ceramic candle filter, biosand filter-standard, and biosand filter-zeolite as alternate household drinking water systems. Amongst all filters, the silver-impregnated porous pot is the best in terms of flux (0.05–2.49 L/h) and separation efficiency (LRV > 5) for feed concentrations varying from 3×10^2–3.68×10^6 CFU/mL. For similar feed concentrations, the ceramic candle filter provided a flux and separation efficiency of 1–4 L/h and 2–4 LRV, respectively.

Ciston et al. (15) studied the role of a developed ceramic membrane skin layer on the microbe stability on zirconia ceramic UF membranes coated with anatase and mixed phase titanium dioxide photocatalysts. From the results it showed that the TiO_2 coatings insignificantly influenced membrane roughness but reduced *Pseudomonas putida* attachment. However, further details with respect to reduction in fouling resistance were not elaborated by the authors.

Vasanth et al. (12) prepared a low cost ceramic membrane using uniaxial dry compaction method and inorganic precursors such as kaolin, quartz, calcium carbonate, sodium carbonate, boric acid, and sodium metasilicate. The membrane sintered at 900–1000°C was characterized to have an average pore size and porosity of 1.3 μm and 30% respectively. At a ΔP of 69 kPa and for feed *E. coli* concentrations of 6×10^4 and 6×10^5 CFU/mL, the membrane provided maximum rejection of 63% and 99% and permeate flux of 3.64×10^{-4} and 1×10^{-4} $m^3/m^2.s$ respectively. Vasanth et al. inferred that the rejection decreased with increasing trans-membrane pressure differential and decreasing feed concentration. The inability of the fabricated membrane to provide LRV above 5 for bacteria is indicative of the need for further engineering improvements in the low cost ceramic membrane technology for bacteria separation applications.

Bielefeldt et al. (16) studied the separation efficiency of clay based commercial ceramic water filters for the separation of *E. coli*. The authors inferred that the membranes did not provide satisfactory performance during long term permeation tests. For a feed bacterial concentration of 1×10^6 CFU/mL, the permeate stream concentrations were about 1×10^1 – 1×10^3 CFU/mL. On the other hand, the filters separation efficiency was improved when silver coating was deposited using colloidal silver solutions. Thus, it is apparent that commercial filters did not provide efficient separation capabilities (in terms of LRV).

A critical analysis of the available literature provides several insights. First, the literature is highly focused towards drinking water treatment applications but not bacteria separation applications, which are also important from the perspective of industrial biotechnology. Commercial bacteria separation applications include pasteurization followed with centrifugation, which involve a heat treatment step. Heat treatment steps could damage heat sensitive compounds that are of immense value in bioprocessing streams. Therefore, low cost ceramic membrane technology might be promising in such processes. Second, Vasanth et al. (12) and Simonis and Basson (17–19) studied the efficacy of low-cost ceramic membranes for bacteria separation applications, but did not present a detailed investigation with respect to bacteria removal from water. Compared with standard alpha-alumina ceramic membranes, low cost ceramic membranes made from clay provide similar flux and separation characteristics at a lower cost and are therefore attractive for faster research commercialization. An important issue for the developed low cost ceramic membranes is to achieve LRV > 4 separation efficiency for bacteria, which is dependent on both pore size distributions and morphologies of the separated microbes. Thus, it is apparent that significant amounts of research activity needs to be devoted towards the development and application of low cost ceramic membranes for microbe separation applications. In this regard, a systematic investigation that accounts for the assessment and identification of relevant membrane morphological characteristics to suit the desired application is very important. While literature does provide few data sets for ceramic membranes, systematic insights with respect to the performance characteristics are not available. For instance, the literature does not elaborate the dependence of membrane fouling on membrane morphology. This is an important issue in the context of the shelf life of the low-cost ceramic membranes. Thus, research emphasis shall be towards minimizing the in situ fouling performance and maximizing the shelf life of low-cost ceramic membranes. Such efforts will further enhance the adaptability of low-cost ceramic membranes for drinking water treatment and bacteria separation applications.

Recently, our research group (Emani et al. (20)) identified a membrane precursor formulation that provides membrane morphologies within sub-micron range pore size (CM1 membrane) and was proven to be highly effective in the clarification of fruit juices. Therefore, CM1 membrane is anticipated towards good MF performance during bacteria separation application studies. This work is a natural extension of the membrane fabrication research to target membranes with variegated membrane morphologies.

The objective of this work is to identify optimal morphological properties that provide maximized combinations of trans-membrane flux and separation efficiency and minimal fouling during the MF of synthetic microbial solutions. This work addresses the preparation and characterization of low cost ceramic membranes for bacteria separation applications. Using

uniaxial dry compaction method, three membranes CM1, CM2, and CM3 were fabricated with diverse membrane morphologies. The morphological characterization was carried out using field emission scanning electron microscopy (FESEM), X-ray diffraction (XRD), porosity and pure water permeation experiments. Subsequently, the membranes were investigated for the direct-flow MF of synthetic solutions prepared with DH5α microbial strain. The optimal membrane MF performance has been targeted by evaluating transmembrane flux, initial flux, time dependent fouling index, average fouling index, and separation efficiency in terms of rejection and LRV. Also, the fitness of competent fouling models was also examined to infer upon the dominance of pore blocking and irreversible fouling mechanisms during the MF experiment.

EXPERIMENTAL WORK

Fabrication of Ceramic Membranes

Three ceramic membranes CM1, CM2, and CM3 with distinct membrane morphologies were fabricated using low cost inorganic precursors such as kaolin (CDH, India), quartz (Research Lab Fine Chem Industry), calcium carbonate (Merck, India), sodium carbonate (Merck, India), boric acid (Merck, India), and sodium metasilicate (CDH, India). Except PVA, the compositions reported in this work for CM1 and CM2 membranes have been with respect to those presented by Vasanth et al. (21). However, the compositions reported in this work including PVA are novel and have not been studied by the authors. The variations in the membrane morphologies were achieved by targeting variation in the inorganic precursor composition and their particle size distributions in the dry powder mixture. Table 1 summarizes the compositions of the inorganic precursors to fabricate CM1-CM3 membranes. For CM1 and CM2 membranes, polyvinyl alcohol (PVA, M. wt. 1, 15,000, Loba Chemicals Ltd., India) was also used with a solution composition of 2 and 4 wt%, respectively. The inorganic precursors with distinct functional attributes enabled to achieve membranes within the pore size range of 0.5–5 μm. The identified inorganic precursor compositions were based on a trial and error fabrication approach that enabled the optimization of the chosen process parameters. Further, for CM1 and CM2 membranes, the powder mixture recipe (Table 1) was dry sieved with 36 (425 μm) and 72 (212 μm) mesh screen, respectively. The sieving step was not deployed to prepare the CM3 membrane.

TABLE 1
Composition of raw materials for the fabrication of various membranes

Material	CM1 (wt %)	CM2 (wt %)	CM3 (wt %)
Kaolin	40	40	40
Quartz	15	15	15
Calcium carbonate	25	25	20
Sodium carbonate	10	10	10
Boric acid	5	5	5
Sodium metasilicate	5	5	10
Polyvinyl alcohol	2	4	–

The membrane fabrication procedure adopted uniaxial dry compaction method after thorough mixing of the raw materials using a ball mill. The experimental procedure was similar to that presented by Emani et al. (20) and Vasanth et al. (21). The dry powder mixtures were compacted using a hydraulic press (Make: Velan Engineering, Tamil Nadu, India) at a fabrication pressure of 49 MPa. Following this, several heat treatment cycle were followed that include drying at 150°C for 12 h followed with heating at a rate of 2°C/min upto 900°C and was eventually kept at 900°C for 4 h. The membranes have been dried at 150°C but not 100°C. This is due to the reason that the green membrane has low moisture content (due to dry compaction method) and hence additional thermal stresses are not induced with high temperature drying.

Finally, the membranes were cooled to ambient temperature by a natural cooling process. For all membranes, subsequent steps for polishing and sonication assisted surface cleaning were similar to that reported by Vasanth et al. (21).

Structural and Morphological Characterization

The morphological and structural assessment of the low-cost ceramic membranes was targeted by carrying out X-ray diffraction analysis (XRD, Make: BRUKER, Model No. D8 Advance, Germany), field emission scanning electron microscopy (FESEM, Make: ZEISS, Model No. ∑IGMA, USA), total porosity determination using the Archimedes principle, and evaluation of pore size distribution from FESEM image analysis. While XRD enabled to infer upon the extent of different phase transformations and crystallinity of the membranes during sintering, the FESEM provided a visual picture and presence/absence of defects and morphological pore size distribution, which was determined using ImageJ software (Version 1.40). The assessment of pore size distributions based on FESEM images was based on the measurement of about 500 pores using the Image J software for evaluation of the average pore size of the membranes. To minimize the impact of sampling size, several micrographs were randomly chosen to evaluate upon the pore size distributions.

Using water as a wetting agent, the total porosity of the membrane was determined by first drying the membrane at 110°C for 6 h to obtain its dry weight. Eventually, the wet weight of the membrane was measured after placing the membrane in water for 24 h at room temperature and subsequently wiping its surfaces with tissue paper. The overall porosity (including dead and permeable pores) was evaluated using the expression:

$$\varepsilon = \frac{(w_2 - w_1)/\rho_w}{\pi \times \left(d/2\right)^2 \times \delta} \quad (1)$$

w_1 Dry weight of the membrane, g
w_2 Wet weight of the membrane, g
ρ_w Density of water, g/cm^3
d Diameter of the membrane, cm
δ Membrane thickness, cm

Microfiltration Studies

Pure Water Permeation and Direct-Flow Microfiltration

Both hydraulic permeability and direct-flow MF experiments were conducted with laboratory fabricated experimental setup. The setup consists of a stainless steel cylindrical unit (SS316, 320 mL capacity) that hosts a circular base plate to keep the membrane in leak proof condition during direct-flow MF and liquid permeation experiments. Prior to MF/water permeation run, the fabricated membrane disc was sandwiched between two rubber o–rings (43 mm diameter) that were kept above and below the ceramic membrane on a circular base plate. During permeation experiments, the feed was filled with water/synthetic solutions in the tubular section of the sealed setup and the chamber was pressurized with nitrogen gas to obtain permeate flux as a function of measured cumulative permeate volume and time period of MF run. The cumulative permeate volume was measured using a water beaker (500 mL) that was kept on a digital weighing balance. Since the fabricated membrane possessed wider average pore size, very high transmembrane fluxes were obtained (22). Hence, significant batch volumes of feed solutions have been used to measure the transmembrane flux for prolonged time periods. The time period between any two batch volumes has been kept very low (about 30 s) to obtain minimal errors in the measured flux data.

The direct-flow MF was carried out using synthetic solutions (DH5α cells suspended in sterile saline water at a pH of 7.2) at a ΔP of 206.7 kPa, which is the typical maximum operating pressure differential for Microfiltration tests. For all membranes, using samples of variant feed concentrations, the membranes were subjected to a number of trails for the removal of *E. coli*. The effective membrane area for permeation is 1.45×10^{-3} m^2.

The synthetic microbial solutions were prepared using DH5αstrain, a coliform type of organism and a good indicator for the potential contamination of water sources. *E. coli* (DH5α strain) was obtained from the Department of Biotechnology, IIT Guwahati, India and was maintained on nutrient agar plates and incubated at 37°C for 24 h. One loop full sample of the bacterial culture was inoculated into 50 mL sterile nutrient broth and incubated overnight at 37°C in an orbital shaking incubator (Make: LabTEch, DaihanLabtech, India Pvt. Ltd., Model: LSI - 3016R) at a speed of 200 rpm. Subsequently, various volumes from the overnight cultivated microbial culture were mixed in 10 L of sterile physiological water (0.9% w/v NaCl) to prepare synthetic microbial solution of variant feed concentrations. In this regard, it is important to note that the feed concentrations cannot be controlled with precision due to variant microbial activity of the prepared samples and an approximate estimate was obtained from preliminary analysis of the microbial culture. Using the data obtained from preliminary analysis, the desired feed concentration was achieved from the synthetic microbial solution.

All experimental investigations related to the evaluation of membrane characterization parameters have been conducted for at least two sets of membranes and the average value of these parameters along with standard deviation have been reported. A similar approach had been followed for the evaluation of permeate characteristics.

The time dependent fouling index ($F(t)$), total fouling index (FI), and average fouling index (AFI) of the ceramic membrane for a MF run have been estimated using the expressions (23):

$$\mathrm{F(t)} = \left(1 - \frac{\mathrm{J}}{\mathrm{J_0}}\right) \times 100 \quad (2)$$

$$\mathrm{FI} = \int_0^{t_{max}} \mathrm{F(t)dt} \quad (3)$$

$$\mathrm{AFI} = \frac{\mathrm{FI}}{t_{max}} \quad (4)$$

where t_{max} refers to the maximum time of operation during a MF run. A combination of higher FI/AFI and lower instantaneous transmembrane flux (measured after 1 minute of experimental run) indicates significant pore blocking and irreversible fouling. Therefore, the magnitude of FI (AFI) and instantaneous membrane flux during direct filtration is indicative towards lower membrane fouling. In this regard, it can be noted that the well-known rule of thumb for membrane technology research is that lower membrane fouling translates to greater longevity of the membrane during insitu applications. By using the trapezoidal rule, FI was determined with the evaluated data of time dependent fouling index F (t) for all experimental runs.

Analytical Methods

After a MF run, the concentrations of bacterial colonies in feed and permeate samples were determined using the spread plate method. In this method, it was assumed that each viable bacterium in the suspension will form an individual colony. This assumption is valid only when the analytical procedures were followed correctly to determine sample concentrations in terms of number of colony forming units (CFU) per unit volume (mL) of the sample solution.

The average percent microbe rejection (R) for a microfiltration run was estimated using the expression (24):

$$R = \left(1 - \frac{C_p}{C_0}\right) \times 100 \quad (5)$$

where

C_P Concentration of permeate, CFU/mL
C_0 Concentration of feed, CFU/mL

The LRV was calculated using the expression (2):

$$\text{Log}_{10}\text{ reduction value (LRV)} = \log 10(C_0) - \log 10(C_p) \quad (6)$$

Few physicochemical parameters such as pH and conductivity were also determined for both feed and permeate samples using a water analysis kit (Make: VSI Electronics, Model: VSI - 06D1, India).

Theory of Membrane Fouling Mechanism

Hermia (25) proposed four empirical models to evaluate the presence of various membrane fouling mechanisms during constant pressure direct-flow filtration. These refer to complete pore blocking (CPB), standard pore blocking (SPB), intermediate pore blocking (IPB) and cake filtration (CF). The procedure for the fitness of various models is similar to that adopted by Nandi et al. (11), which involves the assessment of the measured flux data to fit with any one of the following models:

a) Complete pore blocking: $\ln\left(J^{-1}\right) = \ln\left(J_0^{-1}\right) + k_b t$ (7)

b) Standard pore blocking: $J^{-0.5} = J_0^{-0.5} + k_s t$ (8)

c) Intermediate pore blocking: $J^{-1} = J_0^{-1} + k_i t$ (9)

d) Cake filtration: $J^{-2} = J_0^{-2} + k_c t$ (10)

RESULTS AND DISCUSSION

Surface and Physical Characterization

XRD

The XRD pattern for unsintered raw material mixture and sintered inorganic material membrane for CM1–CM3 membranes is presented in Fig. 1(a–c) respectively. As shown, for all cases, peaks corresponding to kaolin disappeared after sintering the inorganic precursors at 900°C.This is due to the conversion of kaolinite and metakaolinite at the sintering temperature (23). The XRD pattern also confirm upon significant phase transformations during sintering which refer to the appearance of a nephiline phase after sintering.

FLUX

The variation of pure water flux with applied pressure for the membranes is presented in Fig. 2(a). As shown, for a variation in ΔP from 68.9–206.7 kPa, the pure water flux varied from 1.312 – 3.893 × 10^{-4}, 4.728 – 14.145 × 10^{-4} and 33.245 – 88.552 × 10^{-4} m^3/m^2.s for membranes CM1, CM2 and CM3 respectively. Variations in average membrane approximate porosity (determined with Archimedes principle) and average pore size (determined using Hagen-poiseuille equation) for various membranes are presented in Fig. 2(b). As shown, the membrane porosity reduced from 39.4–19.3% with an enhancement in pore size from 0.7–4.5 μm for membranes CM1–CM3, respectively. The significant variation in both pore size and porosity of the membranes is due to the variation in both inorganic precursor compositions and particle size distributions of the inorganic precursor mixture. A critical analysis of the fabrication procedure and inorganic precursor composition indicates that both CM1 and CM2 have almost similar compositions but with variant in PVA concentrations. On a trial and error basis, these variations in PVA concentrations have been identified to be important to achieve the desired membrane morphology. However, experimental fabrication procedures were also slightly different. For CM1 membrane, 36 (425 μm) mesh screen was used to screen the precursor mixture where as for CM2 membrane, 72 (212 μm) mesh screen was used. Thus, for a similar PVA concentration, it is expected that CM2 membrane should have had lower average pore size due to the finer particle size distributions. However, since higher average pore size was obtained for the CM2 membrane, it is apparent that PVA concentration significantly influences membrane morphology and higher PVA concentration in the inorganic precursor mixture enhances the average membrane pore size. On the other hand, the CM3 membrane inorganic precursor formulation does not involve the utilization of PVA and with wide particle sizes of inorganic precursors, the membrane properties are anticipated to be distinct from CM1 and CM2 membranes. In summary, the achievement of low cost ceramic membranes with larger pore size (4.5 μm) is anticipated to be useful for the MF of synthetic microbial solutions, as it is expected that the wider pore size of the membrane could provide higher trans-membrane flux, good separation efficiency and lower fouling.

FESEM

Figures 3(a–c) present the FESEM images for CM1, CM2, and CM3 membranes respectively. The images indicate highly porous texture of the membranes without surface defects such as cracks and pinholes. The maximum observable pores for all membranes are in the range of 2–6.5 μm. Based on analysis of the image, the pore size distributions in various membranes have been determined using ImageJ software (Version 1.40) and has been illustrated in Fig. 4. For all membranes, it can be observed that less than 10% of the pores are within the pore diameter range of 1–15 μm. Also, 25% of the pores exist below 0.85 μm for CM1 membrane, 30% and 36% pores exist for CM2 and CM3 membranes below 1.8 and 4.1μm respectively. Based on the FESEM image analysis, the average pore

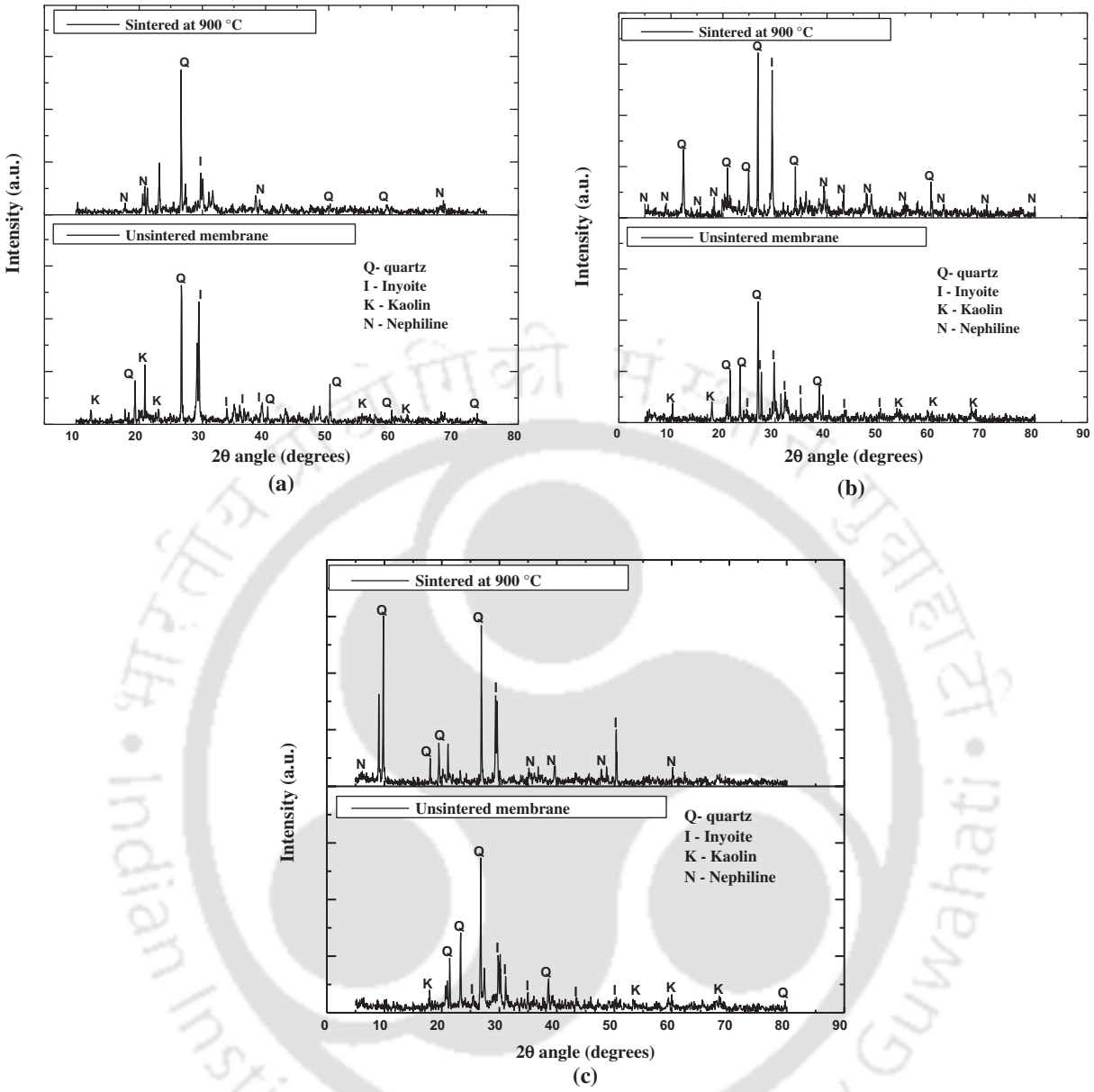

FIG. 1. XRD spectra of unsintered and sintered membranes (a) CM1 (b) CM2 and (c) CM3 membranes.

size is 1.1, 1.9, and 4.9 μm for membranes CM1, CM2 and CM3, respectively. These values are in good agreement with the corresponding pore size values determined using pure water permeation experiments.

A critical comparison of obtained morphologies with those presented in the literature for low cost ceramic membranes indicates that the average pore size and porosity of membrane CM2 is comparable with those presented by Vasanth et al. (12). Using a similar inorganic precursor formulation, Vasanth et al. obtained an average pore size and porosity of 1.3 μm and 30% at a fabrication pressure of 50 MPa, a value slightly higher than the fabrication pressure adopted in this work (49 MPa). Compared to their experimental procedure for the fabrication of the membrane, it is apparent that both precursor composition and particle size distributions significantly influenced morphologies of CM2 and CM3 membranes.

Microfiltration Studies on Various Ceramic Membranes

FLUX

Figures 5(a-c) present the microbial (DH5α) flux decline profiles for CM1, CM2 and CM3 membranes respectively. The feed concentration and flux values corresponding to these membranes have been presented in Table 2.

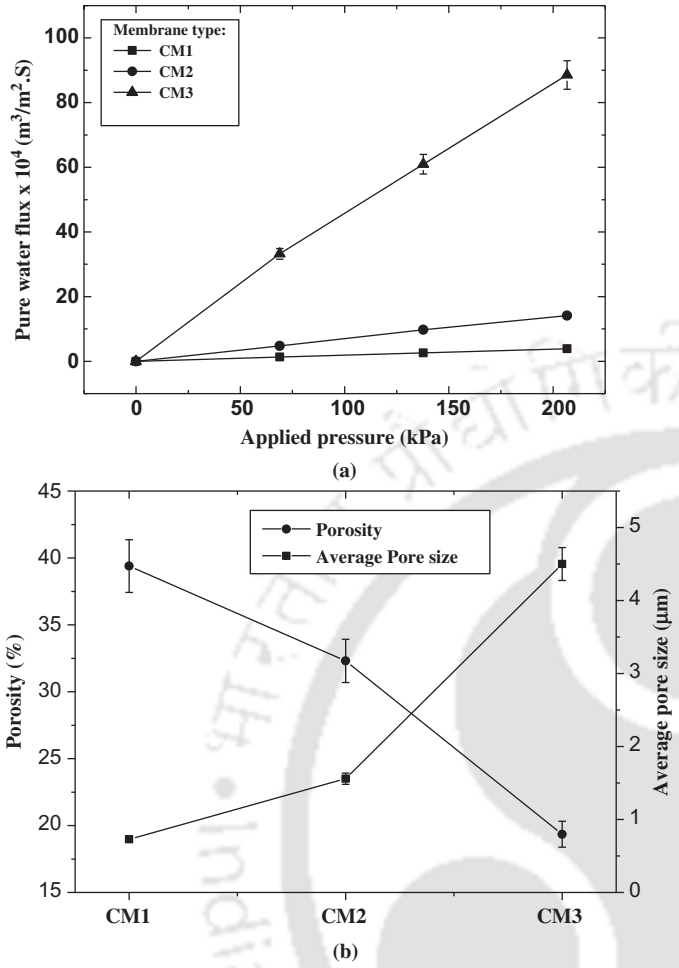

FIG. 2. Variation of (a) Pure water flux with applied pressure and (b) Average pore size and porosity for CM1, CM2 and CM3 membranes.

It can be also observed in Figs. 5(a-c), a common time period does not exist for all membranes. The total experimental run period varied from 12-120 min. The total volume of the solution used for various cases has significantly varied due to the pertinent fouling effects. However, for the CM3 membrane, it can be observed that the total MF run period did not exceed more than 10-12 min. This is due to the large pore size of the membrane.

For CM1 and CM2 membranes, the flux decline profiles did not follow a systematic trend with increasing feed concentrations. For these two membranes, the flux profile for an intermediate feed concentration was located below the flux profile obtained at low and higher feed concentration. These observations are possibly due to the variation in the morphologies of the cultivated microbes in the feed samples which can either significantly contribute towards pore blocking or formation of a dynamic cake filtration layer on the membrane surface. On the other hand, for the CM3 membrane, membrane flux profiles reduced with enhancement in feed concentration. This is due to significant pore blocking at higher feed concentrations. Thus, from an operational perspective, it can be inferred that the membrane CM3 provided pore size distributions that enabled a systematic reduction in flux with increasing feed concentrations.

SEPARATION EFFICIENCY

Figures 6(a-c) illustrates the separation efficiency of CM1–CM3 membranes respectively. The separation efficiency for the membranes has been presented in terms of cumulative permeate count and cumulative permeate volume of the permeate samples. For the CM1 membrane (average pore size of 0.7 μm), the cumulative permeate count varied from 0 - 380, 0 -10, and 0 CFU/mL for feed concentrations of 1.6×10^6, 1.7×10^6, and 8.4×10^6 CFU/mL respectively. These correspond to an LRV value of 5 and 6 for feed concentrations of 1.6×10^6 and 1.7×10^6 CFU/mL respectively, given the fact that LRV cannot be defined for zero permeate count cases. Thus, the separation efficiency of the CM1 membrane varied from 5-6 LRV for variation in feed concentration. Similar trends were obtained for CM2 and CM3 membranes. For CM2 membrane (average pore size of 1.5 μm), 100% removal efficiency was observed at a feed concentration of 0.05×10^6 CFU/mL and the LRV increased from 3 - 6 with an increase in feed concentration from 0.80 - 61 $\times 10^6$ CFU/mL. For the case of CM3 membrane (average pore size of 4.5 μm), the LRV was found to be 2, 3 and 6 respectively for a feed concentrations of 0.004×10^6, 0.0297×10^6, and 14.9×10^6 CFU/mL, respectively. Thus, for the CM3 membrane, the separation efficiency increased with increasing feed concentration, and since CM3 membrane provided the highest flux amongst all the membranes, it can be inferred to possess the most desirable pore size distributions and average pore size for the MF of microbial solutions. However, it is important to note that 100% separation efficiency was not achieved and this indicates further engineering of the ceramic membrane is required. This could refer to an additional bacteriostatic skin layer (such as silver film) to deactivate the growth of the bacterial film on the membrane and omit the passage of microbes into the permeate stream.

Table 3 presents a summary of the performance of various ceramic membranes towards the separation of bacteria. It can be observed that CM3 membrane performance is comparable with those reported in the literature. Table 4 presents a summary of physico-chemical properties of feed and permeate samples for membranes CM1 - CM3 for selected experimental data. Similar results were obtained for other sets of MF runs and have not been reported. It can be observed that for feed samples the pH and conductivity values varied from 6.60-7.34 and 6.69-11.30 μs/cm respectively. Corresponding pH and conductivity samples for permeate streams varied from 8.13–8.98 and 7.86–11.89 μs/cm, respectively. These observations indicate that the pH and conductivity of the permeate samples increased

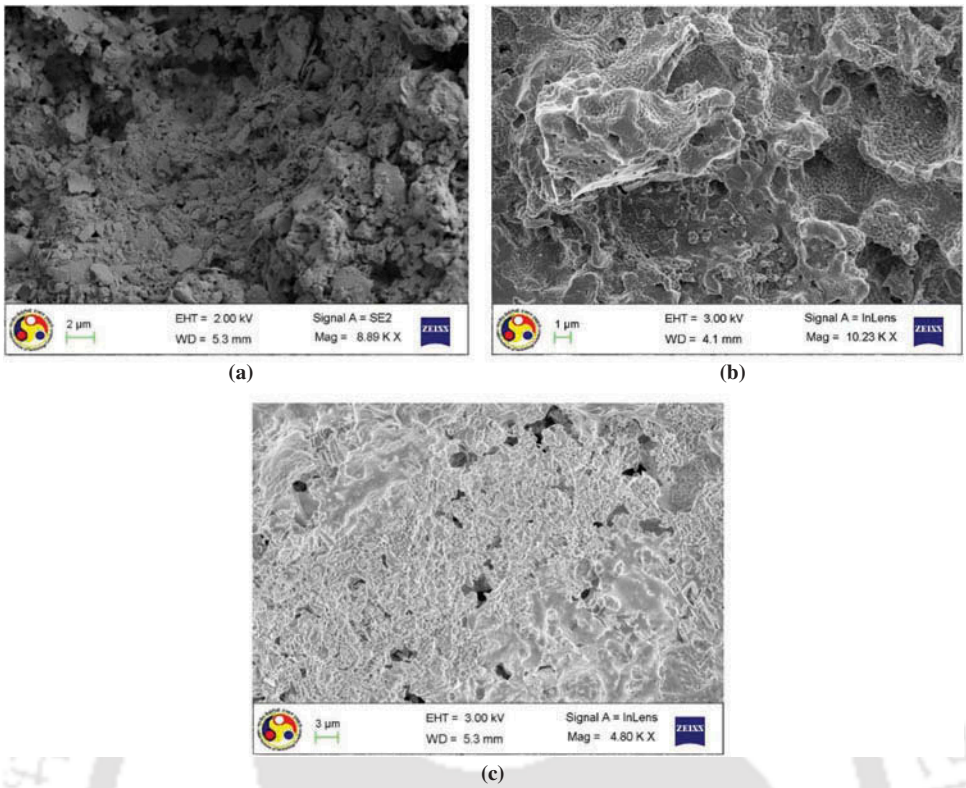

FIG. 3. Field emission Scanning electron micrographs of (a) CM1 (b) CM2 and (c) CM3 membranes.

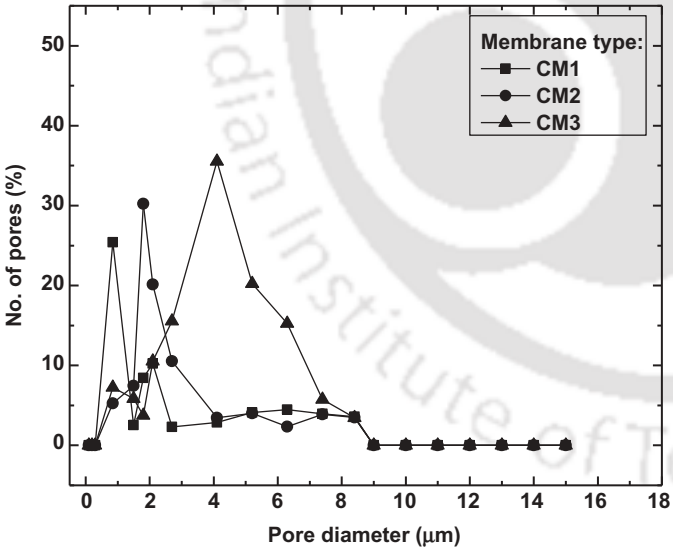

FIG. 4. Pore size distribution for CM1-CM3 membranes.

significantly for the permeate samples. The enhancement in the pH of the permeate samples is due to the presence of alkaline oxides and carbonates in the membrane matrix (26). The conductivity of both feed and permeate samples remained fairly constant.

Figure 7 presents the variation of time dependent fouling index (FI) and average fouling index (AFI) of CM1, CM2, and CM3 at various feed concentrations. Table 2 summarizes the relevant values corresponding to the obtained data for all membranes. Thus, it can be observed that while AFI values for CM1 membrane were the lowest, they were highest for the CM3 membrane. This is due to significant pore blocking for wider membrane morphologies. However, CM1 membrane provided an almost negligible flux after 100 min. of operation due to which reason flux experiments could not be carried out after 100 min. of MF operation. On the other hand, for the CM3 membrane, despite obtaining a very high value of AFI (30), flux experiments were conducted upto a time frame of 10 minutes and further experiments were not conducted due to minimal variation in the flux after 10 minutes time frame. Therefore, the CM3 membrane is regarded to be the best membrane among CM1–CM3. The FI and AFI profiles could not be regressed using mathematical expressions. This is due to their strong dependence on membrane morphology, feed concentrations and microbe morphologies in the feed samples. Thus, further research needs to be carried out to relate the biological activity of feed samples and morphologies of the developed membranes.

Figure 8 presents the best fit models for all membranes at distinct feed concentrations. Corresponding parameters associated to correlation coefficient, slope and intercept of the best

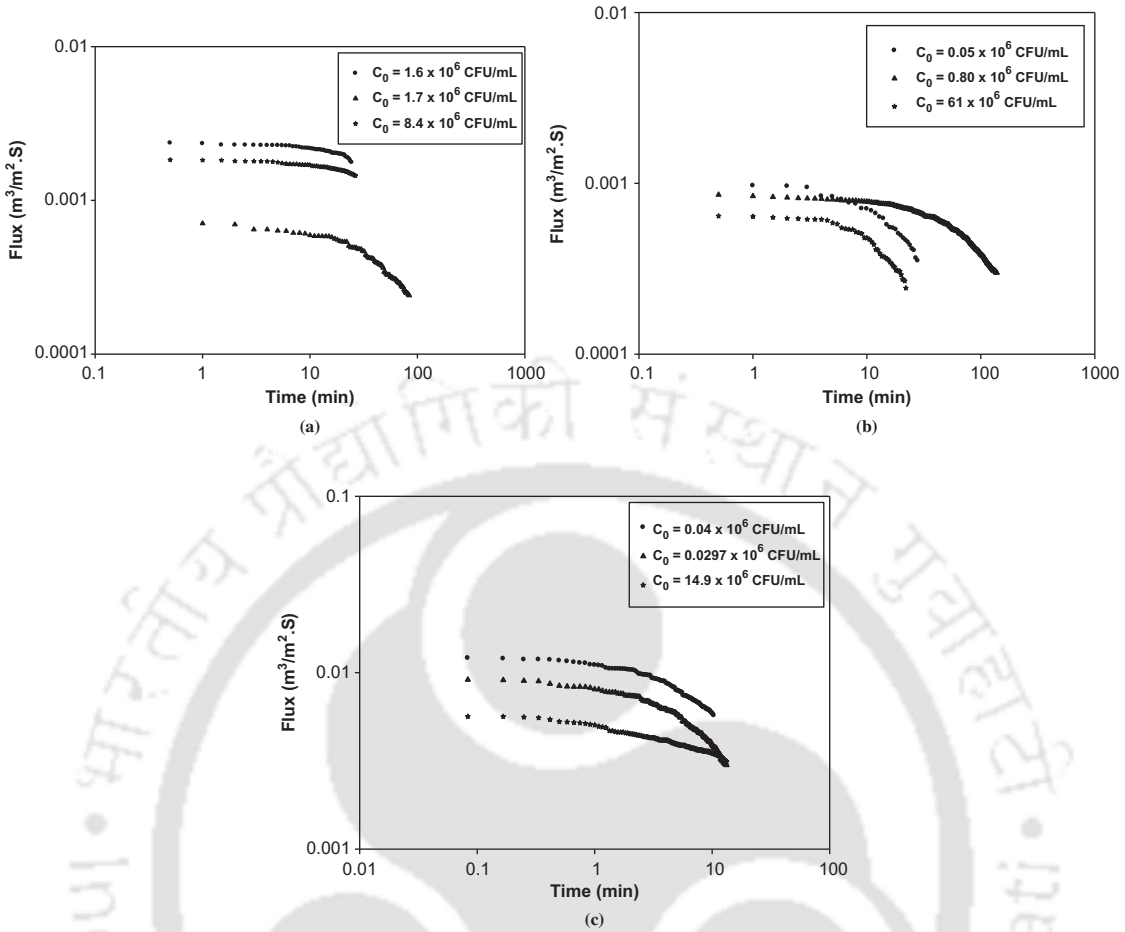

FIG. 5. Variation of transmembrane flux with time at $\Delta P = 206.7$ kPa for membranes CM1-CM3 at various feed microbial concentrations. (a) CM1 (b) CM2 and (c) CM3 membranes.

TABLE 2
A summary of fouling index and average fouling index data for various membranes at different feed concentrations

Membrane Type	Feed (CFU/mL) $\times 10^6$	Flux ($m^3/m^2.s$)	Fouling Index (FI)	Avg. Fouling Index (AFI)
CM1	1.6	2.36×10^{-3}	240	10
	1.7	7.07×10^{-3}	3366	40.6
	8.4	1.83×10^{-3}	2573	9.9
CM2	0.05	9.68×10^{-4}	901.2	33.4
	0.80	8.57×10^{-4}	5397.5	39.4
	61	6.44×10^{-4}	589.8	23.1
CM3	0.004	1.21×10^{-2}	325.3	31.5
	0.0297	9.11×10^{-3}	555.8	4.7
	14.9	5.65×10^{-3}	404.2	30.5

fit fouling models for all membranes is presented in Table 5. Thus, it is apparent that except for a single case for the CM3 membrane, all other cases correspond to the existence of pore blocking mechanisms, which can significantly contribute towards irreversible membrane fouling. However, very high trans-membrane flux values were obtained for the CM3 membrane for a short total MF run time period of 10-12 min, which indicates that the CM3 membrane provided lowest in

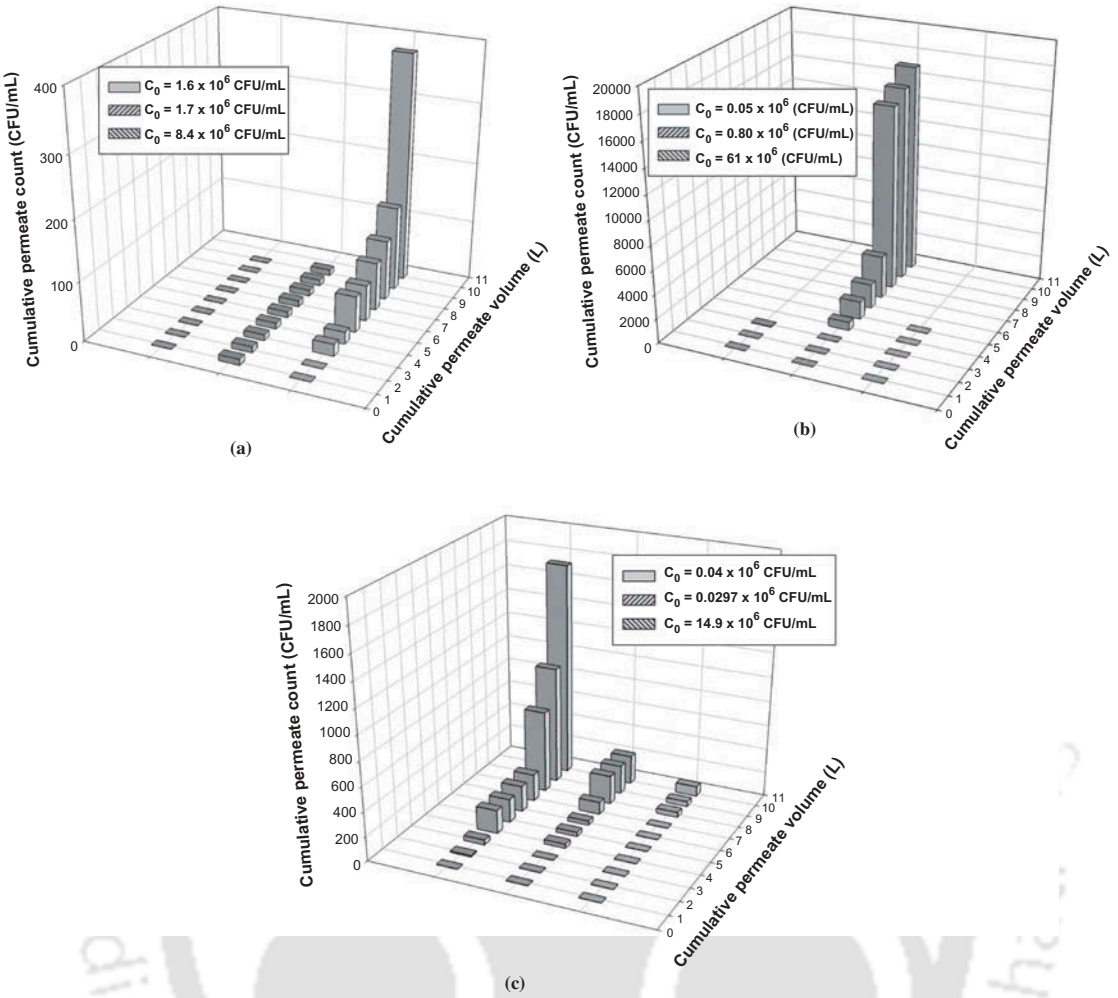

FIG. 6. Variation of cumulative permeate count (CFU/mL) with cumulative permeate volume (L) at various feed microbial concentrations for (a) CM1 (b) CM2 and (c) CM3 membranes.

TABLE 3
A summary of low cost ceramic membranes for bacteriostatic applications

S.No	Authors	Average pore size (μm)	Porosity (%)	Feed concentration (CFU/mL)	Flow rate (LPH)/Flux ($m^3/m^2.s$)	Pressure (kPa)	Removal Efficiency (LRV)
1	Simonsis and Basson (2)	–	64	6×10^4	–	–	4
2	Vasanth et al. (12)	1.3	30	6×10^5	1×10^{-4} $m^3/m^2.s$	69	2
3	Mwabi et al. (14)	–	–	–	1 – 4 LPH*	–	2 – 4
4	Bielefeldt et al. (16)	–	–	10^6	1.9 LPH*	–	3 – 4
5	This Work	4.5 ± 0.2	19.3 ± 1.07	$14.9 \pm 0.5 \times 10^6$	$3.15 \pm 0.05 \times 10^{-3}$ $m^3/m^2.s$	206.7	6

*Membrane area is not given.

TABLE 4
Physico – chemical properties of feed and permeate samples of synthetic solutions during MF at $\Delta P = 206.7$ kPa

Membrane type	Feed concentration (CFU/mL) $\times 10^6$	Feed		Permeate	
		pH	Conductivity (μs/cm)	pH	Conductivity (μs/cm)
CM1	0.36 ± 0.03	6.60 ± 0.05	6.69 ± 0.12	8.13 ± 0.04	7.86 ± 0.13
CM2	0.16 ± 0.02	6.50 ± 0.06	12.52 ± 0.14	8.73 ± 0.07	12.79 ± 0.16
CM3	14.9 ± 0.04	7.34 ± 0.05	11.30 ± 0.11	8.98 ± 0.06	11.89 ± 0.14

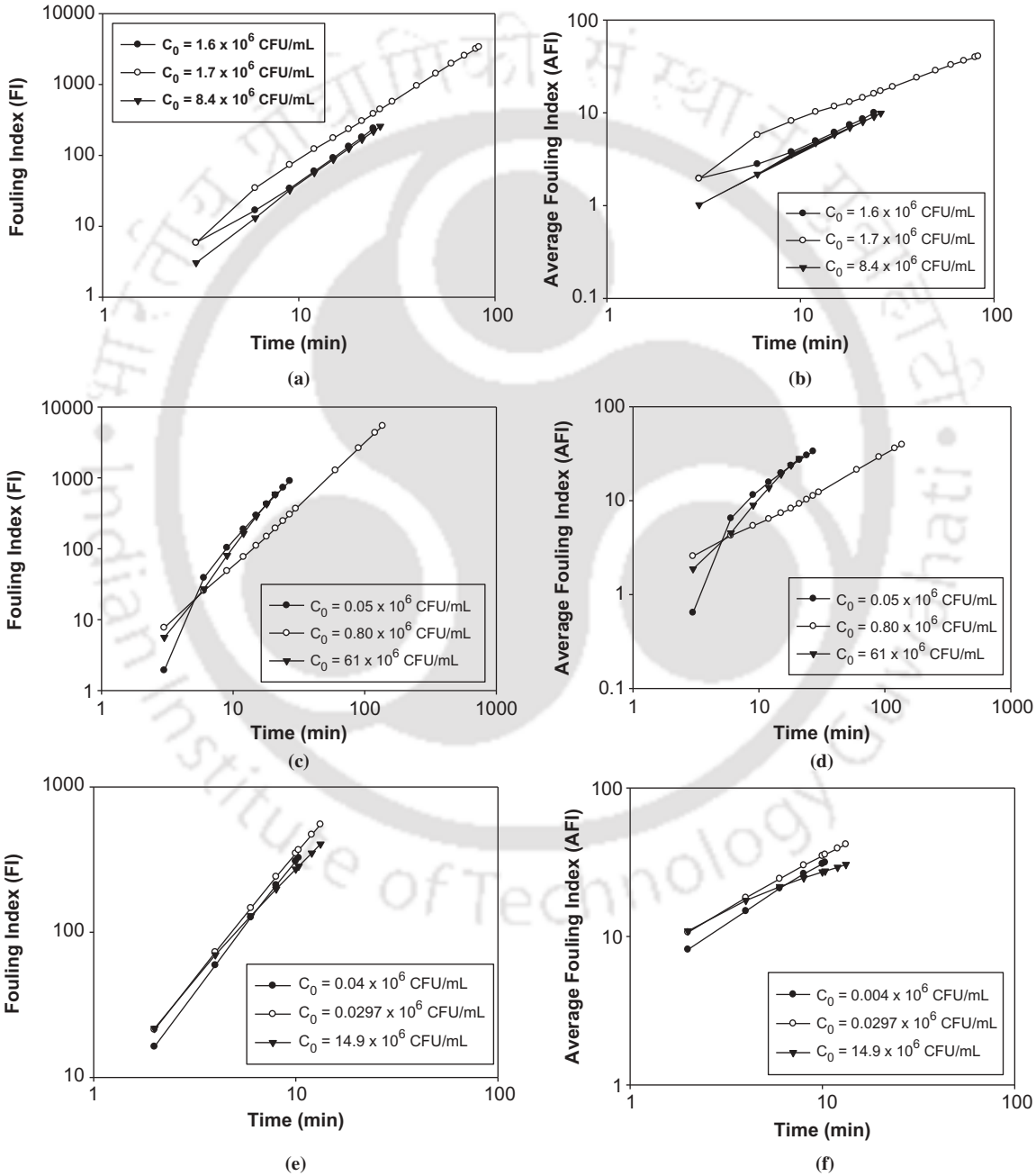

FIG. 7. Variation of FI and AFI for various membranes: (a, c and e) correspond to FI and (b, d and f) correspond to AFI for CM1- CM3 membranes.

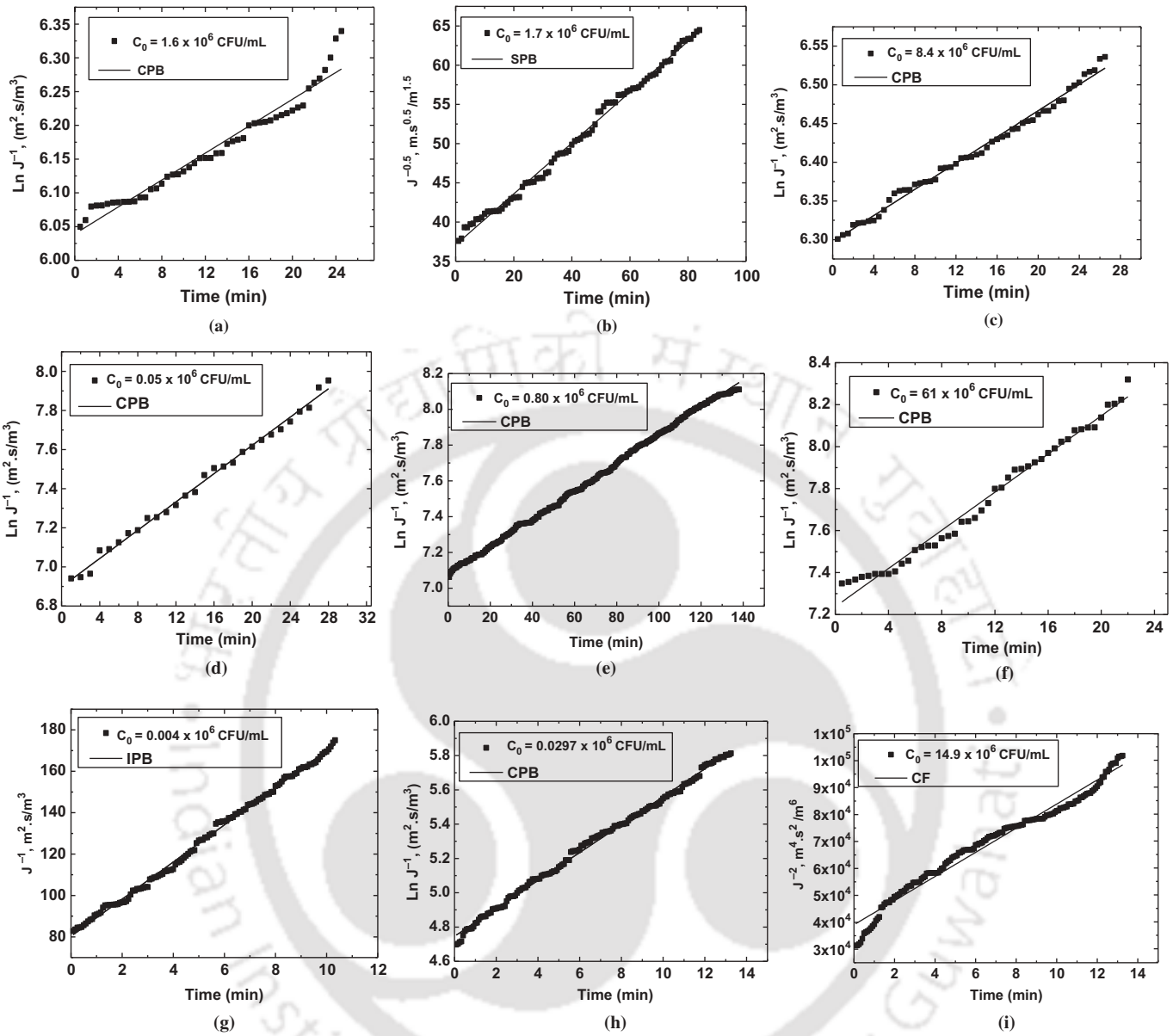

FIG. 8. Fitness of best fit fouling models towards the measured MF data for various membranes at distinct feed concentrations (a-c) CM1 membrane (d-f) CM2 membrane and (g-i) CM3 membrane.

situ fouling. Also, the fitness of cake filtration model for the CM3 membrane at highest feed concentration is indicative towards lower irreversible membrane fouling. In summary, the variation in best fit models for variant feed concentrations and membrane morphology (or average pore size) is indicative towards the complexity associated with morphology and activity of microbes.

Based on general rule of thumb, CM3 membrane should undergo maximum membrane fouling during the MF operation, which is not the case. This is indicative to the fact that the dynamic cake filtration layer formed on the membrane surface behaved distinctly for different membrane pore sizes. While the cake filtration layer for the CM1–CM2 membrane restricted the membrane flux, it favoured higher membrane flux for the CM3 membrane. Thus, it can be analysed that the dynamic microbial cake filtration layer morphology is a strong function of the membrane morphology. Thus, it is apparent that larger average pore size of the membrane is favourable to achieve good properties of the dynamic microbe based cake filtration layer that develops during the MF operation.

The data presented in this work corresponds to flux measurements carried out using batch microfiltration cell using membranes with very high water permeability. About 50–60 batches of microfiltration runs were conducted in a span of 100 minutes

TABLE 5
Summary of parameters associated to all fouling models for dead end MF at $\Delta P = 206.7$ kPa

Membrane type	Feed Concentration (CFU/mL) $\times 10^6$	Complete pore blocking			Standard pore blocking			Intermediate blocking			Cake filtration		
		$k_b \times 10^{-4}$	$\ln(J_0^{-1})$	R^2	$k_s \times 10^{-4}$	$J_0^{-0.5}$	R^2	$k_i \times 10^{-4}$	J_0^{-1}	R^2	k_c	J_0^{-2}	R^2
CM1	1.6	2	6.04	0.954	18	20.45	0.947	800	416.48	0.938	77	170247	0.919
	1.7	2	7.29	0.994	54	37.10	0.995	5522	1243.5	0.987	2999	37024	0.952
	8.4	1	6.30	0.991	17	23.28	0.990	863	540.26	0.988	106	288205	0.981
CM2	0.05	6	6.90	0.994	124	30.54	0.987	10386	842.79	0.970	3777	25105	0.910
	0.80	1	7.08	0.999	29	33.39	0.995	2702	1005.7	0.982	1190	8101.4	0.937
	61	8	7.24	0.985	185	36.16	0.974	18363	1180.8	0.955	9341	64964	0.899
CM3	0.004	12	4.44	0.991	67	9.11	0.996	1494	80.29	0.997	38	4956.4	0.987
	0.0297	14	4.75	0.997	96	10.41	0.995	2747	97.89	0.983	118	8.82	0.930
	14.9	6	5.32	0.917	46	14.25	0.937	1464	201.75	0.953	75	39092	0.974

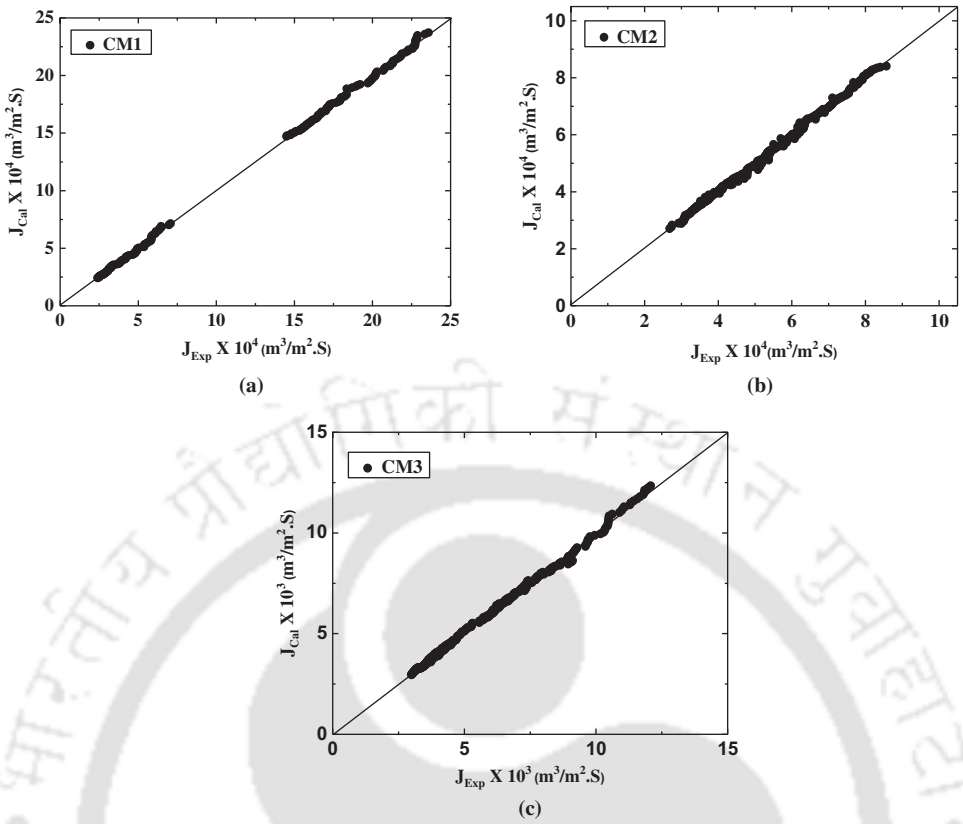

FIG. 9. Parity plots for measured flux and best fit fouling model flux for (a) CM1 (b) CM2 and (c) CM3 membranes.

for some membranes. However, the reduction in membrane flux after 10 batches is significantly low. This indicates that the membranes are promising for commercial applications. Further flux data could be measured, but it did not contribute significant know how of the inherent flux decline trends.

Figures 9(a-c) depict parity plots for the fitness fouling models to represent measured experimental MF flux data for membranes CM1-CM3, respectively. It can be observed that all best fit fouling models had very good fitness with the measured flux data. The maximum and minimum errors have been evaluated to vary from 6 - 7% and 0.002 - 0.007% respectively for membranes CM1 - CM3. Corresponding RMS error values were evaluated to vary in the range of 1.43 - 1.81%.

MEMBRANE COST

The average cost of the fabricated membranes based on retail cost of the materials is about 62\$/m^2. Inclusive of other fabrication costs such as electrical and labor costs, the average cost of fabricated membranes is estimated to be about 80 \$/m^2. Typical ceramic filter candles for gravity fed applications have a dimension of 7×10^{-2} m length and 2×10^{-2} m dia. This corresponds to a membrane surface area of 4.71×10^{-3} m^2. Each ceramic pot filter costs about 1.19\$. Thereby, the retail cost of the ceramic pot filter has been evaluated as 251 \$/m^2. Thus, the fabricated membranes are about 70% less expensive compared with the commercially available membranes.

With respect to other incurred costs during operation, both for CM1 and CM2 membranes, additional costs are incurred to provide sufficient pressure. But CM3 membrane with wider pore size is envisaged to be applicable for gravity fed application. Thus, CM3 membrane is inferred to be the low cost membrane for gravity fed application as a ceramic pot filter.

CONCLUSIONS

Using uniaxial dry compaction method, this work reported three different inorganic precursor formulations to achieve low cost ceramic membranes for bacteria separation applications. Inorganic precursor formulation and size distribution of precursor powder mixture have been identified as the key parameters to influence membrane morphologies. Amongst all membranes fabricated, the CM1 membrane at a feed concentration of 1.7×10^6 CFU/mL provided maximum separation efficiency (100%) but lowest transmembrane flux and lowest initial flux, which are all indicative towards significant pore blocking during the MF run. The long term poor performance of CM1 membrane is possibly due to the incompatibility of membrane pore size distributions towards the filtration of chosen bacterial strain morphologies (2×1 μm) at their feed concentrations. On the other

hand, CM3 membrane with higher average pore size at a feed concentration of 14.9×10^6 CFU/mL provided optimal membrane performance in terms of initial and final transmembrane flux and acceptable values of separation efficiency (99.9999%). For this membrane, the ability of the membrane to provide very high values of transmembrane flux without higher degree of fouling after 10 min. of operation is promising. Also, the lack of competence of either one of the fouling models to represent the measured MF data is indicative towards the complexities associated with the variation in pore blocking mechanisms with variant microbial activity, pore size distribution of the membranes and trans-membrane pressure differentials. In summary, the observations, analysis and suggestions are indicative towards the optimality of CM3 membrane as a viable low cost ceramic membrane towards bacteria separation applications.

FUNDING

The authors sincerely acknowledge Council of Scientific and Industrial Research (CSIR), New Delhi for providing the financial assistance towards carrying out the research reported in this article.

REFERENCES

1. Safe Drinking Water Foundation, Canada, http://www.safewater.org/PDFS/PurposeofDrinkingWaterQualityGuidelinesRegulations.pdf (accessed May 2014).
2. Simonis, J. J.; Basson, A. K. (2011) Evaluation of a low-cost ceramic micro-porous filter for elimination of common disease microorganisms. *Phy. Chem. Earth*., 36:1129–1134.
3. Kent Ro, UV and water purifiers, http://www.kent.co.in/Technology-Mineral-RO (accessed May 2014)
4. Shalini, C.; Pragnesh N. D. (2012) Removal of iron for safe drinking water. *Desalination*, 303:1–11.
5. Salahi, A.; Gheshlaghi, A.; Mohammadi, T.; Madaeni, S. S. (2010) Experimental performance evaluation of polymeric membranes for treatment of an industrial oily wastewater. *Desalination*, 262: 235–242.
6. Girard, B.; Fukumoto, L. R. (1999) Apple juice clarification using microfiltration and ultrafiltration polymeric membranes. *LWT - Food Sci. Technol*., 32: 290–298.
7. Yang, Y. F.; Li, Y.; Li, Q. L.; Wan, L. S.; Xu, Z. K. (2010) Surface hydrophilization of microporous polypropylene membrane by grafting zwitterionic polymer for anti-biofouling. *J. Membr. Sci*., 362: 255–264.
8. Siemens Industry, http://www.industry.siemens.com/topics/global/en/fairs/siww/waterconvention/Documents/02_Poster_Comparison-Ceramic-and-Polymeric-Membranes.pdf (accessed May 2014).
9. Abbasi, M.; Taheri, A. (2014) Modeling of permeation flux decline during oily wastewaters treatment by MF-PAC hybrid process using mullite ceramic membranes. *Indian J. Chem. Technol*., 21: 49–55.
10. Khemakhem, S.; Amar, R. B. (2012) Purification of industrial effluent by microfiltration and ultrafiltration ceramic membranes: comparative study between commercial and elaborated tunisian clay membranes. *Desal. Water. Treat*., 39: 182–189.
11. Nandi, B. K.; Das, B.; Uppaluri, R.; Purkait, M. K. (2009) Microfiltration of mosambi juice using low cost ceramic membrane. *J. Food Eng*., 95: 597–605.
12. Vasanth, D.; Pugazhenthi, G.; Uppaluri, R. (2011) Fabrication and properties of low cost ceramic microfiltration membranes for separation of oil and bacteria from its solution. *J. Membr. Sci*., 379: 154–163.
13. Srivastava, A.; Srivastava, O. N.; Talapatra, S.; Vajtai, R.; Ajayan, P. M. (2004) Carbon nanotube filters. *Nat. Mat*., 3: 610–614.
14. Mwabi, J. K.; Mamba, B. B.; Momba, M. N. B. (2012) Removal of Escherichia coli and faecal coliforms from surface water and groundwater by household water treatment devices /systems: A sustainable solution for improving water quality in rural communities of the Southern African development community region. *Int. J. Environ. Res. Public Health*, 9: 139–170.
15. Ciston, S.; Lueptow, R. M.; Gray, K. A. (2008) Bacterial attachment on reactive ceramic ultrafiltration membranes. *J. Membr. Sci*., 320: 101–107.
16. Bielefeldt, A. R.; Kowalski, K.; Summers, R. S. (2009) Bacterial treatment effectiveness of point-of -use ceramic water filters. *Water. Res*., 43: 3559–3565.
17. Simonis, J. J.; Basson, A. K. (2012) Manufacturing a low-cost ceramic water filter and filter system for the elimination common pathogenic bacteria. *Phy. Chem. Earth*., 50-52: 269–276.
18. Simonis, J. J.; Basson, A. K. (2013) Manufacture of a low-cost ceramic microporous filter for the elimination of microorganisms causing common diseases. *J. Water Sanit. Hyg. De*., 3: 42–50.
19. Simonis, J.; Ndwandwe, M.; Basson, A.; Selepe, T. (2014) Removal of selected microorganisms using silver-impregnated and coated, low-cost, micro-porous, ceramic water filters. *J. Water Sanit. Hyg. De*., 4: 37–42.
20. Emani. S.; Uppaluri, R.; Purkait, M. K. (2013) Preparation and characterization of low cost ceramic membrane for mosambi juice clarification. *Desalination*, 317: 32–40.
21. Vasanth, D.; Uppaluri, R.; Pugazhenthi, G. (2011) Influence of sintering temperature on the properties of porous ceramic support prepared by uniaxial dry compaction method using low-cost raw materials for membrane applications. *Sep. Sci. Technol*., 46: 1241–1249.
22. Nandi, B. K.; Uppaluri, R.; Purkait, M. K. (2009) Effect of dip coating parameters on the morphology and transport properties of cellulose acetate- ceramic composite membranes. *J. Membr. Sci*., 330: 246–258.
23. Agarwal, A.; Pujari, M.; Uppaluri, R.; Verma, A. (2013) Preparation, optimization and characterization of low cost ceramics for the fabrication of dense nickel composite membranes. *Ceram. Int*., 39: 7709–7716.
24. Emani, S.; Uppaluri, R.; Purkait, M. K. (2014) Micro filtration of oil-water emulsions using low cost ceramic membranes prepared with the uniaxial dry compaction method. *Ceram. Int*., 40: 1155–1164.
25. Hermia, J. (1982) Constant pressure blocking filtration laws - Application to power - law non-Newtonian fluids. *Trans. Inst. Chem. Eng*., 60: 183–187.
26. Nandi, B. K.; Uppaluri, R.; Purkait, M. K. (2009) Treatment of oily waste water using low-cost ceramic membrane: Flux decline mechanism and economic feasibility. *Sep. Sci. Technol*., 44: 2840–2869.